A ROBUST DESIGN METHOD FOR MODEL AND PROPAGATED UNCERTAINTY

A Dissertation
Presented to
The Academic Faculty

by

Hae-Jin Choi

In Partial Fulfillment
of the Requirements for the Degree
Doctor of Philosophy in the
School of Mechanical Engineering

Georgia Institute of Technology
December 2005

A ROBUST DESIGN METHOD FOR MODEL AND PROPAGATED UNCERTAINTY

Approved by:

Dr. Farrokh Mistree, Advisor
School of Mechanical Engineering
Georgia Institute of Technology

Dr. David L. McDowell, Co-advisor
School of Mechanical Engineering
Georgia Institute of Technology

Dr. Janet K. Allen
School of Mechanical Engineering
Georgia Institute of Technology

Dr. Hamid Garmestani
School of Materials Science & Engineering
Georgia Institute of Technology

Dr. David Rosen
School of Mechanical Engineering
Georgia Institute of Technology

Dr. Kwok Tsui
School of Industrial & Systems Engineering
Georgia Institute of Technology

Dr. Roshan Vengazhiyil
School of Industrial & Systems Engineering
Georgia Institute of Technology

Date Approved: September 20, 2005

ACKNOWLEDGEMENTS

My achievement would not be realized if there were not the efforts of the people who have given me a precious help.

I give my sincere appreciation to my advisor, Dr. Farrokh Mistree. His continuous encouragement, guidance, and untainted reliance upon me make this work possible. He gave me the primary motivation and inspiration for this research as well as generous support. His broad knowledge and insight guided me from the start of this journey to the end.

I give my special thanks to my co-advisor, Dr. David McDowell, his expertise in materials design and multiscale modeling is the major guidance in this work. His enthusiasm in this area was great encouragement in my work.

I thank Dr. Janet K. Allen. This achievement would not be possible without her help. Her continuous guidance has helped me grow intellectually and personally since I came to Systems Realization Laboratory.

I owe my thanks to other committee members, Drs. David Rosen, Hamid Garmestani, Kwok Tsui, and Roshan Vengazhiyil. I would like to give my sincere thanks to Jitesh Panchal and Ryan Austin. They have given the greatest help to me in this work. Without their help, this research would not be possible. I cherish the support and compassion given by other SRL colleagues – Marco Fernandez, Carolyn Conner Seepersad, Chris Williams, and Matt Chamberlain.

The financial support from AFOSR MURI 1606U81 is greatly appreciated. Those make this work possible.

I offer my deepest thanks to my parents for their continuous encouragement, sacrifice, and love through out this process.

I would like to dedicate this dissertation to my wife, Chee-eun Kim, and my son, Sungjae Choi.

I thank my Load for everything.

TABLE OF CONTENTS

LIST OF TABLES

LIST OF FIGURES

GLOSSARY

Analysis Chain	A Series of Interlinked Analyses or Simulations
ANOVA	Analysis of Variance
CCD	Central Composite Design
cDSP	Compromise Decision Support Problem
Design Process Chain	A Series of Interdependent Design Tasks
DCE	Discrete Constraints Evaluation
DCI	Design Capability Index
DOE	Design of Experiments
DP	Design Parameter
DPM model	Discrete Particle Mixture model (Microscale Simulation)
EMI	Error Margin Index
EOS	Equation of State
FOSM	First-Order, Second Moment
FR	Functional Requirement
GRDPM	Graphical Robust Design Process Model
HD-EMI	Hyper-Dimensional Error Margin Index
IDEF0	Integrated Definition
IDEM	Inductive Design Exploration Method
IDCE	Inductive DCE
LRL	Lower Requirement Limit
MDO	Multidisciplinary Design Optimization
NTM model	Non-equilibrium Thermodynamics Mixture model (Continuum Analysis)
MESM	Multifunction Energetic Structural Material
MPP	Most Probable Point
MPU	Model Parameter Uncertainty
MSU	Model Structure Uncertainty
PDF	Probability Density Function
RCEM	Robust Concept Exploration Method
RCEM-DCI	Robust Concept Exploration Method with Design Capability Index
RCEM-EMI	Robust Concept Exploration Method with Error Margin Index

RPMM	Reactive Particle Metal Mixture
SOSM	Second-Order, Second Moment
SVE	Statistical Volume Element
Type I Robust Design	Insensitive Design to Uncertainty in Noise Factors
Type II Robust Design	Insensitive Design to Uncertainty in Control Factors
Type III Robust Design	Insensitive Design to Uncertainty Embedded in Models
Type IV Robust Design	Insensitive Design to Uncertainty in a Design/Analysis Chain
URL	Upper Requirement Limit

LIST OF SYMBOLS

$A_i(x)$	Performance Functions
$acFe$	Accumulated Mass Fraction of Fe in a Material Specimen
$\mathbf{B_j}$	Discrete Point Vector on a Constraint Boundary
$\mathbf{B_j^i}$	Projected Vector of $\mathbf{B_j}$ along i Direction on the Nearest Boundary of an Output Range
$b_{j,i}$	i th component of $\mathbf{B_j}$
$b_{j,i}^{\ i}$	i th component of $\mathbf{B_j^i}$
$\boldsymbol{\beta}, \hat{\boldsymbol{\beta}}$	Vector of Regression Parameters, Vector of Estimated Regression Parameters
$d_i^-\ d_i^+$	Deviation Variables in a cDSP
$\mathrm{DCI}_{\mathrm{target}}$	Target DCI Value
δ_{max}	Maximum Deflection of a Beam
E	Modulus of elasticity
ε_i	Observed Random Error
$\mathrm{EMI_l}$, $\mathrm{EMI_u}$	Lower and Upper Error Margin Indices
$\mathrm{EMI}_{\mathrm{constraints}}$	Error Margin Index for Constraint Conditions
$\mathrm{EMI}_{\mathrm{target}}$	EMI Target Value
F	Transformation Function
$f_{0,i}(\mathbf{x})$	Mean Response (Performance) Functions
$f_{j,i}(\mathbf{x})$	Uncertainty Bound Functions for a Mean Response Function $f_{0,i}(\mathbf{x})$
G_i	System Goals
$g_i(\mathbf{x})$	System Constraints in a cDSP
$\mathrm{HD\text{-}EMI}_i$	HD-EMI in i performance direction
$\mathrm{HD\text{-}EMI}_{\mathrm{target}}$	Target HD-EMI
I	Information Content
N	Total Number of Samples
n	Number of System Variables
m	Number of System Goals
mean	Mean Vector of an Output Range
$mean_i$	i th component of **mean**
μ_x	Means of System Variables
μ_y	Mean Response

P_{max}	Maximum Load
P	Number of Predictors
p	Number of Equality Constraints
q	Number of Inequality Constraints
R	Radius of a Circular Beam Section
ρ	Density of Material
σ	Scale Factor in Conditional Variance Model
σ_i^2	Observed Variance
σ_u	Ultimate Tensile Strength
$t_{N-P,1-\alpha/2}$	t-value in Student t-distribution with (1-α) Confidence Level, N Samples, and P Predictors in an Approximate Model
T_{ignit}	Critical Temperature for Chemical Reaction Initiation; Weighted Average Hotspot Temperature at First Reaction Initiation
$\boldsymbol{\theta}$, $\hat{\boldsymbol{\theta}}$	Vector of Variance Parameters, Vector of Estimated Variance Parameters
$\sigma^2 v^2(\mathbf{z_i}, \boldsymbol{\theta}, \boldsymbol{\beta})$	Conditional Variance Model
U_p	Particle Velocity
URL	Upper Requirement Limit
W	Weight
$\mathbf{x}$	Vector of Design Variables
$\mathbf{x}_0$	New Observation
x	Volume Fraction of Clay
x_1	Mean Radius of Al Particles
x_2	Mean Radius of Fe_2O_3 Particles
x_3	Volume Fraction of Voids
x_4	Mean Radius of Voids
y	Response
y^{tr}	Transformed Response
$Y_{\max}$, $Y_{\min}$	Maximum and Minimum Responses in a Given Design Space
ΔY	Response Deviation
ΔY_{upper} , ΔY_{lower}	Upper and Lower Deviation from a Mean Response
$\mathbf{z}$	Vector of Variance Factors
$\mathbf{x}_i$, y_i, $\mathbf{z}_i$	Factors, Response Value, and Variance Factors at i^{th} Observation

SUMMARY

One of the important factors to be considered in designing an engineering system is uncertainty, which emanates from natural randomness, limited data, or limited knowledge of systems. In this study, a robust design methodology is established in order to design multifunctional materials, employing multi-time and length scale analyses. The Robust Concept Exploration Method with Error Margin Index (RCEM-EMI) is proposed for design incorporating non-deterministic system behavior. The Inductive Design Exploration Method (IDEM) is proposed to facilitate distributed, robust decision-making under propagated uncertainty in a series of multiscale analyses or simulations. These methods are verified in the context of 'Design of Multifunctional Energetic Structural Materials (MESM)'. The MESM is being developed to replace the large amount of steel reinforcement in a missile penetrator for light weight, high energy release, and sound structural integrity. In this example, the methods facilitate following state-of-the-art design capabilities, robust MESM design under (a) random microstructure changes and (b) propagated uncertainty in a multiscale analysis chain. The methods are designed to facilitate effective and efficient materials design; however, they are generalized to be applicable to any complex engineering systems design that incorporates computationally intensive simulations or expensive experiments, non-deterministic models, accumulated uncertainty in multidisciplinary analyses, and distributed, collaborative decision-making.

CHAPTER 1

MULTISCALE SIMULATION-BASED MATERIALS DESIGN

The principal goal in this dissertation is to establish approaches that are suitable for robust, multifunctional materials design based on a multiscale non-deterministic analyses and simulation chain. In this chapter, we introduce a system-based materials design paradigm incorporating multiscale analysis and simulation. From this introduction, we identify research questions, formulate hypotheses, plan validation and verification of the proposed hypotheses, and introduce the structure of the dissertation.

In Section 1.1, a design paradigm based on multiscale simulation is introduced followed by multiscale simulation-based materials design and Olsen's materials design definition (Olson, 1997). In this section, as a specific example of the multiscale simulation based materials design, the Multifunctional Energetic Structure Materials (MESMs) design problem is introduced. Challenges in system-based design of materials due to uncertainties in multiscale simulation and analyses are identified from the perspectives of material analysis and those of systems design in Section 1.2. Based on the identified problems in multiscale simulation-based materials design, the research scope for this dissertation is framed, introducing strategies for managing uncertainty in a system in Section 1.3. Previous approaches in robust design methodology are briefly introduced and are reviewed critically later in Chapter 2. In Section 1.4 research questions and

hypotheses in this dissertation are posted followed by a discussion of the validation strategy and dissertation structure in Section 1.5.

This chapter is revisited for checking structural soundness of the dissertation when literature review, method development, design examples, and validation of hypotheses are discussed in other chapters.

1.1. MULTISCALE SIMULATION-BASED DESIGN

Growing interest in simulation-based design, as evident from the recent National Science Foundation (NSF) workshop on Simulation Based Engineering Science (SBES) (Workshop Report, 2004), is attributed to the availability of independently developed simulation models at multiple length and time scales. SBES represents an interface between diverse disciplines. Following the NSF workshop on SBES, The US Department of Energy sponsored three workshops on multiscale mathematics (Dolbow, et al., 2004) to identify research and funding opportunities in multiscale modeling. In theses workshops, a number of issues related to multiscale modeling were identified. From a multiscale modeling standpoint, the primary challenge is to *integrate information* generated by different simulation models in a consistent manner so that **the overall system behavior can be predicted from the individual constituent models**. During the two workshops, various application domains that would benefit from multiscale modeling were identified. These domains include, but are not limited to, environmental sciences and geosciences, climate, material science, combustion, biosciences, power grids and information networks, development of biomimetic sensors and devices, and homeland security.

Since it is possible to predict the behavior of systems at multiple scales, the natural next step is to use these models in designing systems at multiple scales. For example, as shown in Figure 1.1, the product is designed at the overall system level or individual components through nanoscale interactions or atomic level chemistry. One significant advantage of designing products at multiple scales is increased design freedom, which enables designers to achieve performance that was not possible by designing at a single scale level (mostly overall system and component levels) before. In contrast to multiscale modeling, the primary challenge faced by the simulation-based design community is to effectively and efficiently *utilize information* generated by a wide range of models that predict system behavior at different scales. In order to address this challenge, there exists a need for a domain independent methodology for designing multiscale systems.

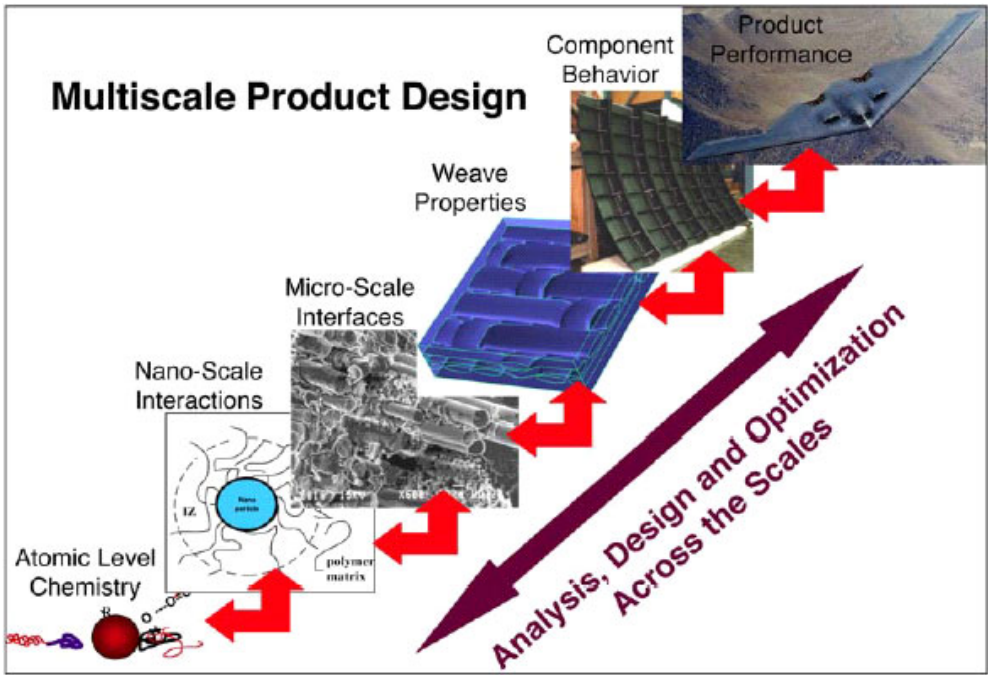

Figure 1.1 Multiscale product design (Workshop Report, 2004)

1.1.1. Multiscale Materials Design

One of the most important challenges among the applications of multiscale SBES is multiscale materials design. Traditionally, materials are selected from a database which lists their properties experimentally established (c.f., Ref. (Ashby, 1999)). However, this approach is changing in favor of tailoring materials for specific products by virtue of continuous development of materials science and computing. The main approach in materials science is deductive mapping from the material processing path, nano-structure and micro-structure, material properties, and up to material performance as shown in Olson's (Olson, 1997) materials hierarchical in Figure 1.2. While Olson's construct sets an important philosophical foundation on which to base materials design, it delegates practical aspects of the goal-oriented (inductive) materials design process to the creative will, depth of insight, experience, and knowledge base of the designer.

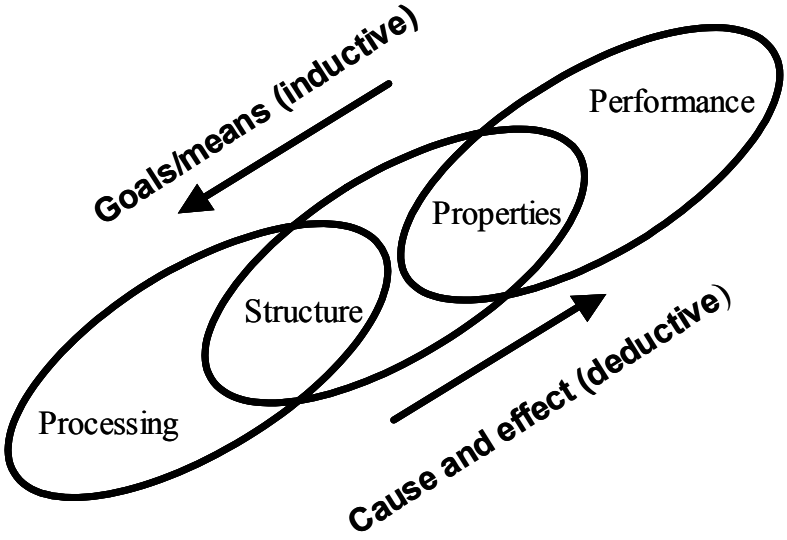

Figure 1.2 Olsen's hierarchical concept of materials by design (Olson, 1997)

Materials design is an inherently multiscale, multifunctional activity. Most applications require materials that satisfy multiple functions, such as structural load

bearing, thermal transport, cost, and long-term reliability. These design requirements cannot be defined in isolation from overall system conditions and requirements. These conditions are associated with the operating environment and the component(s) and the overall system in which a material is integrated.

Desired material properties and performance characteristics often depend on phenomena that operate at different length and time scales, spanning from angstroms to meters and from picoseconds to years. A hierarchy of multiscale models has been developed and applied to specific length and time scales. Each model in the hierarchy is used to provide the formulation of other models on higher scales. The higher scale models capture the collective behavior of lower scale subsystems. It is very difficult to formulate a single model for macroscopic material properties that unifies all of the length scales (McDowell, 1998). For example, first principles models[1], based on theoretical and solid-state physics, can be used on atomistic and molecular levels to predict the structure and properties of ideal designs. However, such models (i.e., first principles models) are computationally expensive to analyze materials with highly heterogeneous microstructures that strongly influence their macroscopic properties. On the other hand, continuum-based models, based on classical continuum theory, are useful for describing properties at a macroscopic scale relevant to many engineering applications; however, they are inappropriate for smaller scale phenomena that require atomistic resolution. Therefore, multiple scale models need to be incorporated to precisely predict a system level product performance considering smaller scale material phenomena.

[1] Models formulated based on elements' principles in the periodic table

In this section, multiscale materials design is introduced as an important challenge among applications of multiscale SBES. In the next section, an example of multiscale materials design, multifunctional energetic structural materials design, is introduced.

1.1.2. Multifunctional Energetic Structural Materials (MESM) Design

In the previous section, we discuss the multiscale approach in the analysis of material behavior. This multiscale approach is being applied to the various fields of material analysis and design. In this section, we introduce a multiscale modeling example for designing materials based on Multifunction Energetic Structural Materials (MESM). MESMs are materials that derive superior energetic characteristics and enhanced mechanical strength properties. MESMs are used to classes for missiles that release their explosive energy after penetrating through a target, as shown in Figure 1.3.

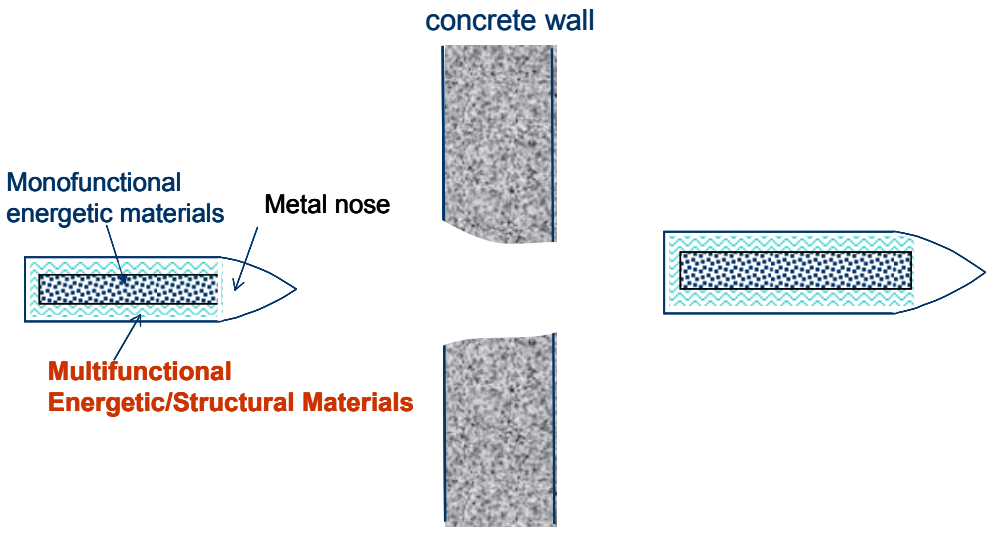

Figure 1.3 Missile penetrator with MESM casing

In such missiles, high explosives are typically encased in a steel projectile that is designed with sufficient structural strength to penetrate targets such as steel or concrete. In such missiles, the steel is used only to provide structural strength as needed to

penetrate through specific targets and shield the high explosives during the penetration process. By replacing the steel (and thus increase the payload) with the MESM, we achieve the function of structural strength while penetrating through the target. Later, the explosive energy released by MESM will add to the energy released by the high explosive. MESMs will be reinforced either by high strength materials such as carbon nanotubes or they will be reinforced at the macrolevel. The challenge is to preserve the energetic characteristics as reinforcement is introduced.

In the development of MESMs, multiscale analytical, experimental and computational tools are employed to engineer the MESMs from micro to nano scales and compare their performance. Ab initio principles are developed for reacting elements to explore stress-induced initiation of reactions in MESMs. MESM developers use an equivalent continuum field concept that allows atomic scale heterogeneity from molecular dynamics calculations to be described in a continuum setting, with appropriate homogenization procedures for scaling up to higher scales. These bridges between multiple scale models are created to analyze both energetic materials and energetic structural materials, in close connection with companion experiments. Material experiments are designed and conducted jointly with the modeling process as necessary to develop and validate the models. Using the multiscale computational models for predicting MESM performance, missile penetrators will be customized by computationally analyzing the penetration performance of the missile as it impacts to concrete targets. The hierarchy of multiscale computational models incorporated for designing MESMs is illustrated in Figure 1.4. In the following four sections, we discuss briefly the multiscale models (the boxes in the scale graph) for multifunctional analyses of MESMs employed for this research.

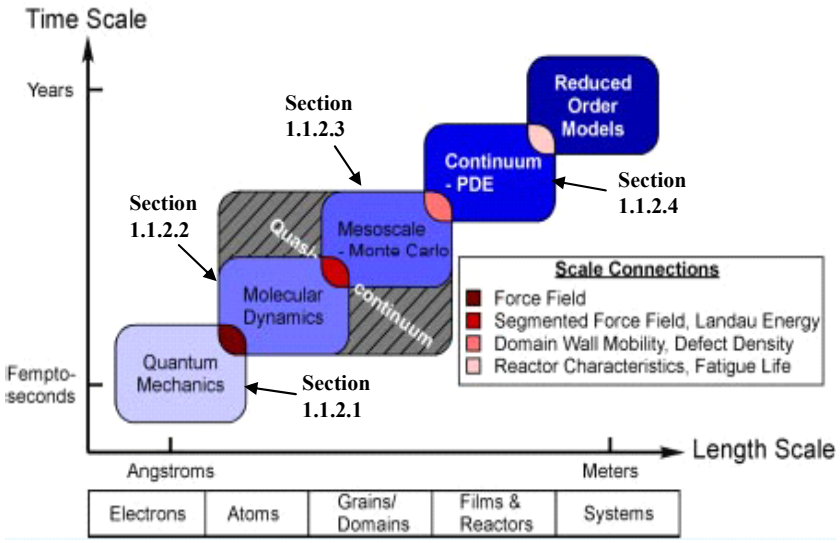

Figure 1.4 Hierarchical materials design

1.1.2.1 Quantum Mechanics Models

Quantum scale models, the smallest scaled computational model in Figure 1.4, are used to determine the equation of state properties of the individual materials and the likelihood of reaction initiation between reactive components. These ab initio models only require environmental properties such as pressure and temperature as inputs since the atomic properties are fundamentally derived. The equation of state results, particularly in the Hugoniot form, are used in the meso-scale discrete particle models to determine the constitutive behavior of the individual components. Evaluation of the transition states and energies that relate to the interaction of reactive components can be processed to determine the likelihood that a reaction will initiate. These probabilities can be used in the meso-scale discrete particle models. Quantum scale models are also used to determine the parameters in potentials used in molecular dynamics models.

1.1.2.2 Molecular Dynamics Models

Molecular dynamics (MD) models, the second smallest scaled models in Figure 1.4, can also be used to investigate the equation of state properties and the probability of reaction initiation, but at larger scales. While quantum scale models are limited to tens of atoms, MD models can investigate the interactions of hundreds of thousands to millions of atoms. The MD models can then be used more effectively to study shock waves through the atoms, size scale effects at reactive component interfaces, and nanoscale domains of the constituents. The MD models can also be compared and verified with quantum scale models. The results of the MD models may be used in the meso-scale discrete particle models.

1.1.2.3 Meso-Scale Models

In the meso-scale model, the third smallest scaled models in Figure 1.4, the constituents are modeled as discrete particles in the nanometer to micron scale range. With a given shock input, the model estimates reaction initiation and structural information within a volume element measuring in the tens to hundreds of microns in length. The randomly generated morphology is created based on statistical information such as volume fractions, size distributions, and nearest neighbor distributions. The structural information in the form of Hugoniot data is used in continuum models for systems model analysis. The reaction initiation aspects of the model can be used to determine the likelihood of reaction propagation and the pressure, temperature effects of the reaction.

1.1.2.4 Continuum Models

Achieving an accurate continuum model for new materials is important to accurately estimate the performance of a system scale model. Structural and reaction information generated from meso scale model are interfaced with the continuum model. Experimental data are often required for validating multiscale analysis models at this scale. Constitutive models and reduced order models are implemented at this scale. The reduced order model in this MESM analysis is a non-equilibrium mixture model which predicts structural and reaction relations based on the 'rule of mixtures,' in which a mixture's property can be calculated by the weighted average of mixture constituents' properties based on their fractions in a mixture.

One of the main objectives is to establish a multiscale materials design framework in order to derive the characteristics for other fuel, oxidant and structural reinforcement combinations based on these multiscale models. In this section, we introduce the multiscale models for designing MESM as an example of multiscale simulation-based materials design. In the next section, the challenges in the multiscale simulation-based materials design are discussed.

1.2. CHALLENGES IN MULTISCALE SIMULATIONS-BASED DESIGN

In the previous section, we introduce the multiscale simulation and analysis models that are incorporated materials design. As discussed, one of the primary objectives in the MESM development is to develop a systematic design framework since there is no available systematic design method incorporating those multiscale simulation models. To establish a framework for this need, we discuss overall challenges in the process of

designing materials based on the multiscale simulation are discussed in this section. Seepersad and coauthors (Seepersad, et al., 2004) address three main challenges in system-based multiscale materials design. Those are decision based collaborative design, collaborative computational infrastructure, and management of uncertainty in computational models. In the following subsections, we discuss briefly about these challenges. In Section 1.2.4, we highlight the uncertainties in multiscale computational models with the microscale MESM shock simulation model.

1.2.1. Collaborative Decision-Based Materials Design

While it is extremely challenging to develop physics-based models that embody relevant process-structure-property relations shown in Figure 1.2 on different scales for diverse functions of materials, the complexity and restricted domain of application of these models limit their explicit linkage across the length and time scales illustrated in Figure 1.4. Instead, they must be linked in a manner that facilitates exploration of the systems-level design space by a collaborative team of experts. This strategy contrasts markedly with attempts to design materials using concurrent multiscale modeling which we view as unrealistic for a number of reasons.

Distributing analysis and synthesis activities also leverages the extensive domain-specific knowledge and expertise of various material and product designers who may be specialized according to length and time scales, classes of materials, and domains of functionality. A fundamental role of each domain-specific expert is to make decisions that involve synthesizing and identifying solution alternatives to achieve desirable tradeoffs between sets of conflicting material property goals. However, material subsystems are interdependent, and the individual decisions associated with them rely on

information and solutions generated by other decision-makers at other levels of the hierarchy. In the end, preferable *systems-level* solutions are sought, and they are not necessarily obtained by 'optimizing' each subsystem individually. Therefore, it is critical to establish multi-objective *decision protocols* for individual designers as well as standards, tools, and mathematical techniques for *interfacing* individual decisions and facilitating information flow among multiple experts.

1.2.2. Collaborative Computational Infrastructure

In order to realize collaborative decision-making between multidisciplinary material experts, it is critical to establish a computing infrastructure for integrating heterogeneous, distributed software applications and databases in a materials design process. An effective *computing infrastructure* needs to automate the details of executing and linking various models, freeing a designer to build upon previous model-based developments and to concentrate on higher-level design issues. The computing infrastructure should be easily extensible and platform independent. A computing infrastructure also needs to archive and organize large amounts of data and facilitate real-time data sharing and visualization as well as systematic communication, translation, and search-based retrieval of design information. Tools are needed for on-line collaboration, communication, and project management, and real-time data sharing and archiving.

1.2.3. Management of Uncertainties in Materials Design

Finally, since materials are complex, hierarchical, heterogeneous systems, it is not reasonable or sufficient to adopt a deterministic approach to materials design. First, microstructure is inherently random at some scales. Second, parameters of a given model are subject to variation associated with variation of material microstructure from

specimen to specimen. Furthermore, uncertainty is associated with model-based predictions for several reasons. Models inevitably incorporate assumptions and approximations that impact the precision and accuracy of predictions. Uncertainty may be magnified when a model is utilized near the limits of its intended domain of applicability and when information propagates through a series of models. Also, to facilitate exploration of a broad design space, approximate or surrogate models may be utilized, but fidelity may be sacrificed for computational efficiency. Experimental data for conditioning or validating approximate or detailed models may be sparse, and they may be affected by measurement errors. Also, variation is associated with the structures and morphologies of realized materials due to variations in processing history and other factors. Often, it is expensive or impossible to remove these sources of variability, but their impact on model predictions and final system performance can be profound. Therefore, systems-level design methods need to account for the many sources of variation and uncertainty. In the next section, uncertainties in materials design are discussed in further detail.

1.2.4. Examples of Uncertainties in Multiscale Materials Design

Engineering systems contain many different kinds of uncertainties found in material and component structures, computational models, input variables, and constraints. Potential sources of uncertainty in a system include human errors, manufacturing or processing variations, operating condition variations, inaccurate or insufficient data, assumptions and idealizations, and lack of knowledge. Manufacturing variations are manifested as tolerances in part dimensions, missing small sized parts or joints, and porosity in the base material. Operating conditions, such as the ambient temperature and

air flowrate, may vary as well. In addition to these sources of uncertainty, the finite element analyses required for systems behavior evaluation incorporate a number of simplifying assumptions. Examples include idealized modeling of boundary conditions as well as mesh size. Many of these simplifying assumptions are required in order to make the analyses fast enough for a complex, iterative design process. Since non-deterministic factors in a system sometimes produce considerable variations in predicted system responses, uncertainty is an important factor for designers to consider when making decisions regarding design specifications.

Realistic nanoscale or microscale computational simulations often address non-deterministic material behavior. This is due to the limited size of material captured in a computational model (i.e., less than representative volume size), non-homogeneous material distribution, random variations in material morphology, etc. These uncertainty factors represent natural variability that is quantifiable by a large enough number of samples in non-deterministic simulations. However, because of the computational burden of those simulations, it is difficult to obtain sufficient data for estimating accurate variances of responses. An equally important source of uncertainty arises from the process of developing computational models of materials. In developing these models, material scientists often employ idealistic assumptions, such as a plane strain assumption in order to reduce the true three-dimensional loading to a more tractable two-dimensional case, idealization of the material microstructure geometry, and boundary conditions. Moreover, there are uncertain constitutive models for nonlinear material behavior due to a lack of complete knowledge regarding fundamental processes. These idealizations and

assumptions incur un-quantifiable uncertainty in a simulation model, which may result in inaccurate estimation of material behavior.

An example of a non-deterministic computer simulation in the MESM design is illustrated in Figure 1.5. The components of the Statistical Volume Element (SVE)[2] in our model system are shown in the figure. Constituent phases include aluminum particles (Al-1100), agglomerates of iron oxide particles (Fe_2O_3), an epoxy binder (Epon 828), and interspersed voids. An SVE of a Reactive Particle Metal Mixture (RPMM) modeled for microscale discrete particle simulations to explore the mechanical and thermal conditions that initiate exothermic reactions is illustrated in Figure 1.5. Analysis of the RPMM is conducted by: (1) generating physically realistic microstructures, (2) performing a shock simulation, and (3) extracting relevant results from the simulation (Choi, et al., 2004).

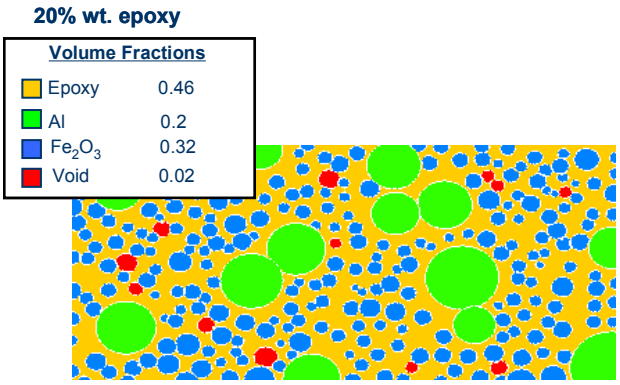

Figure 1.5 Statistical volume element of the Al-Fe_2O_3 RPMM

One of the challenges in the design of an RPMM is that the shock simulation includes a noise factor that is hard to parameterize. Experiments are performed on SVE samples with different particle distributions. Thus, the system response has pseudo-random variability with a fixed set of shock simulation input parameters as shown in Figure 1.6.

[2] Representative volume element that includes statistical information of the explicit microstructure of a mateiral

In the figure, the histogram of responses (the number of reaction sites) of 99 repeated simulations at a given set of input variables is illustrated. This implies that the system has noise factors which have not been modeled. Each instantiation of an SVE of the material incorporates a "pseudo-random" assignment of particle positions using a constrained Poisson point process (this technique is also known as a random sequential addition process (Torquato, 1991)) that prevents particle overlap.

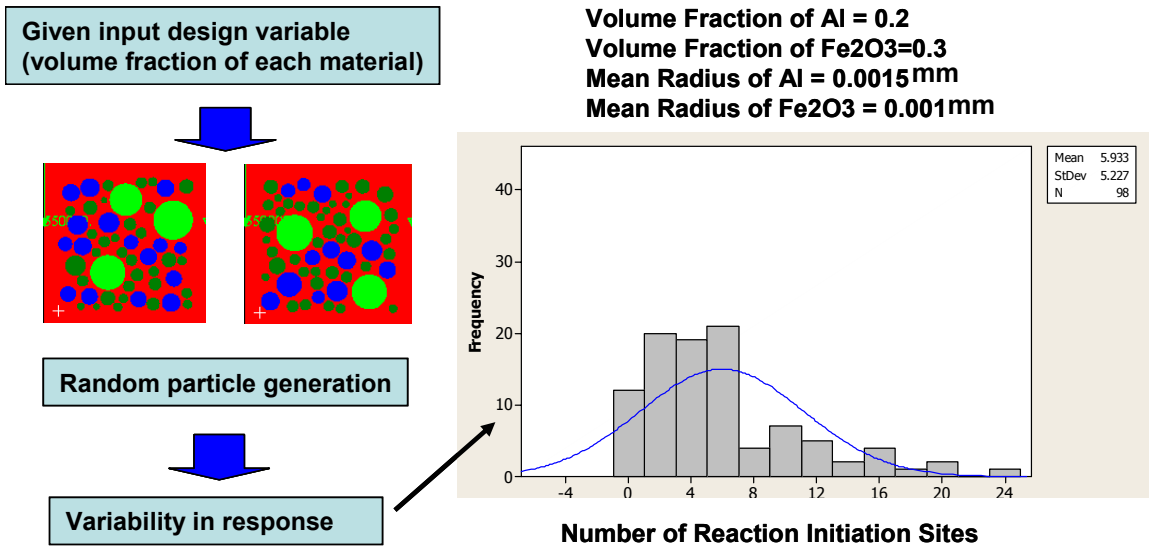

Figure 1.6 Variability in responses due to pseudo-random particle generation process

This randomness is difficult to parameterize in the system model and causes large response variance. However, it must be considered for a designer to ensure his or her design will meet specified performance requirements with regard to reaction initiation. This type of uncertainty is a hallmark of the simulation of innumerable material systems.

In addition to the statistical variability in SVE, the microscale MESM shock simulation model has a number of assumption and idealization due to computational efficiency and limitation of knowledge. The plane strain assumption is invoked in order to reduce the true three-dimensional nature of shock loading to a more tractable two-

dimensional case. A compressive shock wave is propagated though the mixture by applying a velocity boundary condition to the SVE. The velocity boundary condition is ramped up during the first stage of the simulation according to a quadratic function of time in order to avoid spurious oscillations in the solution associated with instantaneous loading. The mechanical behavior of different materials within a single element is governed by a mixture theory that equilibrates pressure in a single iteration. A physically-based constitutive model for iron oxide was not available in the open literature. Therefore, a simple elastic-plastic model has been adopted, consisting of an initial linear elastic response followed by linear isotropic strain-hardening. This may be the source of errors of this computational model, comparing with the real experimental results.

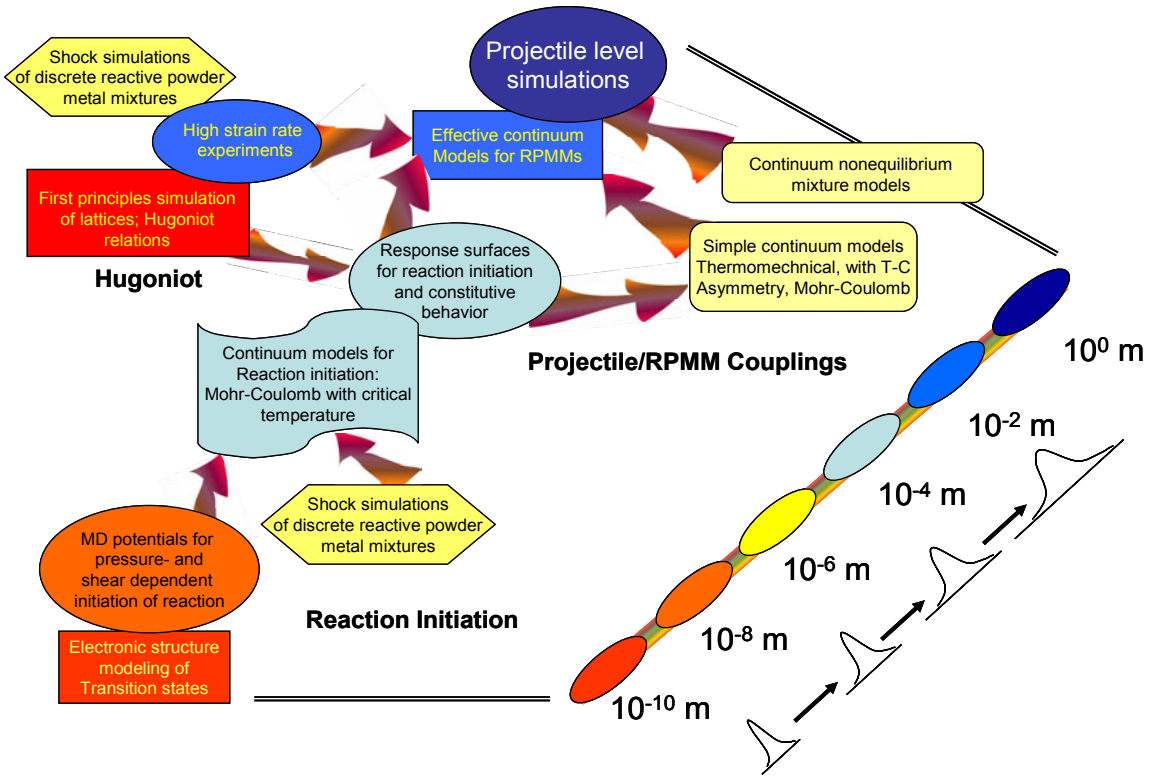

Figure 1.7 Propagated uncertainty in a multiscale simulation chain (McDowell, 2004)

Another important source of uncertainty in multiscale materials design is uncertainty propagated and accumulated along the multiscale simulation chain as shown in Figure 1.7. Aforementioned uncertainties at a single scale model is propagated and expanded by interfacing with simulation models at other scales. For example, the results (e.g., evaluation of the transition states and energies relative to the interaction of reactive components) in the analysis of the quantum mechanics model become the inputs to a microscale analysis model. Parameters in the potentials obtained in the analysis of the quantum mechanics model are the input parameters to potentials used in molecular dynamics models. The Equation–Of-States (EOS) parameters, mechanical properties, and reaction initiation behavior obtained in the microscale analysis model serve as inputs to the continuum level analysis. In this manner, all computational models are mutually interfaced in order to estimate the final performances (e.g., reaction initiation and Hugoniot information) of MESMs and the performances (e.g., depth of penetration and total energy release) of a projectile as shown in Figure 1.7. The uncertainties of the models in the simulation and analysis chain are propagated and accumulated so that the final projectile performance estimation may include a large amount of errors. Therefore, mitigation of this propagated uncertainty in designing materials (e.g., MESMs) and product (e.g., projectiles) is critical.

In this section, we discussed the challenges in multiscale simulation-based materials design, classified in three areas: (1) collaborative decision-making protocols, (2) computational frameworks for distributed collaboration, and (3) the management of uncertainties in materials design. We discussed the uncertainties in material models in detail and concluded it is essential to manage those uncertainties in designing materials

based on multiscale computational models. In the next section, the approaches for managing those uncertainties are discussed.

1.3. FRAME OF REFERENCE: MANAGEMENT OF UNCERTAINTY

For managing the sources of uncertainty discussed in the previous section, two primary approaches are available. One approach is reducing the uncertainty itself, and the other is designing a system to be insensitive to uncertainty without reducing or eliminating it.

1.3.1. Reducing Uncertainty

Reducing uncertainty is feasible when a designer has large amounts of data or complete (or better) knowledge of a system. Kennedy and O'Hagan (Kennedy and O'Hagan, 2000) employ a Gaussian Process model (known as kriging in spatial statistics) for fitting simple model data. They assume the model for detailed simulation data is a combination of the fitted simple model, a linear scale term, and error terms. The linear scale is assumed as an unknown constant and error terms are defined in another Gaussian Process model. By adding some detailed simulation results, unknown scale and error terms are estimated for constructing an approximate model of the detailed simulation. Qian and the co-authors (Qian, et al., 2004) propose a modified calibrated model by modeling the scale term as an unknown linear approximate regression function. These two methods are particularly useful for decreasing the computational expense by reducing the number of samples in fine mesh analyses. However, the common hypothesis underlying the two methods is that it is possible to obtain true (or approximately true)

data. This hypothesis, however, is not valid in many materials design problems. Brooks and Tobias (Brooks and Tobias, 1996) propose detailed guidelines for choosing the best model among available mathematical or computer models by measuring levels of detail, complexity, and corresponding model performance. Sargent (Sargent, 2003) develops a guideline for model validation, which includes data validity, conceptual model validity, computerized model verification, and operational validity. Sargent specifies validation techniques at each stage of this model validation process. Jin and co-authors (Jin, et al., 2003) test various metamodeling techniques for different optimization formulations under uncertainty and compare the accuracy of the approximation results. Simpson and co-authors (Simpson, et al., 2001) also survey sampling and metamodeling techniques and recommend a guideline for the appropriate use of statistical approximation techniques in a given situation.

1.3.2. Robust Design

The second approach for managing uncertainties is designing a system to be insensitive to uncertainty without eliminating or reducing its sources in the system; this is called robust design. In other words, robust design is used to make the system response insensitive to uncontrollable system input variations, thus improving the quality of a designed product. This is also called parameter design. Parameter design alone does not always leads to sufficiently high quality. Further improvement can be achieved by controlling the source of variations. However, the cost associated with controlling the variation sources may be prohibitively high. A robust design approach can be introduced to design at lower cost by sacrificing the achievement of optimal performance.

Typically, in robust design literature, design parameters are divided into three categories: control factors, noise factors, and responses. Control factors, also known as design variables, are parameters that a designer adjusts. Noise factors are exogenous parameters that affect the performance of a product or process but are not under a designer's control. Responses are performance measures for the product or process. The sources of uncertainty mentioned in the previous section reside in system design models, based on which designers make their decision in a scientific manner, with various forms; these are control factors, noise factors, or others, which are discussed in Sections 1.3.3, 1.3.4, 1.4.1, and 1.4.2. It is important for designers to identify *where the uncertainty sources reside in a system model* in order to employ an appropriate uncertainty management method. In the following sections, we discuss the uncertainties in a mathematical formulation of systems design.

1.3.3. Managing Uncertainty in Uncontrollable Parameters-Type I Robust Design

One of the main forms of uncertainty in a system model is uncertainty in uncontrollable independent system parameters, which are known as *"noise factors."* Noise factors are in parametric form and may be quantified and characterized as *continuous numbers with or without probability information*. Noise factors are usually given in system models as environmental factors, operating conditions, boundary conditions, or materials property variances that may be represented as continuous parameters and cannot be controlled by designers. Uncertainty in noise factors can exist as one of the aforementioned uncertainty types; however the most dominant type of uncertainty is variability (natural uncertainty), which can be measured in a statistical way. The degree of uncertainty in noise factors can be decreased by increasing the size of

sampling and/or adapting efficient uncertainty analysis methods, leaving only irreducible statistical variability.

In order to design a system robust to the uncertainty in noise factors, **Type I** robust design was proposed by Taguchi.

Type I Robust Design: Identify control factor (design variable) values that satisfy a set of performance requirement targets despite variation in noise factors.

Type I robust design is used to design systems that satisfy a set of performance requirement targets despite variations in noise factors which are uncertain, uncontrollable, independent, system parameters. Although Taguchi's robust design principles (Taguchi, 1993) are advocated widely in both industrial and academic settings, his statistical techniques, including orthogonal arrays and signal-to-noise ratio, have been criticized extensively, and improving the statistical methodology has been an active area of research (Chen, et al., 1996; Myers and Montgomery, 1995; Nair, 1992; Tsui, 1992; Tsui, 1996). During the past decade, a number of researchers have extended robust design methods for a variety of applications in engineering design (Cagan and Williams, 1993; Chen, et al., 1996; Chen, et al., 1996; Chen and Lewis, 1999; Mavris, et al., 1999; Otto and Antonnson, 1993; Otto and Antonsson, 1993; Parkinson, et al., 1993; Su and Renaud, 1997; Yu and Ishii, 1994). Taguchi robust design method and its modifications are reviewed in Section 2.3.1 in detail.

1.3.4. Managing Uncertainty in Controllable Parameters - Type II Robust Design

The second form of uncertainty in a system model is uncertainty in controllable system variables, which are known as "*control factors*". Similar to noise factors, control factors are also in parametric forms that can be measured and characterized as continuous

numbers with or without probability distribution. Control factors are usually derived from the characterized parameters in system models that relate to system performances, including geometric information, mass, electrical, mechanical, or chemical inputs, amounts of constituents in materials, process control inputs, etc. Designers can determine the means of control factors; however, the deviations of control factors may not be controllable. Therefore, control factors should be characterized in a manner similar to noise factors. In order to design a system robust to the uncertainty in control factors, **Type II** robust design was proposed by Chen and coauthors (Chen, et al., 1996) as shown in Figure 1.8.

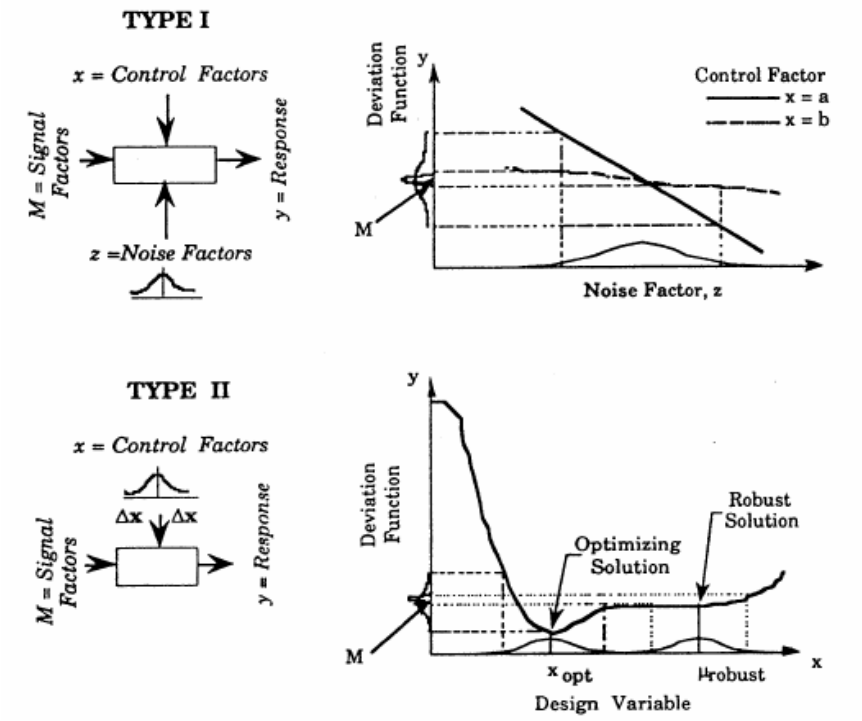

Figure 1.8 Robust design for variations in noise factors and control factors (Chen, et al., 1996)

- ***Type II Robust Design:*** Identify control factor (design variable) values that satisfy a set of performance requirement targets despite variation in control and noise factors.

Type II robust design is used to design systems that are robust to possible variations in system parameters as a design evolves. In **Type II** robust design, designers search for means of control factors that satisfy a set of performance requirement targets despite variation in control factors. A method combining **Types I** and **II** robust design in the early stages of product development, namely, the **R**obust **C**oncept **E**xploration **M**ethod (RCEM) (Chen, 1995) has been developed. RCEM is a domain-independent approach for generating robust, multidisciplinary design solutions. Robust solutions to multi-functional design problems are preference-weighted trade-offs between expected performance and sensitivity of performance due to deviations in design or uncontrollable variables. These solutions may not be absolute optima within the design space. By strategically employing experiment-based metamodels, some of the computational difficulties of performing probability-based robust design are alleviated. RCEM has been employed successfully for a simple structural problem and design of a solar powered irrigation system (Chen, 1995), a High Speed Civil Transport (Chen, et al., 1996), a General Aviation Aircraft (Simpson, et al., 1996), product platforms (Simpson, et al., 2001), and other applications (Chen, et al., 2001).

Increasingly, many researchers studied probabilistic approaches for the uncertainty analysis in which designers estimate the probability distribution of a system response from the probability distribution of input variances. The fundamental goal here is to reduce computational expenses while maintaining estimation accuracy by refining

uncertainty propagation methods. Traditional approaches, such as Monte Carlo Simulation and Latin Hypercube Sampling Techniques, are accurate but computationally expensive. On the other hand, First and Second Order Reliability Methods (FORM/SORM) do not require intensive computing power, but their accuracy is questionable. Recently, uncertainty propagation methods using stochastic variables in mathematical series forms, such as Polynomial Chaos Expansions (Kim, et al., 2004) and the Stochastic Response Surface Method (Isukapalli, et al., 1998), have been used to estimate relatively accurate probability distribution of a system response with reduced computational power. However, these techniques, with the exception of computationally expensive propagation techniques, are based on the assumption that the system model is deterministic. Inexpensive uncertainty propagation in a non-deterministic system model is still a challenging research issue.

In Section 1.3.3 and 1.3.4, **Type I** and **II** robust design approaches are discussed. These two approaches are methods for managing quantified uncertainty (i.e., variability) in input parameters (i.e., noise and control factors). However, as discussed in Sections 1.2.3 and 1.2.4, there are other sorts of uncertainties in multiscale materials design that cannot be managed by **Type I** and **II** robust design approaches. These are response variability due to random microstructure changes, uncertainties due to assumptions in models, and propagated uncertainty in multiscale simulation chains. **These uncertainties cannot be directly configured in parameters.** In order to manage these types of uncertainties in multiscale materials design, it is necessary to establish new types of robust design. We discuss this in the next section, identifying research questions in this dissertation.

1.4. NEW TYPES OF ROBUST DESIGN: RESEARCH QUESTIONS

Clearly, **Types I** and **II** robust design are necessary in the design of multidisciplinary engineering systems, including multiscale materials design. However, as discussed in the previous section, those two robust design approaches are not enough to manage all sorts of uncertainties mentioned in Sections 1.2.3 and 1.2.4. Since the uncertainty in material responses due to random microstructure changes cannot parameterized, this uncertainty cannot be represented in terms of variability in control and noise factors. Instead, this ***uncertainty is embedded in a simulation model (or function),*** not in parameters, and hence is considered 'non-deterministic'. This is also the case for the uncertainties due to assumptions and idealization. The ***propagated uncertainty in a chain of multiple simulations and analyses*** discussed in Section 1.2.4 is another main source of uncertainty in multiscale simulation-based design (such as multiscale materials design) and cannot be handled by the two types of robust design. To overcome this shortcoming, in this dissertation, the following primary research question is proposed.

> ***Primary Research Question****: How can we design complex engineered systems in the presence of uncertainties embodied in modeling of phenomena and in the design and analysis process chain?*

In order to decompose the primary research question into detailed research questions, we investigate the uncertainty embedded in a simulation model (or function) and the propagated uncertainty in a chain of analyses in further detail in the following two sections.

1.4.1. Managing Uncertainty Embedded in System Functions - Type III Robust Design

There are four sources of uncertainty that are associated with uncertainty embedded in system functions of an engineering design problem. Those are (a) non-parametric system noise, (b) un-configured system noise, (c) model parameter uncertainty, and (d) model structure uncertainty.

First, uncertainty of system functions may arise from "***non-parametric system noise***". Non-parametric system noise is the source of noise that is hard for designers to parameterize as numeric forms. If the system responses vary without the variance of noise factors or control factors, the system may include this type of uncertainty. The varieties of microstructure morphology in a SVE discussed in Section 1.2.4 is a good example. However, non-parametric system noise is difficult to represent numerically, resulting in a challenging issue in small scale system design.

Second, system functions could have ***"un-configured system noise"***. This un-configured system noise is similar to non-parametric system noise because the system response varies without input changes. However, in this case, the system has un-configured parameters that could have been parameterized as numeric forms, but were not because of limited knowledge of and/or data for the system. Since this uncertainty can be reduced by increasing the knowledge of the system, it is categorized as model structural uncertainty.

The third factor for the uncertainty embedded in system functions is ***"model parameter uncertainty,"*** which is due to a combination of limited data and non-parametric system noise (or un-configured system noise). For example, if a non-deterministic system analysis is computationally intensive or experimentally expensive,

then the limited data will result in uncertain parameters in metamodels (such as response surface models) of the system response. This is the typical type of uncertainty in materials design that employs computationally intensive models.

The final factor for the uncertainty embedded in a system model is ***"model structural uncertainty"*** that is due to assumptions and idealization in a system. For example, model structural uncertainty includes linearization and discretization errors in finite element analysis, errors in computer codes, employment of uncertain knowledge, and other assumptions due to limited information. The approximate constitutive model and 2-D idealization of the microscale shock simulation discussed in Section 1.2.4 are examples of this type of uncertainty.

We define four sources that incur the uncertainty embedded in a system model or function. The uncertainty embedded in a system model cannot be managed by previous robust design approaches (Type I and II). In order to manage this uncertainty, we propose new type of robust design approach, called **Type III** robust design.

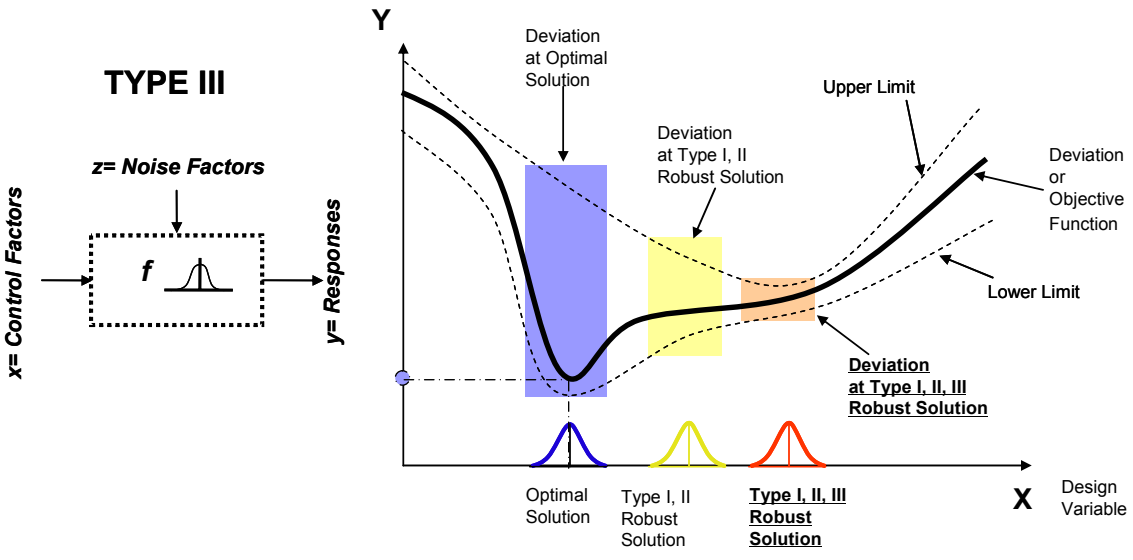

Figure 1.9 Type III robust Design

- ***Type III Robust Design*:** Identify adjustable ranges for control factors (design variable), that satisfy a set of performance requirement targets and/or performance requirement ranges and are insensitive to the variability within the model. For example, in materials design, it is common practice to analyze a representative statistical volume element that specifies a microstructure distribution. As discussed in Section 1.2.4, repeated analyses of various SVEs with identical inputs yield variability in performance at the SVE scale.

Type III Robust Design is illustrated in Figure 1.9. In the figure, the same objective function curve is employed to show the differences among the optimal solution, Type I and II robust solution, and Type I, II and III robust solution. A deviation (or objective) function, which represents the system's response, is illustrated as a solid curve. In addition, two dotted curves are added around the objective function, representing uncertainty limits, which is due to the non-parametric variability, un-configured variability, and model parameter uncertainty as mentioned above. Considering not only the objective function but also the two uncertainty limits, the optimal and Type I and II robust solution have larger performance deviations than the Type I, II, and III robust solution.

Type III robust design becomes more important since modern engineering systems are getting more and more complex (or extremely small) and their behaviors are stochastic. Compared to Type I and II robust design, the **Type III** robust design has not been studied rigorously in engineering systems design. The absence of the studies is due to the ignorance of this uncertainty in most of traditional engineering systems design

problems or the difficulties in quantifying and incorporating this uncertainty into a design exploration process. Hence, the first research question is posted here.

> ***Research Question 1****: How can we get a ranged set of design specifications that are robust to the uncertainty embedded in a model?*

Research Question 1 is based upon the assumption that quantified uncertainty bounds in a model in terms of design variables are available; therefore, the unquantifiable uncertainty (e.g., model structure uncertainty) cannot be addressed by the answer to Research Question 1. It will be addressed in Research Question 4.

For **Type III** robust design, it is required to build error bounds (uncertainty bounds) in a model in a computationally inexpensive manner. The most accurate way to incorporate the embedded uncertainties as well as the uncertainty in control and noise factors during design exploration is to perform actual simulation using statistical techniques (simulation-based design). Monte Carlo Simulation is a popular method to measure variations of performance by simulating input variations (uncertainty analysis). Du and coauthors employed this approach for a relatively simple problem (Du and Chen, 2000). Even though this approach could produce accurate results in design exploration, it requires a large number of experiments (more than 10,000 in many cases) for uncertainty analysis even in a single evaluation during a design exploration process. However, most of our applications – material performance analyses – need intensive computing power (from half an hour to several days for a single simulation run). It is nearly impossible to employ this approach in materials design exploration even if we apply a sampling technique, such as Latin Hypercube sampling, to reduce number of experiments. We

need a computationally inexpensive uncertainty analysis method to solve this problem. Therefore, a subsequent research question arises.

> ***Research Question 2:*** *How can we estimate the amount of variability in the response of a non-deterministic model with variability in input variables in a computationally efficient manner?*

In this section, we defined Type III robust design and research questions. In the next section, we discuss our strategy for managing propagated uncertainty in a design/analysis process chain.

1.4.2. Managing Propagated Uncertainty in a Design and Analysis Process Chain - Type IV Robust Design

The final type of uncertainty in a complex system model is that generated in the design and analysis process chain, which, unlike the aforementioned uncertainties in a system model, arises from the complex design and analysis process chain and not from the system model itself. This type of uncertainty is dominant in multidisciplinary uncertain system design problems, such as Multidisciplinary Design Optimization (MDO), etc., and includes ***errors in decisions made by other designers*** **and** ***accumulated errors*** (propagated uncertainty) by subsequent series of uncertain subsystem models.

Typically, complex multidisciplinary system design requires multiple experts to collaborate to make decisions for designing a system. The outputs of other experts' decisions in a subsystem could be input parameters, constraints, or design spaces of other subsystems or systems design. In many cases, multiple subsystem designs even share common design variables. In these interactions in design activity, a subsystem design error can be propagated to another subsystem or system. Additionally, complex systems

design tends to employ multiple analyses and simulations in a series to predict system responses.

For example, materials design employs multiple steps of analyses or simulations to predict material performance - from processing to material structure, material structure to material property, and material property to material performance (Olson, 1997). In addition, hierarchical multi-time and length scale models are employed to predict material performance. For example, predicting exothermic reaction characteristics of energetic materials based on multiscale simulation models discussed in Section 1.1.2, designers employ the microscale shock simulation model for determining mechanical properties, interfacing with the chemical reaction model (ab initio model) for analyzing reaction initiation in infinitesimal local hot spots between micro-size discrete fuel constituents. In this case, reaction criteria generated by the chemical reaction model serves as input parameters for microscale shock simulation.

- ***Type IV Robust Design*:** Identify adjustable ranges of control factor (design variable) values under potential uncertainty and uncertainty propagation in a design and analysis process chain; account for uncertainty in downstream activities and uncertainty propagation.

Type IV robust design is focused on uncertainty associated with the design process chain as shown in Figure 1.10. Design process uncertainty emanates from: (a) changes in design specifications as a result of downstream or concurrent decisions and design activities or (b) the propagation and potential amplification of uncertainty due to the combined effect of analysis tasks performed in series or in parallel. Both sources of design process uncertainty are common and important for multidisciplinary design and

analysis, including multiscale, multi-physics materials design, with a plethora of shared or coupled variables and analyses performed on multiple length and time scales. The information dependency in multiscale models engenders complex design process chains – hierarchical, parallel, and serial design processes.

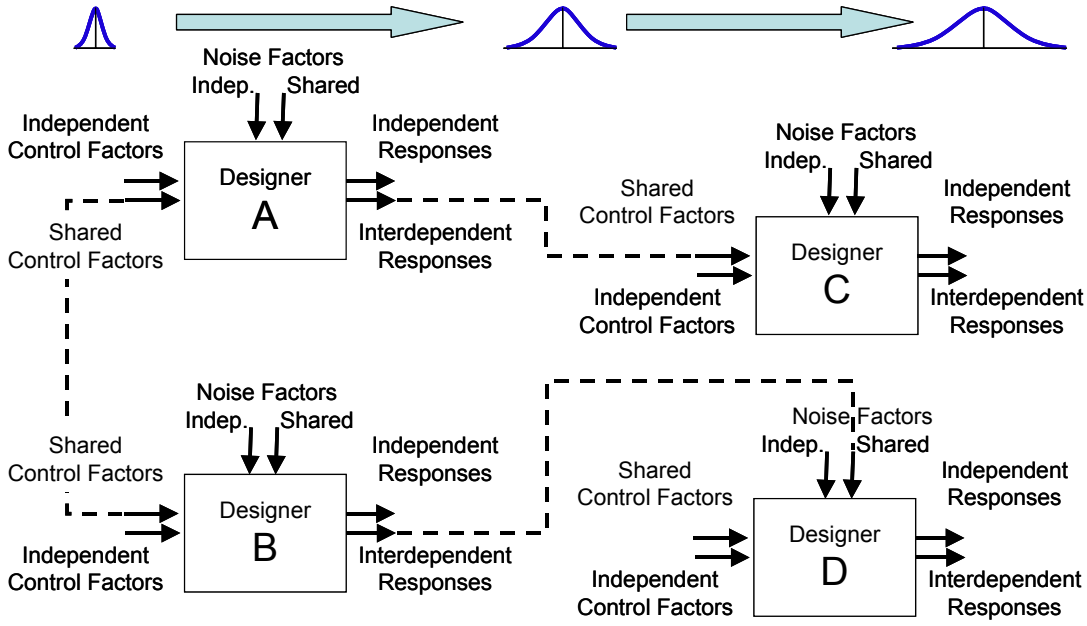

Figure 1.10 Type IV robust design

In complex design processes, the output of a given design (or analysis) task could provide input to subsequent tasks, increasing or decreasing the amount of uncertainty in the system via interdependent variables and parameters, as shown in Figure 1.10. Sometimes, a small deviation in an input variable can produce large variation in the final performance at the end of the design task network. For this reason, it is necessary to represent the amount of uncertainty propagating within a design process chain in a graphical manner so that engineers or designers can easily identify which design tasks

significantly increase the uncertainty of the whole system. This challenge leads us to the third research question.

> ***Research Question 3:*** *How can we represent complex multidisciplinary robust design process chains and their associated uncertainties in a way that is easily identifiable to designers?*

Probabilistic and robust design techniques are being infused into a number of multidisciplinary design optimization (MDO) approaches that have been proposed for formulating and concurrently solving decomposed or partitioned complex system design problems. Categories of MDO methods include: (1) single level optimization approaches in which analyses are distributed and independently executed while a single optimizer is used to evaluate the results (e.g., simultaneous analysis and design (Haftka, 1985)), and (2) multi-level optimization approaches in which analyses are distributed and subsystems are optimized by subsystem-level and system-level optimizers (e.g., concurrent sub-space optimization (Sobieszczanski-Sobieski, 1988; Wujek, et al., 1996) or collaborative optimization (Kroo, et al., 1994)). Comprehensive reviews of MDO approaches are available in the literature (e.g., (Lewis and Mistree, 1998; Sobieszczanski-Sobieski and Haftka, 1997)) and are not repeated here.

A few authors have focused on considering probabilistic as well as deterministic variables and parameters in an MDO context (Du and Chen, 2002; Gu and Renaud, 2001). Other authors have focused on replacing complex, computationally-intensive analysis routines with approximate models (Giunta, et al., 1997; Koch, et al., 1999; Mavris, et al., 1999). While approximate models ease the computational burdens of MDO, they can be inaccurate or inefficient if the responses are highly nonlinear or governed by a large

number of parameters. MDO approaches are fundamentally limited in a distributed design environment in which it is desirable to distribute *synthesis* activities in order to (1) leverage the extensive domain-specific knowledge and expertise of various design stakeholders and (2) avoid solving integrated system-level synthesis or analysis problems that are enormously large and computationally intractable. If decision-making is distributed fully among multiple designers who make decisions independently of one another, the difficulty lies in managing interdependencies among the decisions when any single designer cannot exert global control.

In game theoretic approaches, protocols (e.g., cooperation, non-cooperation, and Stackelberg leader/follower) and mathematical coordination mechanisms—such as rational reaction sets or best reply correspondences—are used to model and incorporate interactions among designers or design teams and their associated analysis and synthesis tools. For complex systems, best reply correspondences are typically based on approximate models that fall prey to accuracy and efficiency issues.

Using the preceding approaches we cannot design process chains for design that spans scales and where uncertainty is embedded in the engineering models and also propagated along the design process chain. For this reason, the final research question arises.

> ***Research Question 4:*** *How can we achieve robustness in designing a multi-disciplinary complex system in which uncertainty is propagated and expanded by exchanging uncertain information between subsystem models in a design and analysis process chain?*

In this section, two new ideas for robust design, **Type III** and **Type IV**, are proposed based on the requirements to facilitate multiscale simulation-based robust design that

respectively emphasizes uncertainty embedded in a model and uncertainty that is propagated along a design and analysis process chain. In the next section, we summarize the requirements in multiscale simulation-based design and research questions. Hypotheses regarding on the research questions are formulated and discussed.

1.4.3. Research Questions and Hypotheses

In this section, we summarize the challenges in multiscale simulation-based design discussed in Section 1.2 and the research questions that have been developed in Section 1.4. The hypotheses for the research questions are posted and discussed. In Table 1.1, the requirements, research questions, and corresponding hypotheses are listed. As outlined in the table, the primary hypothesis and the decomposed hypotheses are formulated from the research questions.

As mentioned in the hypothesis for the primary research question, in this dissertation research, **we establish a design methodology that facilitates Type III and IV robust design as well as Type I and II in order to support multiscale simulation-based design.** The Type III and IV robust design methods allows designers (or design teams) to maintain or maximize their design freedom to achieve robustness in their final solution against uncertainties embodied in simulation models (Type III) and the propagated uncertainties along a design and analysis process chain (Type IV).

Table 1.1 From requirements of materials design to research questions

Challenges in Multiscale Simulation-based Materials Design in Section 1.2	Research Questions posted in Section 1.4	Hypotheses
Collaborative Decision-Based Design ▪ Design and analysis process chain ▪ Multidisciplinary system models ▪ Multi-objective applications ***Collaborative Computational Infrastructure*** ▪ Information and knowledge hierarchy ▪ Distributed heterogeneous computing environment ***Management of Uncertainty*** ▪ Non-deterministic simulations and analyses ▪ Simplifying assumptions and idealization in simulation and analysis models ▪ Limited data due to intensive computation and expensive experiment ▪ Propagated uncertainty in a design and analysis process chain	***Primary Research Question:*** How can we design complex engineered systems in the presence of uncertainties embodied in modeling of phenomena and in the design and analysis process chain?	***Hypothesis for the Primary Research Question.*** The development of Type III and IV robust design will allow a designer (design team) to maximize ranges of values for design variables and maintain the bound of performance parameters in infeasible ranges considering uncertainties embodied in models and process chains.
	Research Question 1 How can we get a ranged set of design specifications that are robust to the uncertainty embedded in a model?	***Hypothesis 1*** The Robust Concept Exploration Method with Error Margin Indices, a method for Type III robust design, provides an effective and efficient mathematical construct to find robust solution range under uncertainty embodied in a model, in which Error Margin Indices are metrics of available margin for potential errors due to uncertainty in models.
	Research Question 2 How can we estimate the amount of variability in the response of a non-deterministic model with variability in input variables in a computationally efficient manner?	***Hypothesis 2*** Increased uncertainty due to reducing experimental expenses is inevitable; however, we can formulate the bounds of model uncertainty based on mean response and prediction interval approach for later use in robust design exploration.
	Research Question 3 How can we effectively represent complex multidisciplinary robust design process chains and their associated uncertainties in a way that is easily identifiable to designers?	***Hypothesis 3*** A graphical robust design process model associated with Error Margin Indices is an effective protocol for designers to identify a complex robust design process chain.
	Research Question 4 How can we achieve robustness in designing a multi-disciplinary complex system where in which uncertainty is propagated and expanded by exchanging uncertain information between subsystem models in a design and analysis process chain?	***Hypothesis 4*** The Inductive Design Exploration Method for Type IV robust design provides an effective mean to find robust multiple ranged sets of design specifications in an inductive manner in a distributed, multidisciplinary systems design problem.

Hypothesis 2: Increased uncertainty due to reducing experimental expenses is inevitable; however, we can formulate the bounds of model uncertainty based on mean response and prediction interval approach for later use in robust design exploration.

In Hypothesis 2, the integrated mean response and prediction interval estimation approach is proposed to capture statistical variations of a response surface model. Hypothesis 2 should be accomplished and validated before proceeding to Hypothesis 1. The main objective of using the techniques is to statistically quantify variability limits in system response with some confidence level, such as confidence or prediction interval of a response surface model, or to measure variability by duplicated sampling in each experimental point and to build a metamodel for the variability itself as well as one for mean system response. The main point of the technique should remain applicable to computationally intensive simulation models; that is, the techniques should be able to capture an appropriate amount of uncertainty even if available data are limited. The predicted error bounds in system response are leveraged robust design exploration method that is established in Hypothesis 1.

Hypothesis 1: The Robust Concept Exploration Method with Error Margin Indices, a method for Type III robust design, provides an effective and efficient mathematical construct to find robust solution range under uncertainty embodied in a model, in which Error Margin Indices are metrics of available margin for potential errors due to uncertainty in models.

In Hypothesis 1, the Robust Concept Exploration Method with Error Margin Indices (RCEM-EMI) is proposed as a design method for facilitating Type I ~ III robust design. Current robust design methods have focused on Type I and II robust design. However, the robust design method for multiscale simulation-based design should support Type I ~ IV. The RCEM-EMI provides a framework for designers to obtain a ranged set of design specifications that are robust against uncertainties in simulation models as well as uncertainty in controllable and uncontrollable variables. In this framework, a mathematical construct (Error Margin Index), which represents the amount of uncertainty in a design decision, is established for effective design solution search. The compromise Decision Support Problem (cDSP) (Mistree, et al., 1992) leveraging EMI is employed to search design specifications of complex (multi-objective) systems, which are the most cases of multiscale simulation-based design, such as MESM design.

Hypothesis 3: A graphical robust design process model associated with Error Margin Indices is an effective protocol for designers to identify a complex robust design process chain.

In Hypothesis 3, graphical representation of a robust design process based on multiscale simulations and analysis is proposed. Designers should easily identify the robust design solution process in a complex design process. Identifying information dependencies among multiple designers in the design process, uncertainty propagation along a design and analysis chain, and associated uncertainty in decision making points is very important. A graphical protocol of robust design process showing all above information would be the most effective way to represent this information. As

Hypothesis 2 is a basis for accomplishing Hypothesis 1, Hypothesis 3 is a basis for identifying a set of robust design specification employing multiscale simulation and analysis models. Traditional approaches for representing a design process are actually bottom-up (deductive) analysis and simulation processes. In Hypothesis 3, we propose to graphically show a design process, which is a top-down (inductive) approach, incorporating determined design specifications and uncertainty associated with the design decision.

Hypothesis 4: The Inductive Design Exploration Method for Type IV robust design provides an effective mean to find robust multiple ranged sets of design specifications in an inductive manner in a distributed, multidisciplinary systems design problem.

In Hypothesis 4, the Inductive Design Exploration Method is proposed to support obtaining a ranged set of design specifications in a design and analysis process chain. The method supports searching for feasible design specifications based on the design process set up by the graphical protocol proposed in Hypothesis 3. The main objective of robust design of complex, multidisciplinary system is that the final predicted system performance should be still satisfied under the accumulated uncertainty (or variability) in the prediction along a design and analysis process chain. In a multidisciplinary robust design approach, the cost of uncertainty propagation for final performance deviation is very high since the number of associated random variables is large and the interfacing between the multidisciplinary systems is very difficult. Therefore, in Hypothesis 4, the method to pass ranged sets of design specifications to other disciplinary systems instead of passing uncertainty analysis information, which will significantly reduce information transfer traffic between multidisciplinary subsystems. Moreover, the Inductive Design

Exploration Method is a goal-oriented search algorithm which reduces design iteration that is often required in the bottom-up exploration approach. For computationally intensive simulation-based design, the Inductive Design Exploration Method will provide significant benefits to save design lead time.

1.5. OVERVIEW AND VALIDATION STRATEGY FOR THIS DISSERTATION

Engineering design is primarily concerned with open problems that involve objective and subjective elements and no single right answer. As Pedersen and coauthors (Pedersen and Emblemsvag, 2000) indicate, there is no single right answer in software design and development because a software framework supporting engineering activity is an engineering system itself. Most of all, subjective elements could be involved to decide the initial design stage of framework implementation. The validation or verification of a method and a result is necessary since a development of a method includes many subjective elements and there is no single right answer.

Pederson and coauthors propose a method called 'Validation Square' with which a researcher can build confidence in the utility of methods and examples with respect to a purpose. Their proposal is associated with whether the method provides design solutions correctly (structural validity) and whether it provides correct design solutions (performance validity). This process of validation is represented in the Validation Square as shown in Figure 1.11.

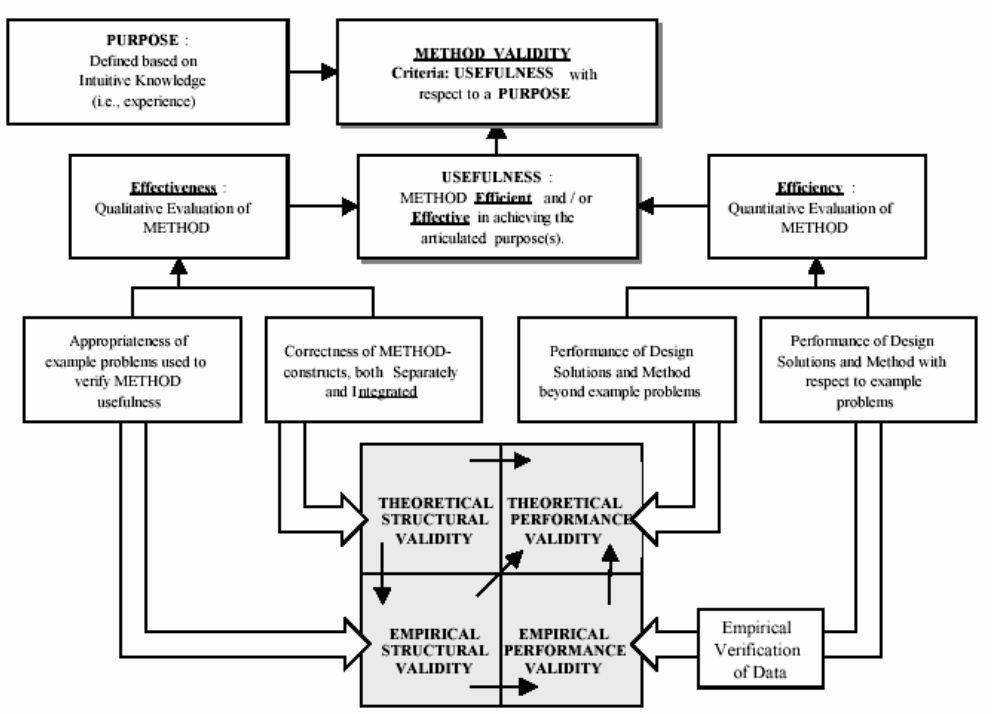

Figure 1.11 Validation square (Pedersen and Emblemsvag, 2000)

Accepting theoretical structural validation means accepting the individual structural/ logical validity as well as accepting overall consistency of the assembly of constructs. Empirical structural validation includes building confidence in the soundness of the example problems to illustrate and verify a suggested design method. Empirical performance validation can be used to build confidence in the utility of a method for the example problems and case studies. Theoretical performance validation includes building confidence in the generality of the method and accepting that the method can be useful for others beyond the example problems. In this dissertation, the validation square is adopted as a guide line for validating the Type III and IV robust design methods. The following tasks are planned for the validation and summarized in Figure 1.12.

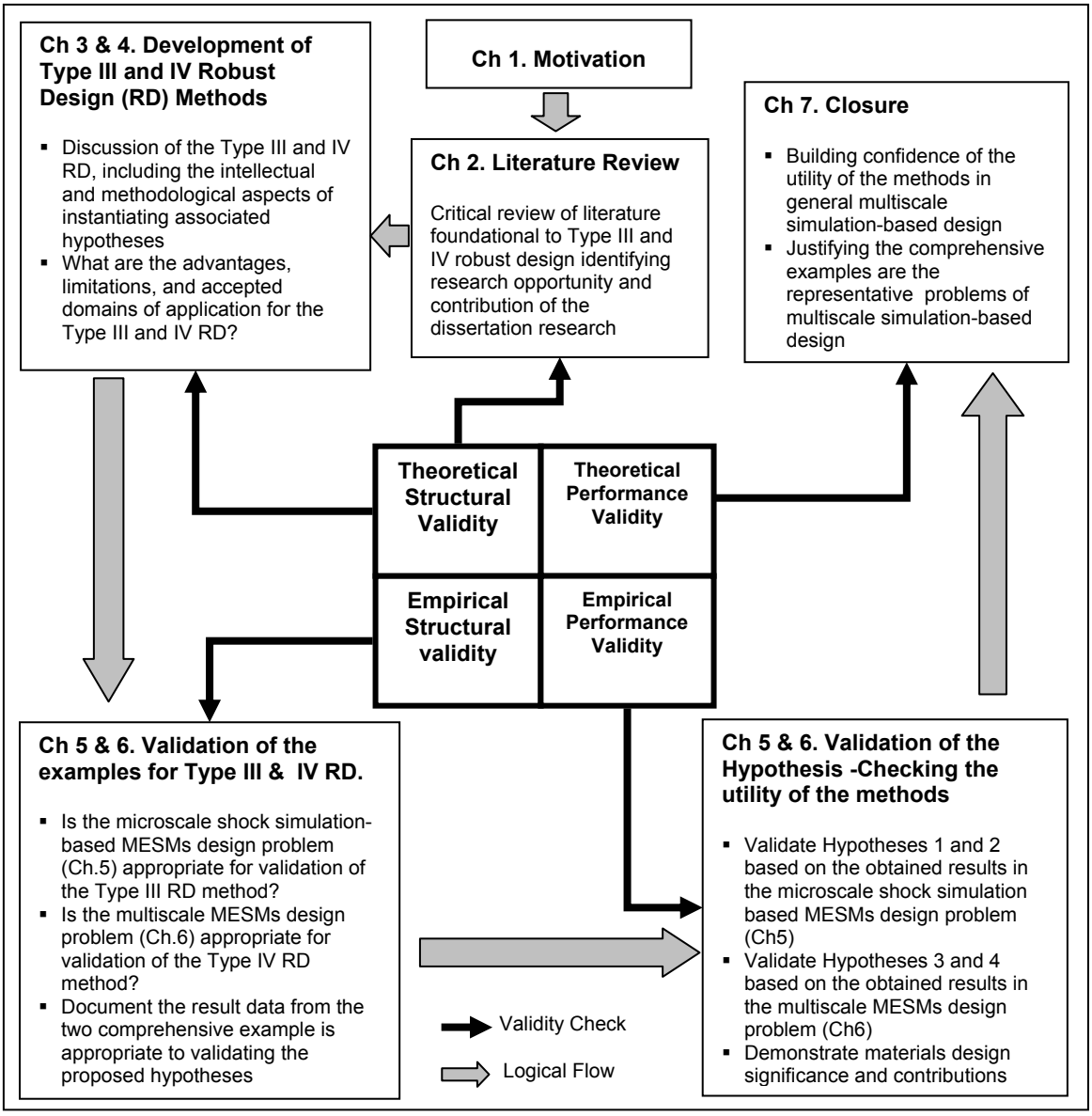

Figure 1.12 Validation strategy of the dissertation

Tasks for checking Theoretical Structural Validation

- Critically review the relevant literature and identify research opportunities. (Chapter. 2)
- Justify that the four hypotheses are logically formulated to appropriately cover the research opportunities. (Chapter. 2)

- Discuss the developed Type III and IV robust design methods are well constructed to instantiate the hypotheses in intellectual and methodological aspects. (Chapter 3 and 4)
- Identify merits, limitations, application domains for the developed Type III and IV robust design methods. (Ch 3 and 4)

Tasks for checking Empirical Structural Validation

- Discuss the challenging aspects of the comprehensive example, microscale discrete particle shock simulation, for Type III robust design and argue that the aspects are appropriate to test Hypotheses 1 and 2. (Chapter. 5)
- Discuss the challenging aspects of the comprehensive example, multiscale simulation-based MESM design, for Type IV robust design and argue that the aspects are appropriate to validate Hypotheses 3 and 4. (Chapter. 6)
- Document the result data are appropriate for testing the hypothesis

Tasks for checking Empirical Performances Validation

- Validate Hypotheses 1 and 2 based on the obtained results in the microscale discrete particle shock simulation. (Chapter 5)
- Validate Hypotheses 3 and 4 based on the obtained results in the multiscale simulation-based MESM design problem. (Chapter 6)

Tasks for checking Theoretical Performances Validation

- Discuss that the hypotheses in this dissertation are also valid for general multiscale simulation-based design problems. (Chapter 7)
- Argue that the comprehensive examples represent the challenging aspect of the general multiscale simulation-based design problems. (Chapter 7)

The dissertation is organized as shown in Figure 1.13.

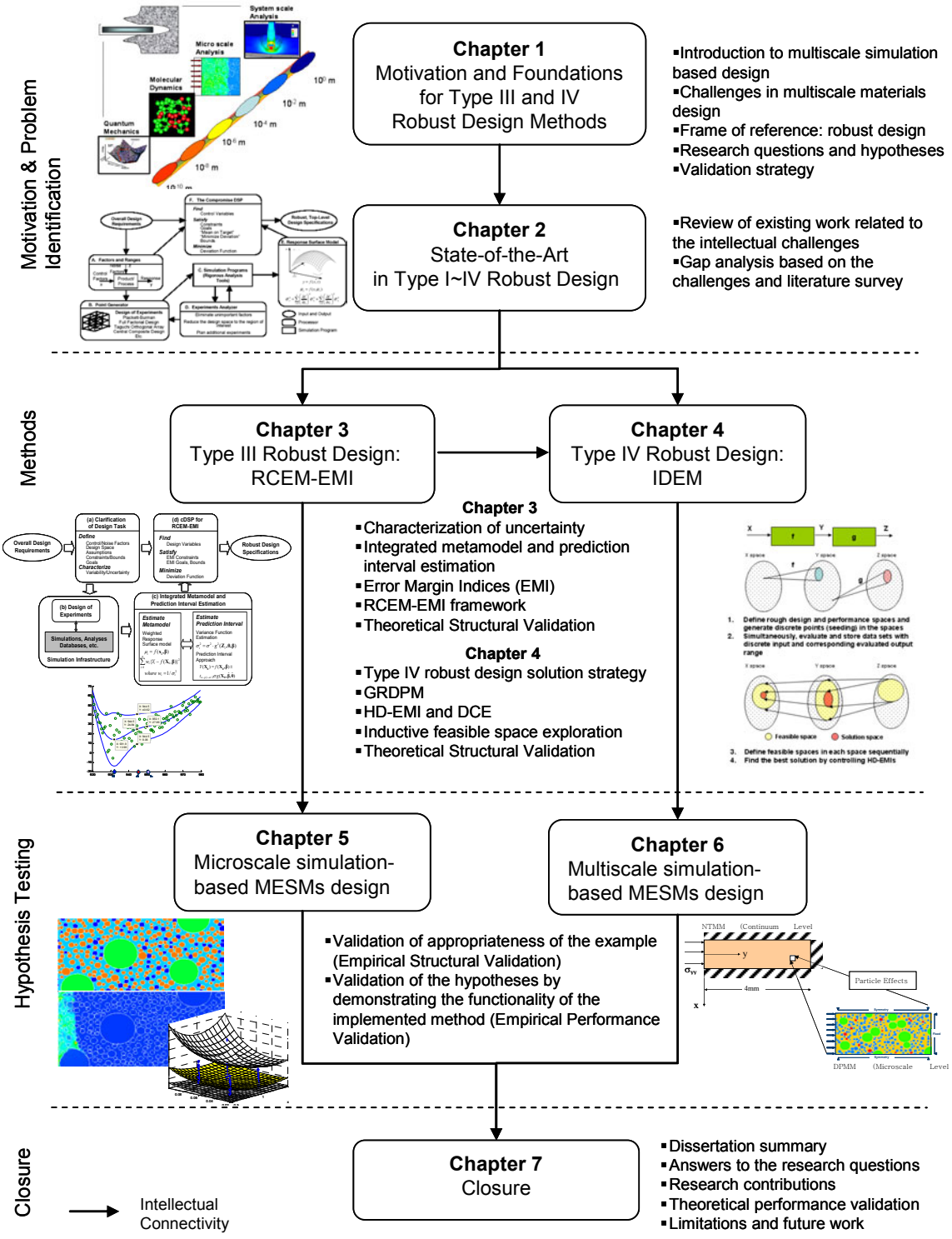

Figure 1.13 A Dissertation overview and roadmap

In Chapter 1, the motivations and foundations are discussed for Type III and IV robust design methods. The principal goal is introduced along with the research questions and hypotheses. The expected contributions are summarized, and a validation strategy is established for the dissertation.

In Chapter 2, the theoretical foundations for the Type III and IV robust design methods are introduced and discussed. Those foundations include uncertainty characterization and quantification, robust design, and multidisciplinary robust design. For theoretical structural validation, relevant literature in each of these research areas is referenced, discussed, and critically evaluated. The purpose is to discuss the availability, strengths, and limitations of methods and constructs that are foundational for Type III and IV robust design methods and to identify research opportunities addressed in this dissertation.

In Chapter 3, the Robust Concept Exploration Method with Error Margin Indices (RCEM-EMI) is proposed as a method for Type III robust design. The Type III robust design is clearly defined and the problem scope that Type III robust design can cover is also defined. The types of uncertainty in materials design are categorized and a strategy for uncertainty quantification is discussed. The goals and overview of the RCEM-EMI are provided. Each step of the RCEM-EMI is discussed in detail. The conceptual and mathematical definitions of Error Margin Indices are provided. The Theoretical Structural Validation of the RCEM-EMI is checked providing advantages, limitations, and applications of the method based on Hypotheses 1 and 2 proposed in Chapter 1.

In Chapter 4, the Inductive Design Exploration Method (IDEM) is proposed as a method for Type IV robust design. Similar to the structure of the Chapter 3, the Type IV

robust design is clearly defined and the problem scope that Type IV robust design can cover is also defined. A graphical representation protocol for the IDEM is presented and discussed in detail. The relationship between the RCEM-EMI and the IDEM and the techniques in the RCEM-EMI that can be used in the IDEM are discussed. The goals and overview of the IDEM are provided. Each step of the IDEM is discussed in detail. Each step of the RCEM-EMI is discussed in detail. The conceptual and mathematical definitions of Hyper Dimensional EMI are provided. The procedure of Discrete Constraints Evaluation (DCE) is provided in detail. The Theoretical Structural Validation of the IDEM is checked providing advantages, limitations, and applications of the method based on Hypotheses 3 and 4 proposed in Chapter 1.

In Chapter 5, a microscale discrete particle shock simulation-based MESM design is presented as an example for demonstrating the effectiveness of the RCEM-EMI (a method for Type III robust design). For the Empirical Structural validity check, the capabilities, limitations, assumptions, and uncertainties associated with the simulation are discussed showing that the example is appropriate for validating the utility of the RCEM-EMI. Each step of the RCEM-EMI is followed in this application. Clarifying the tasks for robust MESM design, the main objectives and constraints of the design problem are identified and formulated. Design of experiments (DOE) for sampling of the simulation data is performed and discussed. Response Surface Methodology is employed to construct mathematical model instead of computational model and the justification of using metamodels is provided. Uncertainty characterization and quantification process for the shock simulation is followed by the building a response surface model. The compromise Decision Support Problem (cDSP) is formulated to find the best solution

considering uncertainty in a model and its parameters (the solution of Type I, II, and III robust design). Finally, we validate Hypotheses 1 and 2 based on the results of this design problem for Empirical Performance Validation.

In Chapter 6, designing MESM with multiscale simulation models is employed to demonstrate the effectiveness of the IDEM (a method for Type IV robust design). Simulation and analysis models involved in this example are discussed in detail. The capabilities of the models and uncertainties associated with multiscale models are discussed. Their interaction, mapping input and output among multiscale models, are provided justifying that the multiscale simulation-based MESM design is an appropriate example for validating the IDEM. The IDEM for designing robust MESM starts with formulating inverse design process, passing ranged set of specifications from the final performance requirement to the initial design space. The formulation is represented based on the graphical entities developed in Chapter 4. The multiscale simulation-based MESM design tasks in the IDEM are overviewed. Each of the tasks is discussed in detail in subsequent sections. Finally, we validate Hypotheses 3 and 4 based on the graphical presentation of the design process and the design results obtained by the IDEM, respectively for the Empirical Performance Validation.

In Chapter 7, the research questions proposed in this dissertation are answered by summarizing the validation results of the hypotheses. Research contributions and achievements are discussed. The critical evaluation of the dissertation research and necessary future works are provided. We take a leap of faith in our accomplishments, arguing that the MESM design example is representative of general multiscale simulation-based design problems.

1.6. SYNOPSIS OF CHAPTER 1

In this chapter, a new paradigm for multiscale simulation-based design is introduced. Multiscale simulation-based materials design is one of the promising areas for tailoring materials for specific needs. Multiscale simulation-based MESM design is introduced in Section 1.1 followed by uncertainties in the simulation and their effect on the system based design of materials. As discussed in Section 1.2, in the perspective of systems based design, uncertainties in multiscale simulation and analyses are managed by either reducing uncertainty or developing systems, including material systems, robust to uncertainty. In Section 1.3, the scope of this dissertation is designing systems to be robust to the uncertainty. Previous robust design methods, Type I and II robust design, have been introduced; however, we identified the types of uncertainties that cannot be addressed by the previous robust design approaches in multiscale simulation-based materials design. In Section 1.4, the research questions and corresponding hypotheses are established. Establishing the research questions, two new types of robust design, Type III and IV robust design, are defined for multiscale simulation-based robust design. As discussed in Section 1.4.1, Type III robust design is identifying of means of control variables that satisfy a set of performance requirement targets despite uncertain system functions. On the other hand, as discussed in Section 1.4.2, Type IV robust design is focused on uncertainty associated with the design process. This type of uncertainty emanates from the propagation and potential amplification of uncertainty due to the combined effect of analysis tasks performed in series or in parallel. The research questions and hypotheses are summarized in Table 1.1. In Section 1.5, a strategy for validating proposed hypothesis with multiscale materials design examples is discussed.

The validation square roadmap shown in Figure 1.12 is used as a guideline for validating the methods in this dissertation. Finally, the structure of this dissertation is also discussed in Section 1.5 and illustrated in Figure 1.13. This chapter is frequently revisited in other chapters in order to evaluate the structural soundness of the dissertation.

In Chapter 1, research questions and hypotheses are identified based on the perspective of the multiscale simulation-based robust design paradigm and brief reviews of previous approaches. In the next chapter, in order to validate the contributions of these proposed works, we critically review existing literature related to uncertainty, robust design, multidisciplinary systems design, and information modeling that are related to the four research questions identified in this chapter.

CHAPTER 2

LITERATURE REVIEW AND JUSTIFICATION OF RESEARCH QUESTIONS

Main issues in robust design methodology are (1) uncertainty characterization and quantification, (2) robust design under uncertainty, (3) robust design for multidisciplinary uncertain systems, and (4) semantic models for representing a multidisciplinary design process. Each of these issues has been studied rigorously. In this chapter, we review the literature related with these issues and find research opportunities for justifying the research questions discussed in Chapter 1.

In Section 2.1, work related to uncertainty characterization and definition is reviewed. In Section 2.2, methods for quantifying uncertainty are discussed in detail. In Section 2.3, methods for robust decision making based on quantified uncertainty are reviewed. In Section 2.4, robust decision making methods in multidisciplinary systems design, an emerging area in robust design, are discussed. In Section 2.5, semantic models for representing a multidisciplinary collaborative design process are discussed. In each section, challenging issues are addressed in developing the approaches. Finally, in Section 2.6, we analyze gaps among the existing methods and post requirements of new robust design methods in order to justify the research questions in Chapter 1.

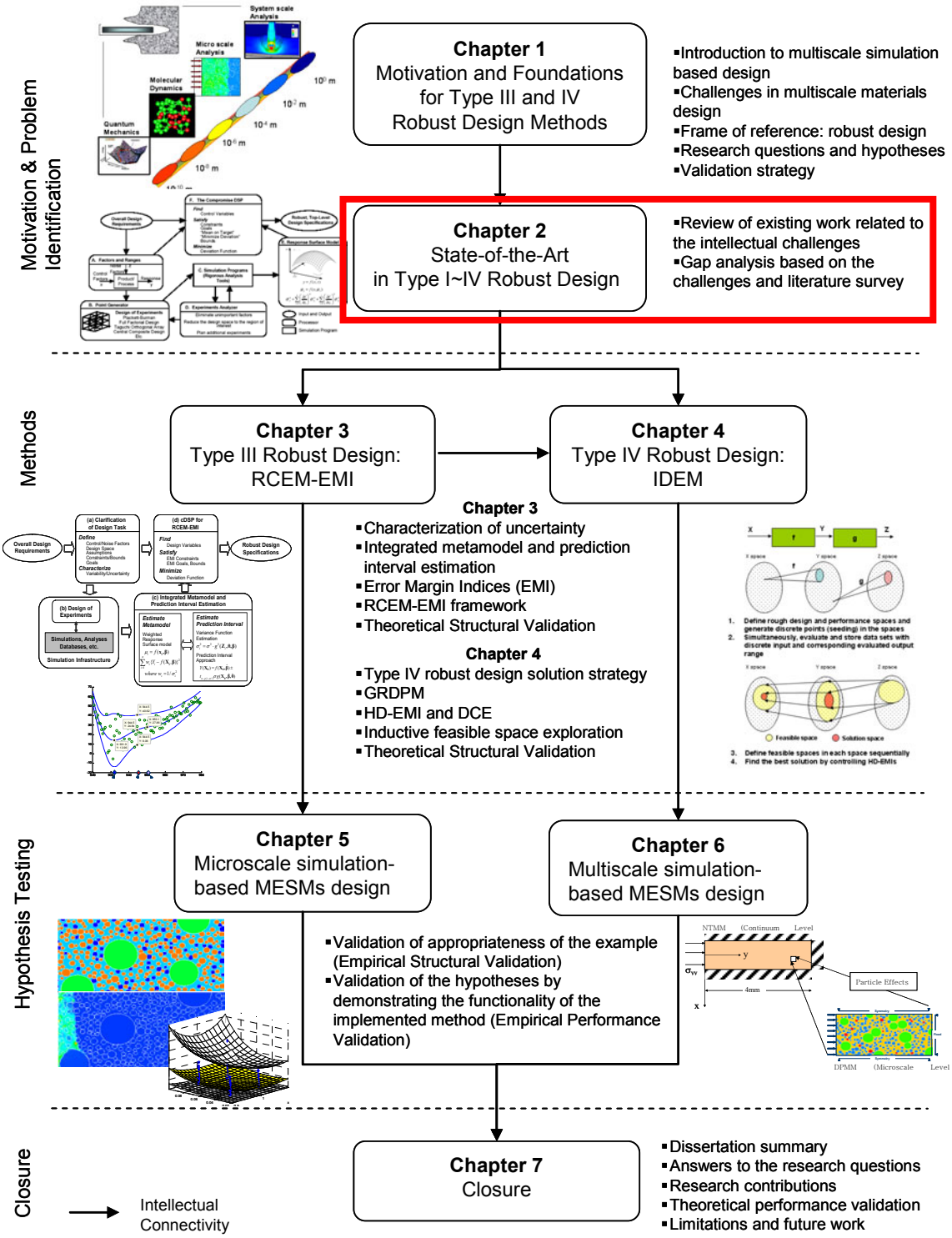

Figure 2.1 Roadmap of this dissertation

2.1. TYPES OF UNCERTAINTY IN DESIGN DECISION MAKING

There are two approaches to classify the types of uncertainty. One is classification according to the nature of uncertainty by Ayyunb and Klir (Ayyub and Chao, 1997), and the other is the source of uncertainty by Der Kiruregian and others (Klir and Yuan, 1995).

2.1.1. Classification by the Nature of Uncertainty

In this section, the classification of uncertainties according to its cause and type of deficiency in available information is discussed.

Classification by Ayyub (Ayyub and Chao, 1997)

Ayyub and coauthors classify uncertainty as either objective or subjective. Objective type of uncertainty (ambiguity) includes physical, statistical, and modeling sources of uncertainty, etc. Subjective type of uncertainty (vagueness) includes expert-based assessment, human error, etc. The ambiguity components in objective type uncertainty are generally due to non-cognitive sources that include: 1) physical randomness; 2) statistical uncertainty due to the use of sampled information to estimate the characteristics of model response; 3) lack of knowledge; and 4) modeling uncertainty that is due to simplifying assumptions of real performances. Vagueness-related uncertainty is due to cognitive sources that include: 1) the definition of certain parameters; 2) other human factors; and 3) defining the inter-relationships among the parameters of problems, especially for complex systems. Other sources of uncertainty can include 1) conflict in information, and 2) human and organizational errors.

- Objective type -> Ambiguity (probability can be analyzed) -> Non-Cognitive Uncertainty Type -> Random analysis approach
- Subjective type -> Vagueness (probability cannot be easily analyzed) -> Cognitive Uncertainty type -> Fuzzy analysis approach
- Or two approach can be combined -> Fuzzy-random analysis approach

Analysis of systems commonly starts with a definition of the system that can be viewed as an abstraction of the real system. The abstraction is performed at different epistemological levels as shown in Figure 2.2. The resulting model can depend largely on an analyst or engineer. During the process of abstraction, the engineer needs to make decisions regarding what aspects should or should not be included in the model.

Classification by Klir and Yuan (Klir and Yuan, 1995)

Klir and Yuan categorize uncertainty on the basis of the type of deficiency in the available information, into vagueness (fuzziness) and ambiguity. They further divided ambiguity into conflict and nonspecificity. Conflict causes a given action to result in different outcomes or conflicting evidence (three experts provide different estimates of the error in the estimate of the stress in a structure). Nonspecificity occurs when multiple outcomes of an action are left unspecified. Measurements from observations of repeated experiments are often precise but are in conflict. Subjective information from experts is often nonspecific. For example, if we ask an expert for a subjective estimate of the difference between the true value of the stress in a structural component and a predicted value of the stress obtained from a finite element model, the expert would estimate a range of differences rather than a precise value. The less confidence the expert feels about the estimation of the difference, the expert will expect the broader range.

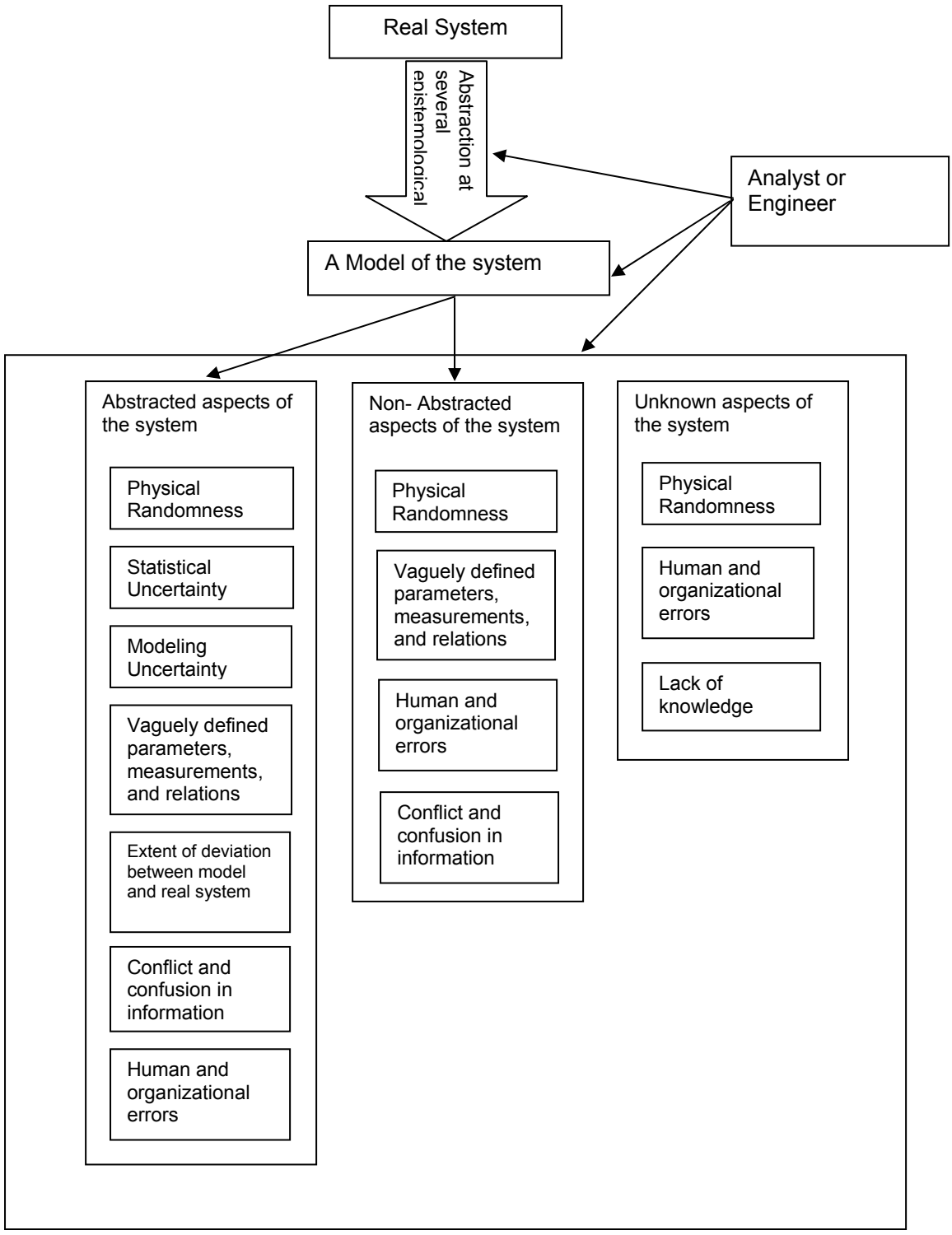

Figure 2.2 Uncertainty types and their relations to real and abstracted systems (Ayyub and Chao, 1997)

2.1.2. Classification by the Source of uncertainty

Uncertainty is often classified as either *Aleatory* (irreducible) or *Epistemic* (reducible) based on the causes of the uncertainty. *Epistemic* uncertainty can be diminished by improvements in measurements and/or model formulation and/or by increasing the accuracy or sample size of data. *Aleatory* uncertainty, on the other hand, is inherent in the physical system and can only be quantified in a statistical sense. In this section, the types of uncertainty that researchers classified according to those different sources of uncertainty are discussed. The summary of the classifications defined by various researchers is illustrated in Figure 2.3. The detailed discussions are followed by the figure.

Classification by Isukapalli and coauthors (Isukapalli, et al., 1998)

As shown in Figure 2.3a, Isukapalli and coauthors classify uncertainty types as (a) the inherent randomness or unpredictability of the physical system ("natural uncertainty/variability"), (b) approximations and simplifications in model formulation ("model uncertainty"), or (c) incomplete knowledge of model parameters/inputs due to insufficient or inaccurate data ("data uncertainty"). Uncertainty can be further categorized into "reducible" and "irreducible". Reducible uncertainty can be lowered by improvements in measurements and model formulation, whereas irreducible uncertainty is inherent in the physical system and can only be quantified in a statistical sense.

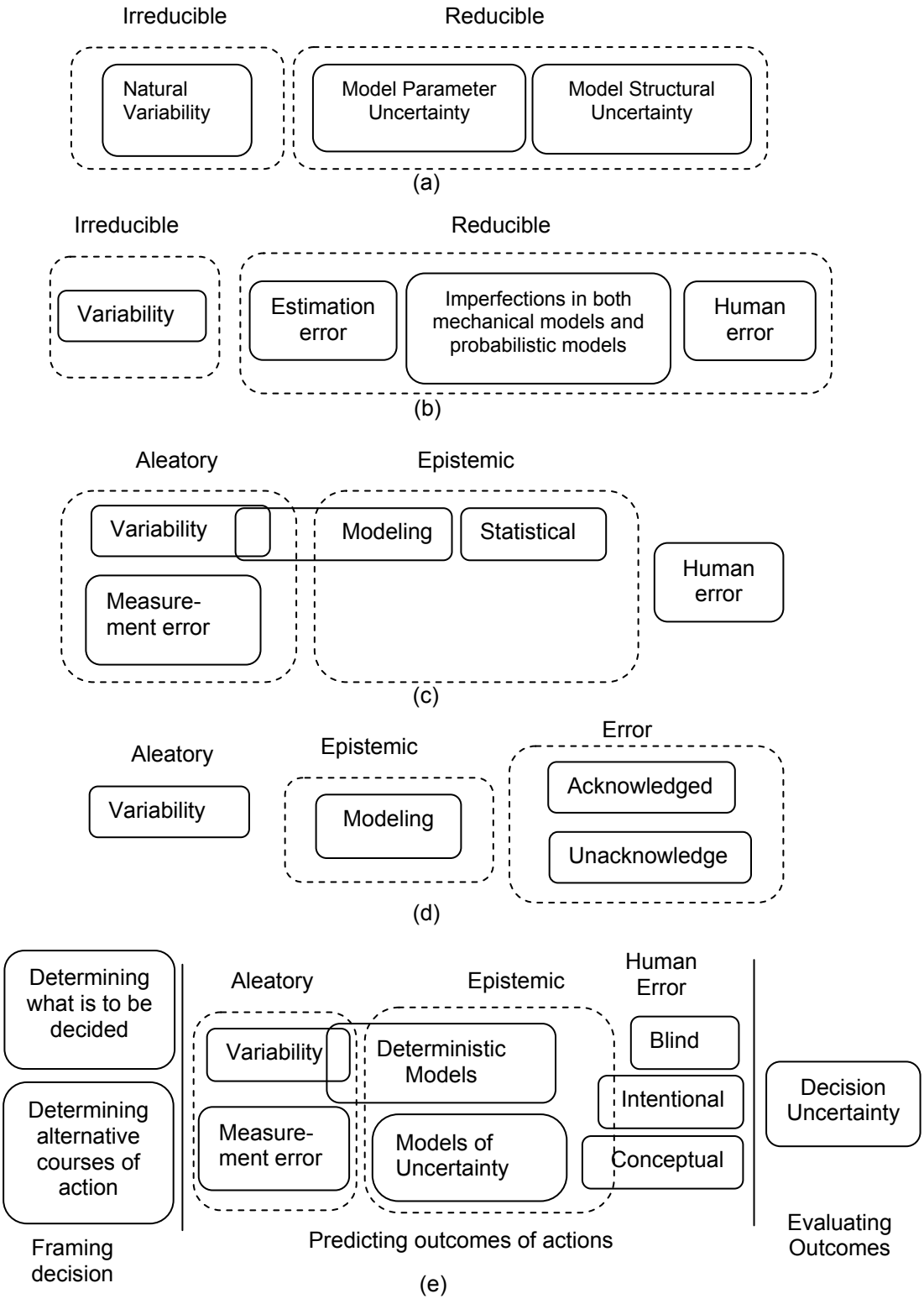

Figure 2.3 Types of uncertainty: (a) classification by Isukapalli, (b) classification by Der Kiuregian, (c) classification by Haukaas, (d) classification by Oberkampt et al., (e) classification by Nikolaidis (Nikolaidis, 2005)

Classification by Der Kiuregian (Der Kiureghian, 1989)

As shown in Figure 2.3b, Der Kiuregian considers the following four sources of uncertainty in structural analysis and design: (1) inherent variability, (2) estimation error, (3) model imperfection, and (4) human error. Inherent variability is equivalent to the natural uncertainty classified by Isukapalli, which is due to the unpredictable randomness in physical systems. Estimation error is due to incompleteness of sampling information and our inability to accurately estimate the parameters of the probabilistic models that describe inherent variability. Model imperfection is due to lack of understanding of physical phenomena (ignorance) and the use of simplified structural models and probabilistic models (errors of simplication). Imperfections in probabilistic models refer to errors in the choice of a parameterized probability distribution. Unlike the classification by Isukapalli, Der Kiuregian includes human errors as the source of uncertainty in a system. Human errors occur in the process of designing, modeling constructing, and operating a system. (1) is irreducible uncertainty and the rest of them, (2) ~ (4), are reducible uncertainties allowed by increasing knowledge about a system and collecting more data.

Classification by Haukaas (Haukass, 2003)

As shown in Figure 2.3c, Haukaas said that the division of aleatory and epistemic uncertainty is not disjunctive since one component of modeling uncertainty is due to missing some random variables in a model and this component is also aleatory uncertainty. Randomly generated micro-structure morphology changes in a material analysis cause randomness in response; however, the microstructure morphology changes cannot be modeled as a random variable. Modeling uncertainty and variability overlap

because modeling uncertainty due to missing random variables in a deterministic model causes variability.

Classification by Oberkampt and Coauthors (Oberkampf, et al., 1999)

In Oberkampt's definition illustrated in Figure 2.3d, error has a broader meaning than the definition of human error. Error includes simplification of mathematical models and approximations in numerical algorithms. Oberkampt and coauthors stated that error is not aleatory or epistemic uncertainty since it is not due to lack of knowledge. The error is further categorized according to whether it is recognized or not. If the error is not recognized then it is unacknowledged error. If the error is recognized but it is allowed to remain then it is acknowledged error. For example, discretization error or round-off error are acknowledged error, while programming error and mistakes are unacknowledged errors.

Classification by Nikolaidis (Nikolaidis, 2005)

Nikolaidis's classification is unique since it is based on the decision-making process. As illustrated in Figure 2.3e, Nikolaidis defines three stages of a decision – framing a decision, predicting the outcomes of actions, and evaluating the payoff of outcomes. In each stage of the decision process, the types of uncertainty are classified by a certain type of uncertain source. When framing a decision, the decision maker is uncertain if he or she has correctly framed what needs to be decided and all relevant features of the problem are considered. Moreover, the decision maker is uncertain if he or she has examined all available alternative courses of action.

When predicting the outcome of an action, Nikolaidis classifies three basic uncertainty types, which are aleatory, epistemic, and human error. As others have described, aleatory

uncertainty is due to natural variability and measurement error. In epistemic uncertainty, the classification by Oberkampf is employed. Epistemic uncertainty is a potential deficiency in any phase of the modeling process that is due to lack of knowledge. Epistemic uncertainty in deterministic models includes use of incorrect models, missing variables, and wrong assumption and idealization. The epistemic uncertainty in non-deterministic models (probabilistic model of uncertainty) is uncertainty in models of uncertainty, such as selecting the wrong type of probability distribution of a random variable and the inability to estimate accurately the parameters of the distribution from a finite sample. As Haukaas stated, Nikolaidis said that variability and epistemic uncertainty in deterministic models partially overlap, indicating that the division of aleatory and epistemic uncertainty is not disjunctive (Nikolaidis, 2005). This is because some random variables in a model are missing and those random variables cause random variability in predictions. Human error is the third source of predicting the outcome of an action. Human error is divided into execution (blind), intentional, and conceptual errors. The boundary between intentional and conceptual errors and epistemic uncertainty is fuzzy.

Classification of uncertainty in a model is very important since the quantification and strategy for decision under those uncertainties should be selected depending on the types of uncertainty. However, as discussed in this section, **there are disagreements among the researchers for defining types of uncertainty.** In Section 2.6, we suggest one of the classifications addressed in this section in order to effectively define types of uncertainty in materials design. In Sections 3.1 and 3.2, we investigate uncertainty in materials design problems and classify associated uncertainty based on the classification scheme in

Section 2.6. In the next section, we review robust design methodologies that manage the uncertainty in systems-based engineering.

2.2. ANALYSIS AND MANAGEMENT OF UNCERTAINTY

In Section 2.1, various classifications of uncertainties are presented. The main reason for classifying uncertainties in engineering systems is that the strategy and methods for managing uncertainty depend on the types of uncertainty. Quantifiable uncertainty, such as aleatory uncertainty, should be quantified, and the quantified degree of uncertainty is considered in the design exploration process. On the other hand, the main approach for dealing with unquantifiable uncertainty, such as epistemic uncertainty, is to reduce the amount of uncertainty by increasing knowledge about uncertain systems, such as collecting real experimental data, reducing computational errors, validating model development processes, etc. Another approach for dealing with unquantifiable uncertainty is to define subjective criteria or functions, such as fuzzy logic, utility, and loss functions in uncertainty. In this section, we explore and review previous studies for dealing with uncertainty in engineering systems.

2.2.1. Analysis of Uncertainty

The first step for robust design is to characterize and quantify uncertainty in a system. Hence, in this section, we reviewed several approaches for quantifying uncertainty and its engineering applications. Uncertainty analysis is estimating output uncertainty (i.e., probability distribution of system response) with variability in input parameters. Analysis of aleatory uncertainty is relatively easier than analysis of epistemic uncertainty if measuring a system behavior is feasible. The most interesting point of the uncertainty

quantification in engineering applications is "**how to efficiently analyze the uncertainty of a system**". Efficiency is an important factor in designing a system with consideration of uncertainty, since uncertainty analyses are necessary at each function evaluation while exploring a design space in a robust system design.

Depending on the types of uncertainty analysis methods, we classify the types as non-probabilistic and probabilistic methods. The probabilistic methods are further classified as statistical and non-statistical approaches. Non-probabilistic methods include Interval Analysis and Fuzzy Logic methods, which are particularly useful when a system model is deterministic – there are no random errors in a system response - and input parameters are uncertain - without probability density functions due to lack of information. If a system model (computational model) is deterministic and input parameters are known as probabilistic density functions, then there are lots of techniques available in literature. If a system model is non-deterministic and input parameters are known as probability density functions then statistical methods for uncertainty analysis are also useful for uncertainty quantification. However, if a system model is non-deterministic and input parameters are uncertain, then no existing method is applicable to uncertainty analysis.

In Table 2.1, available uncertainty analysis methods depending on the characteristics of a system are listed. Among the **non-probabilistic methods**, interval analysis and fuzzy logic have been widely used for uncertainty analysis. In interval analysis, the value of a variable is replaced by a pair of numbers representing the maximum and minimum values that the variable is expected to take. Interval arithmetic rules are then used to perform mathematical operations with the interval numbers.

Table 2.1 Available uncertainty analysis methods depending on system characteristics

System model	Deterministic		Non-deterministic	
Input	Uncertain	Probability distribution	Uncertain	Probability distribution
Available uncertainty analysis methods	**Non-probabilistic methods** ▪ Interval analysis ▪ Fuzzy logic	**Probabilistic methods** - *Statistical methods* ▪ Monte Carlo Simulation ▪ Latin Hypercube sampling, etc. - *Non-statistical methods* ▪ First and second order moment methods ▪ Polynomial chaos expansions ▪ Stochastic response surface methods	**N/A**	**Probabilistic methods** - *Statistical methods* ▪ Monte Carlo Simulation

While interval analysis has been applied successfully to small problems (Das, 2005; Hao and Merlet, 2005; Messine, 2004), practical applications with large simulations have not been found because the results it produces are too conservative. Fuzzy logic (Dubois and Prade, 1978; Dubois and Prade, 1979) can be used to estimate the uncertainty in the output when the input parameter uncertainties are characterized by membership functions. Fuzzy logic calculates approximate behavior of the system using models based on inexact or unreliable data. The membership function represents the degree of membership of the fuzzy variable within a fuzzy set. Uncertainty analysis using fuzzy sets is often called a possibility approach. Fuzzy logic has been widely used in engineering applications (Allen, et al., 1990; Krishnamachari, 1991; Simpson, et al., 1996; Swadi and Bui, 1991; Zimmermann, 1978) where input parameters cannot be modeled statistically. Although fuzzy logic is appealing because of its simplicity, many engineering applications that require higher confidence tend to employ probabilistic methods.

As mentioned earlier, **probabilistic methods** can be further classified into statistical methods and non-statistical methods. **Statistical methods** employ a large number of

samples of the input variables, repeatedly measure system output (response), and statistically analyze the output distributions. Depending on the sampling methods for increasing efficiency of the estimation, there are many techniques available. The classical example of a statistical method for uncertainty analysis is Monte Carlo Simulation. The Monte Carlo methods, which are also called "statistical simulation methods," can be loosely defined to include any method that utilizes sequences of random numbers to perform the simulation. The procedure of the basic Monte Carlo method involves: a) generating a set of values by randomly sampling the known or assumed probability density function for each input variable, b) executing an experiment and collecting the data for each of the generated samples, and c) employing statistics for the output data set to define its probability density function. It is important to know that, even if the Monte Carlo method converges to the exact statistic solution as the number of samples goes to infinity, the convergence of the mean error estimate is slow. Hence, thousands or millions of data samples may be required to get enough accuracy. If the experiment (or simulation) is expensive, then the Monte Carlo method is not a feasible approach for uncertainty analysis. This is fairly common in materials design.

Since the basic Monte Carlo method is computationally (experimentally) expensive, modifications of the Monte Carlo method have been developed to improve the efficiency of uncertainty analysis. One of the most popular modified Monte Carlo methods is the **Latin Hypercube sampling method**. (McKay, et al., 1979) In the Latin Hypercube sampling method, the selection of sample points is highly constrained. For a single random variable, instead of randomly sampling from a complete PDF (Probability Density Function), the range of random values is partitioned into several segments of

equal probability. Each segment corresponds to an equal area under the PDF curve. In each segment, a point is sampled with respect to the complete PDF. In the case of multiple random variables, the values picked in the segments of each random variable are randomly combined with the values in the segments of other random variables without duplicating. A complete description and application examples can be found in Iman and the coauthors' publication. (Iman, et al., 1981; Iman, et al., 1981)

Even though statistical methods have been improved to increase sampling efficiency, they are still computationally and experimentally expensive. For increasing computational efficiency, non-statistical methods have been developed. The most widely used non-statistical uncertainty analysis method is **moment methods**. In moment methods, a Taylor series expansion is employed to estimate response variance based on input parameters variances, as shown in the following equations:

$$Var_{first\_order}[y(x)] = Var(x)\left(\left.\frac{\partial y}{\partial x}\right|_{\bar{x}}\right)^2 \tag{2.1}$$

$$Var_{second\_order}[y(x)] = Var(x)\left(\left.\frac{\partial y}{\partial x}\right|_{\bar{x}}\right)^2 + \frac{1}{2}\left(Var(x)\left.\frac{\partial^2 y}{\partial x^2}\right|_{\bar{x}}\right)^2 \tag{2.2}$$

Equation (2.1) is the First-order, Second Moment (FOSM) method and Eq.(2.2) is the Second-order, Second Moment (SOSM) method. In the FOSM, the variance of the output is equal to the variance of the input parameters multiplied by the square of the first sensitivity derivative evaluated at the mean value of the input. In the SOSM, the higher order term (second order term) is included to increase the accuracy in the estimation of the output. The moment methods are very simple and convenient; therefore, these methods are widely used as approximate methods for estimating the moment of the

output from the moments of the uncertain input parameters. These methods are very useful for exploration of a design space in which many function calls are indispensable. However, the methods are good for Gaussian probability distribution, and it is very hard to apply to other types of probability distributions in input parameters. Also, the result can be inaccurate since these are approximate methods.

Since the approximate methods mentioned above could be inaccurate if the probability distributions of the input parameters are not normal distributions, some researchers (Isukapalli, et al., 1998); (Kim, et al., 2004; Xiu and Karniadakis, 2003) employ Polynomial Chaos expansions. Polynomial Chaos uses a spectral representation of the uncertainty which is then decomposed into separate deterministic and random components. In the Polynomial Chaos expansions, each random variable in the equations of the deterministic mathematical model is expanded into an infinite series of Hermite polynomials. Kim and the coauthors (Kim, et al., 2004) use the Polynomial Chaos expansion method for a robust shape optimization problem. Xiu and Karniadakis (Xiu and Karniadakis, 2003) use a Polynomial Chaos method to solve a transient heat conduction problem. They note that the efficiency of the chaos expansion is problem specific and requires further research.

As discussed above, there are many available uncertainty analysis methods for deterministic system models; however, as shown in Table 2.1 uncertainty analysis methods for non-deterministic system models have not been developed in literature. Monte Carlo simulation is the only method for quantifying non-deterministic system response variation with the probability distributions of input parameters. **If a system**

behavior is non-deterministic due to non-parametric input variation [3], it is impossible to perform uncertainty analysis by employing statistical or non-statistical efficient uncertainty analysis methods since those are typically developed for deterministic methods. However, today, even detailed computer simulations as well as real experiments have random processes inside so that the predicted system's response has irreducible random variability.

Xu and Albin (Xu and Albin, 2003) capture statistical error bounds for a response surface model constructed based on experimental data using a simultaneous confidence interval. They consider the statistically estimated uncertainty in the response surface model for their robust optimization. **However, their approach cannot be used to model the system response variability or to estimate uncertainty propagation with statistical or non-statistical input parameter variation.** Uncertainty analysis for non-deterministic simulation is indispensable for multiscale materials design since the simulation models for heterogeneous material behavior tend to be stochastic. This need leads the dissertation research to Research Question 2. We will revisit this section and justify the Research Question 2 in Section 2.6.

2.2.2. Management of Uncertainty

Aleatory system uncertainty is quantifiable; however, epistemic uncertainty that arises from incomplete knowledge of a system is virtually impossible to quantify. Therefore, the uncertainty that comes from lack of knowledge should be reduced (instead of being quantified) by increasing system knowledge and/or getting more information. Unfortunately, methods for reducing unquantifiable (epistemic) uncertainty have not been

[3] input variation that cannot be modeled as numeric parameters

rigorously studied. Statistical uncertainty due to estimating system behavior in a continuous space by discrete sampling points may be captured using **Confidence and Prediction Interval** (Myers and Montgomery, 1995; Neter, et al., 1996) in a metamodeling technique, such as response surface method. However, these techniques are **only intended for quantifying statistical uncertainty due to lack of sampling data**. **Quantification of epistemic uncertainty has not been found in literature.**

Instead, researchers have focused on procedures to reduce uncertainty and validate a model's accuracy. Jin and the coauthors (Jin, et al., 2003) test various metamodeling techniques for different formulations of optimization under uncertainty and compare the accuracy of approximation techniques. Simpson and the coauthors (Simpson, et al., 2001) also survey various sampling and metamodeling techniques and recommend a guideline for appropriately using statistical approximation techniques in a given problem. Brooks and Tobias (Brooks and Tobias, 1996) propose detailed guidelines for choosing the best model in a mathematical or computer models by measuring levels of detail, complexity and corresponding model performance. Sargent (Sargent, 2003) has developed a guideline for a model validation process. Sargent specifies validation techniques at each stage of a model validation and verification process – obtained data validity, conceptual model validity, computerized model verification, and operational validity.

Besides those techniques for reducing uncertainty or validating system models, there have been attempts to reduce uncertainty using model calibration techniques. The model calibration techniques are the methods for statistically calibrating a mathematical model with a large number of relatively simple (with assumption and idealization) simulation results and some complex and detailed (approximately true) simulation or real

experiment results. Kennedy and O'Hagan (Kennedy and O'Hagan, 2000) employ Gaussian Process model (known as kriging model in spatial statistics) for fitting simple model data. They assume the model for detail simulation data is a combination of the fitted simple mathematical model, a linear scale term, and an error term. The linear scale term is assumed to be an unknown constant and the error term is defined as another Gaussian Process model. By applying some detailed simulation results, they find the unknown scale term and the error term for constructing a better approximate model. Qian and the coauthors (Qian, et al., 2004) propose a modified calibrated model by modeling the scale term as an unknown linear regression function. These two methods are particularly useful for saving computational expense by reducing number of samples in fine meshed analysis. **However, the restriction of these methods is that designers must have some true results. In some cases, we cannot obtain any better data than current data due to severe uncertainty in a system or restrictions of computational or experimental expenses, which is the case of multiscale materials design.** Hence, we need a method with which designers may address this problem.

In this section, methods and techniques for estimating the degree of uncertainty in a system or reducing unquantifiable uncertainty are discussed. Once the amount of uncertainty is estimated, then the next step is how to consider the estimated uncertainty in a system design. One of the main approaches for designing under uncertainty is a robust design methodology. In the next section, we investigate some approaches for robust design of uncertain systems.

2.3. ROBUST DESIGN METHODS UNDER UNCERTAINTY

In system design, the uncertainty mentioned in the previous section is an important factor that has to be considered in the decision-making process. As mentioned, this is because the uncertainty may lead to a wrong decision in systems-based design. The best way for making the right decision is eliminating those uncertainties; however, eliminating uncertainty in a model is practically infeasible and reducing the uncertainty is costly and time-consuming. Accordingly, a robust design paradigm, **designing systems to be insensitive to those uncertainties without eliminating them**, was proposed in systems-based engineering design a few decades ago. In this section, we investigate the previous studies and methods for achieving robustness in system responses.

2.3.1. Taguchi Method – Type I Robust Design

As described in Chapter 1, **Type I** robust design is identifying control factor (design variable) values that satisfy a set of performance requirement targets despite variation in noise factors. **Type I** robust design was proposed originally by Genichi Taguchi (Ross, 1988; Taguchi, 1987; Taguchi, 1993). Taguchi said that robust design is a method for improving the quality of products and processes by reducing their sensitivity to variations, thereby reducing the effects of variability without removing its sources. The principles and methods known as robust design developed by Taguchi became the foundation of product and process design in Japanese industry, which is interested in producing cost effective, high-quality products. High cost for tolerance design, such as using better material, is reduced by parameter design, selecting controllable parameters to achieve robustness in the performance of products and processes against uncontrollable perturbation factors (noise factors). The approach for robust design proposed by Taguchi

includes experimental design (orthogonal array), quality loss function, and signal-to-noise ratio.

In the Taguchi method, the objective is to minimize loss, as he mentioned "the quality of a product is the (minimum) loss imparted by the product to the society from the time the product is shipped." He proposed a Quality Loss Function as illustrated in Figure 2.4.

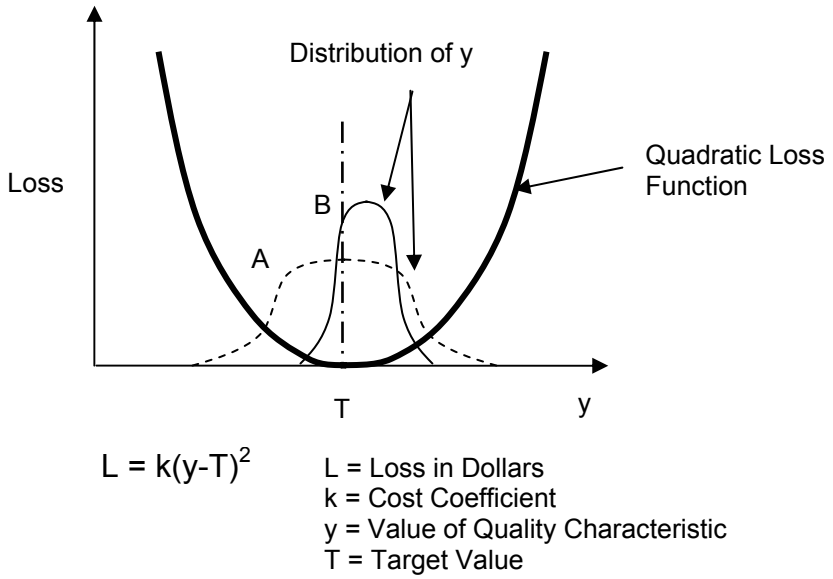

Figure 2.4 Taguchi's quadratic quality loss function

He found that the simple quadratic function approximates the behavior of loss in many instances (Byrne and Taguchi, 1986). Considering the two different distributions (A and B) of the product output, the average quality loss of B is smaller than that of A. Therefore, the objective of robust design is to find a design configuration that yields the distribution B rather than A. Phadke (Phadke, 1989) said the average quality loss depends on two components, which are the deviation of the average value of y from the target and the mean squared deviation of y around its own mean.

Taguchi proposes three stages of engineering design which are system design, parameter design, and tolerance design. He notes that too many tolerance-driven

engineers skip directly from system design to tolerance design and ignore the critically important parameter design stage, in which designers find desirable parameters to minimize quality loss.

Taguchi's robust design approach for the parameter design starts with clear classification of parameters into control factors and noise factors. As mentioned in Section 1.3.4, the control factors are design parameters that can be controlled easily without increasing cost. Noise factors are uncontrollable or are hard (expensive) to control. Taguchi recommends an orthogonal array as the experimental design. Control factor conditions (orthogonal combination of various levels) reside in an inner array and noise factors conditions in an outer array. The experimental results in all combinations of control factors and noise factors conditions are recorded. For evaluation of nominal response, an average of responses (experimental results with varying noise factor condition while fixing control factor condition) at each control factor condition is identified. Taguchi proposed a signal-to-noise ratio for measuring sensitivity analysis of responses to variation of noise factors instead of a statistical test (F-test) using a traditional approach (ANOVA). Based on an average response plot (mean of response variation) and signal-to-noise ratio (deviation of responses), designers select the best combination of the level of each control factor.

Taguchi's robust design philosophy has been applied to various problems in industry and academia since the mid 1980's. His approach is practical, intuitive, and relatively simple. It has been applied to many industry problems and achieved successful outcomes. However, there have been many arguments regarding Taguchi's approach and many researchers suggested improvements and extensions of Taguchi's robust design method.

The orthogonal array of the experimental design in Taguchi's robust design has been criticized as inefficient and costly since it requires an unnecessarily large number of experiments. Welch and coauthors (Welch, et al., 1990) and Shoemaker and coauthors (Shoemaker, et al., 1991) presented a combined single array for both control and noise factors instead of separating them. Vining and Myers (Vining and Myers, 1990) and Shoemaker and coauthors (Shoemaker, et al., 1991) developed approximate models of mean and variance using response surface models.

The signal-to-noise ratio for capturing response variation has been criticized on the ground that designers could miss useful information since the signal-to-noise ratio confounds both the mean and variance of response in its formulation. The use of the signal-to-noise ratios for decision-making is only effective when at least one factor influencing the mean should be separated from the factors influencing the variance. However, the effects on the mean are confounded with the effects on the variance when the factors influencing the mean cannot be separated. Statisticians (Box, 1988; Tsui, 1992; Vining and Myers, 1990) suggested modeling the mean response and variance directly or by statistical data transformation instead of using signal-to-noise ratio.

Taguchi's robust design method may be adapted to unconstrained problems. However, constraints are typically important in engineering applications. To include constraints in robust design formulation, Parkinson and coauthors (Parkinson, et al., 1993) proposed 'feasibility robustness' for designs that satisfy constraints despite variations in control and noise factors. They present a worst case that uses first order Taylor series expansion for calculating the amount of variation that needs to be considered in constraints evaluations by variation of control and noise factors. Otto and Antonsson (Otto and

Antonsson, 1991) adopt a constrained optimization approach for robust design, in which they used a modified version of Taguchi's signal-to-noise ratio as the objective function. Du and Chen (Du and Chen, 2000) include probability based constraint evaluation (reliability design) in feasibility checking. For probability constraint evaluation, they found the Most Probable Point (MPP) in the interface region between control and noise factors' combined probability distribution and a constraint bound.

The Taguchi method has been criticized and alternative approaches have been presented by many researchers. However, his philosophy of robust design has been adapted in many applications in industry and has achieved successful outcomes; it is a milestone as a design philosophy, achieving not only optimization but also insensitivity to environmental perturbations (noise factors).

The Taguchi method is only valid when the noise factor can be leveled and experimentally set up in order to analyze the contribution of the variations in noise factors to a system performance. **If noise factors cannot be quantified as numeric parameters or quantitative levels, then this method is not valid.** However, as discussed in Sections 1.2.4 and 1.4.1, the types of uncertainty in materials design problem tend to be unparameterizable.

2.3.2. Robust Design in Suh's Axiomatic Design

Taguchi's robust design method has been employed in an embodiment or detail design stage in the product realization process by changing the appropriate parameters for achieving robust system performance to noise factors. In contrast to Taguchi's robust design, Suh's Axiomatic Design provides a robust design approach for selecting a design concept among available candidates in conceptual design stage.

Axiomatic Design is a principle-based design method focused on the concept of domains. The primary goal of axiomatic design is to establish a systematic foundation for design activity by two fundamental axioms and a set of implementation methods. (Suh, 1990) The two axioms are:

- Axiom 1: The Independence Axiom: Maintain the independence of functional requirements
- Axiom 2: The Information Axiom: Minimize the information content in design

In the axiomatic design approach, the design process is modeled as a mapping between a set of functional requirements (FRs) in the functional domain and a set of design parameters (DPs) in the physical domain. The mapping process is represented by the design equation:

$$\mathbf{FR} = \mathbf{[A]DP}\,, \qquad (2.3)$$

where $A_{ij} = \frac{\partial FR_i}{\partial DP_j}$

Suh defines an uncoupled design as a design in which FRs and DPs can be mapped one-to-one. This means that only the diagonal terms of [**A**] are non-zero. He defines decoupled design as a design in which [**A**] can be arranged as triangular matrix by appropriate order changes of FRs and DPs. He defines a coupled design as a design whose [**A**] cannot be arranged as a triangular or diagonal matrix by order changes of the FRs and DPs. These are illustrated as

$$\begin{bmatrix} FR_1 \\ FR_2 \\ FR_3 \end{bmatrix} = \begin{bmatrix} X & 0 & 0 \\ 0 & X & 0 \\ 0 & 0 & X \end{bmatrix} \cdot \begin{bmatrix} DP_1 \\ DP_2 \\ DP_3 \end{bmatrix} \quad \text{Uncoupled}$$

$$\begin{bmatrix} FR_1 \\ FR_2 \\ FR_3 \end{bmatrix} = \begin{bmatrix} X & 0 & 0 \\ X & X & 0 \\ X & X & X \end{bmatrix} \cdot \begin{bmatrix} DP_1 \\ DP_2 \\ DP_3 \end{bmatrix} \quad \text{Decoupled} \qquad (2.4)$$

$$\begin{bmatrix} FR_1 \\ FR_2 \\ FR_3 \end{bmatrix} = \begin{bmatrix} X & X & X \\ X & X & X \\ X & X & X \end{bmatrix} \cdot \begin{bmatrix} DP_1 \\ DP_2 \\ DP_3 \end{bmatrix} \quad \text{Coupled}$$

From the Axiomatic Design perspective, uncoupled design enabling one-to-one mapping between FRs and DPs is the best design among all and satisfies the independence axiom. The decoupled design is also acceptable in the perspective of the independence axiom since we can sequentially select design parameters that make system's function requirements. However, coupled design does not satisfy the independence axiom, since it is hard to control design parameters to satisfy all functional requirements. Suh suggested that designers use the independence axiom to select the best design configuration first among all available design candidates.

Once the system's functional configuration has been selected, the next process is to select selecting design parameters to minimize information content, which is very similar to robust design philosophy. The information axiom provides the means of evaluating the quality of designs, thus facilitating a selection among available design alternatives. The selection of an appropriate design in the perspective of the information axiom is accomplished by comparing the information content of the design candidates. Information content is defined in terms of entropy, which is expressed as the logarithm of the inverse of the probability of success p as

$$I = \log_2 \frac{1}{p} \tag{2.5}$$

In case of uniform probability distribution of design range, the above equation can be written as

$$\mathrm{I} = \log_2 \left(\frac{\text{System Range}}{\text{Common Range}} \right) \tag{2.6}$$

As shown in Figure 2.5, the design range is the desirable system range for meeting functional requirements, the system range is the deviation of functional requirement of a candidate system, and common range is the overlapping region between the design range and the system range. The information content (I) is minimized by maximizing probability of success (p). Maximizing p can be achieved by minimizing system range and/or maximizing common range. In the perspective of the information axiom, a designer should select a design candidate that has minimum information contents based on the calculation of probability of success.

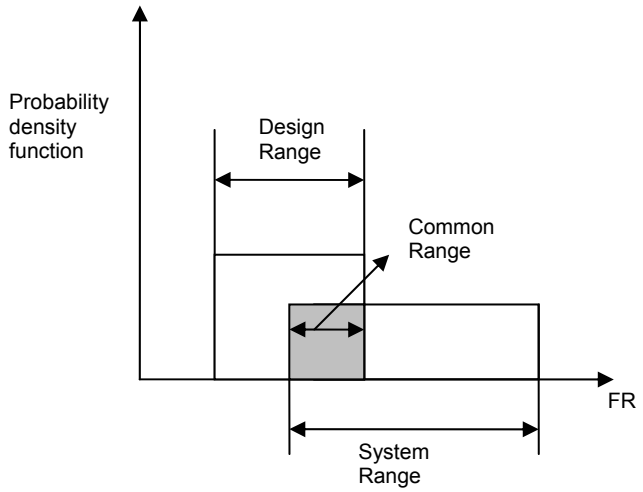

Figure 2.5 Design, system, and common range for calculating probability of success

Suh (Suh, 1990) uses conditional probability to calculate the information content of a decoupled design. The philosophies of the Taguchi method and Axiomatic Design are different. As shown in Figure 2.6, the two methods could result in two different decisions.

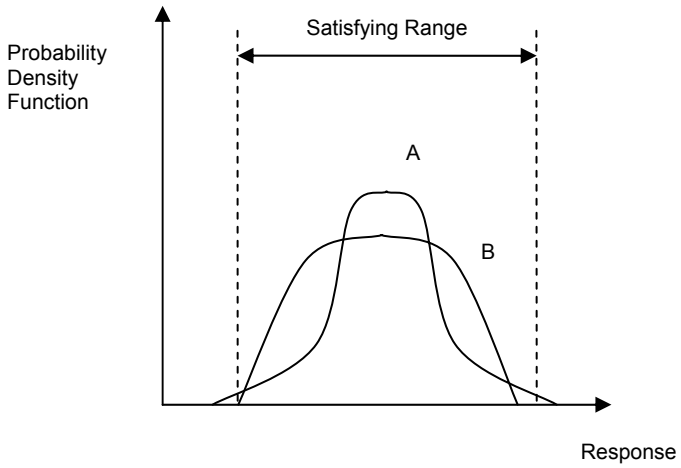

Figure 2.6 Two alternative designs with satisfying range

Using Taguchi method, designers select design A by virtue of signal-to-noise ratio, but using the axiomatic design, designers select design B according to the information axiom. We cannot simply conclude which method is better than the other. The method should be appropriately selected depending on the type of design problems. If the boundary of the satisfying range is strict, then we had better select the axiomatic design rather than the Taguchi method. If the probability of hitting the target is more important, then we need to choose Taguchi method for our decision making. However, the Taguchi method is clearly a parametric design method that can be utilized in a detail design stage and Suh's axiomatic design is a decision-making tool that is more appropriate for a conceptual design stage.

Suh's axiomatic design, however, lacks a procedure of analyzing performance sensitivity due to disturbance factors. Information axiom is a metric that indicates a designer's specific preference in terms of system performance, but is not a systematic

procedure (or method) for designer to follow for designing robust systems. Moreover, it cannot deal with the unparameterizable variability just like the Taguchi method. Therefore, the axiomatic design is not the method that facilitates robust materials design under the uncertainty mentioned in Section 1.2.4.

2.3.3. The Robust Concept Exploration Method / Design Capability Indices - Type I and II Robust Design

Taguchi's robust design method and Suh's Axiomatic Design are two different robust design methods that can be used in a discrete design space depending on the stage in a design process. However, we often need to explore an entire continuous design space to find favorable concepts, which is especially important in a conceptual design stage. Suh's axiomatic design is useful once we have a number of discrete design alternatives, but these methods cannot actively search a continuous design space. In addition, Taguchi's robust design is typically useful for achieving a design insensitive to deviations in noise factor, but that cannot include the performance deviations due to perturbations in control factors. In response to these needs, Chen and coauthors (Chen, et al., 1996; Chen, et al., 1996) propose the Robust Concept Exploration Method (RCEM) for searching a conceptual design configuration for robust performance that is insensitive to deviation of noise and control factors in a conceptual design stage.

As shown in Figure 2.7, Chen and coauthors classify robust design tasks into two categories. One is **Type I** robust design, which is insensitive to variation in noise factors. The other is **Type II** robust design, which is insensitive to variation in control factors. In **Type I** robust design, designers prefer to set control factor x at a since variation in the deviation function with respect to the variation in noise factor (z) is less at $x=a$ than $x=b$ as shown in the figure. It is equivalent to Taguchi's robust design method.

The Robust Concept Exploration Method

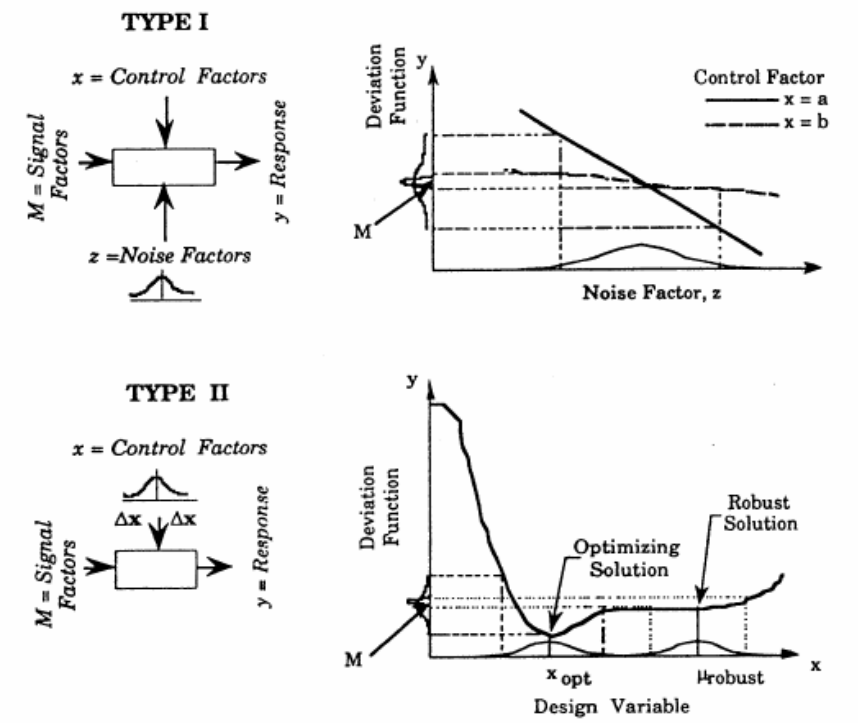

Figure 2.7 Robust design for variations in noise factors and control factors (Chen, et al., 1996)

In addition to **Type I** robust design, **Type II** robust design considers the variation in control factors. As shown in Figure 2.7, when the variation in a control factor exists, the optimizing solution produces larger variance in deviation in a response than the robust solution does in some cases. Therefore, they suggest finding a flat region rather than an optimal point, at which system's performance will be degraded significantly at slight deviation from the optimal decision point.

The RCEM is a systematic approach for finding a ranged set of design specifications that produce robust performance in variations of noise and control factors by integrating statistical experiments, approximate models, robust design techniques, multidisciplinary analyses, and multiobjective decisions. The computing infrastructure of the RCEM is illustrated in Figure 2.8.

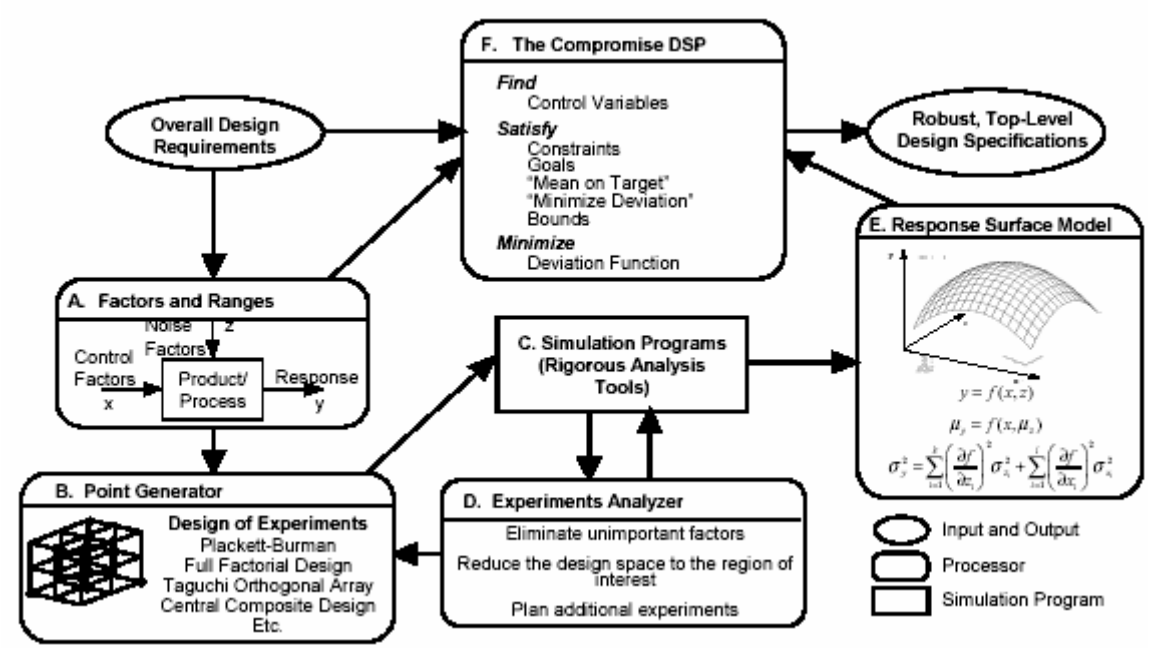

Figure 2.8 Computing infrastructure for Robust the Concept Exploration Method (Chen, et al., 1996)

As shown in the figure, design parameters are classified as noise factors and control factors in stage A (Factors and Ranges). Experiments (or simulations) are designed in stage B (Point Generator) to get the most accurate response surface model (approximate model) with the minimum sampling. Based on the experiment specification, designers perform experiments or simulations and get the result data in stage C (Simulation Program). In stage D (Experiments Analyzer), designers analyze result data statistically and eliminate unimportant factors that do not affect system performance. They reduce the design space in order to get more accurate response surface models and plan additional experiments within a reduced design space. The stages C and D are sequentially repeated until the best set of data is obtained for building response surface models. In stage E (Response Surface Model), designers build response surface models based on the obtained data. In stage F (The Compromise DSP), to find a ranged set of design

specifications that are robust against deviations of noise and control factors, Chen and coauthors employed the compromise Decision Support Problem (cDSP) (Bascaran, et al., 1987; Bras and Mistree, 1993; Chen, et al., 1995; Mistree, et al., 1992).

The compromise Decision Support Problem is a mathematical decision construct that supports decision making by combining multiple objectives and constraints into a single construct. The cDSP borrows the deviation formulation technique from goal programming (Ignizio, 1983) and constraint evaluation from mathematical (linear and nonlinear) programming. The cDSP is different from goal programming since it has the capability of combining constraint conditions that most engineering applications require. In traditional mathematical programming, the objective function typically represents a single goal by which the desirability of a design solution is measured. All other characteristics of a design are modeled as hard constraints. On the other hand, the compromise DSP is more flexible than traditional mathematical programming because it accommodates multiple constraints and objectives, as well as both quantitative information and information – such as bounds and assumptions – that may be based on a designer's judgment and experience (Marston, et al., 2000). In the compromise DSP, multiple goals have been considered conventionally by formulating the deviation function either with Archimedean weightings or preemptively (lexicographically) (Mistree, et al., 1992).

The RCEM employs the compromise Decision Support Problem as a mathematical construct for finding a solution since a robust design is a multi-objective problem for each system goal, bringing the mean of performance to target as well as minimizing performance deviation. The RCEM has been employed successfully for a simple

structural problem and design of a solar powered irrigation system (Chen, et al., 1995), a High Speed Civil Transport (Chen, et al., 1996), a General Aviation Aircraft (Chen, et al., 1996) , product platforms (Simpson, et al., 2001), and other applications (e.g., (Chen, 2001)).

The Robust Concept Exploration Method is a robust design method for finding ranged sets of robust design specifications in the conceptual design stage. Unlike the Taguchi method and Suh's Axiomatic Design, in the RCEM, designers can explore the entire continuous design space for finding a robust solution under the variations of noise and control factors. In the RCEM, an approximate model is employed instead of analysis or simulation model for fast function evaluation for exploring a design space. A system performance deviation by input variations is calculated by the second order moment method discussed in Section 2.2.1. The first order Taylor series expansion in Equation (2.7) may be used in order to reduce computational expense due to a large number of samples, as when Monte Carlo Simulation is used to measure performance sensitivity, i.e.,

$$\Delta y = \sum_{i=1}^{k} \left| \frac{\partial f}{\partial x_i} \Delta x_i \right| + \sum_{i=1}^{m} \left| \frac{\partial f}{\partial z_i} \Delta z_i \right| , \tag{2.7}$$

where y: response, x: control factor, z: noise factor, f: response surface model

This approximate approach is often required since it is virtually impossible to perform Monte Carlo simulation to estimate response deviations at every function call while exploring the design space. The RCEM is unique among the robust optimization methods since it employs the compromise Decision Support Problem in order to compromise the achievements of multiple goals (performance means and variance) by controlling deviation variables from the multiple targets.

Despite these advantages, the RCEM has limitations in its capabilities. Since it employs approximate models, the function evaluation is not as accurate as actual analysis or simulation. The response surface method that has been used for building an approximate model in RCEM is not appropriate for computational models (computer analysis or simulation model) since the computational models are deterministic and do not have unbiased errors. Simpson and coauthors (Simpson, et al., 1998) suggested using the kriging model instead of the response surface model for a computer simulation or analysis model in RCEM since the kriging model interpolates all observation points. The estimation of performance variation based on the employed mathematical techniques, such as first order Taylor series expansion, could be inaccurate when the variations in noise and control factors are large and/or the model function is highly nonlinear. Lin and coauthors (Lin, et al., 1999) suggested using three point goal formulation instead of Taylor series expansions when variations in noise and control factors are large. Recently, some robust design approaches have employed stochastic techniques, such as polynomial chaos expansions (Kim, et al., 2004) and stochastic response surface (Isukapalli, et al., 1998), to increase efficiency in estimating the performance variations, increasing accuracy with limited number of samples.

The Robust Concept Exploration Method with Design Capability Indices (RCEM-DCI)

In the early stages of design process, we do have explicit information regarding the target value of a system performance. If the target of a performance is uncertain, then cDSP (and goal programming) that deals with deviation from the target value could produce a different solution than the designer intend. Instead, ranged requirements could

be given for a system performance, such as the performance of a system should be better than a lower requirement limit, smaller than an upper requirement limit, or between lower and upper limits. Chen and coauthors (Chen, et al., 1996; Chen, et al., 1999) propose Design Capability Indices (DCIs) as metrics for system performance and robustness; these are used as goal formulations in cDSP formulation instead of directly using the means and variances of system performances.

The DCIs are mathematical constructs for efficiently determining whether a ranged design specification is capable of satisfying a ranged set of design requirements. When the index is negative, the mean of system performance is outside of the system requirement range. If the index is greater than unity, then the design will meet the requirement satisfactorily. Therefore, a designer's objective is to force the index to unity so that the larger portion of performance deviation falls into the range of design requirements. Forcing the index to unity is achieved by reducing performance deviation and/or locating the mean of performance deviation farther from requirement limits. The procedure to evaluate the index is illustrated in Figure 2.9; C_{du},$C_{dl,}$ and C_{dk} in the figure are calculated as

$$C_{dl} = \frac{\mu - LRL}{3\sigma}; C_{du} = \frac{\mu - LRL}{3\sigma}; C_{dk} = \min\{C_{dl}, C_{du}\} \tag{2.8}$$

The Design Capability Indices calculated in this manner are employed in cDSP for finding a ranged set of design specifications.

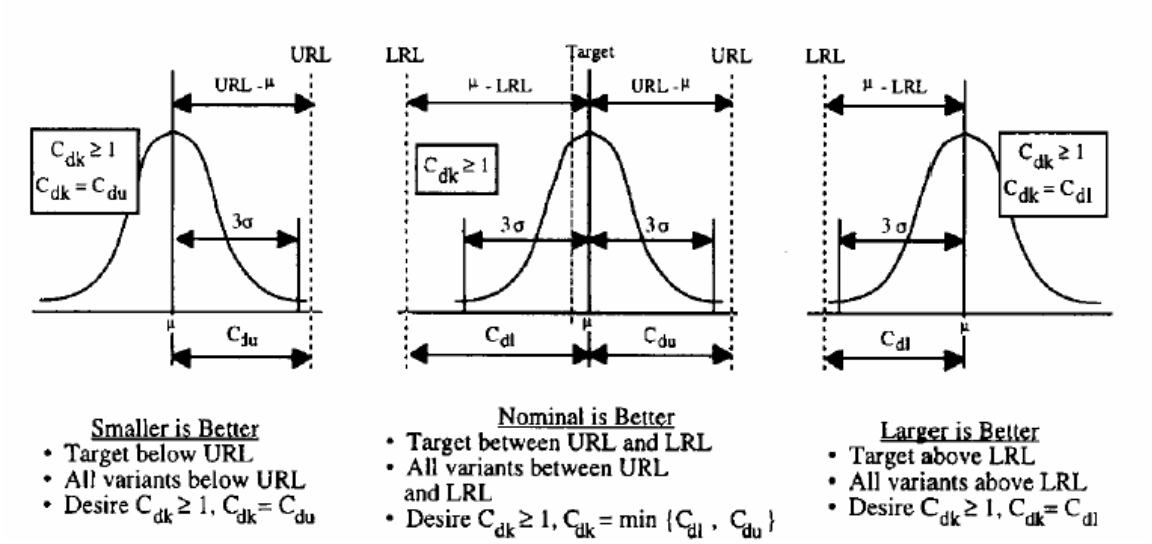

Figure 2.9. Design Capability Indices (Chen, et al., 1999)

The Robust Concept Exploration Method with Design Capability Indices (RCEM-DCI) provides the following advantages. With the DCI, a designer can efficiently check whether a family of designs can satisfy design requirements while eliminating the tedious task of evaluating large numbers of discrete or continuous design specifications. In addition, a designer can consider multiple aspects of quality improvement by adjusting the location of the mean of the performance distribution as well as the variation. Finally, the DCI is easy for a designer to compute and understand using a simple index number as discussed in the previous paragraph. The advantages of RCEM-DCI have been approved by applying this technique to some engineering problems, such as design of a solar powered irrigation system (Chen, et al., 1999), multidisciplinary decision making in design of a circuit board (Xiao, et al., 2002), and design of a Linear Cellular Alloy (Seepersad and Allen, 2003).

On the other hand, the RCEM-DCI has an important underlying assumption. **The assumption is that the models (approximate models, simulations, or engineering equations) incorporated to compute the DCIs are accurate; otherwise, the estimated**

spread of design performance will not be accurate. The RCEM and RCEM-DCI are important references of this dissertation since a method for Type III robust design established in this work is based on the construct of the RCEM-DCI. At the end of this chapter, the research opportunities to extend the capability of the RCEM-DCI are discussed in detail.

2.4. ROBUST DESIGN OF MULTIDISCIPLINARY SYSTEMS

Robust design heavily relies on the result of uncertainty analysis. There are two types of uncertainty analysis considering variation in input and/or model. One is single disciplinary or all-in-one integrated analysis and the other is multidisciplinary uncertainty analysis. As shown in Figure 2.10, the all-in-one approach analyzes the effect of uncertainty in initial design variables (x1 and x2) on the final performance (z); however, a multidisciplinary approach predicts the effect of uncertainty in each model in the system.

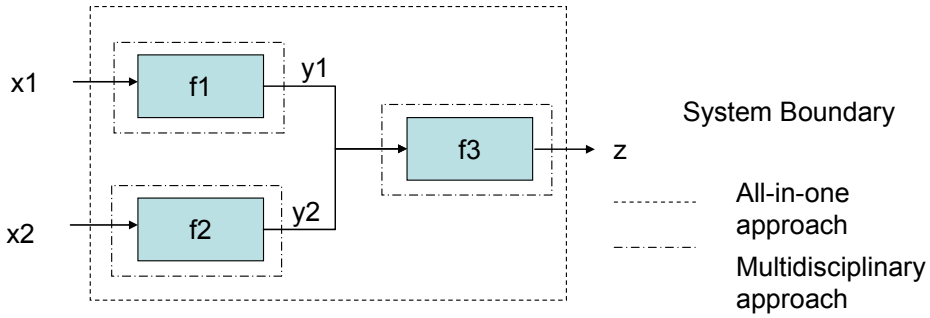

Figure 2.10 System boundary of all-in-one and multidisciplinary approaches

The single step (all-in-one) uncertainty analysis approach is rigorously studied to improve the accuracy of uncertainty analysis with limited data. The available methods are Monte Carlo simulation, Latin Hyper Cube Sampling, first and second moment methods,

and polynomial chaos expansions as discussed in Section 2.2.1. This approach is employed in many robust design methods (e.g., Taguchi method, RCEM, etc.). However, the all-in-one approach has a critical drawback in implementing all-in-one simulation or experimental models in multidisciplinary design problems. If the decomposed models are controlled by different disciplines or reside in a distributed environment, interfacing a large number of individual sub-systems in order to formulate an all-in-one simulation imposes great cost even if many computational frameworks for system integration are available.

Because of this drawback, some researchers proposed multidisciplinary uncertainty analysis and robust design methods. Only two studies have been found in this area. Gu and coauthors (Gu, et al., 2000) propose worst case propagated uncertainty analysis and robust optimization. With their approach, the first order sensitivity analysis is performed in each of the sub-systems. Final system response deviation is estimated by propagating the result of individual sub-system uncertainty analysis. Du and Chen (Du and Chen, 2002) propose efficient analysis methods to accommodate a generic probabilistic approach instead as an alternative to using worst case sensitivity analysis estimate the amount of uncertainty more accurately. In Section 2.4.1 and 2.4.2, we critically review the two approaches with respect to the requirement for robust materials design methods described in Section 2.6.

2.4.1. Robust Optimization with the Worst Case Uncertainty Propagation

In the robust optimization with the worst case uncertainty propagation (Gu, et al., 2000), worst case uncertainty propagation is employed as an uncertainty analysis method to reduce computational load; it sacrifices accuracy of the results because an uncertainty

analysis, such as Monte Carlo simulation, mostly needs a large number of samples. The authors emphasized the importance of management of uncertainty in a coupled problem of multidisciplinary system design because a coupled problem usually requires an iterative procedure for calculating "state variables" (intermediate linking variables between multidisciplinary models), and the iterative procedure keeps propagating the uncertainty in state variables. The uniqueness of this approach is that, while analyzing uncertainty, it considers not only variability of input variables but also potential bias errors of numerical procedure in a model.

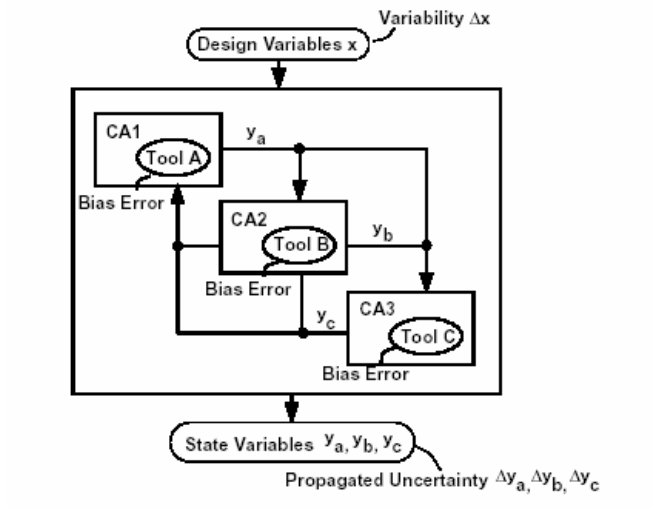

Figure 2.11 Models of multidisciplinary system design(Gu, et al., 2000)

In Figure 2.11, the authors illustrate a multidisciplinary system analysis in which a number of disciplines exchange information. The uncertainty in the states (state variables – $\mathbf{y}_a$, $\mathbf{y}_b$, and $\mathbf{y}_c$) computed by a given discipline is dependent on the variability in the design variables ($\mathbf{x}$), the bias errors in the states computed by other disciplines (contributing analyses – CA1, CA2, and CA3), and the bias error of the discipline tool (Tool A, B, and C) itself (Gu, et al., 2000). The main purpose of this approach is to

include the "propagation" of the uncertainty through the multidisciplinary system analysis. Propagated deviations of responses are given by

$$\begin{Bmatrix} \Delta y_a \\ \Delta y_b \\ \Delta y_c \end{Bmatrix} = \begin{Bmatrix} \left|\frac{dy_a}{dx}\right| \\ \left|\frac{dy_b}{dx}\right| \\ \left|\frac{dy_c}{dx}\right| \end{Bmatrix} |\Delta x| + \begin{bmatrix} |B_{aa}| & |B_{ab}| & |B_{ac}| \\ |B_{ba}| & |B_{bb}| & |B_{bc}| \\ |B_{ca}| & |B_{cb}| & |B_{cc}| \end{bmatrix} \begin{Bmatrix} |\delta_a(x, y_b, y_c)| \\ |\delta_b(x, y_a, y_c)| \\ |\delta_c(x, y_a, y_b)| \end{Bmatrix}, \quad (2.9)$$

where $B = \begin{bmatrix} B_{aa} & B_{ab} & B_{ac} \\ B_{ba} & B_{bb} & B_{bc} \\ B_{ca} & B_{cb} & B_{cc} \end{bmatrix} = \begin{bmatrix} I_a & -\frac{\partial T_a}{\partial y_b} & -\frac{\partial T_a}{\partial y_c} \\ -\frac{\partial T_b}{\partial y_a} & I_b & -\frac{\partial T_b}{\partial y_c} \\ -\frac{\partial T_c}{\partial y_a} & -\frac{\partial T_c}{\partial y_b} & I_c \end{bmatrix}^{-1}$, T_a, T_b, and T_c are analysis tools and $\frac{dy_a}{dx}, \frac{dy_b}{dx}, and \frac{dy_b}{dx}$ are "global sensitivities" (sensitivity of state variables versus single design vector). The first term of the right hand side of the equation is variability in state variables due to variability in design variables and the second term is that due to bias errors of tools. An important assumption is made for formulating the second term. The assumption is that the tool's bias error at the true variable position is about the same as that at the nominal position of input variables, such as $\delta_a(x^{true}, y_b^{true}, y_c^{true}) \cong \delta_a(x, y_b, y_c)$. Based on this assumption, the authors estimate the

approximate region of the true value of the state variables in order to consider the variability in state variables in robust design optimization.

Gu and the coauthors' approach is a computationally efficient method for estimating propagated uncertainty in the presence of variability in design variables and tools. Their method has been validated on simple and complex highly coupled examples showing that their approach is valid for quickly and pretty accurately estimating bounds on performance variability. The approach has been employed in robust design optimization to find design variables that lead to robust performance under variability in input variables and bias error of contributing analysis tools.

A few disadvantages, however, exist in this method. **First, all multidisciplinary models should be provided as differentiable forms in terms of design variables and state variables.** In reality, the models could be a mathematical form that is not differentiable or simulation (or analysis) itself. This is common in materials design. Another drawback of this approach is that **the estimated performance deviation bound could be inaccurate with the existence of large error between the potential true value and the biased nominal value.** An implicit assumption that the authors have not mentioned in the article is that the propagated uncertainty in the state variables is not expanded very far so that higher order terms of the Taylor series expansion are still ignored. Because of accumulated bias errors due to large number of iterations for finding nominal state variables, the gap between true state variables and biased nominal state variables could be large enough so that we should consider higher order terms in Taylor series expansions. In materials design, high degree of non-linearity in materials

simulation models tends to cause large amount of bias errors in estimated models; therefore, it is a serious problem in materials design.

2.4.2. Robust Optimization with the System Uncertainty Analysis (SUA) and the Concurrent Subsystem Uncertainty Analysis (CSSUA)

In Du and Chen's approach, they quantify propagated uncertainty in multidisciplinary systems using the System Uncertainty Analysis (SUA) and Concurrent Subsystem Uncertainty Analysis (CSSUA). Their configuration of a multidisciplinary system is illustrated in Figure 2.12. The subsystems have coupled variables (**Yij**), called linking variables in their paper, shared variables (**X**s) and independent variables (**X**i). Each subsystem produces system output (**Z**i).

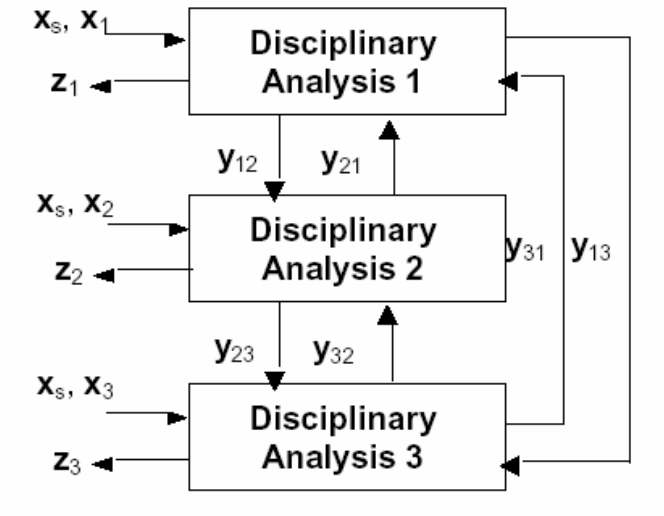

Figure 2.12 A multidisciplinary system (Du and Chen, 2002)

The procedure for quantifying system variation is as follows:

- Find mean values of Yij with given mean of Xs and Xi
- Estimate variation of Yij with given mean and variation of Xs and Xi and derived mean of Yij using First-Order Reliability Method

- Find mean value of Zi with given mean of Xs and Xi and derived mean of Yij
- Estimate variation of Zi with derived means and variations of Yij and given means and variations of Xs and Xi using First-Order Reliability Method (FORM)

Basically, the technique for estimation of deviation in variables (Yij and Zi) is similar to the technique used in Gu's approach mentioned in Section 2.4.1 but the authors use FORM instead of the Worst Case Analysis method. Therefore, the authors' approach is less conservative than Gu's approach. The difference between the SUA and the CSSUA is in Step 1. In the SUA, implicit iteration loops for finding means of Yij are often necessary and are computationally expensive. To reduce computation time, the authors use a suboptimization for finding means of Yij with parallel employment of subsystem analyses in the CSSUA. The authors argued that, when the system level analysis (finding Yij) for a system design is computationally expensive, the CSSUA reduces design lead time with parallelizing the computation. Finally, the above procedure is incorporated to a robust optimization loop to find a robust solution of the shared and independent design variables.

The SUA and CSSUA methods have similar limitations Gu's approach mentioned in previous section. In the SUA method, if the model for Yij is in an implicit form, then a large number of iterations are required to find Yij variables and the iteration will expand bias errors of the model as the number of iterations is increased. Finally, **the derived mean value of linking variables (Yij) deviates far from the unknown true position and estimated mean, and the deviation of system outputs at the incorrect mean of**

linking variables could be incorrect. Additional critical evaluation of this method is addressed in Section 2.6.

In this section, we reviewed uncertainty estimation methods, robust design methods, and multidisciplinary robust design method for propagation of uncertainty. Based on the observations, we summarize the challenges (gaps between the existing methods) in those three areas for system-based materials design in Section 2.6. In the next section, we review the graphical process representation protocols that are useful for describing a multidisciplinary robust design process network.

2.5. DESIGN PROCESS REPRESENTATION

Design process representation is an important process since the process is usually complex, collaborative, and geographically distributed, and design results are sensitive to the design process in a complex system design. A project manager and designers should agree and share the formation of a design process for efficient collaboration. In view of these needs, graphical representations of a process – processes for design, analysis, manufacturing, etc – have been studied. In this dissertation, we review two previous approaches. One is Integration Definition of Functional modeling (IDEF0), which is the industry standard for describing a process in graphical manner, and the other is P-Diagram, which has been used for describing robust design tasks. In the following two sections, we discuss the two protocols and identify the benefits and limitations. Based on this discussion, research opportunities are identified and the Research Question 3 is justified in Section 2.6.

2.5.1. Integration Definition of Functional modeling (IDEF0)

During the 1970s, the U.S. Air Force Program for Integrated Computer Aided Manufacturing (ICAM) sought to increase manufacturing productivity through systematic application of computer technology. The ICAM program identified the need for better analysis and communication techniques for people involved in improving manufacturing productivity. As a result, the ICAM program developed a series of techniques known as the IDEF (ICAM Definition) technique which included the following (NIST, 1993):

- IDEF0, used to produce a "function model". A function model is a structured representation of the functions, activities or processes within the modeled system or subject area.
- IDEF1, used to produce an "information model". An information model represents the structure and semantics of information within the modeled system or subject area.
- IDEF2, used to produce a "dynamics model". A dynamics model represents the time-varying behavioral characteristics of the modeled system or subject area.

In 1983, the U.S. Air Force Integrated Information Support System program enhanced the IDEF1 information modeling technique to form IDEF1X (IDEF1 Extended), a semantic data modeling technique. Currently, IDEF0 and IDEF1x techniques are widely used in the government, industrial and commercial sectors, supporting modeling efforts for a side range of enterprises and application domains. A design process model can be described using the IDEF0 function model. In this section, we discuss the capability of the IDEF0 function model and investigate if the IDEF0 model is appropriate for describing a complex process for designing multidisciplinary systems in Section 2.6.

IDEF0 is a modeling technique based on graphics and related text that are presented in an organized and systematic way to gain understanding, to support analysis, to provide logic for potential changes, to specify requirements, or to support systems level design and integration activates (NIST, 1993). An IDEF0 model is composed of a hierarchical series of diagrams that gradually display increasing levels of detail describing functions and their interfaces within the context of a system. The graphic diagrams define functions and functional relationships via box and arrow syntax and semantics.

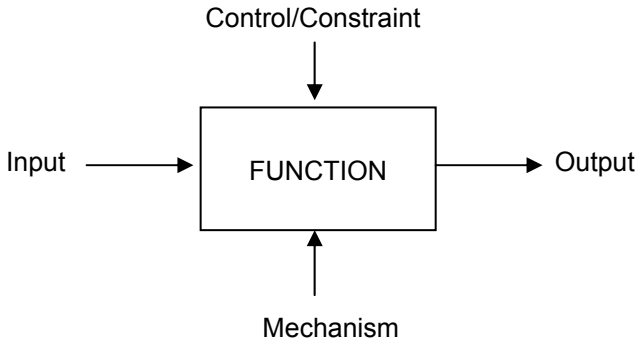

Figure 2.13 Inputs, Controls, Outputs, and Mechanisms (ICOMs) protocol of IDEF0 model

The semantics of IDEF0 model entities are defined as follows. A **Box** provides a description of activity in a designated function. The label of the box is an active verb or verb phrase that describes the function. An **Arrow** indicates information flow between multiple boxes. As shown in Figure 2.13, an arrow contains separate meaning depending on the side of the box that an arrow is connected to. Arrows entering the left side of the box are inputs. **Inputs** are transformed or consumed by the function to produce outputs. Arrows leaving a box on the right side are outputs. **Outputs** are the data or objects produced by the function. Arrows entering the box on the top are controls. **Controls** describe the conditions or circumstances that govern the function. The assumption is that an arrow is a control unless it obviously serves only as input. The bottom of a box is

reserved to indicate a **Mechanism**, which may be the person or device which carries out the function. Basically, the inputs and outputs show what is done by the function, control shows why it is done, and the mechanism shows how it is done.

A Data Flow Diagram (DFD), which is a network of ICOMs and Boxes, is used to model data flows in a system. In DFDs, each box can be further detailed into a separate sheet in which multiple decomposed ICOMs and Boxes are interconnected. An example of DFDs, representing a design process for truss structured high-speed robot arm (Wang, 2001), is illustrated in Figure 2.14.

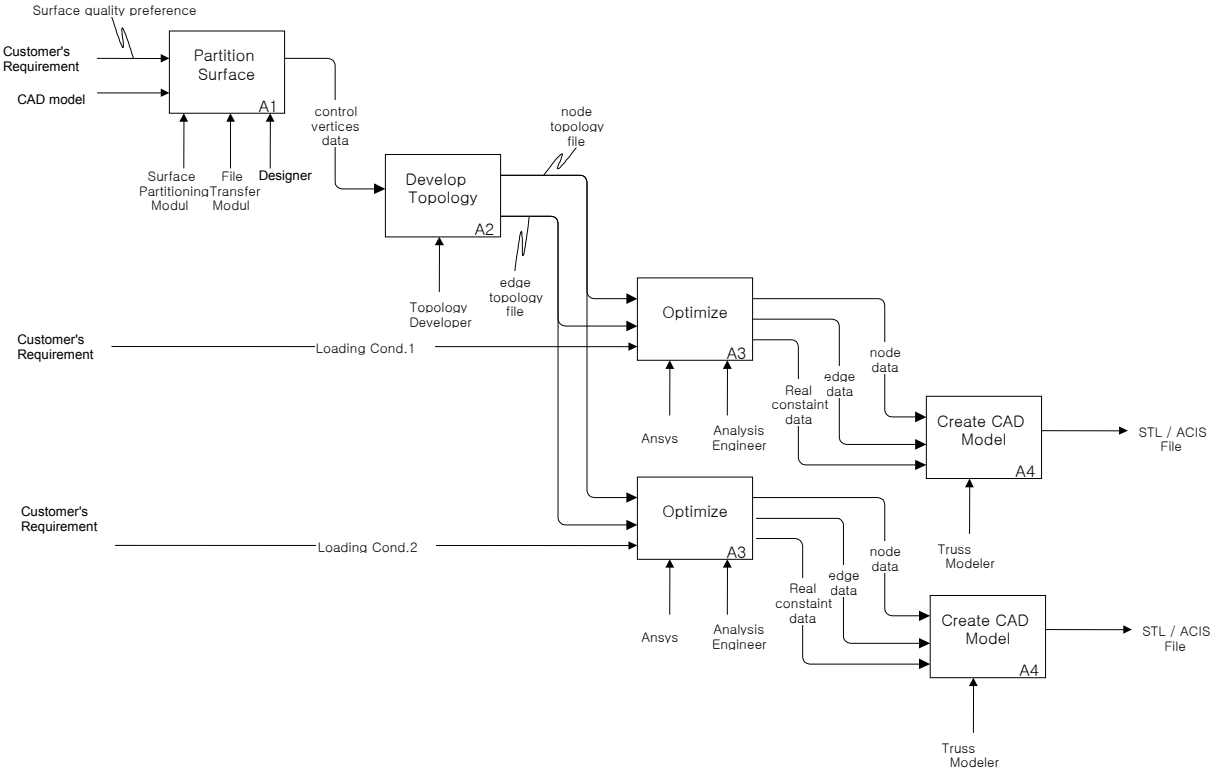

Figure 2.14 An example of DFDs of IDEF0 function model (Choi, 2001)

The IDEF0 function model has many advantages. It can be used for describing a process explicitly, comprehensively, and graphically across an entire system function process including hierarchical function relations. It is useful for explicit information sharing by graphical representation among analyst, developer, designer and project

manager. It has been successfully tested and proven in the U.S. Air Force, other government developments projects, and private industries. There are a number of commercial products that can be used for efficiently developing an individual process model using IDEF0.

In a multidisciplinary (multiscale) system design process, multiscale simulation models tend to have **various sorts of uncertainties** and those exist in activities (Boxes) and related information and tools (ICOMs). However, there is no way to represent the existence of uncertainty in systems (or processes). Based on the review of the IDEF0 models, these critical requirements for describing robust design process are not satisfied by the IDEF0 model. We discuss these limitations for applying the IDEF0 model to the representation of a multidisciplinary system design process, and justify why Research Question 3 in this dissertation is important to be answered in Section 2.6.

2.5.2. P-Diagram

Phadke (Phadke, 1989) proposes a block diagram representation of a system (product or process), which is called P-Diagram. The P-Diagram is specially established in order to represent quality characteristics in a system. In Figure 2.15, a block diagram of a product or process is illustrated.

As shown in the figure, Phadke classifies parameters that can influence the quality characteristic or response of a product into the three types, which are signal factor (M), noise factor (x), and control factor (z). Signal factors are the parameters set by a user or an operator of a product to express the intended value for the response of the product. (Phadke, 1989).

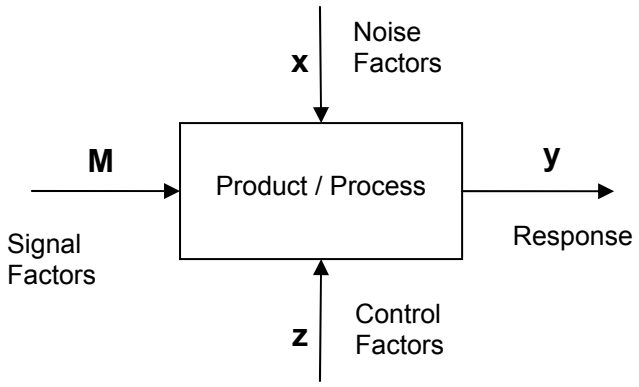

Figure 2.15 The block diagram of a product/process: P diagram (Phadke, 1989)

For example, the speed setting on a table fan for controlling air flow rate and the steering wheel angle for turning an automobile are the signal factors. The signal factors are selected by the design engineer based on the engineering knowledge of the product being developed (Phadke, 1989). Noise factors are some parameters that cannot be controlled by the designer or are very expensive to control. Only the statistical characteristics (such as mean and variance) of a noise factors can be known or specified, but the actual value is uncertain. The noise factors make response deviate from the target specified by the signal factor, and lead quality loss. Control factors are parameters that can be specified freely by a designer. Designers are responsible for selecting (designing) the control factors. Phadke recommends using the P-diagram to represent a manufacturing process or even a business system and says that identifying important responses, signal factors, noise factors, and control factors in a specific project are important tasks.

Chen and the coauthors (Chen, et al., 1996) use P-diagram in the RCEM for representing their system parameters. P-diagram is useful for classifying the parameters involved in a product or a process and describing a robust design task based on semantic graphical representation. **However, it is difficult to use for representing a process (a series of events) since it cannot represent a decision-making process that illustrates**

selected decisions on tasks (designed control factors) and its influence on other tasks (mean and variance of the response at the selected control factors). This need leads us to Research Question 3. Justification of this challenge is discussed in Section 2.6.

From Sections 2.1~2.5, we review and critically evaluate the methods and approaches in regard to the challenges in multiscale simulation-based systems design. In the next section, we summarize the limitations of the reviewed methods and justify why the research questions formulated in Chapter 1 appropriately address the requirements.

2.6. THEORETICAL STRUCTURAL VALIDATION: RESEARCH OPPORTUNITIES AND JUSTIFICATION

In this chapter, methods and approaches related to the issues addressed by multiscale simulation-based robust materials design are discussed. These methods and approaches include uncertainty classifications in engineering systems (Section 2.1), uncertainty analysis and management methods (Section 2.2), robust design methods (Section 2.3), multidisciplinary robust design methods (Section 2.4), and semantic graphical process representation approaches (Section 2.5). As a process for theoretical structural validation as shown in Figure 2.16, we critically evaluate the capabilities of those methods and approaches with respect to the needs of multiscale simulation-based materials design mentioned in Chapter 1. Finally, we identify research opportunities from these reviews and justify the research questions and hypotheses posted in Section 1.4.3.

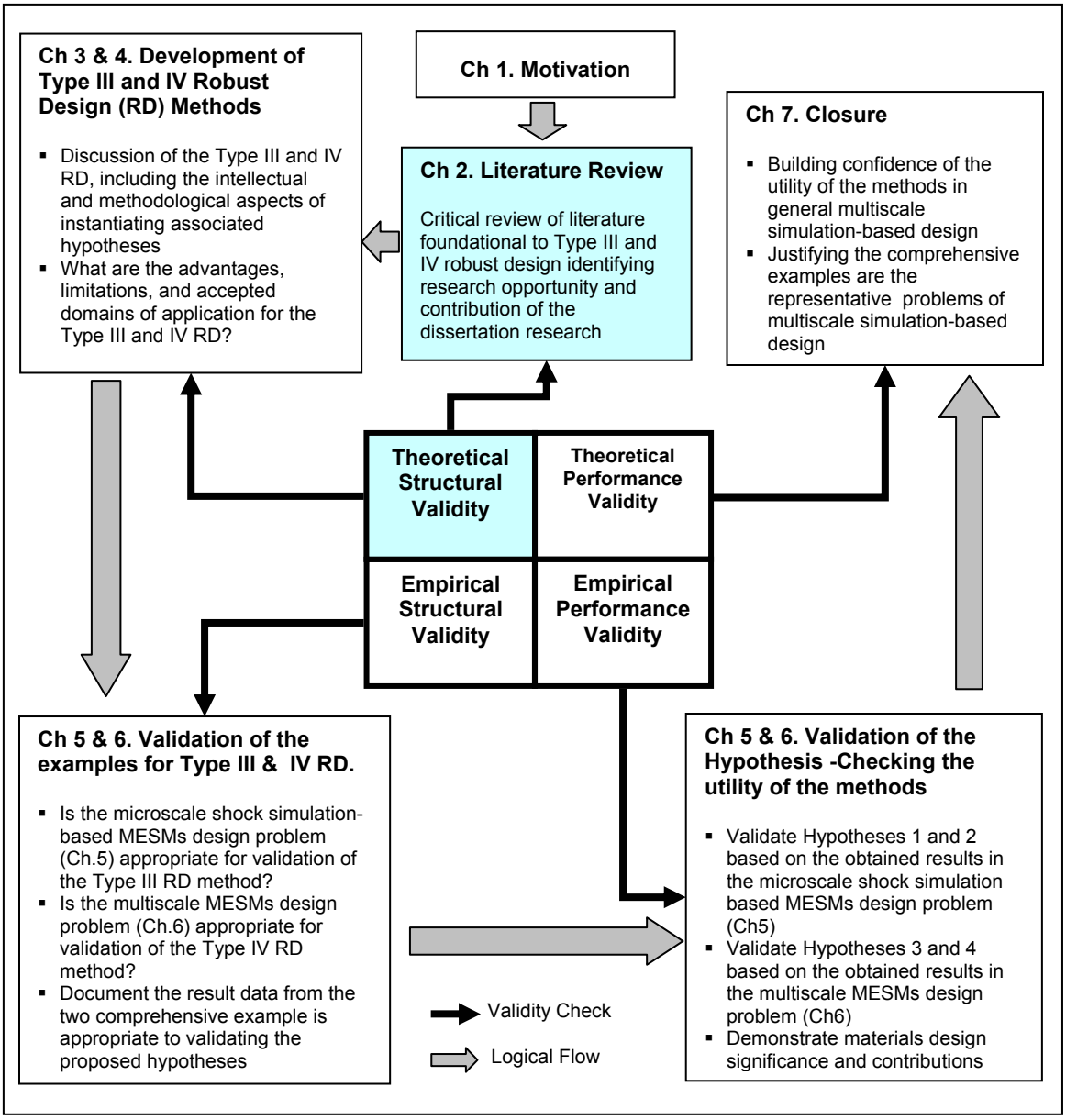

Figure 2.16 Validation square roadmap

In Table 2.2, the evaluation results in existing methods regarding the issues addressed by designing material systems are summarized. Based on the evaluation results, we justify that the research questions are properly formulated.

Table 2.2 Summary of critical evaluation of existing methods

Issues	Methods	Evaluation results	Justification
Classification of uncertainty	Classification by the nature of uncertainty	▪ The classification is difficult to incorporate with mathematical modeling in systems design	N/A
	Classification by the sources of uncertainty	▪ There are disagreements among the researchers for defining types of uncertainty. ▪ None of the reviewed approaches studied explicitly the type of uncertainty in computational models that predict material behaviors.	N/A
Analysis and management of uncertainty	Existing methods for uncertainty analysis (Interval analysis, Monte Carlo method, etc.)	▪ Uncertainty analysis methods for non-deterministic system models have not been developed in literature except for Monte Carlo (MC) method. ▪ The MC method is computationally intensive to apply into materials design	Computationally efficient uncertainty quantification method is required – R.Q. 2
	Methods for reducing uncertainty	▪ Designers must have some true results. In some cases, we cannot obtain any better data than current data due to severe uncertainty in a system or restrictions of computational or experimental expenses, which is the case of multiscale materials design	Robust design approach is necessary – R.Q. 1
Robust design under uncertainty	Type I robust design (Taguchi method)	▪ No study has been done for establishing robust design methods for designing a system to be insensitive to uncertainty and unquantifiable variability (such as morphology changes in materials discussed in Section 1.2.4) in a system model.	Type III robust design is necessary – R.Q. 1 and R.Q. 2
	Type II robust design (RCEM, DCI)		
Robust design of multidisci-plinary systems	Gu and coauthors' approach	▪ Estimated performance deviation bound could be inaccurate with the existence of large error between the potential true value and the biased nominal value. ▪ unquantifiable model structural uncertainty is not considered ▪ If one of the models in the series is changed, then whole process after the changed model needs to be repeated for estimation of propagated uncertainty.	New method for Type IV robust design is necessary – R.Q. 3 and R.Q. 4
	Du and Chen's approach		
Design process representation	IDEF0	▪ It is impossible to represent the existence of uncertainty in systems (or processes).	Robust design process modeling protocol including the aspects of uncertainty is necessary – R.Q. 3
	P-Diagram	▪ It is difficult to use for representing a process (a series of events) since it cannot represent a decision-making process that illustrates selected decisions on tasks (designed control factors) and its influence on other tasks (mean and variance of the response at the selected control factors).	

As discussed in Section 2.1, many classifications and taxonomy have been suggested by researchers as discussed. These are categorized by the nature of uncertainty and the sources of uncertainty. Since a multiscale simulation-based design incorporates multiple computational models that predict system behaviors, it is better to adapt the **classification by the sources of uncertainty**. We may classify the uncertainties involved in a development process of a simulation model as epistemic uncertainty, and inherited uncertainties that a simulation model produces as aleatory uncertainty. For example, one of the epistemic uncertainties is the uncertain boundary conditions assumed in a computational analysis model. The boundary conditions may involve some idealization processes which could not be real system conditions. The non-deterministic behavior of a computational model due to random process, simulating real world condition on a system, is an example of aleatory uncertainty.

None of the reviewed approaches, however, studied explicitly the type of uncertainty in computational models that predict material behaviors. Since there are already well configured uncertainty classifications as shown in Section 2.1.2 depending on the sources of uncertainty, we will not classify our own taxonomy in this dissertation. Instead, we will **investigate instances of computational material models and select the best classification** among the reviewed classifications for describing the types of uncertainty in multiscale computational materials behavior models. **The purpose of the classification of uncertainties is to select or establish an appropriate approach for dealing with uncertainty**. For example, designers should measure the variability of aleatory uncertainty and consider the variability effects on the system design, such as robust design or design for reliability. However, since we cannot measure the amount of

epistemic uncertainty, we need to reduce the uncertainty increasing our knowledge or establish other types of robust design technique than aforementioned robust or reliable design techniques.

In Section 2.2, the methods and techniques for estimating the degree of uncertainty in a system or reducing unquantifiable uncertainty are reviewed. High fidelity computer simulations as well as real experiments tend to incorporate with random processes inside so that predicted system responses include irreducible random variability. However, as shown in Table 2.1, **uncertainty analysis methods for non-deterministic system models have not been developed in literature except for Monte Carlo method.** Monte Carlo method is the only method for quantifying a non-deterministic response variation with input parameters probability distributions, but it is computationally too intensive. Therefore, **an uncertainty analysis method for non-deterministic simulation, which is computationally efficient, is indispensable.** This requirement leads to Research Question 2. In Research Question 2, we propose to establish a computationally efficient uncertainty propagation method for non-deterministic simulation, which is indispensable for robust design exploration that calls the uncertainty analysis routine many times.

In Section 2.3, we review robust design methods for designing a system to be insensitive to uncertainty. As discussed in this review, we may design a system to be insensitive to noise factors' variation using the Taguchi method and a system to be insensitive to control and noise factors' variation using Robust Concept Exploration. However, **no study has been done for establishing robust design methods for designing a system to be insensitive to uncertainty and unquantifiable variability**

(such as morphology changes in materials discussed in Section 1.2.4) in a system model.

In the RCEM, uncertainty in a metamodel cannot be considered while exploring a design space; therefore, if the metamodel is uncertain due to lack of data or higher order of non-linearity, then the design exploration result could be inaccurate. Additionally, in the RCEM, the variability in control factors as well as noise factors is considered in the robust design process; however, the RCEM employs only the most probable fitted function of the potential set of metamodel candidates that has been constructed from simulation or experimental data. Even though random variability of a system is quite large, the RCEM employs only the most probable fitted function without considering the large variance. In other words, non-deterministic behavior of a system cannot be taken into account in systems design. **Neither the Taguchi method nor Suh's axiomatic design can meet the aforementioned requirements.** In this sense, the Research Question 1 is a particularly important challenge for multiscale simulation-based design problems, such as materials design, since the simulation model in small scale simulation tend to be non-deterministic due to random structures of heterogeneous materials, as mentioned in Chapter 1.

In Section 2.4, multidisciplinary robust design methods for propagation of uncertainty along a multidisciplinary analysis chain are reviewed. However, these methods have the following limitations for applying into a multiscale simulation-based design problem.

- The previous methods, Gu and Du's approaches mentioned in Section 2.4.1 and 2.4.2, still need **intense information interface across the boundary of sub-system** in order to estimate final performance variation. This is true even if the

amount of information passed is reduced compared with all-in-one uncertainty analysis. This is because the uncertainty analysis process and design exploration (optimization) process are tightly coupled. Whenever new design variables are given, the subsystems analysis should be done in response to the request in real time. This sequential uncertainty propagation in those methods becomes more difficult in a distributed environment.

- In those methods, **the full power of parallel computing still cannot be employed.** In the CSSUA method, the authors parallelize the associated subsystem analyses computing for identifying the means of linking variables; however, since the robust optimization process is sequential and the uncertainty analysis process is a sub-process of the optimization, we cannot fully parallelize the uncertainty analysis process that takes most of the computing power. Parallel computing is a beneficial approach since the computational intensity in multiscale simulation is extremely high.
- The mean and variance (or worst case deviation) of only the final performance are considered in the design optimization. Those of the linking variables are not considered for determination of design variables, for which a designer may miss a better solution in consideration of model structural uncertainty. There is **no consideration of unquantifiable model structural uncertainty** in sub-systems. We discuss it in detail in Chapter 5.
- As mentioned in Sections 2.4.1 and 2.4.2, those methods analyze the amount of uncertainty when **each sub system model has been configured as a differentiable mathematical model**. However, in multiscale materials design,

the model could not be such a mathematical model but a simulation or analysis itself.

- If one of the models in the series is changed, then **whole process after the changed model needs to be repeated** for estimation of propagated uncertainty. It is very important when uncertainty analysis of a system consistently used in a product life cycle.

Research Question 4 is formulated to overcome the aforementioned limitation in the multidisciplinary robust design methods.

2.7. SYNOPSIS OF CHAPTER 2

In this chapter, existing formulations and approaches for robust design are critically reviewed. In Section 2.1, the related works in the area of uncertainty characterization and definition are reviewed. Uncertainty is classified by the nature or source of uncertainty. In each classification, a number of approaches are proposed. In this review, we found that the classification by the source of uncertainty is more appropriate for dealing with uncertainties in multiscale simulation-based design. In Section 2.2, methods for quantifying uncertainty are discussed in detail. There are many available methods for quantifying uncertainty (variability), but few of them are applicable to non-deterministic simulation or experimental model. It is also identified that the computational intensity for uncertainty analyses is an important challenge for multiscale simulation-based materials design. In Section 2.3, methods for robust decision making based on the quantified uncertainty are reviewed. The available methods for Type I and II robust design and those extensions are reviewed. From this review, it is identified that new robust design

methods in order to deal with other types of uncertainties in multiscale simulation-based materials design are necessary. In Section 2.4, robust decision making methods in multidisciplinary systems design, which is an emerging area in robust design, are discussed. Two approaches that were recently developed are critically reviewed. From this review, new requirements for solving multiscale, multifunctional materials design problems are established. In Section 2.5, graphical semantic models for representing a multidisciplinary collaborative design process are discussed. In each section, sensitive issues are addressed in developing the approaches. Finally, in Section 2.6, gaps among the existing methods are identified and requirements of new robust design methods are posted in order to justify the contributions of the research questions in Chapter 1.

In the next chapter, we discuss a new type of robust design method, Type III robust design, in order to accommodate multiscale simulation-based systems design extending Type I and II robust design reviewed in this chapter.

CHAPTER 3

TYPE III ROBUST DESIGN: THE ROBUST CONCEPT EXPLORATION METHOD WITH ERROR MARGIN INDEX (RCEM-EMI)

The main purpose of this chapter is to develop a method that facilitates Type III robust design. In Sections 3.1 and 3.2, types of uncertainty in engineering systems, including material systems, are characterized. In Section 3.3, Type III robust design is defined along with the Type I and II that have been reviewed in Section 2.3. In Section 3.4, a robust design method, called the Robust Concept Exploration Method with Error Margin Index (RCEM-EMI) is proposed and the overall procedure of the RCEM-EMI is introduced. In Sections 3.5~3.9, the RCEM-EMI is explained in detail. we discuss clarification of design tasks (Section 3.5) and DOE using distributed collaborative simulation infrastructure (Section 3.6). In Section 3.7, we discuss the third step of the RCEM–EMI, which is estimating mean and prediction interval models. Uncertainty quantification methods in Section 2.2 are revisited and efficient uncertainty estimation methods for computationally expensive experiments and simulations are introduced. In Sections 3.8 and 3.9, the mathematical construct of the Error Margin Indices is explained, followed by a compromise Decision Support Problem formulation with the Error Margin Indices. The Design Capability Indices described in Section 2.3.3 are revisited in Section 3.8. In Section 3.10, the validity of theoretical structure of the RCEM-EMI is checked based on a simple example. The RCEM-EMI approach is summarized in Section 3.11.

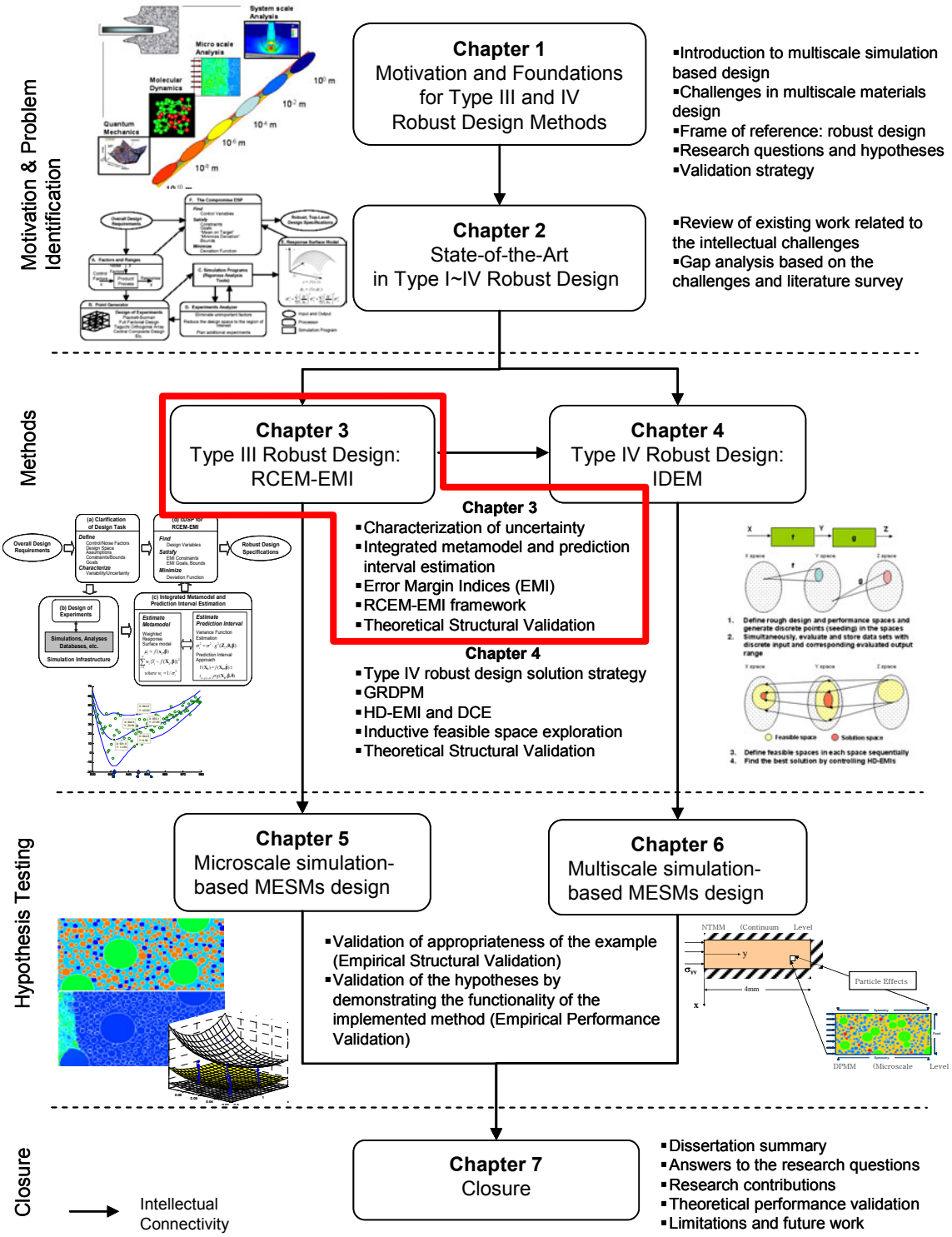

Figure 3.1 Dissertation roadmap

3.1. CHARACTERIZATION OF UNCERTAINTY

Potential sources of uncertainty in a system include human errors, manufacturing or processing variations, operating condition variations, inaccurate or insufficient data, assumptions and idealizations, lack of knowledge, and many others. Manufacturing variations are manifested as tolerances in part dimensions, missing small sized parts or joints, and porosity in the base material. Operating conditions, such as the ambient temperature and air flowrate, may vary as well. In addition to these sources of uncertainty, the finite element analyses required for evaluation of system behavior incorporate a number of simplifying assumptions. Examples include idealized modeling of boundary conditions as well as mesh size. Many of these simplifying assumptions are required in order to make the analyses fast enough for a complex, iterative design process. Since non-deterministic factors in a system sometimes produce considerable errors in predicted system responses, uncertainty is an important factor for designers to consider when making decisions regarding design specifications.

Before discussing the method for Type III robust design, it is necessary to categorize the types of uncertainty in a model, since quantification of the uncertainty in the model depends on these uncertainty types. Extending the classification of uncertainty types by Isukapalli and coauthors (Isukapalli, et al., 1998), the types of uncertainty are categorized as follows.

- Variability (natural uncertainty): uncertainty due to the inherent randomness or unpredictability of a physical system; this is irreducible and can only be quantified in a statistical sense. ***The variability can be further classified as parameterizable and unparameterizable. Parameterizable variability can be***

configured as variance in numeric form, but unparameterizable variability cannot.

- Model parameter uncertainty (data uncertainty): this is incomplete knowledge of model parameters/inputs due to insufficient or inaccurate data; it is reducible by sufficient data or accurate measurements.
- Model structure uncertainty (model uncertainty): this is uncertain model formulation due to approximations and simplifications in a model; it is reducible by improving model formulation.

These uncertainty types coexist within any system. While some types can dominate a system, others may be essentially negligible. For example, the uncertainty associated with Linear Cellular Alloy (Seepersad, et al., 2004), is partially natural, irreducible uncertainty (i.e., manufacturing variability) and partially reducible uncertainty (i.e., human measurement error and resulting inaccuracy of data). Variations in wall thickness typically indicate the existence of manufacturing variability while measurement error is assumed to be negligible. Strictly speaking, however, the uncertainty in wall thickness exhibits both types of uncertainty, and manufacturing variation is the dominant factor in the system. Another relevant example is measuring variability in a system response based on a limited number of data points. Here, the uncertainty of the system response may be attributed to both natural uncertainty and parameter uncertainty due to the limited number of data points. As the amount of data increases, the parameter uncertainty is reduced, and the system variability dominates the measurement interval. Multiple types of uncertainty coexist in any system, which makes identification of dominant sources of uncertainty a difficult and important step in the design process.

3.2. UNCERTAINTIES IN MATERIALS DESIGN

In this section, the microscale shock simulation model for designing Multifunctional Energetic Structural Materials (MESM) that is briefly introduced in Section 1.1.2 is discussed as the examples of uncertainty in materials design. The MESMs, which may be composed of Reactive Powder Metal Mixtures (RPMMs), can deliver superior energetic performance. In order to study the microscale shock-induced reaction initiation behavior of the RPMM, the microscale shock simulation model is developed by Austin and McDowell in the Georgia Institute of Technology (Austin, 2005).

Analysis of the Al-Fe_2O_3 RPMM is conducted by: (1) generating a physically realistic microstructure, (2) performing a shock simulation, and (3) extracting relevant results from the simulation. The components of the statistical volume element (SVE) in the shock simulation model are shown in Figure 3.2.

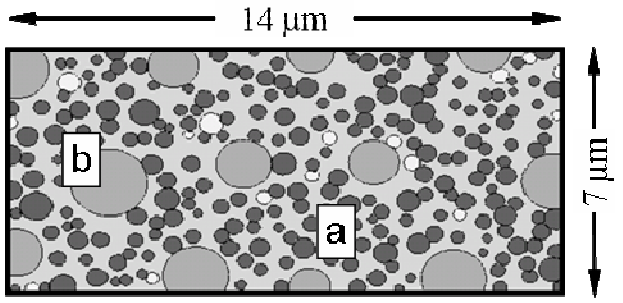

Figure 3.2 Depiction of a Statistical Volume Element (SVE) of the Reactive Particle System (20% epoxy content by weight). Markers indicate: (a) iron oxide agglomerates and (b) aluminum particles; the white circular entities are voids (Austin, 2005)

Constituent phases include aluminum particles (Al-1100), agglomerates of iron oxide particles (Fe_2O_3), an epoxy binder (Epon 828), and interspersed voids. This two-dimensional microstructure is randomly generated using a constrained Poisson process. Particles/voids are assumed to be spherical in three dimensions, and their respective sizes

are normally distributed according to mean particle/void sizes and corresponding variances; particle/void locations are uniformly distributed in the plane.

In the following three sections, the types of uncertainty in materials design are discussed based on this simulation model.

3.2.1. Variability (Natural Uncertainty) in the RPMM Shock Simulation

One of the challenges in designing an RPMM is that the input variables may have variability by natural randomness. For example, the volume fraction of each material, that is a controllable factor (or control factor), could have random variability. Even though a designer determines a volume fraction of Al as a design solution, the real volume fraction of Al may vary from the design specification due to the randomness in material processing. It could produce unexpected performance (reaction initiation) variation in a manufactured RPMM. Additionally, some input variables cannot be controlled or are difficult for a material designer to control, and the variability in the uncontrollable factors (noise factors) affect on the material's performance. For example, the variances of particles' size among the RPMM input variables are very hard or expensive for designers to control. In designing an RPMM, it is necessary for a material designer to consider the variability in controllable and uncontrollable factors since the variability could cause a serious system performance defect. These are "*parameterizable variability*" due to natural randomness, which is not reducible.

Another type of variability due to the random particle generation process is discussed in the previous section. The simulation results – the estimations of reaction initiation - have random variability even with a fixed set of all input variables. This implies that the system has other noise factors which have not been modeled as input parameters. During

the shock simulation, each instantiation of an SVE of the material for purposes of analysis incorporates "random" assignment of particular positions using a constrained Poisson point process that prevents particle overlap.

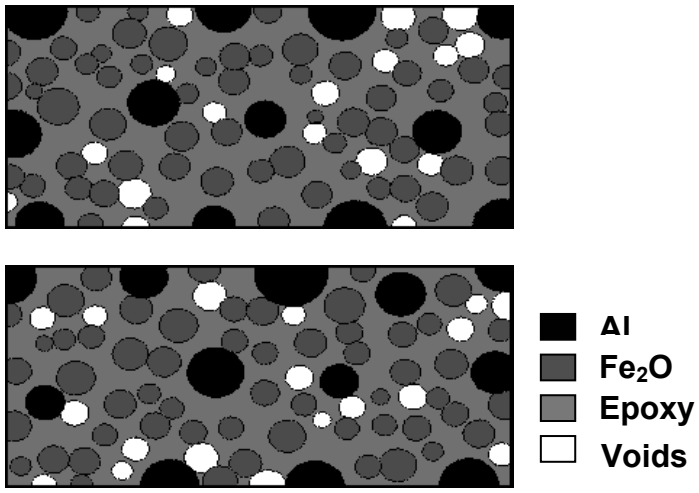

Figure 3.3 An example of the random assignment of particle microstructure with a fixed set of input parameters

This randomness, shown in Figure 3.3, is difficult to parameterize as a numeric variable in the system model. Furthermore, the randomness causes large variances in the simulation results and should be considered in designing the geometric attributes of the mixture so that a designer ensures his or her design will meet specified performance requirements with regard to reaction initiation. The material's performance variance due to the randomness, which is difficult to parameterize, is defined as "*unparameterizable variability*". Unparameterizable variability should be considered in exploring the design space to find solutions that are robust against this variability. This type of uncertainty originating from microstructure variation is a hallmark of the simulation of performance of innumerable material systems.

3.2.2. Model Parameter Uncertainty (MPU) in the RPMM Shock Simulation

As discussed in Section 3.1, different types of uncertainty can co-exist in an engineering model. The RPMM shock simulation model also has the mixed type of uncertainty because of two different uncertainty sources, which are unparameterizable variability discussed above and lack of data due to the computationally intensive shock simulation. If a system, mostly based on computer simulation, is deterministic, then material designers need to perform single simulation at each evaluation point during a design exploration process (such as, optimization process). However, **if a system is non-deterministic due to unparameterizable variability, then designers need a large enough numbers of samples** at each evaluation since the accuracy of a system variability estimation depends on the sampling size.

The most accurate way of designing a non-deterministic system considering both unparameterizable variability as well as variations in control and noise factors is to perform Monte Carlo simulation and obtain statistical analyses of the variability. This approach requires an extremely large number of experiments (more than 1,000~10,000 in many cases) for the variability analysis even at a single evaluation point during a design exploration process. If the sampling size is not large enough, then the estimated system behavior, such as the estimation of system performance mean and variance, based on the small size samples are not accurate enough. The uncertainty in estimating a system's behavior due to lack of data in a computationally intensive shock simulation is model parameter uncertainty. In general, analyzing nonlinear and dynamic behavior of materials with explicit microstructures, such as the shock simulation of an RPMM,

requires a large amount of computational resources; this is another hallmark of materials design involving evolutionary, non-equilibrium processes.

3.2.3. Model Structure Uncertainty (MSU) in the RPMM Shock Simulation

As discussed in Section 3.1, Model Structure Uncertainty (MSU) is due to uncertain assumption and idealization. In the RPMM shock simulation discussed in the previous section, there are a number of assumptions and simplifications that cause MSU. First, the actual geometry of the constituent particles in the mixture is quite complex, and it needs to be approximated in the finite element models. The shapes of individual iron oxide subparticles are block-like rectangles as shown in Figure 5.2; however, the shapes of the iron oxide agglomerates formed by the subparticles are difficult to quantify. The real geometry of voids in the mixture is unknown, since it is difficult to differentiate the shape of voids from the microscopic images. This complexity of the actual microstructure is simplified so that the cross sections of all constituents are circular.

Second, the geometry of the microstructure is further simplified by assuming 2-D circles (i.e., cylinders in 3-D); however, the actual shape of the particles in the mixture is spheres. This simplification is necessary in explicit Eulerian hydrocode[4] calculation, since the computational expense of 3-D calculations is very large. Because of the simplification, generated area fractions of constituent particles are significantly less than those measured from the sectional micrograph of the mixture.

Third, this computational model includes uncertainty due to the limited knowledge of the constitute model of iron oxide. No model whatsoever (physically-based or empirical)

[4] The Eulerian hydrocode (RAVEN) has been made available to us by David Benson of the University of California, San Diego.

is currently available in the open literature for the iron oxide phase (Austin, 2005); therefore, a simple elastic-plastic model has been adopted, consisting of an initial linear elastic response followed by linear isotropic strain-hardening.

Forth, the combustion phenomena of the shock induced reaction initiation in the mixture are quite complicated; therefore, a number of assumptions and approximations must be made to idealize the processes involved in thermal explosion. In this model, it is assumed that the reaction rate depends on the temperature only. This assumption neglects (i) the consumption of reactants, and (ii) any temperature dependence of the pre-exponential factor (Austin, 2005). This uncertainty is one of the reasons for multiscale modeling incorporating a continuum level non-equilibrium thermodynamics mixture model discussed in Section 6.1.

In addition to the aforementioned assumptions and simplifications, there are a number of other assumptions are made. It is assumed that the SVE in the shock simulation is subjected to a nominally one-dimensional shock wave in a 2-D multi-material Eulerian hydrocode which takes into account the effects of heat transfer. The plane strain assumption is invoked in order to reduce the true three-dimensional nature of shock loading to a more tractable two-dimensional case. A compressive shock wave is propagated though the mixture by applying a velocity boundary condition to the SVE. The velocity boundary condition is ramped up during the first stage of the simulation according to a quadratic function of time in order to avoid spurious oscillations in the solution associated with instantaneous loading. Mesh density of the finite element model for the mixture also affects on the simulation results. Higher mesh density will produce more accurate results, but it is limited by the computational expenses.

These assumptions and idealizations due to improving computational efficiency, lack of data, and incomplete knowledge of the system causes the errors in the estimation of the RPMM behaviors based on the simulation results. The inaccuracy due to the above causes is the example of Model Structure Uncertainty. In the next section, the methods and techniques for managing these uncertainties in multiscale simulation-based materials design are reviewed.

3.3. TYPE III ROBUST DESIGN

Based on the definitions and sources of uncertainty discussed in Section 3.1 and 3.2 and the available types (Type I and II) of robust design discussed in Chapter 1, it is necessary to define a third type of robust design, called Type III robust design. **Type III robust design focuses on obtaining design solutions that are insensitive to variability or uncertainty embedded within the model used.** This embedded uncertainty typically differs from uncertainty in noise and control factors because variability or uncertainty may exist in the parameters of constraints, metamodels, and equations. This is due to ***the unparameterizable variability and model parameter uncertainty*** mentioned in Section 3.2. A robust design method incorporating Type I, II, and III has not yet been studied and is the focus of the work presented here. Type I and II robust design methods are illustrated in Figure 3.4 comparing with the optimal solution.

A deviation (or objective) function, which represents the system's response, is illustrated as the solid curve in Figure 3.4. The objective of the design is to minimize the objective function. The normal optimal solution, which is obtained based on the solid objective function, lies on the minimum point of the curve.

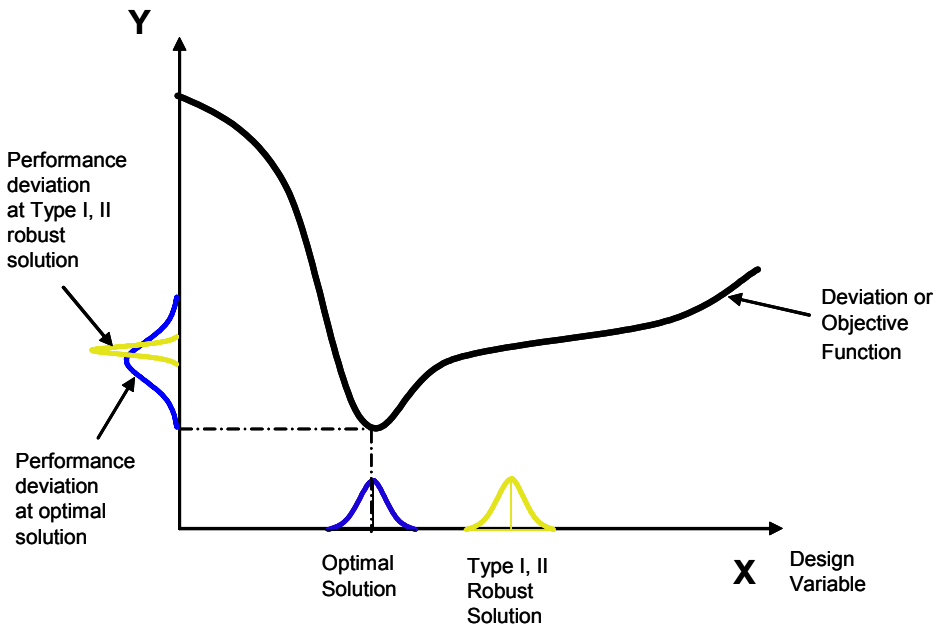

Figure 3.4 An illustration of Type I and II robust design

Considering the variation in design variable x, designers find a flat region beside the optimal point in Type I and II robust design approach, because the distribution of the performance at the Type I and II robust design solution point is smaller than the distribution of the performance at the optimal solution point even though the mean performance is a bit sacrificed. This means the system performance is robust against outer disturbance (variation in x) at the robust solution point.

On the other hand, Type III Robust Design is illustrated in Figure 3.5. In the figure, the same objective function curve is employed to show the differences among the optimal solution, Type I and II robust solution, and Type I, II and III robust solution. A deviation (or objective) function, which represents the system's response, is also illustrated as a solid curve. In addition, two dotted curves are added around the objective function representing uncertainty limits, which is due to unparameterizable variability, model parameter uncertainty, or both. Considering not only the objective function but also the

two uncertainty limits, the optimal and the Type I and II robust solution has larger performance deviation than the Type I, II, and III robust solution.

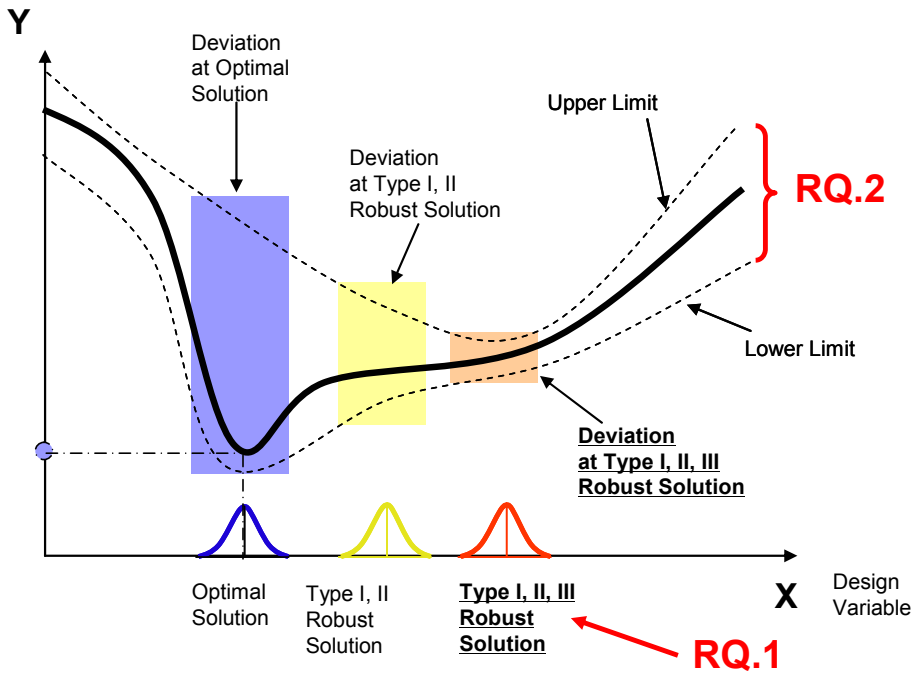

Figure 3.5 An illustration of Type I, II, and III robust design

For this reason, designers need to search for the Type I, II, and III robust solution rather than the other two solutions when the objective function has variability and model parameter uncertainty. Research Question 1 is formulated in Section 1.4 to effectively find the Type I, II, and III robust solution. Research Question 2 is formulated to efficiently capture the uncertainty limits. Based on the discussion in Sections 3.2~3.3, we identify two main requirements for multiscale simulation-based robust design. A robust design method should (a) **be computationally efficient** and (b) **incorporate all types of robust design, namely, Types I, II, and III.** The strategy proposed in this chapter is a robust design method incorporating an approximate model and uncertainty bounds of the model, which takes into account input parameters variation,

unparameterizable variability and model parameter uncertainty in models in order to find robust ranged sets of design specifications. Approximate models and error bounds are used in order to reduce the computational expenses for uncertainty analyses so that the design method could be applicable to computationally intensive simulation or expensive experiments. An approach for Type I, II, and III robust design is discussed in the next section.

3.4. THE ROBUST CONCEPT EXPLORATION METHOD WITH ERROR MARGIN INDICES: TYPE I, II, AND III ROBUST DESIGN

In this section, the Robust Concept Exploration Method with Error Margin Indices (RCEM-EMI) is proposed as a method for Type I, II, and III robust design. The overall procedure of the framework is shown in Figure 3.6.

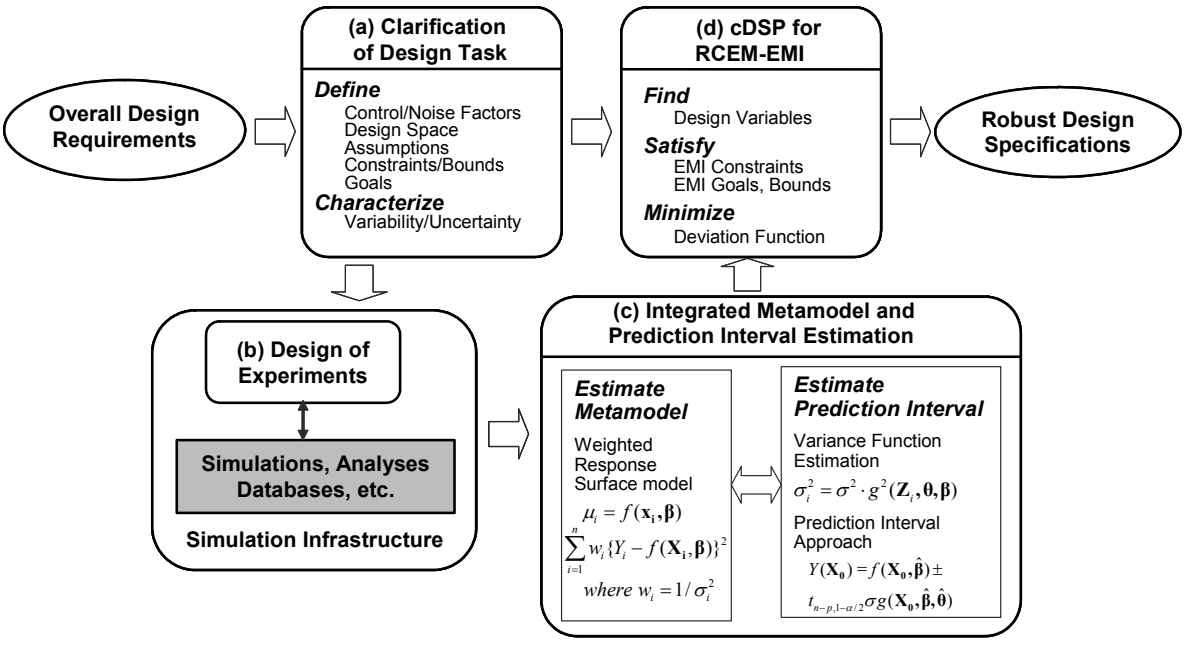

Figure 3.6 The RCEM-EMI construct

Following the RCEM-EMI construct, designers obtain robust ranged sets of design specification from design requirements. The procedure consists of (a) clarification of the design task, (b) DOE and simulation, (c) integrated metamodel and prediction interval estimation, and (d) design space search using the cDSP for the RCEM-EMI. In Step (a), a designer first clarifies his or her task based on the given design requirements by defining design variables, a design space, assumptions, constraints and bounds, and design goals. The designer also characterizes variability and uncertainty in design variables and the system model itself.

In Step (b), simulations are designed and performed using the simulation infrastructure given the design space and variables from Step (a). The obtained results of the simulations are transferred to Step (c).

In Step (c), a designer formulates a metamodel for rapid mapping of the design space to performance based on the data obtained in Step (b). The metamodel should be iteratively updated based on the estimated variance function until the estimation parameters in the metamodel and variance functions converge. The prediction interval estimation task in this step provides upper and lower uncertainty bounds around the mean response model.

In Step (d), the response surface model and upper/lower bounds from Step (c) alongside the variability in design variables from Step (a) are synthesized in the cDSP for the RCEM-EMI. The cDSP for the RCEM-EMI is solved using a search algorithm in order for a designer to find robust ranged sets of design specifications.

In this section, the steps of the RCEM-EMI are overviewed. In the following sections, the approaches in the steps of the RCEM-EMI are explained in detail. In Section 3.5,

clarification of the design task (Step a) is discussed. In Section 3.6, the computational infrastructure for DOE and simulation (Step b) is discussed. In Section 3.7, the procedure for integrated metamodeling and prediction interval estimation (Step c) is discussed. In Sections 3.8 and 3.9, cDSP for solution search incorporating Error Margin Indices (EMIs) (Step d) is discussed.

The mathematical constructs for metamodeling, variance function modeling, and EMI goal formulation are introduced in Sections 3.7 ~ 3.9. The sections include detailed mathematical approaches for (a) quantification of variability and parameter uncertainty, (b) formulation of Error Margin Indices, and (c) robust decision making based on the cDSP with EMIs.

3.5. CLARIFICATION OF DESIGN TASK

In this section, a process for clarifying a design task, which is Step (a) of the construct of the RCEM-EMI shown in Figure 3.6, is discussed. This task is an important step since the design goals, design parameters, uncertainty identification, and strategy for design exploration are determined in this process.

First, design goals need to be identified from design requirements. *What performance criteria (responses) should be selected?* For example, if designers are interested in cooling an electronic chip, they need to measure the heat transfer rate in the system. When designers need to identify the capability of penetration of a missile, then they need to measure the depth of penetration into a target. In other words, designers need to identify a parameter that indicates the system capability for a specific purpose when designing a system. Once goal parameters for a design task are identified, then it is

necessary to identify target values. In the RCEM-EMI, requirement limits need to be identified. Depending on the type of a goal, the designer's preferences can be classified as 'smaller is better', 'nominal is better', or 'larger is better'. For each type, the requirements that need to be identified are an upper requirement limit, upper and lower requirement limits, and a lower requirement limit, respectively. For example, a requirement limit for a cooling device design is a minimum heat transfer rate (a lower requirement limit) that is necessary for proper operation. Higher heat transfer rate is desirable.

Once goals and requirement limits are formulated, then the next step is identifying control and noise factors that affect the system performances. As discussed in robust design method reviews in Section 2.3, factors that can be easily controlled by designers or manufacturers are control factors, and factors that cannot be controlled are noise factors. The number of control and noise factors determines the number of experiments (or simulations) that are necessary for establishing a system metamodel and variance function model in Step (c) in the RCEM-EMI. It is important to eliminate the factors that are relatively unimportant for system responses. Chen and coauthors (Chen, et al., 1996) proposed an iterative screening procedure for identifying unimportant factors using the response surface method.

Once control and noise factors are identified, system constraints need to be established in terms of the factors. System constraints include design space, which are bounds on control and noise factors, and any other constraint conditions that are necessary. After design goals and factors are identified, the next step is identifying uncertainty in a system. As discussed in Section 3.1 and 3.2, uncertainty in a system could be variability in

control and noise factors (parameterizable variability), variability embedded in system behavior (unparameterizable variability), assumption and idealization of system analysis model or experiment (model structure uncertainty), and limitation of data acquisition (model parameter uncertainty). Examples of uncertainty classification using a microscale shock simulation-based RPMM (Reactive Particles Metal Mixture) design problem are discussed in Section 3.2. In the RCEM-EMI, it is recommended to identify uncertainties in a system and classify those in terms of the types discussed in Section 3.1. This is an important task for the RCEM-EMI as well as any other robust design task.

3.6. DESIGN OF EXPERIMENTS (DOE) AND SIMULATION

Based on the control and noise factors identified in the previous section, it is necessary to design experiments (plan simulation) – Step (b) in Figure 3.6 - that should be performed for building an accurate mean response model and conditional variance models. There are many DOE techniques available for characterizing a system response in terms of the control and noise factors. Taguchi (Taguchi, 1987) employed an orthogonal array arranging control factors in an inner array and noise factors in an outer array. Statisticians (Shoemaker, et al., 1991; Tsui, 1992) argued that the efficiency of experiments is improved by replacing the orthogonal array with a single array that includes both control and noise factors. They also suggested the single array approach since the interaction effect between control and noise factors can be appropriately captured.

In the RCEM-EMI, a DOE technique using the single array approach is incorporated. Among the DOE technique, we recommend Central Composite Design (Myers and

Montgomery, 1995) for building a response surface model since the prediction errors of the Central Composite Design are identical across the entire design space. However, designers may employ any other DOE techniques, such as two or three level factorial design, Latin HyperCube sampling (McKay, et al., 1979), Box-Behnken (Myers and Montgomery, 1995), etc., for obtaining the most accurate response surface model with the minimum number of experiments (or simulations). Another important task is the metamodeling of prediction variance for the non-deterministic simulation results. Therefore, it is necessary to get replicated or near replicated experiments at each designed experimental point to effectively capture a conditional variance model. The number of replications for accurately capturing a conditional variance model depends on system characteristics.

While collecting experimental data based on DOE specifications, designers have to perform a number of simulations or experiments in a series or parallel. Sometimes, they may need to connect to a remote machine where simulation software is installed. In this case, it is necessary to employ a distributed, collaborative design framework, such as Web-DPR (Choi, 2001; Xiao, et al., 2001), X-DPR (Choi, et al., 2003), Phoenix Integration (Phoenix Integration Inc., 2001), and iSIGHT/FIPER (Engineous Inc., 2001). These design frameworks are useful for automating serialized and parallelized multiple simulation executions and collecting result data across geographically distributed computing resources. Some of the software frameworks (e.g., iSIGHT/FIPER) also provide statistical and design tools for supporting design tasks in general.

3.7. INTEGRATED ESTIMATION OF REGRESSION MODEL AND PREDICTION INTERVAL

Variability quantification is an important initial step in any robust design task. In this section, an approach for quantifying unparameterizable variability for later use in a robust design exploration method is discussed in detail - Step (c) in Figure 3.6. In Taguchi's method, response variability is quantified using a cross array which is an orthogonal combination of an inner array for the levels of control factors and an outer array for the levels of noise factors. However, Taguchi's method is limited to quantifying response variability in a discrete space of control factors. To overcome this limitation, two approaches have been developed.

The approach taken in this dissertation is to model response mean and variability in a continuous design space; this is known as *modeling of location and dispersion*. In this approach, the mean and variance of response variability are modeled and the unknown parameters in the models are estimated by either maximizing the pseudolikelihood estimator or minimizing the least-square estimator. Davidian and Carroll (Davidian and Carroll, 1987) published an excellent review of the earlier works for response variance function models and parameter estimation techniques. Vining and Myers (Vining and Myers, 1990) proposed a dual response surface modeling approach for location and dispersion modeling. Engel (Engel and Huele, 1996) proposed a joint modeling strategy of location and dispersion by a generalized linear modeling approach.

In the other approach, called *response modeling* (Shoemaker, et al., 1991; Welch, et al., 1990), the inner and outer arrays in the Taguchi method are merged into a single array to effectively capture the interaction effects between noise and control factors. A response is

modeled as a function of both the control and noise factors instead of computing the variance over the noise replicates. In RCEM, Chen and co-authors (Chen, 1995) employ the response modeling approach for quantifying response variability due to control and noise factor variation.

In this approach, both of the aforementioned approaches for quantifying variability are employed. The location and dispersion modeling approach is used for quantifying unparameterizable variability and the response modeling approach for quantifying response variability due to parameterizable noise factors. The response modeling approach is not feasible because the noise factor, pseudo random particle placement in an SVE, cannot be parameterized. The modeling and estimating of the location and dispersion models are similar to those of generalized linear modeling (Engel and Huele, 1996). However, the approach in this dissertation includes a predication interval to estimate bounds around an estimated mean function with some confidence level and to incorporate those bounds with the goal formulation that is discussed in Section 3.8. This approach differs from other robust design approaches that consider only response variability in their robust design formulation. An overall procedure for building metamodels for response and prediction interval is illustrated in Figure 3.7.

STEP 1: The first step is transforming raw data. Since the obtained data often represents non-linear behavior of materials, it is necessary to transform raw data (y) into another form so that a mean response model (e.g., response surface model) can fit the transformed data (y^{tr}) accurately. The required transformation is defined by

$$y^{tr} = F(y) \ , \tag{3.1}$$

where F is the transformation function.

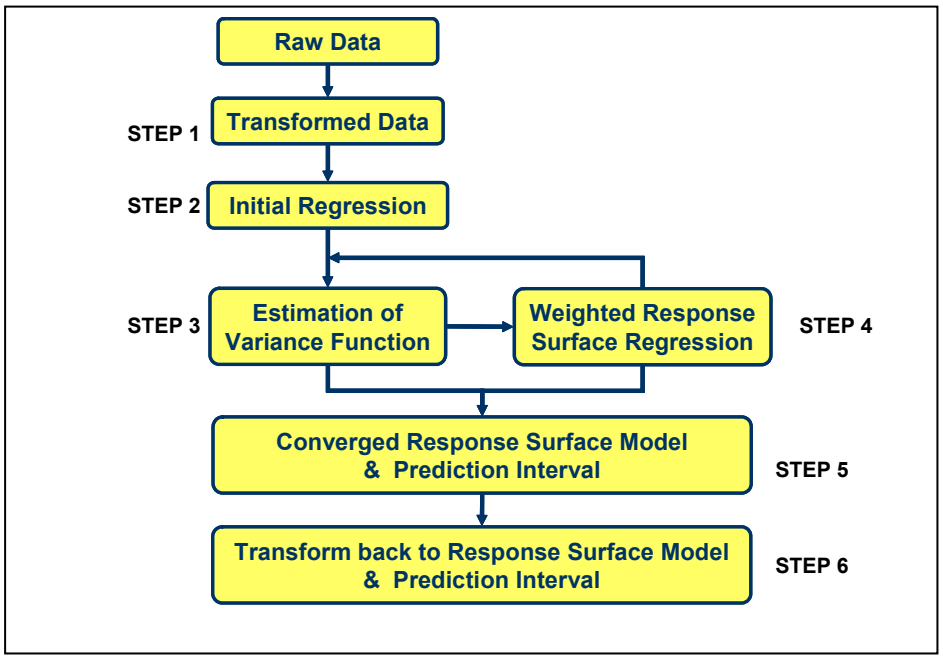

Figure 3.7 Steps for integrated metamodeling and prediction interval estimation

STEP 2: y^{tr} is regressed using a mean response model, $f(\mathbf{x_i}, \boldsymbol{\beta})$, where $\mathbf{x_i}$ is a sample vector of design variables and $\boldsymbol{\beta}$ is a vector of regression parameters. In this dissertation, a quadratic response surface model is employed for $f(\mathbf{x_i}, \boldsymbol{\beta})$. A residual plot should show a normal distribution, $\varepsilon_i \sim N(0, \sigma_i^2)$ as long as the raw data are properly transformed. The regression is represented as

$$y_i^{tr} = f(\mathbf{x_i}, \boldsymbol{\beta}) + \varepsilon_i \tag{3.2}$$

where i = 1, ..., N (total number of samples).

A major assumption of a regression is that the variances (σ_i^2) of the random error distributions are constant over the entire design space. This is called homoscadasticity. However, in reality, the variances are not always constant across the entire design space but may vary by several factors (e.g., design variables, noise factors, etc.). This is

referred to as heteroscadasticity. The unparameterizable variability is one of the primary sources for heteroscadasticity. In this step, a mean response model is initially estimated by obtaining a vector of estimated regression parameters ($\hat{\boldsymbol{\beta}}$) that is used in the next step.

STEP 3: The response variance should be modeled in terms of factors. A generalized representation of a conditional variance model, proposed by Davidian and Carroll (Davidian and Carroll, 1987) is given by

$$\sigma_i^2 = \sigma^2 \cdot v^2(\mathbf{z_i}, \boldsymbol{\theta}, \hat{\boldsymbol{\beta}}) \tag{3.3}$$

where i = 1, ... , N (total number of samples), σ is a scale factor, $\mathbf{z_i}$ is a vector of variance factors, $\boldsymbol{\theta}$ is a vector of variance parameters, and $\hat{\boldsymbol{\beta}}$ is the vector of estimated regression parameters obtained in STEP 2. Many different types of conditional variance models have been proposed. In industrial contexts, Box and Meyer (Box and Meyer, 1986) as well as many others (Chan and Mak, 1995; Engel and Huele, 1996; Grego, 1993; Nair and Pregibon, 1988) suggest

$$\sigma_i^2 = \exp(\boldsymbol{\theta} \cdot \mathbf{x}_i^{'}) \tag{3.4}$$

where i = 1, ... , N (total number of samples), σ is assumed to be unity, and $\mathbf{z_i}$ are assumed to be $\mathbf{x_i}$ with given $\hat{\boldsymbol{\beta}}$. An exponential form effectively represents heteroscadastic variance since estimated variances are always positive, and $\boldsymbol{\theta}$ can be efficiently estimated via log-link conversion, which is discussed below.

For estimating $\boldsymbol{\theta}$, variance model fitting methods, such as maximum pseudolikelihood method (Aitkin, 1987; Gong and Samaniego, 1981), least squares on squared residuals estimation (Amemiya, 1977; Jobson and Fuller, 1980), least squares on absolute residuals estimation(Glejser, 1969; Theil, 1971), or logarithm method (Engel and Huele, 1996;

Harvey, 1976) are required. The pseudolikelihood estimation function for estimating $\boldsymbol{\theta}$ in Eq. (3.3) is

$$l(\boldsymbol{\beta},\boldsymbol{\theta},\sigma) = -N\log\sigma - \sum_{i=1}^{N}\log\{v(\mathbf{z_i},\boldsymbol{\beta},\boldsymbol{\theta})\} - (2\sigma^2)^{-1}\sum_{i=1}^{N}\{y_i - f(\mathbf{x_i},\boldsymbol{\beta})\}^2 / v^2(\mathbf{z_i},\boldsymbol{\beta},\boldsymbol{\theta})\} \quad (3.5)$$

Applying Eq.(3.4) to Eq.(3.5) with transformed data (y_i^{tr}), the pseudolikelihood estimation function becomes

$$l(\boldsymbol{\theta}) = -\frac{1}{2}\sum_{i=1}^{N}[\boldsymbol{\theta}\cdot\mathbf{x_i'} - \{y_i^{tr} - f(\mathbf{x_i},\hat{\boldsymbol{\beta}})\}^2 / \exp(\boldsymbol{\theta}\cdot\mathbf{x_i'})] \quad (3.6)$$

By maximizing this function, a vector of estimated variance parameters ($\hat{\boldsymbol{\theta}}$) is obtained with given $\hat{\boldsymbol{\beta}}$. The estimation function of the logarithm method for estimating $\boldsymbol{\theta}$ in Eq. (3.3) is

$$ls(\boldsymbol{\beta},\boldsymbol{\theta},\sigma) = \sum_{i=1}^{N}[\log\{y_i - f(\mathbf{x_i},\boldsymbol{\beta})\}^2 - \log\{\sigma^2 v^2(\mathbf{z_i},\boldsymbol{\beta},\boldsymbol{\theta})\}]^2 \quad (3.7)$$

Applying Eq.(3.4) to Eq.(3.7) with transformed data (y_i^{tr}) , the logarithm least-squares estimation function is

$$ls(\boldsymbol{\theta}) = \sum_{i=1}^{N}[\log\{y_i^{tr} - f(\mathbf{x_i},\hat{\boldsymbol{\beta}})\}^2 - \boldsymbol{\theta}\cdot\mathbf{x_i'}]^2 \quad (3.8)$$

By minimizing Eq.(3.8), $\hat{\boldsymbol{\theta}}$ is obtained with given $\hat{\boldsymbol{\beta}}$. Although two methods for estimating $\boldsymbol{\theta}$ in the conditional variance model are introduced, the logarithm method is employed in this chapter. The maximum pseudolikelihood method is used for the materials design problem in Chapter 5 since it is suitable for any type of random error distributions.

STEP 4: Once a conditional variance model for heteroscadastic observations is estimated, the initial mean response model must be refit using the weighted regression method (Neter, et al., 1996). With this approach, the mean response model becomes more robust to the effect of adding large variance data (such as, outliers). For estimating the updated $\hat{\boldsymbol{\beta}}$, we minimize the weighted squares of residual given by

$$wls(\boldsymbol{\beta}) = \sum_{i=1}^{N} w_i \{y_i - f(\mathbf{x_i}, \boldsymbol{\beta})\}^2 \quad \text{where,} \quad w_i = 1/\sigma_i^2 \tag{3.9}$$

By applying the estimated conditional variance model in STEP 3 to Eq.(3.9), we obtain a weighted least square estimation function, which is

$$wls(\boldsymbol{\beta}) = \sum_{i=1}^{N} w_i \{y_i^{tr} - f(\mathbf{x_i}, \boldsymbol{\beta})\}^2 \quad \text{where,} \quad w_i = \exp(-\hat{\boldsymbol{\theta}} \cdot \mathbf{x_i}') \tag{3.10}$$

Based on the updated mean response model, the conditional variance model obtained previously must be re-estimated obtaining the updated $\hat{\boldsymbol{\theta}}$. STEP 3 and 4 should be iterated until $\hat{\boldsymbol{\beta}}$ converges.

STEP 5: After the converged mean response model and the conditional variance model based on the procedure (up to STEP 4 iteratively) is identified, an interval around the regression function at a new observation ($\mathbf{x_0}$) is identified using the prediction interval estimation with a 100(1-α) % confidence level as

$$y(\mathbf{x_0}) = f(\mathbf{x_0}, \hat{\boldsymbol{\beta}}) \pm t_{N-p,1-\alpha/2} \sigma \cdot v(\mathbf{x_0}, \hat{\boldsymbol{\beta}}, \hat{\boldsymbol{\theta}}) \tag{3.11}$$

where p is the number of predictors and (1-α) is the confidence level. Applying Eq.(3.4) to Eq.(3.11), the transformed estimated prediction interval is

$$y^{tr}(\mathbf{x_0}) = f(\mathbf{x_0}, \hat{\boldsymbol{\beta}}) \pm t_{N-p,1-\alpha/2} \cdot \exp\left(\frac{\hat{\boldsymbol{\theta}} \cdot \mathbf{x_0}'}{2}\right) \tag{3.12}$$

STEP 6: Convert the mean response model and prediction interval estimation into the original function. Therefore, the prediction interval in the original coordinate is

$$y(\mathbf{x_0}) = F^{-1}\left\{ f(\mathbf{x_0}, \hat{\boldsymbol{\beta}}) \pm t_{N-p,1-\alpha/2} \cdot \exp\left(\frac{\hat{\boldsymbol{\theta}} \cdot \mathbf{x_0}'}{2} \right) \right\} \tag{3.13}$$

In this section, an integrated, iterative variability and uncertainty quantification method for quantifying uncertainty bounds due to unparameterizable variability and limited sample size is discussed. In Sections 3.8 and 3.9, a design exploration technique for searching Type I, II, and III robust design specifications using quantified uncertainty bounds is discussed. In the design exploration process, the mean response model, $F^{-1}(f(\mathbf{x_0}, \hat{\boldsymbol{\beta}}))$, is used as a mean function, and the upper and lower limit functions of the prediction interval in Eq. (3.13) are used for the uncertainty bounds enveloping the mean function.

3.8. ERROR MARGIN INDEX (EMI)

Error Margin Indices (EMIs) are metrics indicating the degree of reliability of a decision that satisfies system constraints or bounds. The EMIs are used in search algorithms to find ranged sets of design specifications that meet a range of system requirements. The procedure for obtaining the EMIs is as follows: (a) obtain the upper and/or lower deviation of a response and (b) calculate the EMIs based on this deviation.

3.8.1. Estimating the Response Deviation with Uncertainty Bounds

The first step in finding a design variable vector, $\mathbf{x} = \{x_1, x_2, ..., x_m\}$ ensuring a robust response, is to estimate the response variance due to variations in the design variable

vector, $\mathbf{x}$, using a first order Taylor series expansion. Assuming that variations in input variables are small, the response variance is

$$\Delta Y = \sum_{i=1}^{m} \left| \frac{\partial f}{\partial x_i} \right| \cdot \Delta x_i \ , \tag{3.14}$$

where m is the number of design variables.

The representation of the response deviation in Eq. (3.14) is close to the worst case scenario, which assumes that all fluctuations occur simultaneously in the worst possible combination (Chen, et al., 1999). However, the variation (ΔY) in the equation is the response variance due to input variance only. *It does not include the response variation due to the variability of the model itself*.

The following procedure is necessary to consider the effect of model variability on system response variation. Assuming a system model has 'n' uncertainty bounds, a response variation from each of them is obtained using

$$\Delta Y_j = \sum_{i=1}^{m} \left| \frac{\partial f_j}{\partial x_i} \right| \cdot \Delta x_i \ , \tag{3.15}$$

where i=1, 2, …, m and j = 1, 2, …. , n (the number of uncertainty bounds). As an example, a case of two uncertainty bounds (e.g., bounds on a prediction interval) with a single design variable is illustrated in Figure 3.8. In this example, normal distributions are used for demonstration purposes.

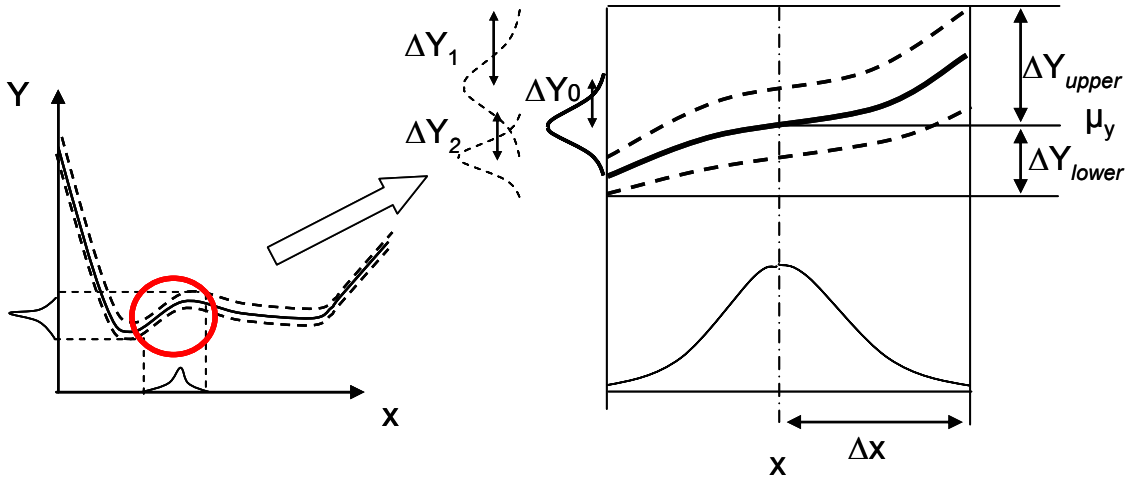

Figure 3.8 Formulation of uncertainty bounds due to variations in a design variable and a model

The most probable model (e.g., a mean response model of a system) is shown as a solid curve with two uncertainty bounds (e.g., bounds on a prediction interval) shown as dotted curves in Figure 3.8. On the right hand side of the figure, the corresponding response variations of the system model and the uncertainty bounds within the interval of the design variable's variance are illustrated. The variations of the three distributions are estimated using Eqs. (3.14) and (3.15). Evaluating multiple variances for a system model and *n* uncertainty bounds with the same procedure, minimum and maximum responses caused by variability in *m* design variables and models are evaluated using

$$Y_{\max} = Max\left\{ f_j(\mathbf{x}) + \sum_{i=1}^{m} \left| \frac{\partial f_j}{\partial x_i} \right| \cdot \Delta x_i \right\} \text{ and } Y_{\min} = Min\left\{ f_j(\mathbf{x}) - \sum_{i=1}^{m} \left| \frac{\partial f_j}{\partial x_i} \right| \cdot \Delta x_i \right\}, \quad (3.16)$$

where $j=0,1,2, \ldots, n$, $f_0(\mathbf{x})$ is the mean response model and $f_1(\mathbf{x}) \ldots f_n(\mathbf{x})$ are uncertainty bound functions.

Upper and lower deviations, which are the deviations from the mean response to the maximum and minimum responses, respectively, are represented as

$$\Delta Y_{upper} = Y_{\max} - f_0(\mathbf{x}) \text{ and } \Delta Y_{lower} = f_0(\mathbf{x}) - Y_{\min}, \quad (3.17)$$

where $f_0(\mathbf{x})$ is the mean response, $Y_{\max}$ is the maximum response, $Y_{\min}$ is the minimum response, ΔY_{upper} is the upper deviation, and ΔY_{lower} is the lower deviation.

Using this procedure, the response variation of a model which has different types of uncertainty bounds including one-sided, two-sided, and crossed error bounds can be evaluated while considering uncertainty in a model. The response deviations (ΔY_{upper} and ΔY_{lower}) can be calculated from any system model functions (e.g., metamodels and/or engineering equations). In this section, we use the prediction interval models obtained in Section 3.9 as upper and lower bounds of the uncertainty.

3.8.2. Evaluating the Error Margin Index

The Error Margin Indies (EMIs) are calculated using the same mathematical construct underlying the Design Capability Indices (DCIs). The mathematical construct is shown in Figure 3.9. The normal distributions in this figure are given as examples. The DCIs are calculated using the mean response (μ_y) obtained by the mean response model, $f_0(\mathbf{x})$, and deviation (ΔY) from a response distribution of a system model (dotted distributions in the figure); ΔY is calculated based on Eq. (3.14). For example, in the "Smaller is Better" (Figure 3.9a), the DCI is $(URL-\mu_y)/\Delta Y$, where URL is Upper Requirement Limit. On the other hand, the EMI is calculated including μ_y and upper/lower deviations (ΔY_{upper} *and* ΔY_{lower}) from a combined distribution of a system model and uncertainty bounds (solid distributions in the figure); the deviation is calculated based on Eqs. (3.15), (3.16), and (3.17). In the case where "Smaller is Better", the EMI is $(URL-\mu_y)/\ \Delta Y_{upper}$. In other words, the DCI includes only the response deviation of a system model due to the

variations of design variables. The EMI, on the other hand, includes the response deviations of error bounds as well as the system model.

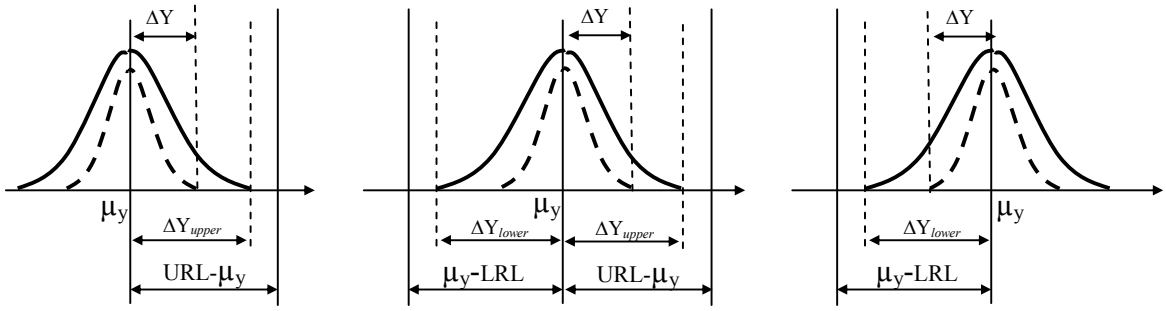

(a) Smaller is better
$EMI = (URL-\mu_y)/\Delta Y_{upper}$
$EMI \geq 1$

$DCI = (URL-\mu_y)/\Delta Y$
$DCI \geq 1$

(b) Nominal is Better
$EMI = Min [EMI_l, EMI_u]$
where,
$EMI_l = (\mu_y-LRL)/\Delta Y_{lower}$
$EMI_u = (URL-\mu_y)/\Delta Y_{upper}$
$EMI \geq 1$

$DCI = Min [DCI_l, DCI_u]$
where
$DCI_l = (\mu_y-LRL)/\Delta Y$
$DCI_u = (URL-\mu_y)/\Delta Y$

(c) Larger is better
$EMI = (\mu_y-LRL)/\Delta Y_{lower}$
$EMI \geq 1$

$DCI = (\mu_y-LRL)/\Delta Y$
$DCI \geq 1$

Figure 3.9 Mathematical construct of Error Margin Indices based on Design Capability Indices

In all cases depicted in Figure 3.9, the EMI becomes larger as decisions become more reliable. In a "Smaller is Better" case, the EMI becomes larger when the location of μ_y is farther from the Upper Requirement Limit (URL) and/or ΔY_{upper} gets smaller. An EMI of unity means that an uncertainty bound just meets a requirement limit. EMIs smaller than unity indicate that a requirement limit may be violated due to uncertainty in the model. The same is true when the EMI is formulated for "Larger is Better" case in Figure 3.9c. In this case, the larger EMI can be achieved by locating μ_y farther from the Lower Requirement Limit (LRL) and/or reducing ΔY_{lower}. In the "Nominal is Better" case, depicted in Figure 3.9b, both the upper and lower EMIs need to be calculated, and the worst case (the smaller EMI) is selected. The EMIs formulated in this manner are leveraged in a solution search algorithm to find solution sets which are robust to model variability as well as to variations in input variables.

3.9. COMPROMISE DECISION SUPPORT PROBLEM (CDSP) FOR THE RCEM-EMI

The last step – Step (d) in the RCEM-EMI - is to identify robust solution based on EMI. In many engineering application, including materials design problems are multifunctional systems. As discussed in Section 1.1.2, the MESM is also multifunctional material; therefore, balancing those multiple performances of a system is important in engineering systems design.

In this dissertation, we employ the compromise Decision Support Problem (cDSP) (Mistree, et al., 1992) in order to design multifunctional materials based on EMIs. The cDSP is a mathematical formulation to identify compromised design solutions in the presence of multiple conflicting goals. The cDSP is a hybrid formulation that incorporates concepts from both traditional mathematical programming and goal programming; see Table 3.1. The cDSP and mathematical programming are similar to the extent that they refer to system constraints that must be satisfied for feasibility. They differ in the way the deviation or objective function is modeled. In the cDSP, as in goal programming, multiple objectives are formulated as system goals involving deviation variables, and the deviation function is modeled using deviation variables rather than system or decision variables. The cDSP differs from goal programming, however, because it is tailored to handle common engineering design situations in which physical limitations are manifested as system constraints (mostly inequalities) and bounds on the system variables.

Table 3.1 The mathematical construct of the compromise Decision Support Problem

Given

n, number of system variables
p, number of equality constraints
q, number of inequality constraints
m, number of system goals
$g_i(\mathbf{x})$, constraint functions
G_i, system goals
$A_i(\mathbf{x})$, performance functions

Find

$\mathbf{x}$ (system variables)
d_i^-, d_i^+ (deviation variables)

Satisfy

System constraints:

$g_i(\mathbf{x}) = 0 \qquad i=1,...,p$
$g_i(\mathbf{x}) \leq 0 \qquad i=p+1,...,p+q$

System goals:

$A_i(\mathbf{x})/G_i + d_i^- - d_i^+ = 1 \quad i=1,...,m$

Bounds:

$x_i^{min} \leq x_i \leq x_i^{max}$
$d_i^-, d_i^+ \geq 0$ and $d_i^- \cdot d_i^+ = 0 \qquad i=1,...,n$

Minimize

$Z = [f_1(d_i^-, d_i^+), \ldots, f_k(d_i^-, d_i^+)]$ *Preemptive*
$Z = \Sigma W_i (d_i^- + d_i^+)\ \Sigma W_i = 1$ *Archimedean*

The conceptual basis of the compromise DSP is to minimize the difference between that which is desired (the goal, G_i) and that which can be achieved ($A_i(\mathbf{x})$) for *multiple* goals. This is accomplished by minimizing the deviation function, Z, expressed in terms of deviation variables. The deviation function provides a measure of the extent to which multiple goals are achieved. In the compromise DSP, multiple goals are considered conventionally by formulating the deviation function either with Archimedean weightings or preemptively (lexicographically)) (Mistree, et al., 1992). In traditional mathematical programming, the objective function typically represents a *single* goal, by which the desirability of a design solution is measured. All other characteristics of a design are modeled as hard constraints.

Using the EMI formulation, the cDSP for the RCEM-EMI is formulated and solved to achieve a range of design solutions, robust to the variation in design variables, unparameterizable variability, and model parameter uncertainty. The mathematical formulation of the cDSP is shown in Table 3.2.

Table 3.2 A cDSP in the RCEM-EMI for robust design under uncertainty in design variables and models

Given

Response functions, $f_{0,i}(\mathbf{x})$ where (i = 1,..., n), $\mathbf{x} = \{x_1, x_2, ..., x_m\}$

where n is the number of responses and m is the number of design variables.

Error boundary functions, $f_{j,i}(\mathbf{x})$ (j= 1,..., k)

where k is number of error bounds for each response .

System Constraints, $g_h(\mathbf{x})$ (h = 1, ...,z)

where z is the number of constraints.

Ranges for the design requirements, URL_i and LRL_i

Target EMI for each response, $EMI_{target,i}$

Deviations of the control variables, $\sigma_{\mathbf{x}}$ or $\Delta\mathbf{x}$

Find

The location of the mean of the control variables $\mu_{\mathbf{x}}$

Deviations d_i^+, d_i^-

Satisfy

Constraints: $EMI_{constraint,\ h} \geq 1$

Goals: $EMI_i / EMI_{target,i} + d_i^- - d_i^+ = 1$

Bounds: $a_i \leq x_i \leq b_i$

$d_i^-, d_i^+ \geq 0$

$d_i^- \bullet d_i^+ = 0$

Minimize

Deviation Function $Z = \sum_{i=1}^{n} [w_i (d_i^- + d_i^+)]$ *where* $\sum_{i=1}^{n} w_i = 1$

The mean response functions, $f_{0,i}(\mathbf{x})$, and the uncertainty bound functions of each mean response function, $f_{j,i}(\mathbf{x})$, should be obtained by the method shown in Section 3.7. System constraints, $g_h(\mathbf{x})$, are formed from demands and wishes in requirements respectively. LRLs and/or URLs are the demands in responses for a multidisciplinary system. Deviations (variability) of control variables should be given. A solution search algorithm is used to find the mean values of control variables $\mu_{\mathbf{x}}$ and the deviations, d_i^+,

d_i^-, from targets. Solutions must satisfy the system constraints considering variability and uncertainty in the model. These system constraints are formed by $EMI_{constraint,h} \geq 1$ for multiple constraints. $EMI_{constraint,h}$ can be calculated based on $g_h(\mathbf{x})$ with the same procedure discussed in Section 3.8. Multiple goals are formulated in terms of given EMI target values ($EMI_{target,i}$). In the cDSP, ranged sets of design specifications for multiple targets are obtained by minimizing an objective function.

3.10. THEORETICAL STRUCTURAL VALIDATION OF THE RCEM-EMI

In this section, the theoretical structural validity of the RCEM-EMI is checked. The mathematical construct and overall procedure of the RCEM-EMI are followed using a simple example. Confidence in the soundness of the RCEM-EMI construct is established. The utility and limitation of the RCEM-EMI is also checked in this section.

The example is a ninth order polynomial function that has heteroscadastic random error variance. It is assumed that this polynomial function is a true system function and the system function has random errors in sampled data. Based on the randomly generated data, the utility of the RCEM-EMI is validated by comparing the design solution of the RCEM-EMI with the true design solution incorporating the true function.

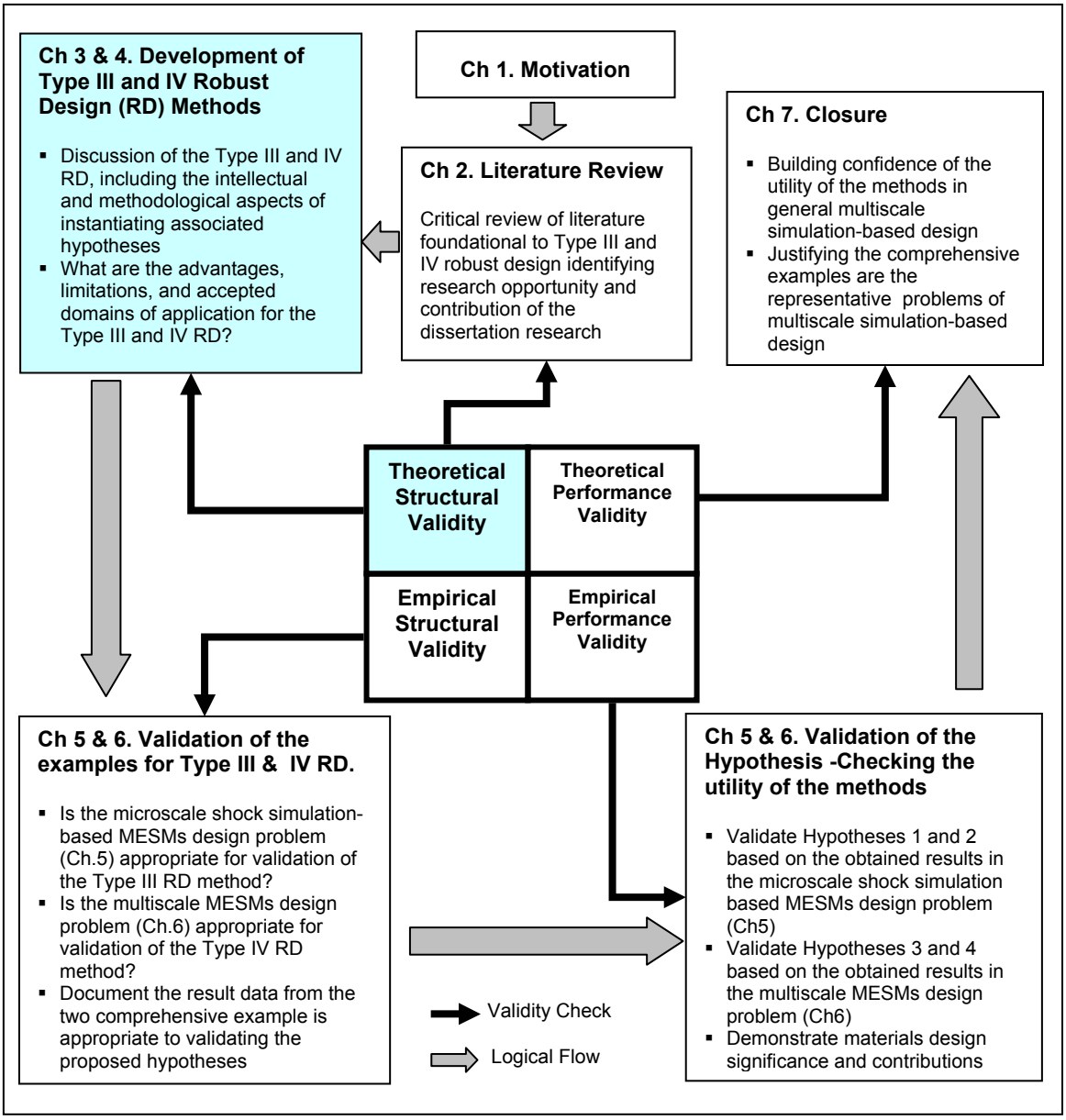

Figure 3.10 Validation square roadmap

3.10.1. Introducing the Example

The system function, which is a ninth order polynomial function with heteroscadastic random error variance, is shown in Table 3.3. The polynomial function is introduced by Lin and coauthors (Lin, et al., 1999). Heteroscadastic random error is included to make the function non-deterministic. The error variance is defined as a normal distribution

with the standard deviation, 200/f(x), which has the maximum error variance at the minimum performance.

Table 3.3 A ninth order polynomial function with heteroscadastic error variance

$$f(x) = \sum_{i=1}^{9} a_i (x - 900)^{(i-1)} + \varepsilon(x)$$

, *where*

$a_1 = -659.23$ $a_4 = 0.82691$ $a_7 = -3.2446 \times 10^{-6}$

$a_2 = 190.22$ $a_5 = -0.021885$ $a_8 = 1.6606 \times 10^{-8}$

$a_3 = -17.802$ $a_6 = 0.0003463$ $a_9 = -3.5757 \times 10^{-10}$

$\varepsilon(x) = N(0, \{200 / f(x)\})$

3.10.2. Clarifying Design Task

Using the defined example function introduced in the previous section, our design task is to find the robust design specification of the design variable (x) with consideration of non-deterministic random error and variability in the design variable (control factor).

Table 3.4 Clarification of the design task

- Objective
  Find x
- Requirements
  Upper Requirement Limit = 40
  Smaller is the better
- Design space: x = [920, 980]
- Deviation in x: $\Delta x = \pm 5$
- System function : *f(x)*

The design requirements are as follows: (a) Upper Requirement Limit (URL), which means the designed system performance should be smaller than URL, is 40 and (b) the smaller performance is the better. The design space considered for the design exploration

from 920 to 980. The design variable has natural uncertainty (variability) of ±5, which is the control factor variability. As discussed in the previous section, the system function is defined as the ninth order polynomial function with the heteroscadastic random errors.

3.10.3. Obtaining Sample Data

Using the defined non-deterministic system function, 86 random samples are generated as shown in Figure 3.11. As expected from the system function, we have the larger random error variance in the smaller mean response region and vice versa. The solid curve shown in the scattered samples is the mean function, which is the polynomial function without random errors.

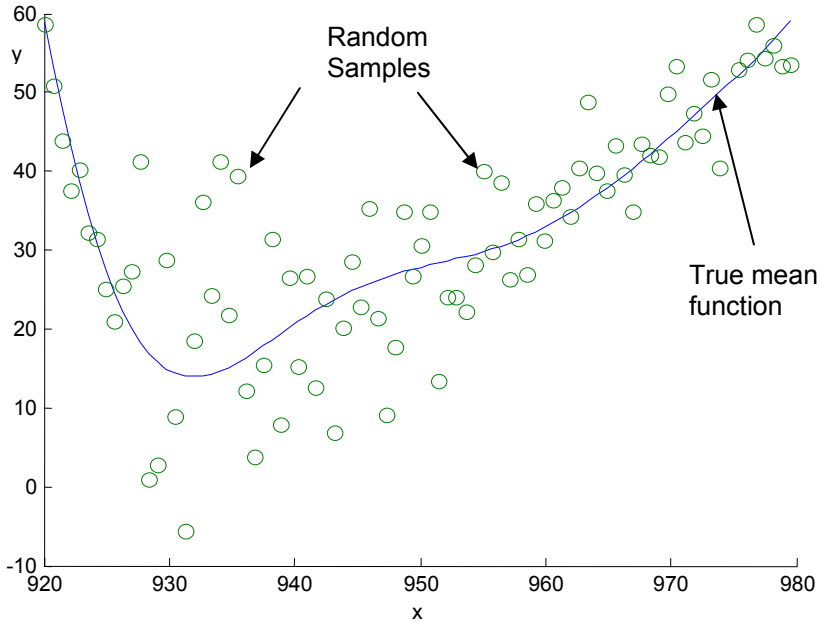

Figure 3.11 Random sampling results in the design space

The obtained samples will be used in the next section for building regression and variance functions assuming that we do not know the true mean and variance functions.

3.10.4. Estimating Regression Model and Prediction Interval

In this section, a mean response function and its conditional variance function are modeled and estimated based on the random samples obtained in the previous section using the framework discussed in Section 3.7.

The mean response model is represented as

$$\begin{aligned} &f(\mathbf{x},\boldsymbol{\beta}) = \boldsymbol{\beta}\cdot\mathbf{x}' \\ &where,\ \ \mathbf{x} = [1, x, x^2], \boldsymbol{\beta} = [\boldsymbol{\beta}_0, \boldsymbol{\beta}_1, \boldsymbol{\beta}_2]. \end{aligned} \tag{3.18}$$

The conditional variance model is an exponential function with a quadratic polynomial power. The factors for the variance model are assumed as the design variable and scale factor (σ) is assumed as unity. Therefore, the variance model is given by

$$\begin{aligned} &\sigma^2 g^2(\mathbf{x},\boldsymbol{\beta},\boldsymbol{\theta}) = \exp(\boldsymbol{\theta}\cdot\mathbf{x}') \\ &where,\ \mathbf{x} = [1, x, x^2], \boldsymbol{\theta} = [\theta_0, \theta_1, \theta_2]. \end{aligned} \tag{3.19}$$

To estimate the parameters ($\boldsymbol{\theta}$) in the conditional variance model, we minimize the estimator in the logarithm method given by

$$\sum_{i=1}^{N} [\log\{y_i - f(\mathbf{x_i}, \hat{\boldsymbol{\beta}})\}^2 - \boldsymbol{\theta}\cdot\mathbf{x_i}']. \tag{3.20}$$

First, an initial estimation of the parameters in the mean response model $\hat{\boldsymbol{\beta}}_{init} = [\ 2.5200\text{e+}004, \text{-}5.3475\text{e+}001,\ 2.8393\text{e-}002]$ is obtained by the least square regression method. With given initial parameter estimation ($\hat{\boldsymbol{\beta}}_{init}$) of the mean response model, the initial parameter vector in the conditional variance model, $\hat{\boldsymbol{\theta}}_{init} = [3.1136\text{e+}002, \text{-}6.0406\text{e-}001,\ 2.9379\text{e-}004]$, is estimated by minimizing Eq. (3.20). Based on the estimated variance model, the parameters in the mean response

model are re-estimated based on the weighted regression method. The estimation of the updated $\hat{\boldsymbol{\beta}}$ is obtained by minimizing the weighted sum of square of residuals given by

$$\sum_{i=1}^{n} w_i \{y_i - f(\mathbf{x_i}, \boldsymbol{\beta})\}^2 \quad \text{where,} \quad w_i = \exp(-\hat{\boldsymbol{\theta}}_{init} \cdot \mathbf{x_i}') \tag{3.21}$$

At this point, we have updated estimation of the mean response model, $f(\mathbf{x}, \hat{\boldsymbol{\beta}}_{updated})$, where $\hat{\boldsymbol{\beta}}_{updated}$=[1.7455e+004, -3.7218e+001, 1.9865e-002]. Based on the updated mean response model, the above procedure, (a) re-estimating the parameters in the conditional variance model, (b) obtaining weight factors, and (c) re-estimating the parameters in the mean response model, is iterated until the parameters in the mean response model converge.

After twenty seven iterations, the converged parameter vectors for the mean response model and the conditional variance model are

$$\hat{\boldsymbol{\beta}}_{converged} = [1.4678e+004, -3.1414e+001, 1.6833e-002] \text{ and}$$

$$\hat{\boldsymbol{\theta}}_{converged} = [3.9076e+002, -7.5037e-001, 3.5992e-004].$$

Once the converged mean and conditional variance models have been identified, a prediction interval (model parameter uncertainty) at new observation ($\mathbf{x_0}$) is estimated at (1-α) confidence level according to

$$y(\mathbf{x_0}) = \hat{\boldsymbol{\beta}}_{converged} \cdot \mathbf{x_0} \pm t_{n-p,1-\alpha/2} \cdot \exp\left(\frac{\hat{\boldsymbol{\theta}}_{converged} \cdot \mathbf{x_0}'}{2} \right), \tag{3.22}$$

where n is the number of samples (*n=86*), and p is the number of predictors (*p=3*). The converged mean response model and the prediction interval are illustrated in Figure 3.12. The circular dots are the obtained samples. The central curve represents the mean

response model. The upper and lower curves are respectively the upper and lower prediction limits at 95% confidence level.

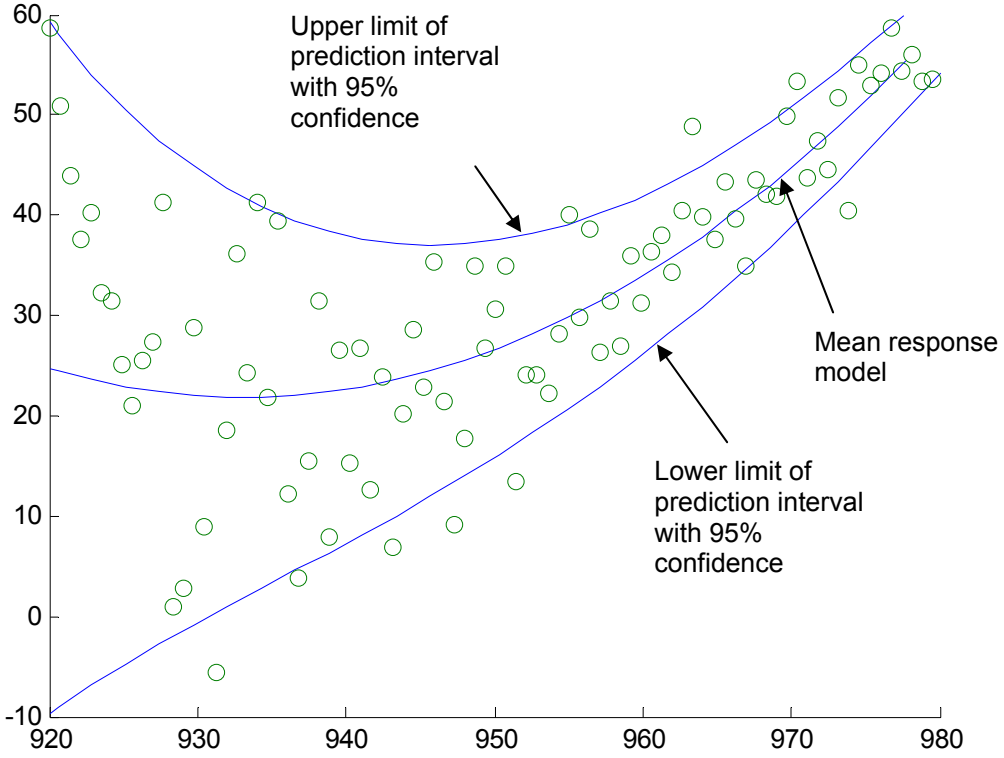

Figure 3.12 The converged mean function and prediction Interval

3.10.5. Finding Design Solutions Based on cDSP for the RCEM-EMI

With the specifications identified in Section 3.10.2 and the mean and prediction interval models obtained in Section 3.10.4, a cDSP is formulated incorporating the EMI to achieve robust system responses with ranged sets of design specifications, as shown in Table 3.5.

Table 3.5 An example of cDSP for the RCEM-EMI

Given

- Response functions: $f_0(x) = \hat{\boldsymbol{\beta}}_{converged} \bullet \mathbf{x}'$
- Lower prediction bound: $f_1(x) = \hat{\boldsymbol{\beta}}_{converged} \cdot \mathbf{x} - t_{n-p,1-\alpha/2} \cdot \exp\left(\frac{\hat{\boldsymbol{\theta}}_{converged} \cdot \mathbf{x}'}{2} \right)$
- Upper prediction bound: $f_2(x) = \hat{\boldsymbol{\beta}}_{converged} \cdot \mathbf{x} + t_{n-p,1-\alpha/2} \cdot \exp\left(\frac{\hat{\boldsymbol{\theta}}_{converged} \cdot \mathbf{x}'}{2} \right)$

$$\mathbf{x} = [1, x, x^2]$$

where, $\hat{\boldsymbol{\beta}}_{converged} = [1.4678e+004, -3.1414e+001, 1.6833e-002]$

$\hat{\boldsymbol{\theta}}_{converged} = [3.9076e+002, -7.5037e-001, 3.5992e-004]$

$n = 86,\ p = 3,\ \alpha = 0.05$

- Satisfying Performance Ranges: URL = 40, the smaller is the better.
- Target EMI for each response: $EMI_{target} = 10$
- Deviation of the control variable: $\Delta x = \pm 5$

Find

- The location of the mean of the control variables $\mu_{\mathbf{x}}$
- Deviations d^+, d^-

Satisfy

- Goals: $EMI / EMI_{target} + d^- - d^+ = 1$

  where, $EMI = \{URL - f_0(x)\} / \{Y_{max} - f_0(x)\}$

  $$Y_{\max} = Max\left\{ \left(f_0(x) + \left| \frac{\partial f_0}{\partial x} \right| \cdot \Delta x \right), \left(f_1(x) + \left| \frac{\partial f_1}{\partial x} \right| \cdot \Delta x \right), \left(f_2(x) + \left| \frac{\partial f_2}{\partial x} \right| \cdot \Delta x \right) \right\}$$

- Bounds: $920 \le x \le 980$

  $d^-, d^+ \ge 0,$

  $d^- \bullet d^+ = 0$

Minimize

- Deviation Function: $Z = d^-$

The functions, $f_0(\mathbf{x})$, $f_1(\mathbf{x})$ *and* $f_2(\mathbf{x})$ are given from the mean response model and the upper and lower prediction interval limits identified in Section 3.10.4. Other required inputs are given from the specifications identified in Section 3.10.2. The Upper Requirement Limit (URL) is set to 40. The target EMI is set to 10. The deviations of design variables (control variables) are also identified in Section 3.10.2. The objective of solving the cDSP is to find the mean location of design variables (x_1) for achieving the target EMI as much as possible.

3.10.6. Theoretical Structural Validation Result

The optimal and RCEM-DCI solutions are identical and the RCEM-EMI solution is different from them. The values in the shaded cells at the solutions of the optimization and RCEM-DCI approaches are calculated using the RCEM-EMI approach. The shaded values are not achievable using the optimization or the RCEM-DCI method.

Table 3.6 The RCEM-EMI solution results comparing with the solutions of optimization and RCEM-DCI

	x	Mean of *y*	Estimated minimum *y*	Estimated maximum *y*	EMI	DCI
Optimization	933.1	**21.819**	*-0.5997*	*44.305*	*0.8085*	*52.912*
RCEM-DCI	933.1±5	21.819	*-0.5997*	*44.305*	*0.8085*	***52.912***
RCEM-EMI	946±5	24.620	**8.8142**	**36.767**	**1.2661**	6.9962

The optimal and the RCEM-DCI solutions are found on 933.1 of the design variable. Using traditional optimization, the maximum performance is searched using only the mean response model. The maximum mean of y (21.819) is achieved. At the optimal solution, maximum DCI (52.912) is also achieved. On the other hand, using the RCEM-EMI approach, a robust design solution is found at 946. At the RCEM-EMI solution, the

maximum EMI (1.2661) is achieved over the entire design space. The minimum and maximum estimated numbers of reaction sites are 8.8142 and 36.767, respectively. It is estimated with the consideration of the deviation in the design variables, unparameterizable variability, and model parameter uncertainty. In other word, taking the deviations in the design variable and unparameterizable variability into account, the minimum number of reaction sites is estimated as 8.8142 and the maximum 36.767 with 95% confidence level.

As shown in Table 3.6, the mean performance is the best at the optimal and RCEM-DCI solution; however, if designers consider unparameterizable variability, the performance deviations (the interval between estimated minimum and maximum) at the two solution points are larger than that at the RCEM-EMI solution point as shown in estimated minimum (-0.5997) and maximum (44.305) responses. This is because the optimization and RCEM-DCI approaches ignore the unparameterizable variability in the system during the design exploration, and the variability is quite large in the example function as shown in Table 3.6. At the optimal and RCEM-DCI solution, it is not certain that the system performance is satisfactory to the URL (the response cannot exceed 40) since the maximum estimated response is 44.305 with 95% confidence. The smaller response variation and smaller estimated maximum response (36.767) are achieved at the RCEM-EMI solution point while sacrificing the mean response (24.620). This result is supported by the plots shown in Figure 3.13.

The graphs in Figure 3.13 are the models estimating mean responses and prediction intervals of the responses in terms of the design variable (x). As expected, the optimal solution is on the peak (minimum) of the mean response model.

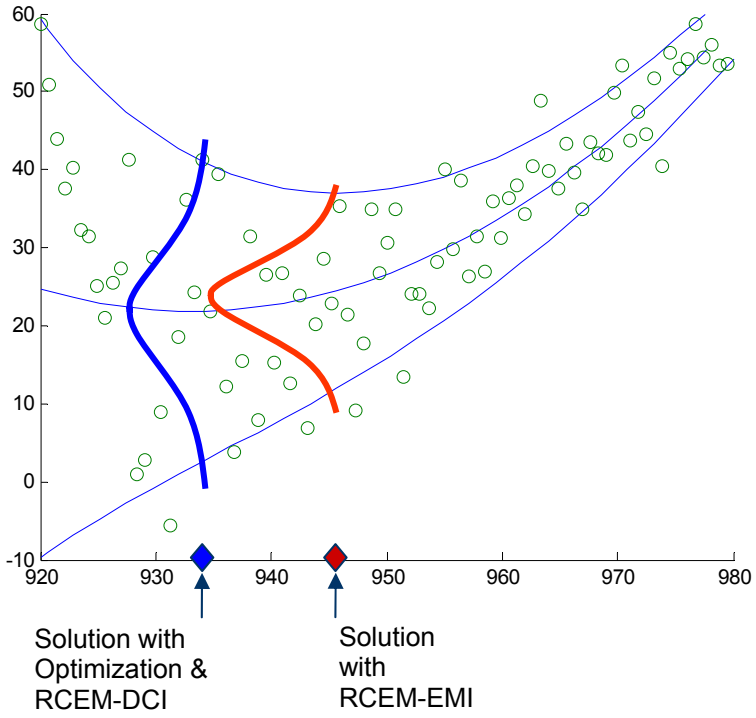

Figure 3.13 The Optimal, RCEM-DCI, RCEM-EMI solutions in the mean response and prediction interval models

The RCEM-DCI solution is also on the peak of the mean response model since the mean response model is sufficiently flat at the peak position. At the RCEM-EMI solution, as mentioned, the mean response (24.620) is a little sacrificed compared with that (21.819) of the RCEM-DCI and optimal solution; however, the deviation of response is much smaller (27.953) at the RCEM-EMI solution than that (44.9074) of other solutions. Consequently, we believe that the design specifications identified by the RCEM-EMI produces more robust performance against the heteroscadastic random errors (unparameterizable variability), taking the variation in the design variables into account as well.

Additional important information the RCEM-EMI approach can provide is that the more accurate response deviation since it captures unparameterizable variability. In

contrast, other two approaches cannot. Therefore, if designers decide their design variable with only the mean model, the system's performance could be unsatisfactory to the performance requirement (URL in this case). By employing the RCEM-EMI, the information for the system's performance deviation due to unparameterizable variability as well as control and noise factors' variability can be provided with some confidence level.

Compared to conventional robust optimization techniques, another advantage of the RCEM-EMI is that designers can easily apply it into an engineering application. One of the difficulties in deciding a robust solution in traditional robust optimization technique is trading off between performance and performance sensitivity. In the RCEM-EMI approach, those two performance criteria are integrated into one EMI formulation; therefore, it is not necessary for designers to worry about trading off the two. This approach is even more useful when designers have a ranged performance requirement, such as URL and/or LRL.

Now, we compare the solutions using the estimated model based on 86 samples and the quadratic polynomial function in Figure 3.13 with the solution identified with the true model shown in Figure 3.14. As shown in Figure 3.14, the true solution considering unparameterizable variability is 944.5. On the other hand, the optimal solution is 931.9 and RCEM-DCI solution is 950.1 without considering unparameterizable variability. As expected the optimal solution is on the peak point of the true mean model and the RCEM-DCI solution is on the flat region of the mean model only considering the deviation in the design variable. However, considering unparameterizable variability, the true response

deviations at optimal solution with 95% confidence is quite large and violates the URL as shown in the figure.

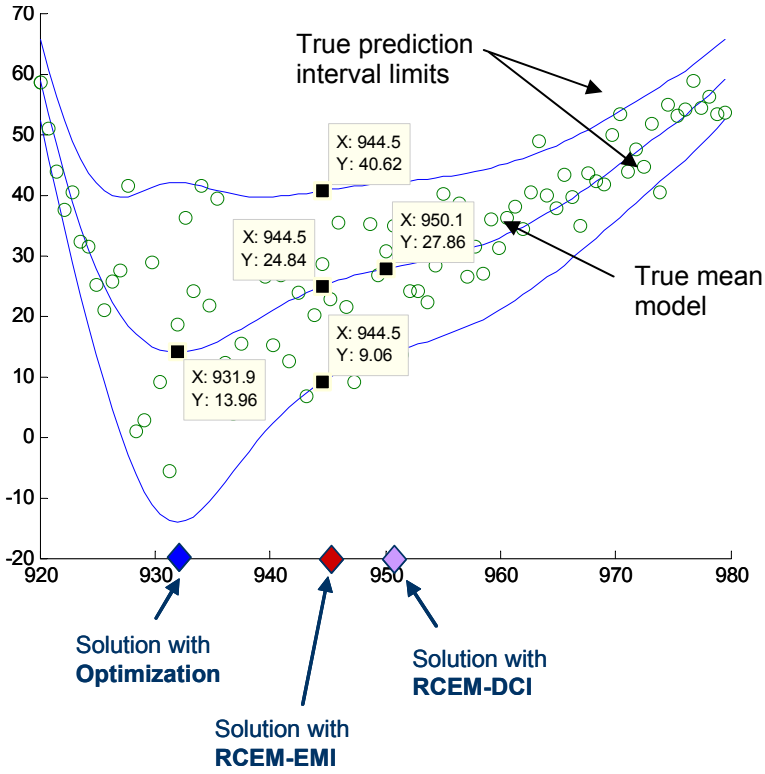

Figure 3.14 Optimization, RCEM-DCI, and RCEM-EMI solutions based on the true models.

In addition, the solution based on the RCEM-DCI approach violates the URL even if the deviation of the response is smaller. Therefore, the solution finding process searches for the solution point compromising those two at the RCEM-EMI solution point. The performance deviation at the RCEM-EMI solution point is smaller than that at the optimal point and larger than that at the RCEM-DCI solution point. However, the mean performance at the RCEM-EMI solution point is not as good as that at the optimal solution but better than that at the RCEM-DCI solution point.

Metamodeling is an approximate way for representing a system behavior; therefore, there is uncertainty (model structure and parameter uncertainty) in metamodels. As shown in Figure 3.14, the metamodels for the mean response and prediction limits in

highly non-linear region (the left portion that is smaller than the optimal solution point) are incorrect. This inaccuracy is originated from the fact that the order of the metamodel is not high enough to characterize the highly non-linear behavior of the true model - model structure uncertainty. Fortunately, all the solutions in metamodels and true models are in the right portion of the optimal solution point where the metamodels are pretty accurate. Therefore, the amount of model structure uncertainty may be assumed as to be small enough to be ignored in the design space that is larger than the location of the optimal solution point in the true model.

Comparing the metamodels (mean model and prediction interval models) in Figure 3.13 with the true models in Figure 3.14, the metamodels are reasonably accurate at the region except the highly non-linear part using 86 samples. The estimated response variation between upper and lower limits at the solution of the RCEM-EMI is 27.21 with 95% confidence. The true response variation between upper and lower limits of 95% normal distribution at the solution point is 30.16. There is some difference but this could be due to model structure uncertainty mentioned earlier.

Uncertainty in a model, including natural, parameter, and model structure uncertainty, can be ignored in some cases. However, in most engineering applications, the uncertainty in the system model must be considered when decisions (design of system specifications) are made. Many robust design methods have been developed, but few of them explicitly consider uncertainty in models. Taking this source of uncertainty into account, a robust design method, the Robust Concept Exploration Method with Error Margin Index (RCEM-EMI), is presented in this chapter. The RCEM-EMI helps a designer make a decision under system's random variability and/or model parameter uncertainty in a

model. Applying the RCEM-EMI in a simple example, we identified the following advantages over conventional optimization and robust design method (RCEM-DCI) from the results shown in Section 3.10.5.

- The RCEM-EMI directly inherits the advantages of the RCEM-DCI; therefore, it is efficient for evaluating a family of designs, easy to understand and easy to compute, and incorporates multiple aspects in quality improvement (Chen, et al., 1999). The RCEM-EMI supports designers in avoiding the difficulties in trading off between performance and performance variability
- A system's performance with respect to the design specification identified by the RCEM-EMI is more robust against variability that is difficult to parameterize, such as random material micro-structure change that causes large variations in system performance. Additionally, it can provide information whether the design result will satisfy the ranged performance requirements or not with some confidence level, which cannot be provided by other robust design methods.

3.11. SYNOPSIS OF CHAPTER 3

In this chapter, the Robust Concept Exploration Method with Error Margin Indices (RCEM-EMI) is proposed and discussed in detail. The RCEM-EMI is developed in order to answer Research Questions 1 and 2.

Types of uncertainties in a simulation-based materials design are discussed Section 3.1 and classified as variability, model parameter uncertainty, and model structure uncertainty in Section 3.2. From this uncertainty classification, Type III robust design is

clearly defined for achieving system performance robustness to uncertainty embedded within the model used in Section 3.3. The RCEM-EMI for instantiating Type I, II and III robust design are discussed step by step in Sections 3.4~3.9. These steps are summarized in Figure 3.6. In these steps, a robust design task is clarified, experiments are designed and simulation data is acquired, metamodels and prediction intervals are estimated, the Error Margin Indices (EMIs) and those mathematical constructs are defined, and a ranged set of robust design solutions is searched. The theoretical structure of the RCEM-EMI is validated based on a simple example in Section 3.10. In this concept validation example, the design specification obtained with the RCEM-EMI is compared with traditional optimization and a robust design method (RCEM-DCI). The estimated prediction interval is checked with the true interval model and validated to establish that the mathematical structure is sound. In Chapter 5, a comprehensive example, shock simulation-based microscale MESM design, is employed to fully validate the utility of RCEM-EMI in a materials design engineering problem.

In the next chapter, another type of robust design method, an extension of Type I, II, and III, for dealing with propagated uncertainties in multiscale simulation-based systems design. The developed techniques, integrated estimation of a metamodel and prediction interval in Section 3.7 and Error Margin Indices in Section 3.8 in this chapter are extended in the next chapter.

CHAPTER 4

TYPE IV ROBUST DESIGN: THE INDUCTIVE DESIGN EXPLORATION METHOD (IDEM)

In this chapter, we discuss the development of a method for Type IV robust design. The implemented method is the Inductive Design Exploration Method (IDEM), using the Discrete Constraints Evaluation (DCE) and Hyper Dimensional Error Margin Indices (HD-EMI). Type IV robust design includes Type I, II, and III robust design; therefore this chapter is related to the RCEM-EMI described in Chapter 3.

In Section 4.1, we discuss model structure uncertainty and propagated uncertainty in an analysis chain in materials design. In Section 4.2, Type IV robust design is clearly defined. In this section, Type I, II, and III robust design methods mentioned in Chapter 1 are revisited. In Section 4.3, we establish a strategy for Type IV robust design discussing the relationship between Type III robust design and Type IV robust design. As the RCEM-EMI for Type III robust design starts with the clarification of the design tasks, The IDEM for Type IV robust design begins by configuring the robust design process based on given design goals and tools. In Section 4.4, graphical entities are developed in order to efficiently describe a robust design process incorporating multiple tools (multidisciplinary analyses, simulation, and experiments). In Section 4.5, the overall procedure of the IDEM is discussed. In Sections 4.6~4.8, the constituent techniques of the IDEM are discussed. Seeding and evaluating discrete points are discussed in Section 4.6.

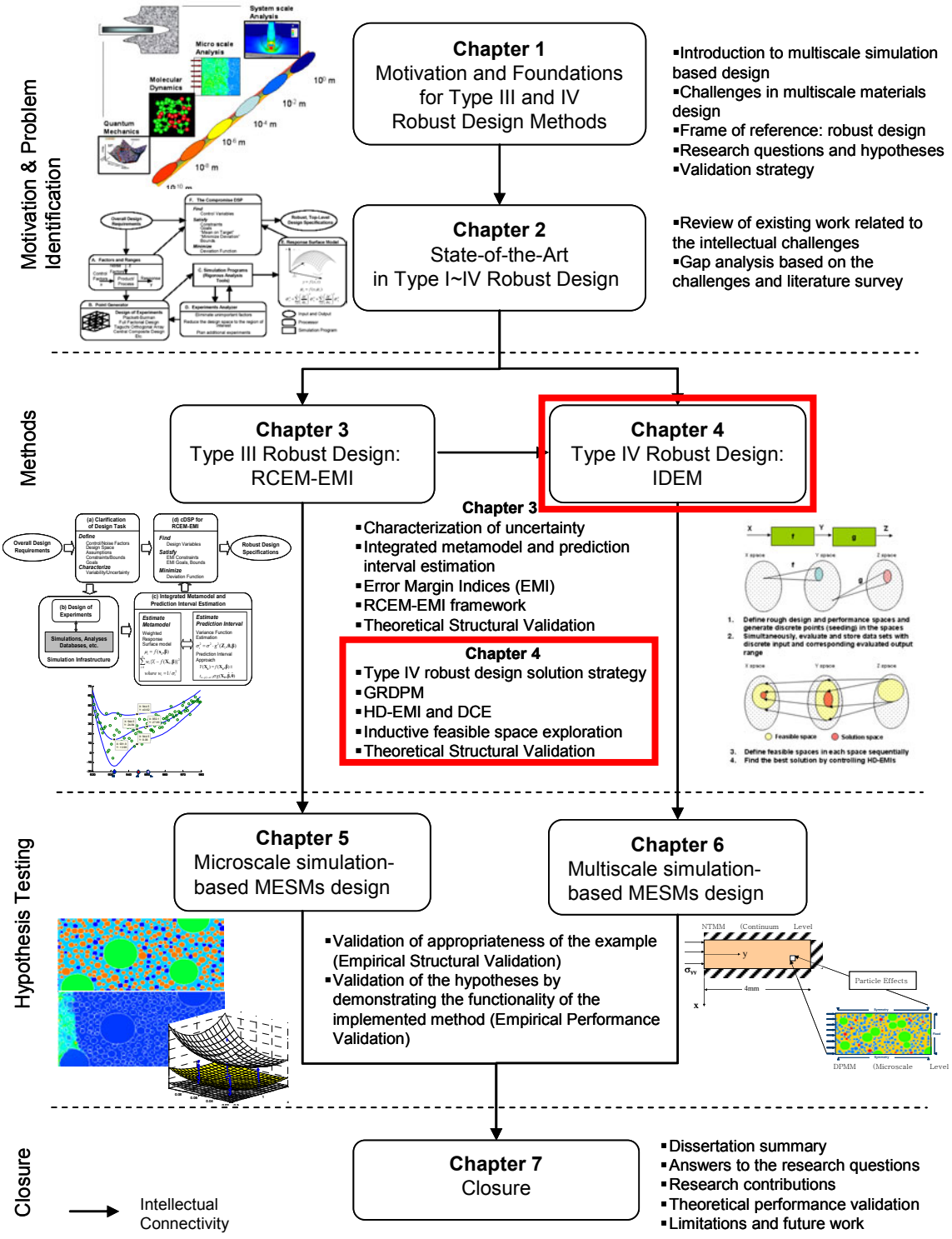

Figure 4.1 Dissertation roadmap

In Section 4.7, the Discrete Constraints Evaluation technique is discussed including the definition of Hyper-Dimensional Error Margin Indices, a technique for finding exact constraints boundaries, and an inductive (top-down) feasible space finding method. In Section 4.8, a compromised DSP is used in order to find the best solution among multiple feasible discrete solutions. In Section 4.9, the validity of the theoretical structure of the IDEM is checked based on a clay-filled polyethylene cantilever beam design problem.

The IDEM, a method Type IV robust design, described in this chapter is further validated with a multiscale simulation-based MESM design example in Chapter 6.

4.1. MODEL STRUCTURE UNCERTAINTY AND PROPAGATED UNCERTAINTY IN A MODEL CHAIN

Typically, materials are selected using databases of experimentally determined material properties (c.f., Ref. (Ashby, 1999)). However, the paradigm is changing to tailoring materials for specific performance required for specific products. The approach in materials science is deductively mapping a processing path, nano-structure and micro-structure, material properties, and performance. This corresponds to Olson's (Olson, 1997) materials hierarchical diagram shown in Figure 1.2.

How do we design systems considering variables, constraints and models that embed relevant aspects of the material microstructure through overall system configuration? (Belytschko, et al., 2004) A new multidisciplinary approach of systems-based design of materials that combines inductive (top-down) engineering with deductive (bottom-up) science is essential. However, there are a number of challenges for facilitating systems-based design of materials and products. These include, among others, uncertainty, heavy computational requirements, mathematical models with highly nonlinear behavior, hierar-

chies of information and simulation, multidisciplinary collaboration, and distributed environments for simulation and decision-making.

An important source of uncertainty arises from the process of developing computational models of materials. In developing the models, material scientists often employ idealistic assumptions, e.g., a plane strain assumption in order to reduce the true three-dimensional loading to a more tractable two-dimensional case, idealization of the material microstructure geometry, and boundary conditions. Moreover, there are uncertain constitutive models for nonlinear material behavior due to a lack of complete knowledge about fundamental processes. These idealizations and assumptions contribute un-quantifiable uncertainty to a simulation model, termed "model structure uncertainty," this may also may result in inaccurate estimation of material behavior. This is discussed in Sections 1.2 and 3.2 in detail.

Another challenge in materials design is that these uncertainties are propagated through a multiscale model chain and the final performance estimate may have large degree of uncertainty. We call this "propagated uncertainty." A simple example of such an analysis chain is illustrated in Figure 4.2.

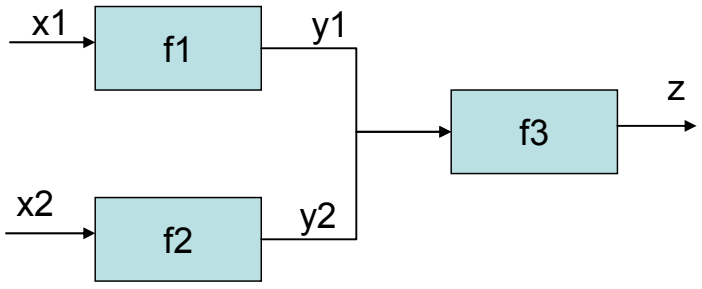

Figure 4.2 An example of information flow in a model chain

Design variables, x1 and x2, may be parameters in a material's processing or structure that may be tailored by materials designers. The functions, f1 and f2, may be simulation

models for predicting the material's properties, y1 and y2, such as modulus of elasticity, ultimate strength, yield strength, Hugoniot relation, etc. Finally, the derived materials properties are then interfaced to a product-level model, f3, such as continuum models and finite element models in order to estimate system performance, z, including such requirements as structural integrity, energy release rate, etc.

The main concern is that input parameters, x1 and x2, and multiscale models, f1, f2, and f3, for predicting materials and system behavior tend to be uncertain or to vary stochastically. For example, the parameter, x1, is an input to the lower scaled model, f1; x1 has a variance associated with it. The y1 is the response from the model in which the input uncertainty is increased because of the combination of variances of x1 and x2 and error in the model itself. The same effect may be applied to model, f3. Parameters, y1 and y2, are inputs with variances to the f3, which produces response, z, with increased uncertainty due to the combination of variances in y1 and y2 with the uncertainty in the model, f3. In this way, uncertainty accumulates through multiple steps of a model chain and making the variance of the final response unexpectedly large.

This is an important issue since negligible errors in parameters, such as x1 and x2, may accumulate to a large degree of uncertainty at the highest system levels, which could incur serious design defects. Therefore, it is necessary for us to identify the propagated uncertainty in system models to find a robust solution against it. In this chapter, we discuss a new robust design method that is capable of dealing with uncertainty in multiscale models of materials and its propagation through a design and analysis chain to system-level responses.

4.2. TYPE IV ROBUST DESIGN

As discussed, we propose another type of robust design, namely Type IV robust design, in addition to Type I, II, and III robust design in this chapter. Type IV robust design is focused on uncertainty associated with the design process and model structure uncertainty (unquantifiable or potential uncertainty). As discussed in Section 1.4.2, Type IV robust design results in ranged sets of design specifications that are robust to the propagated and expanded uncertainty in a process and to the unquantifiable potential uncertainty (model structure uncertainty) a model might have. Process uncertainty emanates from the propagation and potential amplification of uncertainty due to the combined effect of analysis tasks performed in series or parallel – usually performed by different groups of people with different expertise. The sources of design process uncertainty are particularly common and important for multidisciplinary design and analysis, such as multifunctional, multiscale materials design, etc., with a plethora of shared or coupled variables and analyses performed on multiple length and time scales. The unquantifiable potential uncertainty, which is also called model structure uncertainty, is due to modeling assumption and idealization. It is difficult for us to quantify in statistical sense. Model structure uncertainty is discussed in detail in Section 3.2.

Existing robust design methods – the Taguchi method, RCEM, and the RCEM-EMI - cannot deal with the uncertainty propagation in a design/analysis process chain and model structural uncertainty. For example, using the RCEM, designers find a robust solution for a single task; however, they cannot consider the uncertainty propagation in multiple design tasks. If we use conventional the RCEM for multiscale materials design, the multiple design tasks must be represented as a single robust design task. In doing so,

some problems arise. First, meta-models in the RCEM include accumulated errors, since one meta-model is constructed for the entire design process chain. It is not appropriate to use the incorrect meta-model for design exploration. Second, if a design method does not use a meta-model, then simulations in an analysis chain should be integrated and plugged in a robust design exploration procedure. Restrictions on computing power and the difficulty of integrating geographically distributed systems make the integration more difficult. These problems are common in other design methods (Chen, et al., 1996; Parkinson, et al., 1993; Sundaresan, et al., 1995).

We reviewed existing multidisciplinary robust optimization techniques, Gu and Du's approaches, in Section 2.4. However, those approaches have limitation for applications in multiscale simulation-based design as discussed in Section 2.6. Based on the identified limitation, the requirements for a method instantiating Type IV robust design are discussed in the next section.

4.3. STRATEGY FOR TYPE IV ROBUST DESIGN SOLUTION SEARCH

The limitations of existing multidisciplinary robust design methods discussed in Section 2.4 are identified in Section 2.6. Based on the identified challenges, the requirements of new method for Type IV robust design are listed in Table 4.1. The problems in the existing method are listed in the left column of the table and the requirements for an effective and efficient method for Type IV robust design are listed in the right column of the table.

In the following sections, we formulate a strategy for accommodating these requirements in developing a method for the Type IV robust design, and these

requirements are checked for evaluating the implemented design method in Section 4.9.3. For describing this approach, we employ the process model illustrated in Figure 4.2.

Table 4.1 Requirements list of new method for Type IV robust design

Limitations in existing multidisciplinary robust design methods (from Section 2.6)	Requirements of new method for Type IV robust design (solutions for existing problem)
▪ Intense information interface across the boundary of sub-system for estimating final performance variation because of tightly coupled uncertainty analysis process and design exploration process. ▪ The methods still cannot employ the full power of parallel computing. ▪ No consideration of unquantifiable model structural uncertainty in sub-systems ▪ Each sub system model has been configured as a differentiable mathematical model. ▪ If one of the models in the series is changed, then whole process after the changed model needs to be repeated for estimation of propagated uncertainty.	▪ Mitigating uncertainty propagation within design and analysis chains. ▪ Modularizing sub-systems' uncertainty analysis ▪ Considering unquantifiable model structure uncertainty in achieving ranged set of robust design specifications ▪ Decoupling uncertainty analysis process and design exploration process ▪ Incorporating simulation and experimental models as well as mathematical models for uncertainty analysis and design exploration. ▪ Comprehensive process representation of propagating uncertainty in a design process.

4.3.1. Finding Ranged Sets of Design Specifications by Inductive Design Exploration

Olson originally proposed the inverse (inductive) materials design as discussed in Section 1.1.1 (Olson, 1997). However, the inverse design process proposed by Olson cannot be accepted for the general purpose of materials design. A detailed process of the Olson's hierarchical mapping for materials design is illustrated in Figure 4.3. As shown in the figure, a materials scientist usually employs an abstraction process of materials information representation for the purpose of efficient computation in mapping between domains (processing, structure, property, and performance).

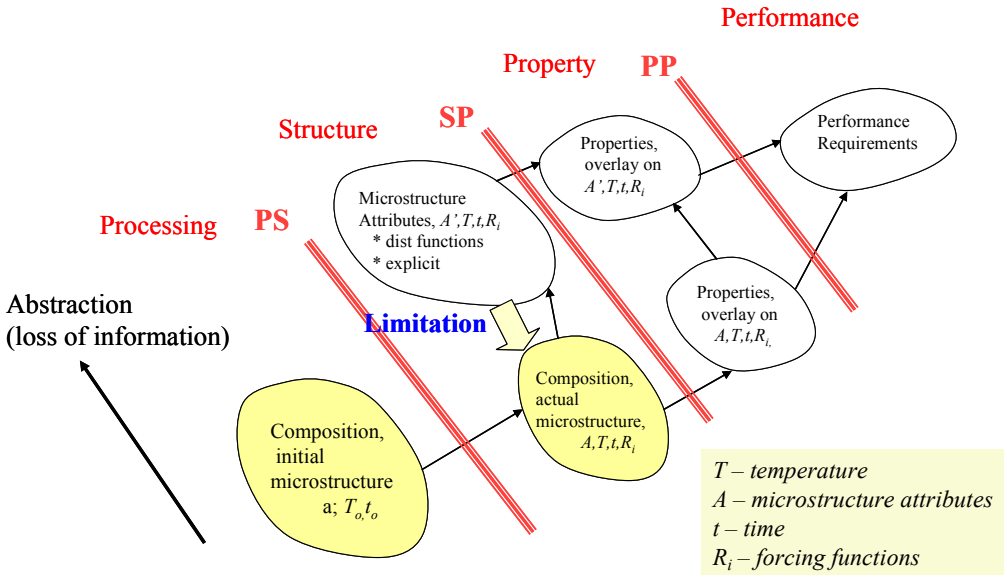

Figure 4.3 Limitation in inverse strategy in Olson's materials design (McDowell, 2004)

For example, explicit microstructure information of a material could be abstracted to a reduced order form of microstructure representation using an appropriated technique (e.g., homogenization) in order to increase computational feasibility with scarifying detailed actual microstructure information. Therefore, the reduced form of a microstructure in a computer model could represent multiple actual microstructures. In other word, many actual material microstructures could map into a single reduced one. For this reason, the information mapping in the order of processing, structure, property, and performance is possible; however, the inverse mapping is limited.

In our approach, the basic idea for finding ranged sets of robust solutions against the propagated uncertainty in a multiscale model chain is **to pass down the feasible solution range in an inverse manner, from desired given final performance ranges to the design space.** For identifying feasible solution range, **we use only material models for bottom-up calculation, not the materials models for the inverse calculation**. We label

this inverse approach as '*inductive design exploration,*' borrowing the word 'inductive' from Olson's materials design hierarchy.

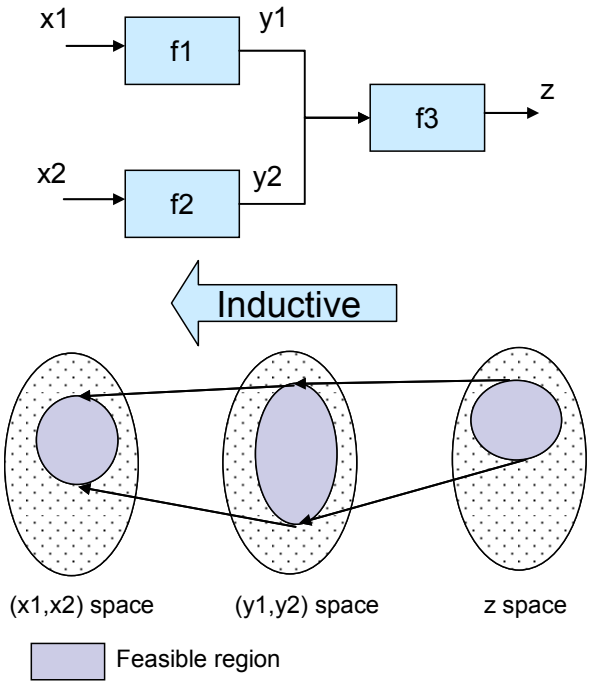

Figure 4.4 A schematic diagram of the inductive design exploration concept

In the example illustrated in Figure 4.2, designers sequentially find the feasible region in the space of (y1, y2) and (x1, x2) with given required performance range in z space. Here, the models, f1, f2, and f3, are functions that have the capability of bottom-up calculation (e.g., producing output, y1, based on input, x1,). The inductive design exploration approach allows for a designer to *find not only a single robust solution, but also ranged robust solution sets from which a designer may choose the best solution without using inverse calculations*.

4.3.2. Parallelizing Function Evaluations

As discussed in Section 2.2, the computational expense of uncertainty analysis is high; therefore, it is critical to parallelize function evaluations that include uncertainty analyses

in a design exploration process. However, as mentioned in Section 2.6 and Table 4.1, design exploration (such as, optimization) and the function evaluations (i.e., uncertainty analyses) process are tightly coupled in the previous approaches. Considering the large amount of resources and time required for uncertainty analysis, it is desirable for us to decouple those two processes so that we can parallelize uncertainty analysis process. In the method for Type IV robust design, the decoupling involves concurrently evaluating the means and deviations of performances, storing the results in a database, and exploring a design space by retrieving the results.

4.3.3. Handling Model Structure Uncertainty

In the Type IV robust design, designers should focus on not only the mean and deviation of a final performance, but also those of interdependent variables, such as the variables, y1 and y2, in Figure 4.2. A simple example is illustrated in Figure 4.5.

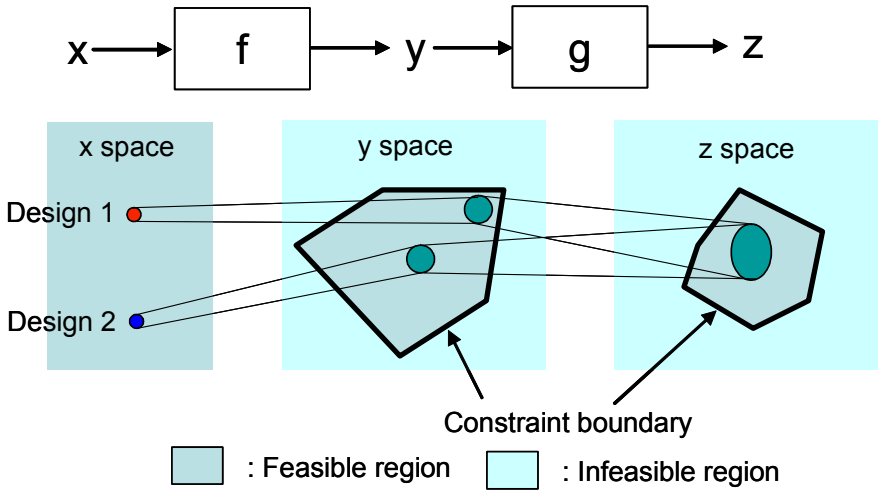

Figure 4.5 An example of sensitivity in interdependent variables

In the figure, x is a design variable, y an interdependent variable, and z a final performance. The interdependent variable y is the output of projecting function f as well as the input of projecting function g. An input in the design space (x-space) is mapped

onto the interdependent variable space (y-space) by projecting function 'f' and the projected region in the interdependent variable space (y-space) is projected again onto the final performance space (z-space) by projecting the function 'g'. A projection function is an evaluation function for estimating mean and deviation of an output. Given a requirement range (feasible region) on the final performance space, e.g., system performance should be greater than some minimum limit, feasible regions in the interdependent variable space (y space) may be obtained constructing a constraint boundary in the space.

If we assume that we have two candidate solutions, Design 1 and 2, for which final performances are identical, then which design we should select among the two candidates? **We believe that Design 2 is better than Design 1 because the projected range of Design 2 in the interdependent variable's space (y-space) is farther from the constraint boundary than Design 1.** In other words, Design 2 is more reliable against potential errors (unquantifiable model structure uncertainty) in the projecting function, f. Current robust design methods discussed in Sections 2.3 and 2.4 cannot handle this issue since the method only focuses on the final performance range. The method for Type IV robust design should be able to select a robust design solution which accounts for this problem.

As mentioned in Section 4.2, the approach for Type IV robust design is determining a solution that is robust against accumulated errors at the final performance but also *potential* errors (model structure uncertainty) in intermediate interdependent variables. With this approach, we believe that the better solution should be obtained considering

model structure uncertainty that is difficult for us to quantify as well as the quantified propagated uncertainty.

In this section, a strategy for solving Type IV robust design is discussed. In the next section, a graphical robust design process model is discussed, which is used for representing this 'top-down' design approach in a visual manner.

4.4. GRAPHICAL ROBUST DESIGN PROCESS MODEL (GRDPM)

One of the most important requirements in Type IV robust design is that we need a protocol for comprehensively representing design process and the parameters' value interlinked with individual subsystems. In this section, a graphical process representation protocol is proposed for designers to capture an entire design process, decision values in design variables, and interlinked parameters in the design process. In Section 4.4.1, semantically rich graphical entities are introduced and explained. In Section 4.4.2, examples of the design process network based on the entities are illustrated.

4.4.1. Entities in the Graphical Robust Design Process Model (GRDPM)

In this section, graphical entities used in GRDPM description are defined. By combining these graphical entities, designers may represent a complex design processes (such as, multiscale materials design processes).

As shown in Table 4.2, depending on the types of geometry, thickness, pattern, and direction, types of values or models are determined. Depending on geometry types, lines represent numeric values, which may be parameters, such as control factors, noise factors,

etc. Boxes represent system models getting inputs and producing outputs, which could be simulation models, system functions, or equations.

Table 4.2 Graphical entities in GRDPM

Symbols	Semantics
Geometry	
▪ Arrow:	Value
▪ Box:	Model
Thickness	
▪ Single line or box:	Discrete
▪ Double line or box :	Ranged
Pattern	
▪ Solid line or box:	Certain
▪ Dotted line or box:	Uncertain
Direction	
▪ Arrow from the left to a box:	Given value or parameter
▪ Arrow out of a box to the right:	Variable to be determined
▪ Arrow from the top into a box:	Goal or required response
▪ Arrow out of a box to the bottom:	Output response

Depending on the thickness of lines or boxes, single lines represent discrete values or deterministic models and double lines represent continuous ranged values or non-deterministic models. Depending on the patterns of lines or boxes, solid lines or boxes mean values or models without uncertainty. Dotted lines or boxes indicate values or models with uncertainty inside. The characteristics of parameters or values are represented based on the directions of arrows. An arrow from the left into a box represents a given input variable or parameter. An arrow out of a box to the right represents a design variable to be determined by a design task. An arrow from the top into a box represents a requirement or constraint in responses. An arrow out of box to the bottom is performance or response output.

Combining those types, we can express the parameters and models in a design process. Some of the examples are illustrated in Figure 4.6.

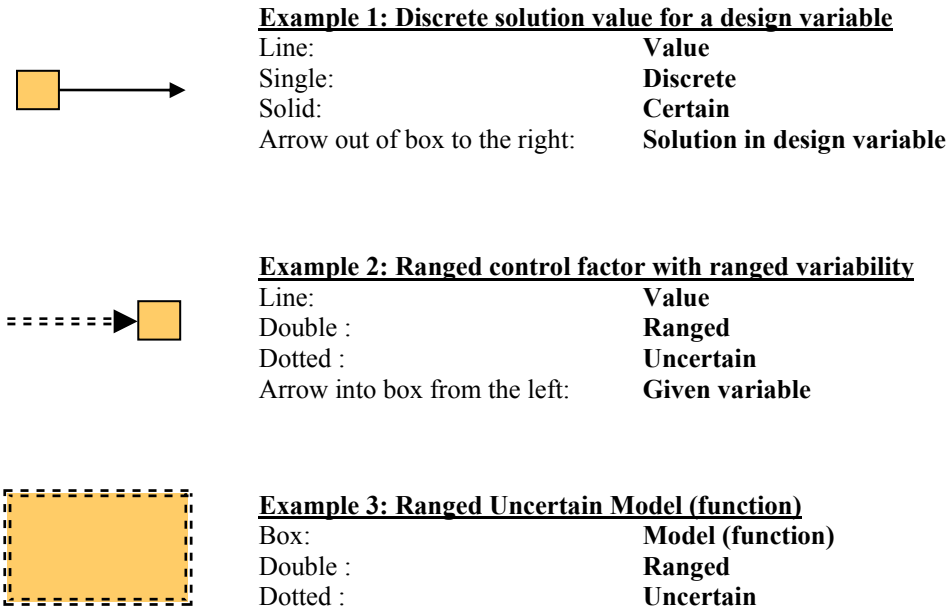

Figure 4.6 Combinations of the graphical entities in GRDPM

4.4.2. A GRDPM for Describing a Complex Robust Design Process

A complete example of a complex design process is discussed in this section. In Figure 4.7, two-level interlinked models, which may be analysis or simulation models in multiple length scales or any hierarchical series of models, are illustrated using P-Diagram discussed in Section 2.5.2.

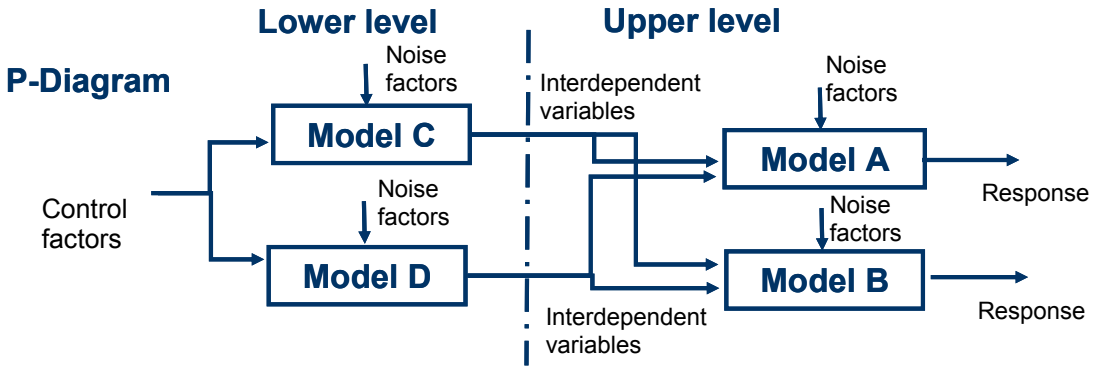

Figure 4.7 Two-level interlinked models represented using P-Diagram

In this model chain, we have two models for each level. In the lower level, we have Models C and D, and, in the upper level, Models A and B. Shared control factors are inputs to Models C and D. Models C and D have independent noise factors, respectively. The response of Model C is again a shared input parameter to Models A and B. Similarly, the response of Model D is a shared input parameter to Models A and B. Models A and B have independent noise factors and produce separate responses. The responses of Models C and D, which become also the control factors of Models A and B, are named as interdependent variables, which connect the lower level models and the upper level models.

As discussed in Section 2.5.2, the P-diagram is difficult to use for representing a design process (a series of events) since it cannot represent a decision-making process illustrating selected decisions (i.e., designed control factors) on design tasks based on each model, nor can it influence of the decisions (i.e., mean and variance of the response at the selected control factors) to other design tasks. For example, in the P-diagram of Figure 4.7, designers cannot find design results (i.e., specifications in control factors) and associated system performances at the specifications. The P-diagram is converted using GRDPM.

In Figure 4.8, a multi-level and multi-objective design process is illustrated using GRDPM defined in Section 4.4.1. In this design process chain, we have two main goals (*single line for discrete Goal A and Goal B*). Each of them has a ranged (*double line*) bound by given requirements and we have two levels (the upper and lower levels) of design tasks interfacing multidisciplinary hierarchical sub-systems. The design process chain starts from the top level design task, Design A, with deterministic model (*single*

solid line box), which has Goal A with noise factors and control factors. A designer (or a design team) in Design A passes robust solution ranges (*double solid line*) to a designer in Design B, which is at the same level but in a different discipline. For shared control variables, the designer in Design B selects his or her design variables within the solution range established by the designer in Design A. The model in Design B embodies model uncertainty (*double dotted box*); therefore, the designer in Design B is required to find a robust solution space against control factor variation, noise factors, and model uncertainty. As shown in the figure, the upper level and lower level are connected in a hierarchical manner, which means that given solution ranges from Design B become bounds in a system performance in Design C. Those two levels are also connected in a sequential manner, which mean that given solution ranges from Design B become bounds in control factors of Design C. With these inputs from the designer in Design B, a designer in Design C passes solution ranges of control factors to a designer in Design D. Finally, the designer of Design D selects his/her solution within the range of control factors given from the design in Design C.

These multilevel design tasks are represented using GRDPM in Figure 4.8. Independent control factors could be in each design task, which is not shown in this example. Independent control factors are not passed down along the design process chain, but shared control factors are.

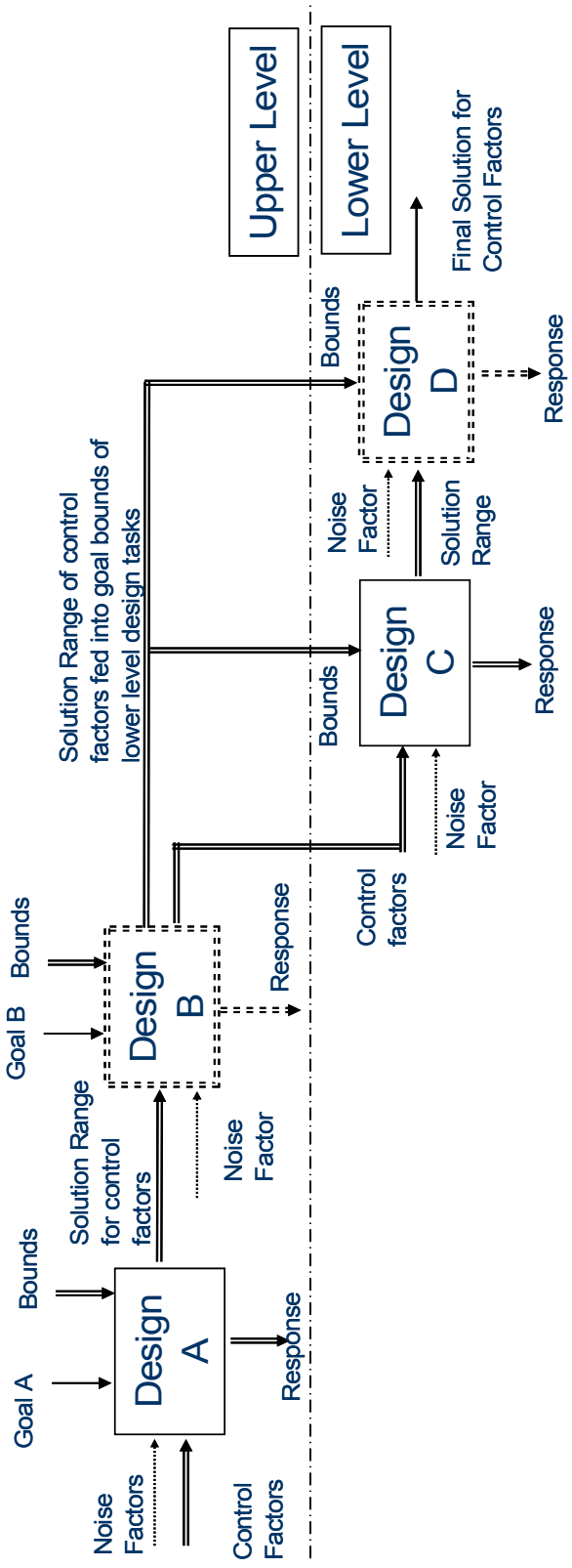

Figure 4.8 A GRDPM example of a two-level robust design process

In this section, we discuss a graphical information model, namely Graphical Robust Design Process Model (GRDPM), for describing a complex design process, such as a multiscale simulation-based materials design process. The graphical entities in GRDPM are used for effectively describing a top-down (inductive) design process in a method for Type IV robust design, which is discussed in the following sections.

4.5. THE INDUCTIVE DESIGN EXPLORATION METHOD (IDEM)

In this section, we discuss the overall procedure of the Inductive Design Exploration Method (IDEM), which is a method for implementing Type IV robust design. In developing the IDEM, the strategy for Type IV robust design discussed in Section 4.3 is instantiated. The strategy in the solution procedure is to find sets of design specifications which pass the feasible solution space in a top-down manner maintaining '*design freedom'* as much as possible. *Design freedom is defined in this dissertation as the ratio of the feasible ranges versus entire design space*. When upstream design variables need to be determined in order to identify the feasible ranges that are passed down to lower-level design tasks, designers should specify the design variables to maximize the design freedom. Once the feasible design spaces are identified based on the inductive design exploration process, the best solution is set by a strategy for trading off the degree of achieved robustness against the individual subsystem model structure uncertainty to decide the most effective robust design solution. The overall procedure for the proposed method is illustrated in Figure 4.9.

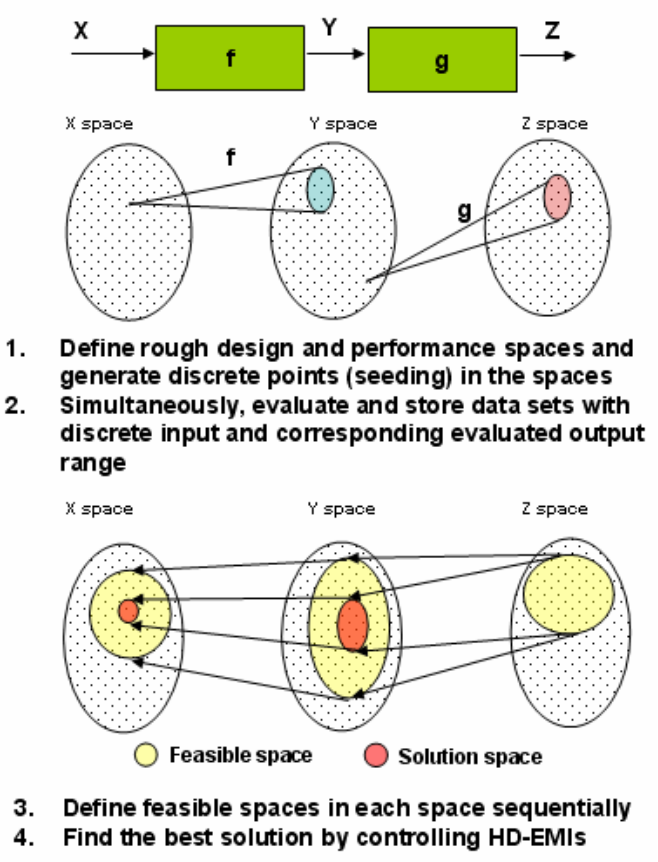

Figure 4.9 Solution finding procedure for the IDEM

The example used for describing the overall procedure in Figure 4.9 is the same process as shown in Figure 4.5. The objective is to find the best ranged sets of design specifications in X space in consideration of the models' (f and g) uncertainty and propagated uncertainty in the process. The procedure includes the following steps.

- Rough design and performance spaces (X, Y, and Z space) need to be defined and then discrete points in each of the spaces are generated.
- The generated discrete points are evaluated based on the projecting functions (f and g) and corresponding data sets composed of a discrete input point and output range are stored in database.

- Feasible regions in Y and X spaces are sequentially identified with a given final performance range in Z space.
- The best solution range is specified by trading off the amount of allowable margin from the identified boundary of the feasible regions in Step 3 for increasing reliability against potential errors in the projecting functions (f and g).

Although the example illustrated above is simple, the procedure is available for finding robust ranged set of specifications in all types (sequential, parallel, and hierarchical) of subsystem networks.

The details of the above procedure are explained in the following sections. In Section 4.6, we discuss generating discrete points in each space and parallel function evolution for generating data sets composed of discrete input and ranged output. In Section 4.7, we discuss obtaining feasible ranges in each space by calculating HD-EMIs at each discrete point, creating an exact border between feasible and infeasible spaces, and thus inversely finding the feasible design space with the IDCE technique. Finally, in Section 4.8, we discuss how to determine the best solution among feasible candidates by controlling HD-EMIs.

4.6. DISCRETE FUNCTION EVALUATION – PROJECTING DISCRETE INPUT TO OUTPUT SPACE

In this section, the basic idea of discrete function evaluation, projecting discrete input to an output space is introduced. Single function evaluations receive a discrete input vector and, if necessary, deviation of input along each dimension of the input vector. Function evaluation produces *a range of output, not a single deterministic output,* under the effects of the input variables' deviation and functional variability; therefore, in this

dissertation, we define the function evaluation as a '*projection.*' A projection is calculated based on any available uncertainty analysis techniques. However, in this dissertation, we leverage the integrated regression model and prediction interval estimation technique discussed in Section 3.7, since it estimates an output deviation considering uncertainty in the model as well as input parameters in a computationally effective way.

In many cases, an *output space could be multi-dimensional* if multiple attributes are evaluated in parallel. For example, in Figure 4.2, the input space is two-dimensional (x1, x2), the output space two-dimension (y1, y2), and we have the two evaluation functions (f1, f2). It is assumed that an output is evaluated by single projecting function; therefore, the rank of the projecting function vector should be identical to the rank of output vector.

What if we have an analysis chain with shared variables? As shown in Figure 4.10, an analysis chain may have shared input in two parallel analysis models. In the figure, the projecting functions, f1 and f2, share a design variable (x2) while both have independent variables. Projecting between multiple inputs with or without share variables and multiple output space involves the following process unlike the simple projection with only independent inputs. The process for projecting shared input and output space is as follows:

- ***Seeding:*** Obtain all combinations of discrete input of associated input variables.
- ***Splitting:*** Group the combinations created in the 'Seeding' process by the input groups of evaluation functions. The divided discrete evaluation point sets are sub-seeds. Among the points in each set, duplicated points are eliminated and, finally, we have the sub-seeds for each evaluation function.

- ***Projecting:*** Evaluate each sub-system function at the points in sub-seeds in order to get corresponding output ranges of each projection.
- ***Merging:*** Combine the multiple response ranges obtained from 'Projecting' process in order to formulate response ranges for each point in the original seeds.

The above procedure is described in Figure 4.10 assuming each design variable has 2 discrete points, respectively; x1 has [1,2]; x2 has [a,b]; and x3 has [I, II]. An instance of the output range is represented as y1_1 for effective illustration.

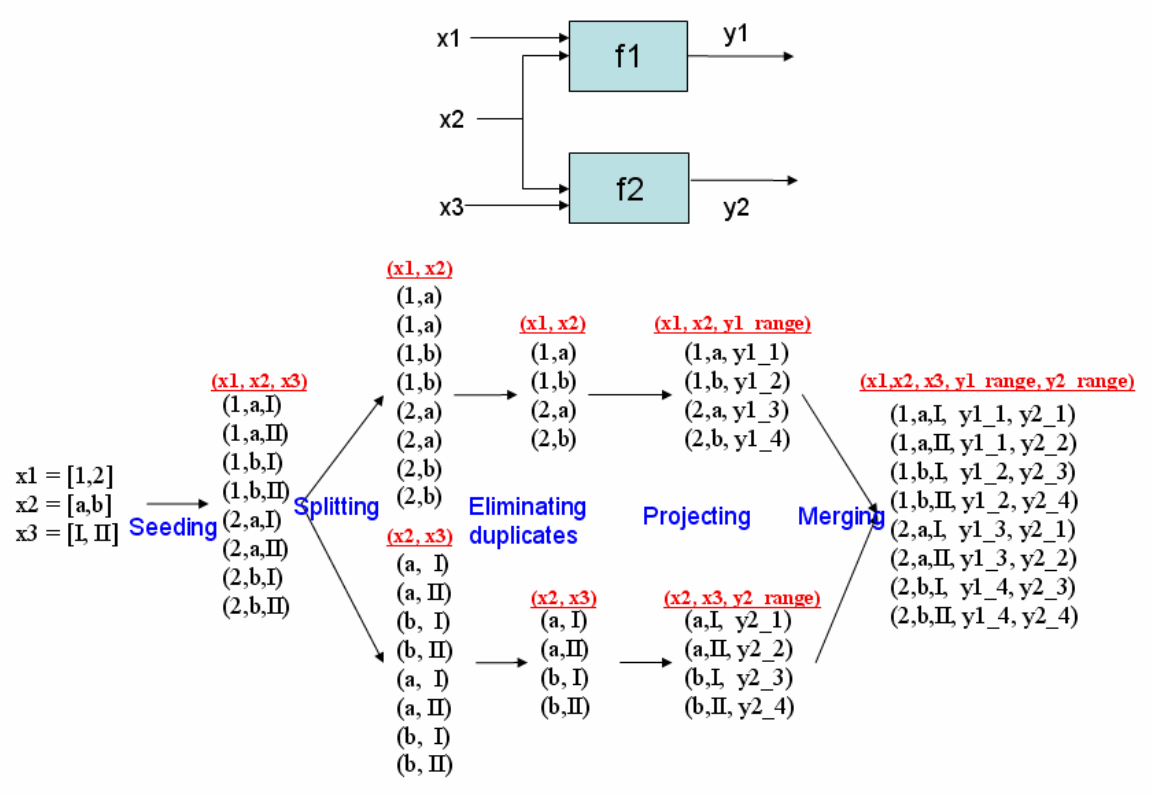

Figure 4.10 An example of function evaluation with multiple inputs and outputs with shared variables

- ***Seeding:*** we have two discrete points for x1, two for x2, and two for x3; therefore, all combinations of these discrete points of the design variables are created. In this process, we obtain the original seeds.

- ***Splitting:*** From the original seeds created by the seeding process, we divide them into two seed groups. One group is the (x1, x2) seed group with first and second columns of original seeds for the projecting function, f1. The other group is the (x2, x3) seed group with second and third columns of original seeds for the projecting function, f2. Once the two groups are formulated, duplicate seeds are eliminated in each of the seed groups.
- ***Projecting:*** The seeds group, (x1, x2), is evaluated to identify the range of y1 by projecting function, f1, and the seeds group, (x2, x3), is evaluated to identify the range of y2 by the projecting function, f2. The projection results are stored as data formed as input seed and output range, such as (x1, x2, y1_range) and (x2, x3, y2_range).
- ***Merging:*** the two separate input seeds and output range groups, (x1, x2, y1_range) and (x2, x3, y2_range) are merged together. Finally, the ranges of y1 and y2 at each discrete point in the original seeds, (x1, x2, x3, y1_range, y2_range), are obtained.

This process facilitates independent projections for f1 and f2 that are beneficial for *parallel computation* to increase efficiency discussed in Section 4.3.2.

The projection process discussed in this section provides corresponding output range at each discrete input point. In the next section, we discuss a method for evaluating whether the obtained output ranges satisfy with given constraint bounds in an output space.

4.7. INDUCTIVE DISCRETE CONSTRAINT EVALUATION (IDCE)

With stored the data evaluated in Section 4.6, designers find feasible ranges in all spaces: design and intermediate spaces, sequentially using the Inductive Discrete Constraints Evaluation (IDCE) technique discussed in this section. The procedure of IDCE technique includes the followings;

(a) Finding satisfactory seeds in an input space with given constraints (bounds) in an output space based on Hyper Dimensional Error Margin Indices (HD-EMIs),

(b) Obtaining exact border contours for feasible regions in an input space creating exact border points between satisfactory and unsatisfactory discrete points,

(c) Sequentially, repeating Step (a) and Step (b) along an inductive design process in order to find the lower level feasible regions using the exact borders obtained in Step (b) as constraint bounds in the output space.

Finally, we obtain satisfactory seeds and boundaries of feasible regions in a design space based on IDCE process. Step (a) is discussed in Section 4.7.1, Step (b) 4.7.2, and Step (c) 4.7.3.

4.7.1. The Hyper-Dimensional Error Margin Indices (HD-EMIs)

The first step of IDCE is checking if the projection of each discrete point from an input space to an output space is within given satisfying output ranges. In this dissertation, we propose Hyper Dimensional Error Margin Indices (HD-EMIs) as metrics for the feasibility check. HD-EMIs are extensions of the Error Margin Indices (EMIs) discussed in Chapter 3 from single performance (i.e., output) dimension to hyper-dimensional performance space.

To calculate HD-EMIs, It is required to determine whether the mean of an output range is in the feasible range or not. Since the feasible range in output space is represented as a discrete point set, it is not easy to check the feasibility. The approach proposed in this dissertation is to evaluate the nearest neighbor points from the location of the mean point as shown in Figure 4.11.

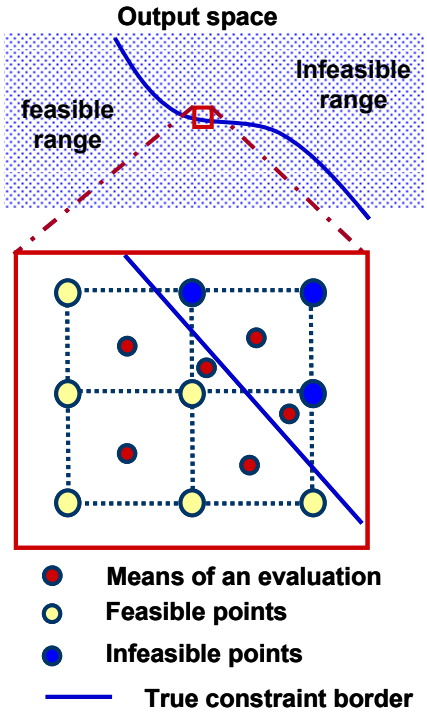

Figure 4.11 Feasibility evaluation technique

If more than half of the nearest neighbor points are satisfactory points, then we assume that the mean is in the feasible range. For more conservative applications, all nearest neighbor points must be satisfactory points for the mean to be in the feasible range. Based on the first criterion, two red dots (i.e., output means) in the upper right square in the detail view are unsatisfactory. Based on the conservative criterion, only one red dot in the lower left square is satisfactory. In both cases, we cannot avoid

discretization error; therefore, it is necessary to obtain finer resolution in an output space for better accuracy, specifically near the constraint borders.

When the mean of an output range is not in the feasible range, then the HD-EMI value is -1, which means the input point is unsatisfactory for the constraint bound in the output space, and we are finished with that calculation. When the mean is inside the feasible range, then it is required to identify the HD-EMI in each output direction.

The HD-EMI in each output direction has an individual value. As described in Figure 4.12, the $HD\text{-}EMI_i$, defined as the HD-EMI in the *i* direction, is the minimum HD-EMI among all HD-EMIs evaluated based on discrete points on a constraint boundary (***B***), their projected points on a boundary of an output range in *i* direction ($\boldsymbol{B}^i$), and the mean of the output range (***mean***). As the EMI increases, the output becomes more likely satisfactory, which means the output range moves farther from the constraint boundary.

$$HD-EMI_{all} = -1 \qquad \text{(if mean is in infeasible range)}$$

$$HD-EMI_i = Min\left(\frac{\left|mean_i - b_{j,i}\right|}{\left|mean_i - b^i_{j,i}\right|}\right) \qquad \text{(if mean is in feasible range)}$$

where, i = 1, ... , number of direction,

j = 1, ... , number of discrete points on constraint boundaries

mean the mean vector of an output range

$mean_i$ i th component of **mean**

$\mathbf{B_j}$ a discrete point vector on constraints boundaries

$b_{j,i}$ the *i* th component of $\mathbf{B_j}$

$\mathbf{B^i_j}$ the projected vector of $\mathbf{B_j}$ on the nearest boundary of output range along *i* th direction

$b^i_{j,i}$ the *i* th component $\mathbf{B^i_j}$

Figure 4.12 Calculation of HD-EMIs

For a better understanding, the details of the HD-EMI calculation are described in Figure 4.13.

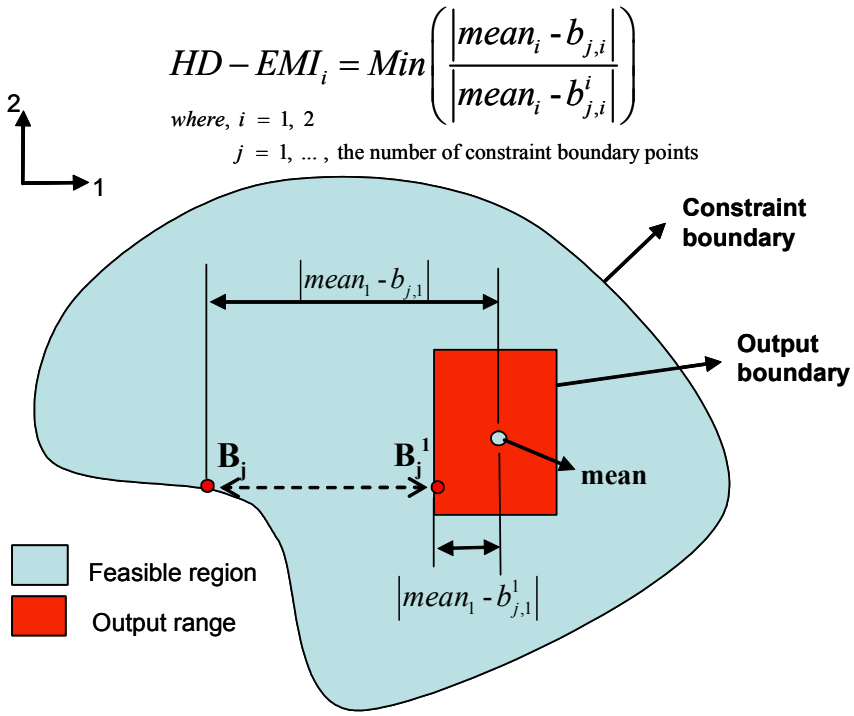

Figure 4.13 HD-EMI calculation in a direction

In the figure, the output space is two dimensional and the feasible region in the output space is described as a contour (constraint boundary). A rectangular region (a hypercube in multidimensional case) representing an output range at a discrete input has a mean inside. All points on the constraint boundary are projected on the output range boundary producing projected points. For example, a point ($\mathbf{B_j}$) on the contour is projected on the boundary of output range (rectangular) in Direction 1, and a projected point ($\mathbf{B_j^1}$) is created. The projection cannot travel through the output region so it does not create any projected points on the other side of the output range boundary. Once we have $\boldsymbol{B_j}$ and $\boldsymbol{B_j^1}$, we can obtain a candidate HD-EMI in Direction 1, which is the ratio of the distances between the ***mean*** and $\boldsymbol{B_j}$ versus the ***mean*** and $\boldsymbol{B_j^1}$ in Direction 1. This HD-EMI

calculation is performed for all other discrete contour points that can be projected in Direction 1 on the output boundary. Among the calculated HD-EMIs, the minimum is the HD-EMI_1, HD-EMI in Direction 1. The HD-EMI_2 is also obtained by the same technique. In mathematical form, the HD-EMI for each performance direction is

$$HD-EMI_i = Min\left(\frac{\left|mean_i - b_{j,i}\right|}{\left|mean_i - b^i_{j,i}\right|}\right) \tag{4.1}$$

In a multidimensional case, HD-EMIs for all other directions are also calculated in this way. Since HD-EMIs are calculated based on all constraint boundaries' points in an output space and the minimum HD-EMI are selected for each direction, we can obtain accurate HD-EMIs even if we have isolated multiple feasible regions.

The HD-EMIs obtained in this process are used to formulate exact discrete constraint boundary points in the input space as discussed in the next section.

4.7.2. Generating Exact Boundary Points in Input Space

An important issue in the discrete constraint evaluation approach is inaccuracy due to the discretization of a space. Because of the resolution problem, a constraint evaluation could be a rough estimation, which means some output ranges that are evaluated to be satisfactory may be unsatisfactory for the exact solution. Discretization errors can be alleviated by increasing resolution, which will also increase the amount of computation required. This problem occurs frequently in the vicinity of a border between satisfactory and unsatisfactory regions, and an HD-EMI calculation requires accurate measurement of the distance from an output range boundary to the constraints boundaries. Therefore, my point of interest is creating the exact constraint border points for accurate calculation of HD-EMIs.

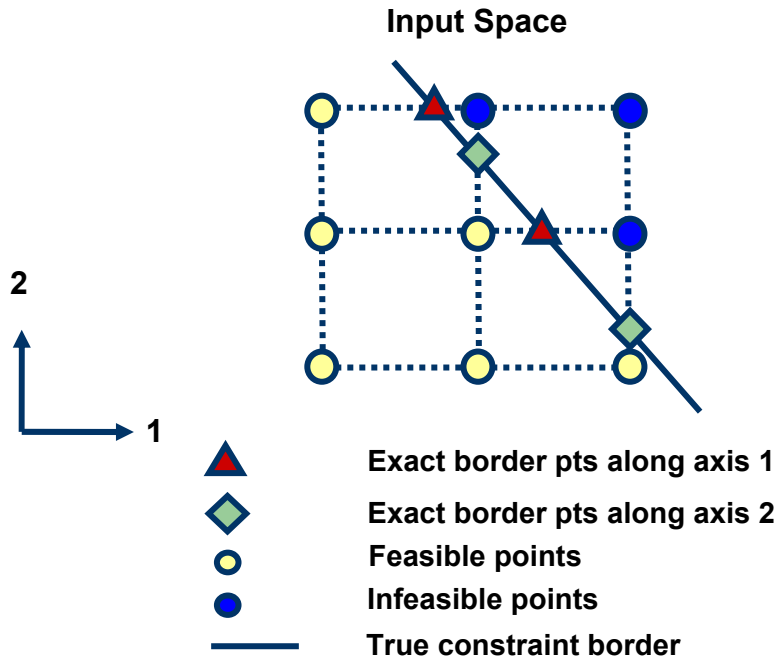

Figure 4.14 True boundary points generation

As shown in Figure 4.14, the true border is located in between discrete satisfactory and unsatisfactory points in an input space. We need to get the location of the discrete points that lie on the true border. To obtain the true boundary points, the diamond points, between the satisfactory and unsatisfactory points along the Direction 2, we fix the value of the Direction 1 as a constant and determine the true location in the Direction 2 using a numerical root finding method. To achieve the exact points, the triangular points, between the satisfactory and unsatisfactory points along the Direction 1, we fix the value of the Direction 2 and obtain the true location in the Direction 1 by a numerical root finding method. In this way, we can find the points on the true constraint boundary in an input space. Since this algorithm for finding true constraint boundaries evaluates all intervals between satisfactory and unsatisfactory points, we may evaluate not only a

single feasible region, but also multiple isolated feasible regions in an input space unless a feasible region is smaller than the discrete resolution.

Gradient based methods, such as the Newton-Raphson Method, are not appropriate as root finding methods because the HD-EMIs, used for constraint evaluation, are not in an explicit form. In this dissertation, we use the Bisection Method (Booth, 1967); however, False Position Methods are also applicable.

4.7.3. IDCE using the HD-EMIs for Type IV Robust Design

As mentioned, the IDCE is finding feasible spaces of input variables (design space) based on given final output ranges (i.e., performance requirements), this is an inverse method for using the analysis process chain shown in Figure 4.2. The IDCE process based on the analysis process in Figure 4.2 is illustrated in Figure 4.15.

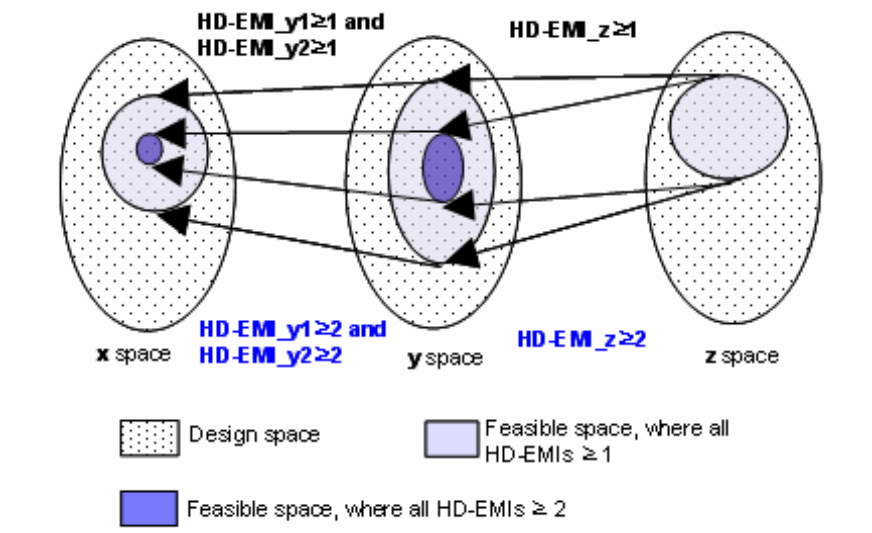

Figure 4.15 An example of the IDCE controlling HD-EMIs

The evaluation procedure starts with an assumption that a required range of the final performance, z, is given as shown as the gray area in z-space in the figure. From the given required range in z-space, we obtain a feasible range in y-space. In this step, first,

we find feasible discrete points in y-space by evaluating if the HD-EMI in z-space at each discrete point is greater than or equal to one. Second, we identify exact border contours between the feasible and infeasible discrete points in y-space. This is to identify the discrete points in y-space of which the HD-EMIs in z-space are equal to one, using the process described in Section 4.7.2. Once we obtain the feasible regions in y-space, the next step is to find feasible regions in x-space based on the identified feasible region in y-space in the previous step.

If we have multiple feasible discrete points in a design space, it means we have more room for tailoring design variables. In this case, we may increase the required HD-EMIs in the spaces of y and z, which may reduce the feasible ranges in x- and y-spaces, respectively. For example, if we set the HD-EMIs in the y- and z- spaces as two, then the feasible regions in x- and y- spaces will be reduced to the darker grey shown in Figure 4.15.

For selecting the best solution among feasible sets of solutions, the required HD-EMI value in each direction in each space should be selected statistically. A designer leaves wider margins between an output range and constraint boundaries by increasing the HD-EMI for the projecting function whose potential error, such as model structural uncertainty, is larger than others. This strategy is discussed in detail in the following section.

4.8. COMPROMISE DECISION SUPPORT PROBLEM FOR DETERMINING THE BEST SOLUTION

The HD-EMIs are important factors for a designer who seeks to determine the most desirable robust solution against model structure uncertainty, because HD-EMIs represent

margins for potential errors in projections for estimating output range by indices. In this section, we discuss how to strategically choose the required HD-EMIs at the output spaces in the IDCE process.

As shown in Table 4.3, the best HD-EMIs selection process is formulated using the compromise Decision Support Problem (cDSP). The purpose of the cDSP in this formulation is to identify the best set of HD-EMIs by trading off the achievement of target HD-EMIs. For example, the target HD-EMI for a more uncertain function (or model) is higher than others. We may also put higher weighting factor for the corresponding deviation in the objective function (Z).

Table 4.3 The cDSP for searching the best HD-EMIs

Given

$\boldsymbol{HD\text{-}EMI_{target}}$

z_{range} : required range of final performance

Find

HD-EMI, x

Satisfy

Constraints

$g(\boldsymbol{HD\text{-}EMI}, z_{range}) = \{\boldsymbol{x}\}$: the IDCE procedure

$Num\{\boldsymbol{x}\} \geq 1$

$HD\text{-}EMI_i \geq 0$ *or 1, where, i=1,2,..,* ***rank(HD-EMI)***

Goal

$HD\text{-}EMI_i/HD\text{-}EMI_{,target,i} + d_i^- - d_i^+ = 1$

$d_i^-, d_i^+ \geq 0$

$d_i^- \bullet d_i^+ = 0$

Minimize

$Z = f(d_i^-, d_i^+)$ *where i=1,2,..,* ***rank(HD-EMI)***

The given information in the cDSP includes a vector of target HD-EMIs in all output spaces, $\boldsymbol{HD\text{-}EMI_{target}}$, the required final performance (z) range, and the IDCE procedure,

*g(**HD-EMI**),* which produces a number of feasible design solutions (x) with the required ***HD-EMI*.** The rank of ***HD-EMI*** is the number of the projecting functions. In the example shown in Figure 10, the rank of the ***HD-EMI*** is three since the projecting functions are f1, f2, and f3 for estimating y1, y2, and z, respectively. A designer's objective is to find the best combination of the ***HD-EMI***. The constraints are the number of feasible design solution sets, *{**x**},* which must be greater than or equal to one. In addition, all HD-EMIs should be positive, which means at least the mean of an output range should satisfy the constraints in the output space. In some cases, designers may require all HD-EMIs to be greater than or equal to one so that entire output range can satisfy the constraints. Note that this is more conservative than the previous case. The deviations from the HD-EMI targets are minimized based on the objective function, $Z = f(d_i^-, d_i^+)$, in an Archimedean or Preemptive formulation. Trading off the achieved HD-EMIs in output (or performance) spaces allows us to put relatively higher HD-EMI in output space of which the model is more structurally uncertain. To this point, we have discussed the strategy and a method for Type IV robust design, the IDEM. In the next section, we validate the structure of the IDEM with a simple material and product design integration problem.

4.9. THEORETICAL STRUCTURAL VALIDATION OF THE IDEM

In this section, we check the validity of the IDEM structure based on a simple cantilever beam design example, which is the Theoretical Structural Validity check in the Validation Square method shown in Figure 4.16.

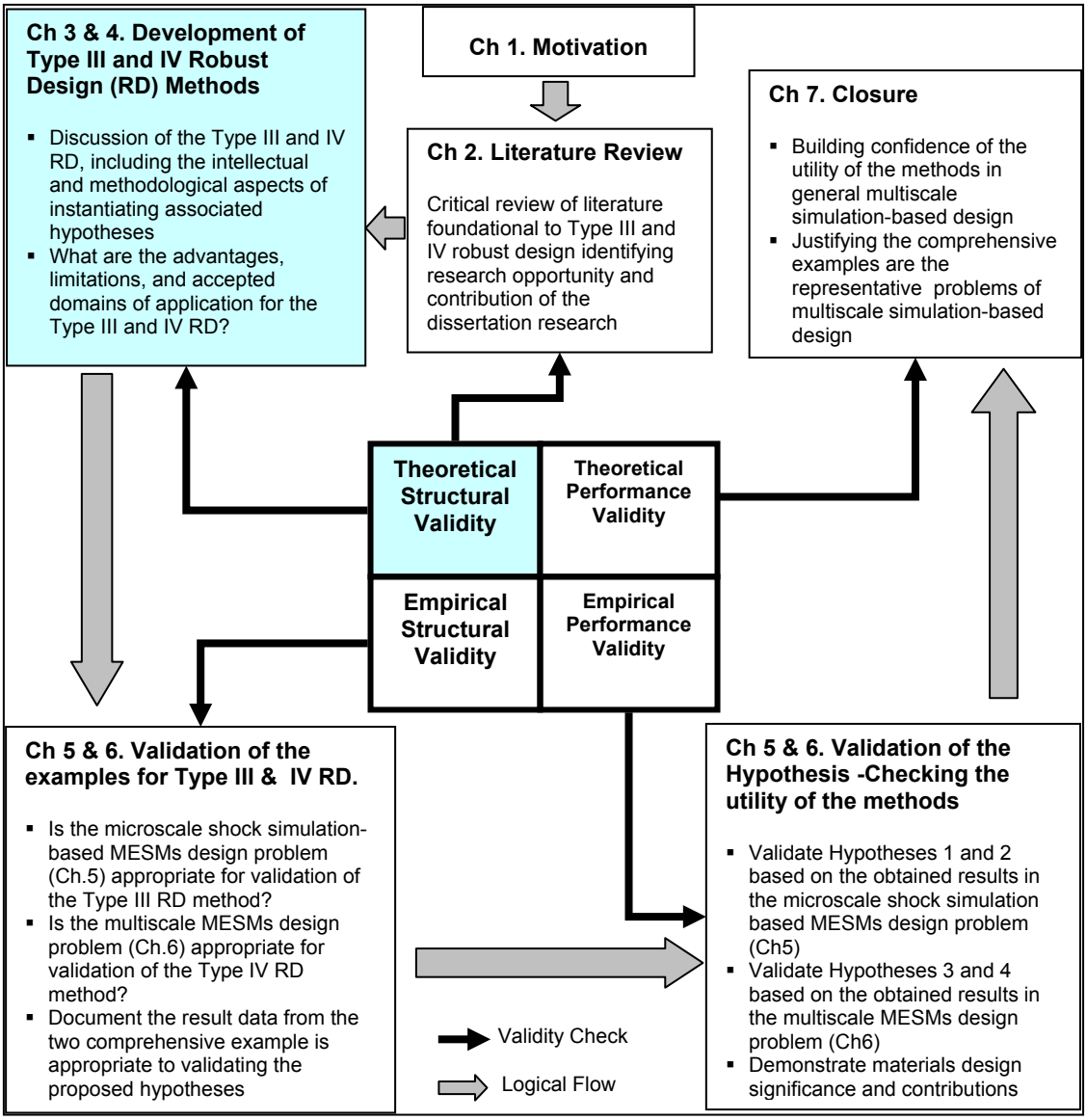

Figure 4.16 Validation square roadmap

4.9.1. A Clay filled Polyethylene Cantilever Beam Design

Many engineering polymers that contain fillers and extenders are particulate composites used for various engineering applications (Askeland, 1994). Adding clay particles into polyethylene as an extender, designers can tailor the composite material's properties for a specific need.

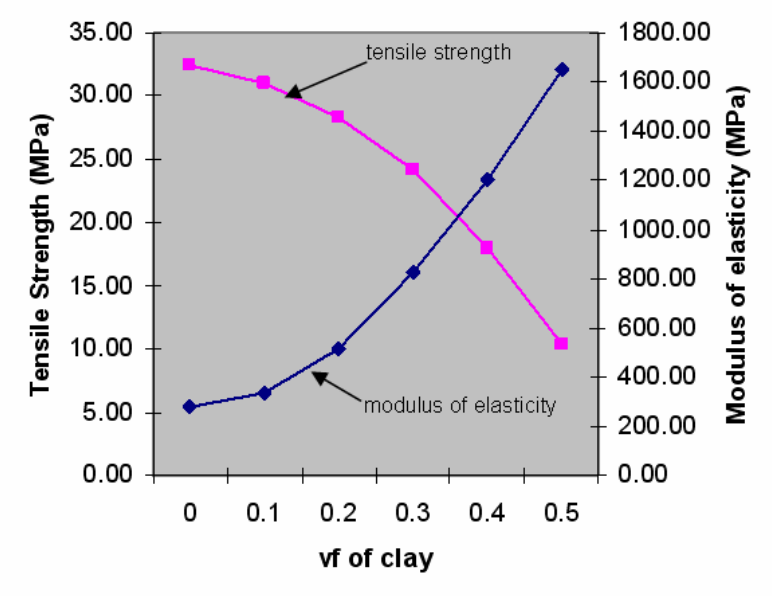

Figure 4.17 Effect of clay on the properties of polyethylene (Askeland, 1994)

As shown in Figure 4.17, the tensile strength of the composite decreases and the modulus of elasticity increases as the volume fraction of clay in polyethylene increases; therefore, it is important to tailor the volume fraction of clay in polyethylene for desirable product performance.

The example of a circular sectional cantilever beam and its materials design are shown in Figure 4.18.

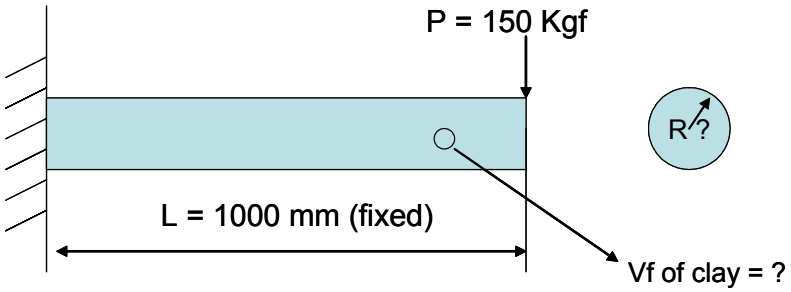

Figure 4.18 A cantilever beam problem

Our design objective is to design the radius of the cantilever beam and the volume fraction of clay in polyethylene for the beam material with following requirements.

Requirements

- The deflection with 150 *kgf* load at the end of the beam must not exceed 35 mm and a smaller deflection is better.
- The beam must withstand at least the maximum *500 kgf* without failure and being able to withstand a larger load is better.
- The weight of the whole beam must not exceed *30 kgf*, and a lighter beam is better.

Assumptions

- The material's behavior is assumed to be linear elastic and perfectly plastic.
- The weight of the beam itself can be ignored while estimating deflection and maximum load.

Based on the design requirements mentioned above, a design process for the cantilever beam is depicted in the Figure 4.19. First, the volume fraction of clay (x) is an input of f1, f2, and f3 that is used to calculate the density (ρ), modulus of elasticity (E), and tensile strength (σ_u) of the composite material, respectively. The properties of the composite materials and the radius of the beam are the inputs of f4, f5, and f6 that estimate the beam weight (W), beam deflection (δ_{max}), and maximum load (P_{max}), respectively.

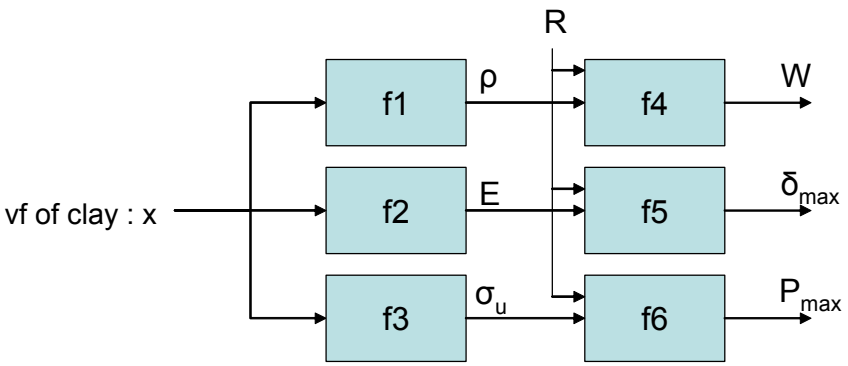

Figure 4.19 Cantilever beam design process.

The details of the functions are illustrated in Figure 4.20.

$$f_1(x) = \rho(x) = x\rho_{clay} + (1-x)\rho_{polyethylene} + \varepsilon_\rho(x)\ (kg/m^3)$$
$$f_2(x) = E(x) = 4875.6x^2 + 365.42x + 264.96 + \varepsilon_E(x)\ (Mpa)$$
$$f_3(x) = \sigma_u(x) = -80.028x^2 - 3.9152x + 32.331 + \varepsilon_{\sigma_u}(x)\ (Mpa)$$
$$f_4(\rho, R) = W(\rho, R) = \pi R^2 L\rho \cdot 10^{-3} + \varepsilon_w(\rho, R)\ (kg)$$
$$f_5(E, R) = \delta_{\max}(E, R) = 9.8PL^3/3EI + \varepsilon_{\delta_{\max}}(E, R)\ (mm)$$
$$f_6(\sigma_u, R) = P_{\max}(\sigma_u, R) = \sigma_u I/9.8LR + \varepsilon_{P_{\max}}(\sigma_u, R)\ (kgf)$$
$$where,$$
$$\rho_{clay} = 1150\ (kg/m^3),\ \rho_{polyethylene} = 940\ (kg/m^3)$$
$$L = 1000(mm), I = \pi R^4/4$$
$$\varepsilon_\rho(x) = \pm 0.1 \bullet f_1(x), \varepsilon_E(x) = \pm 0.1 \bullet f_2(x), \varepsilon_{\sigma_u}(x) = \pm 0.1 \bullet f_3(x)$$
$$\varepsilon_w(\rho, R) = \pm 0.1 \bullet f_4(\rho, R), \varepsilon_{\delta_{\max}}(E, R) = \pm 0.1 \bullet f_5(E, R),$$
$$\varepsilon_{P_{\max}}(\sigma_u, R) = \pm 0.1 \bullet f_6(\sigma_u, R)$$

Figure 4.20 Engineering models and conditions.

We simply assumed that all projecting functions (*f_1, f_2, f_3, f_4, f_5, and f_6*) could have ±10% error in their outputs. For the sake of demonstrating the capability of Type IV robust design capability, it is also assumed that there is no uncertainty in input variables (volume fraction of clay and beam's sectional radius). To consider the variability of input variables as well as parameter uncertainty in functions, the output deviation should be estimated with the uncertainty analysis method introduced for Type III robust design (Choi, et al., 2004).

4.9.2. Robust Design using the Inductive Design Exploration Method (IDEM)

The proposed IDEM has been implemented in MATLAB® and executed for the beam problem. In this section, we discuss the results of the example that are produced by the implemented code. The resolutions between discrete points are fixed as 5(mm),

20(kg/m^3), 100(Mpa), 4(Mpa), 0.01 for *R, ρ, E, σ_u, and x*, respectively. First, we search entire feasible ranges in property space (the spaces of *R, ρ, E*, and σ_u) with given performance requirements described in Section 4.9.1. The HD-EMIs (*HD-EMI$_4$, HD-EMI$_5$, HD-EMI$_6$*) for projecting functions (*f4, f5, and f6*) are set as greater than unity. Among the obtained feasible space of *R, ρ, E* , and σ_u, we select the value of *R* (radius of beam) that has the largest feasible space for the rest of the properties (*ρ, E* , and σ_u) because we want to maintain the *design freedom* as large as possible until the end of the design process, as discussed in Section 4.5. In Figure 4.21, this design procedure is illustrated using the Graphical Robust Design Process Model (GRDPM).

As discussed in Section 4.4, the requirements' ranges are the given ranged values for required performance. Therefore, the required ranges for weight, maximum stress, and maximum load are displayed as the solid double arrows from the top of the design task boxes (design with f4, f5, and f6). The model functions, f4, f5, and f6, have ranged uncertainty inside; therefore, the style of the boxes are double dotted boxes in style.

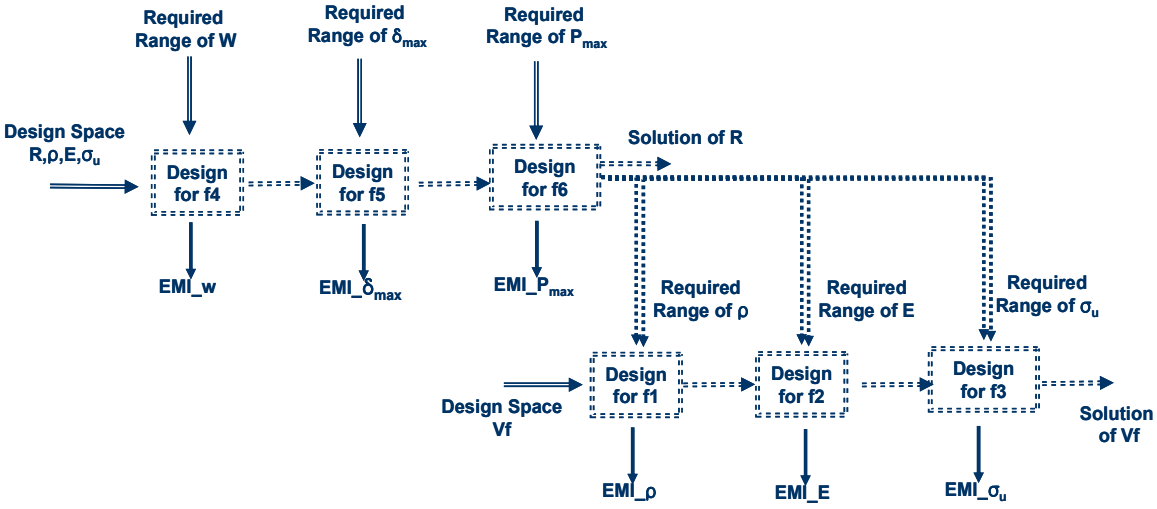

Figure 4.21 GRDPM for designing clay-filled polyethylene cantilever beam.

Shared design variables are passed from the design activities (f4, f5, f6) and then get the solution ranges for the radius of beam (R) at the end of the three design tasks. As the achieved responses from the design activities, the EMIs are achieved for the weight, maximum stress, and maximum load, which are represented as single solid lines since the EMI values are discrete and certain. The identified feasible interdependent solution space, properties (ρ, E , and σ_u) space, is transferred to the lower level as required response ranges of the design activities (design with f1, f2 and f3). The property space is identified by uncertain models at the upper level; therefore, the required range is uncertain and the types of the lines are double and dotted. At the lower-level design tasks, one design variable (volume fraction of clay) is shared by the tasks. Passing down the identified feasible ranges of the design variable, the final solution of the volume fraction of clay as well as the EMI at each design task is identified.

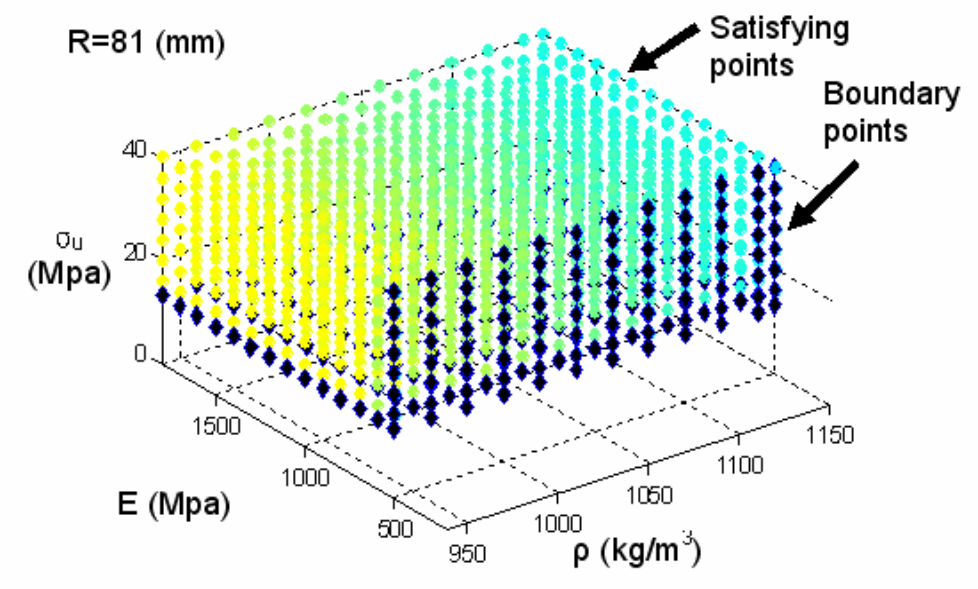

Figure 4.22 An achieved feasible range in tensile strength, modulus of elasticity, and density space

As the exploration results of the upper level design tasks, the largest feasible space is achieved by determining that R is 81(mm) and the feasible space of the composite

materials' properties is shown in Figure 4.22. Satisfactory discrete points (circular points) and boundary points (diamond points) between the feasible and infeasible spaces are shown in the figure.

With the feasible range achieved in the ρ, E, and σ_u-space shown above, the feasible space of the volume fraction of clay (x) is identified by setting the HD-EMIs ($HD\text{-}EMI_1$, $HD\text{-}EMI_2$, and $HD\text{-}EMI_3$) for projecting functions ($f1$, $f2$ and $f3$) as unity. The achieved feasible space of the volume fraction of clay is between 0.19 and 0.42. This means that the achieved space of the volume fraction of clay, [0.19, 0.42] and radius of beam section, 81 (mm) guarantee that the beam performance satisfies the given requirements under parameter uncertainty (10% variability of the performance) of the projecting functions (f_1, f_2, f_3, f_4, f_5, and f_6) and its propagation into the final performance space.

Since the achieved feasible design space can be further reduced, designers may select the HD-EMIs with various scenarios. In this dissertation, we formulate four different scenarios in order to obtain a single design solution within the obtained feasible space as follows:

- Scenario 1: Find the optimal design specifications for maximizing the maximum load and minimizing the maximum deflection considering parameter uncertainty in the projecting functions.
- Scenario 2: Find the robust design specification taking potential errors (model structural uncertainty) in the projecting function, f2 (the analysis model between x and E) into account.

- Scenario 3: Find the robust design specification considering potential errors (model structural uncertainty) in the projecting function, f3 (the analysis model between x and σ_u)
- Scenario 4: Find the robust design specification equally considering potential errors in the projecting functions, f2 and f3.

These scenarios are described in the cDSP formulation shown in Table 4.4.

Table 4.4 The cDSP for a cantilever beam and clay-filled polyethylene material design

Given

$HD\text{-}EMI_{target,i} = 10$, where $i=1,..,6$
$W = [0,30]$ (kgf), the smaller is the better
$\delta_{max} = [0,35]$(mm), the smaller is the better
$P_{max} = [500, inf]$(kgf), the larger is the better

Find

$HD\text{-}EMI_i$, R, and x

Satisfy

Constraints

$g(HD\text{-}EMI_i, W, \delta_{max}, P_{max}) = \{(R, x)\}$
$Num\{(R,x)\} \geq 1$
$HD\text{-}EMI_i \geq 1$, where $i=1,2,..,6$

Goal

$HD\text{-}EMI_i/HD\text{-}EMI_{target,i} + d_i^- - d_i^+ = 1$
$d_i^-, d_i^+ \geq 0$
$d_i^- \bullet d_i^+ = 0$

Minimize

Objective function Z

$Scenario1: Z = \sum d_i^-$ where, $i=5, 6$
$Scenario2: Z = d_i^-$ where, $i=2$
$Scenario3: Z = d_i^-$ where, $i=3$
$Scenario4: Z = \sum 0.5 d_i^-$ where, $i=2$ and 3

The targets for all HD-EMIs are given as 10. The performance requirements in weight, deflection, and maximum load are given. The objective of the cDSP is to find HD-EMIs at projecting functions, the radius of beam, and the volume fraction of clay in the material by minimizing the weighted summation of deviations between the achieved HD-EMIs

and its targets. The constraints on all HD-EMIs must be greater than or equal to 1 and the number of solutions found by the IDCE in R and x must be at least one. The objective functions are formulated according to the four scenarios.

The results of the design exploration are shown in Table 4.5. In all scenarios, the achieved $HD\text{-}EMI_1$ are infinite since constraint boundaries in the direction of density do not exist in defined property spaces, which means the entire density region within the property space is the feasible region satisfying the performance requirement.

Table 4.5 Design results with the four scenarios.

Scenarios		1	2	3	4
R (mm)		***81***	***81***	***81***	***81***
x		***0.42***	***0.42***	***0.21***	***0.32***
achieved HD-EMIs	*1*	*inf*	*inf*	*inf*	*inf*
	2	*6.09*	***6.09***	*1.02*	***4.33***
	3	*2.08*	*2.08*	***5.31***	***4.26***
	4	*1.98*	*1.98*	*2.28*	*2.12*
	5	***9.24***	*9.24*	*1.69*	*6.08*
	6	***1.53***	*1.53*	*3.05*	*2.56*
Weight (kgf)	*Min*	*17.17*	*17.17*	*16.43*	*16.82*
	Mean	*21.19*	*21.19*	*20.28*	*20.76*
	Max	*25.64*	*25.64*	*24.54*	*25.12*
δ_{max} *(mm)*	*Min*	*9.3*	*9.3*	*21.3*	*13.4*
	Mean	*11.34*	*11.34*	*26.03*	*16.45*
	Max	*13.9*	*13.9*	*31.82*	*20.1*
P_{max} *(kgf)*	*Min*	*571.53*	*571.53*	*965.20*	*789.26*
	Mean	*705.73*	*705.73*	*1191.70*	*974.48*
	Max	*854.08*	*854.08*	*1442.05*	*1179.22*

In Scenario 1, maximizing the objective function, the equally weighted summation of the deviations from the targets of $HD\text{-}EMI_5$ and $HD\text{-}EMI_6$, design specifications are identified as 81(mm) and 0.42 for R and x, respectively.

In Scenario 2, the maximum $HD\text{-}EMI_2$ is identified with the assumption that the projecting function f_2 has potential errors. Considering the potential errors in projecting function f_2, the $HD\text{-}EMI_2$ is maximized and the design exploration process has found the

solution, in which the projected output range (the range of modulus of elasticity) is farther from the constraint boundary created in the property space (ultimate strength, modulus of elasticity, and density) inversely from the given performance requirement as shown in Figure 4.22. The achieved HD-EMIs and design solutions are identical to those achieved in Scenario 1. *When the two performances must be optimized as Scenario 1 or the projecting function, f_2, has potential error, then the design specification obtained by Scenario 1 and 2 should be the designers' decision.*

The design solutions found in Scenario 3, are 81(mm) and 0.21 for R and x, respectively, which are different from those of Scenario 1 and 2. Considering potential errors in projection function f_3, $HD\text{-}EMI_3$ is maximized by the same procedure described in Scenario 2. In Scenario 3, the maximum load performance increases while sacrificing the achievement of minimizing maximum deflection compared with Scenarios 1 and 2. However, the solutions in Scenario 3 increase the robustness of the system performance against potential errors in the projection function, f_3. This means that although the true projecting function may be shifted from the current one, the output performances have more chance to be satisfied with the given performance requirements. *In case that the projection function, f_3, may have a large potential error, the design solution obtained in Scenario 3 is the right choice.*

In Scenario 4, maximizing the objective function, an equally weighted summation of deviations from the targets of $HD\text{-}EMI_2$ and $HD\text{-}EMI_3$, the design specifications of R and x are identified as 81(mm) and 0.32. The system performances of this scenario are still as good or better compared than those of Scenario 1 although this scenario is focused on robustness against potential error in projecting function f_2 and f_3. Considering the two

candidate solutions by Scenario 1 and 4, the better deflection performance is achieved in Scenario 1 and the better maximum load performance is achieved in Scenario 4. However, since all performances for the two scenarios meet the given requirement in this case, a designer might select the solutions in Scenario 4 since HD-EMI_3 obtained in Scenario 1 is lower than that found in Scenario 4 even if the final performances of the two scenarios are equally good. *Considering potential errors in the projection function, f_2 and f_3, we believe the design solution in Scenario 4 is a better decision than Scenario 1 because Scenario 4 provides equally good margins for potential errors in the projecting functions, f_2 and f_3 and the performance of Scenario 4 is as good as those of Scenario 1.*

As induced from the results, using the IDEM based on IDCE and HD-EMI, a designer may decide the specifications of materials and product simultaneously and systematically. Ranged sets of design specifications are identified for a given product's performance requirements considering propagated uncertainty in a model chain. With the feasible solutions sets, designers may have more freedom for their decisions and can choose to emphasize product performance or robustness against the uncertainty in employed models.

4.9.3. Theoretical Structural Validation Results

Challenging issues in robust design methods are addressed in Section 4.1. In Section 4.2, we identify the need for Type IV robust design to facilitate hierarchical materials and product design synthesis. Type IV robust design is designing a system that is insensitive to uncertainty in a design process – propagated uncertainty and model structural uncertainty. For instantiating the Type IV robust design concept, we develop the Inductive Design Exploration (IDEM) incorporating the Inductive Discrete Constraints

Evaluation (IDCE) and the Hyper-Dimensional Error Margin Index (HD-EMI) techniques. In this section, we check whether the instantiation of Type IV robust design is successfully performed or not by arguing the IDEM satisfies the requirements listed in Table 4.1.

The main advantage of the IDEM is that it provides a ranged set of design specifications rather than single solutions. Designers have more choices for adjusting the solutions to meet their specific interests. Regarding the requirements in Table 4.1, the IDEM facilitates

- Identifying feasible solution ranges, including isolated multiple feasible solution ranges, with the consideration of propagated uncertainty in an analysis model chain with given performance requirements,
- Modularizing sequential uncertainty propagation for estimating final performance deviation into stepwise projections from input to output space. When an analysis model in an analysis chain is changed, we need to evaluate only the projecting in which function the changed model is involved,
- Strategically selecting a design solution within feasible solution ranges either emphasizing product performance or robustness against uncertainty in hierarchical models,
- Parallelizing computations by decoupling design exploration processes and function evaluation which may incorporate computationally expensive uncertainty analysis,

- Decoupling input and output of analysis chain; a designer needs only a data file that includes the mapping between input and output from a distributed model for later design exploration, and
- Graphically representing a robust design process that includes associated uncertainty in values and models, types of information (ranged or discrete values), and decision-making results.

Although the IDEM is designed to be generally applicable to hierarchical design synthesis problems, it has some limitations which can be improved in the future. The IDEM may be computationally intensive for exploring a design space in which the number of design variables is large. For use of this method, we recommend for readers: (a) to reduce the number of design variables by a screening procedure (eliminating the design variables that do not significantly affect system performances), (b) to use metamodeling techniques for computationally intensive simulation models, and (c) to employ parallel computation for function evaluations.

Since the IDEM evaluates discrete points, it is impossible to avoid discretization errors. We have included an exact boundary generation technique for reducing the discretization errors. However errors still exist in the constraints boundary representation and the feasibility check of output means.

To overcome these limitations, we may need to develop algorithms for positioning discrete evaluation points with uneven resolutions across the space for efficient evaluation of the feasible space by discrete points. For example, we may include additional evaluation points in the vicinity of a constraint boundary while keeping larger resolution on the region with is farther from constraints bounds. Additionally, we may

need to sequentially reduce design and interdependent variables spaces focusing on the space in which our decision will be made.

4.10. SYNOPSIS OF CHAPTER 4

In this chapter, the Inductive Design Exploration Method (IDEM) is developed in order to answer Research Questions 3 and 4. The IDEM is a unique method since designers may find multiple (or ranged) sets of design specifications rather than a single solution. The IDEM consists of the Inductive Discrete Constraints Evaluation (IDCE) technique, Hyper Dimensional Error Margin Indices (HD-EMI), and the strategic selection technique of the best solution. Type IV robust design includes Type I, II, and III robust design; therefore this chapter is related to the RCEM-EMI described in Chapter 3.

In Section 4.1, model structure uncertainty and propagated uncertainty in an analysis chain in materials design is discussed. Achieving robustness in performance under these uncertainties is another important challenge in multiscale simulation-based materials design. In Section 4.2, Type IV robust design is clearly defined in order to deal with those uncertainties discussed in Section 4.1. In Section 4.3, a strategy for Type IV robust design is discussed based on the requirements derived from the critical evaluation of the existing approaches in Section 2.6. The IDEM for Type IV robust design begins with configuring a design process based on given system goals and simulation tools.

In Section 4.4, the Graphical Robust Design Process Model (GRDPM) is developed in order to efficiently describe a robust design process incorporating multiple tools (multidisciplinary analyses, simulation, and experiments), associated uncertainties, and decision-making. In Table 4.2, semantic entities in GRDPM are defined and the examples

of GRDPM are illustrated in Figure 4.6 and Figure 4.7. The overall procedure of the IDEM is discussed in Section 4.5 and illustrated in Figure 4.9. In Sections 4.6~4.8, the constituent techniques in the IDEM are discussed. Seeding and evaluating discrete points is discussed in Section 4.6. If shared variables exist in multiple function evaluation, a special seeding process is required as shown in Figure 4.10.

In Section 4.7, The Inductive Discrete Constraints Evaluation (IDCE) technique is discussed including the definition of Hyper-Dimensional Error Margin Indices, a technique for finding exact constraints boundaries, and an inductive (top-down) feasible space finding method. The Hyper Dimensional Error Margin Indices (HD-EMI) is defined extending the Error Margin Index (a single performance index) to multiple performance indices. The mathematical construct of the HD-EMI is described in Figure 4.12 and Figure 4.13. The exact constraints border finding technique is developed for reducing discretization error in the IDEM. In Section 4.8, a compromised DSP is used in order to find the best solution among multiple feasible discrete solutions. The best solution, the most reliable solution under model structure uncertainty (potential uncertainty), is identified by controlling the achieved HD-EMIs.

In Section 4.9, the theoretical structure of the IDEM is validated based on a clay-filled polyethylene cantilever beam design problem. Using the IDEM, feasible spaces in the chain of the multiscale design process are sequentially identified with consideration of the propagated uncertainty in the analysis chain. As listed in Table 4.5, the best solutions in four different design scenarios are identified considering potential uncertainty in the analysis models. The IDEM, A method for Type IV robust design, described in this chapter is further validated with a multiscale robust MESM design example in Chapter 6.

CHAPTER 5

MICROSCALE DISCRETE PARTICLE SHOCK SIMULATION-BASED ROBUST DESIGN OF MULTIFUNCTIONAL ENERGETIC STRUCTURAL MATERIALS

The purpose of this chapter is to validate Hypotheses 1 and 2 in Section 1.4. In the hypotheses, Type III robust design is proposed for achieving ranged sets of design specifications that are robust to not only variations in control and noise factors but also to the variations in system functions and constraints. Type III robust design is instantiated as a method, called the Robust Concept Exploration Method with Error Margin Index (RCEM-EMI). In Chapter 3, the implementation details including overall procedure and mathematical construct of the constituent of the RCEM-EMI framework are discussed. The soundness of the structure of the method is validated based on a simple example at the end of Chapter 3.

In this chapter, the utility of the RCEM-EMI is validated using a comprehensive material design example. This example is designing Multifunctional Energetic Structural Materials (MESM) based on a microscale discrete particle shock simulation. The simulation predicts the number of reaction initiation sites in a few micron sized materials' window filled with multiple aluminum and iron-oxide particles with epoxy binder.

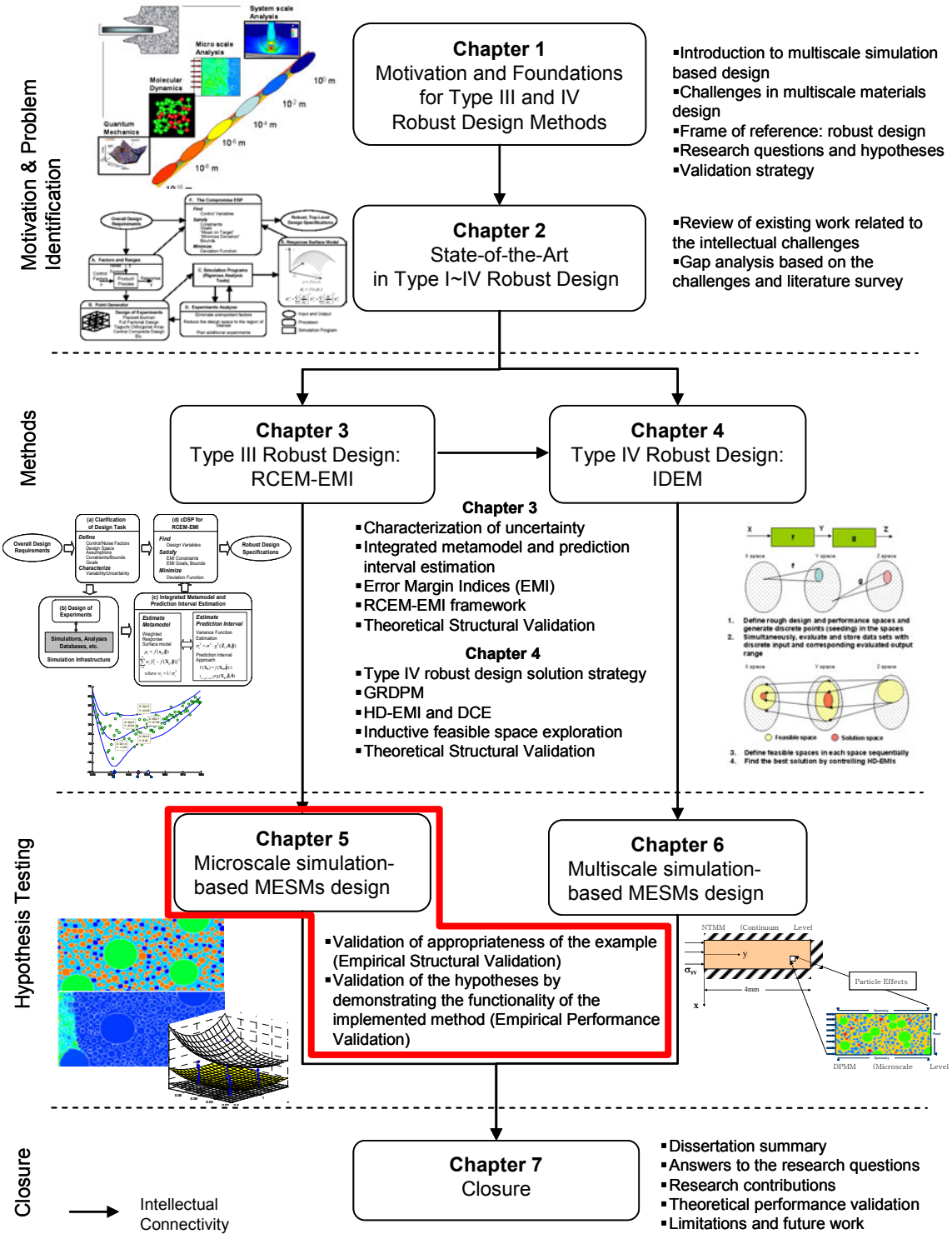

Figure 5.1 Dissertation roadmap

This simulation differs from other computational simulations since a random particle generation process is associated and the results of the simulation have random variability. Based on this simulation, the objective of this design problem is customizing the sizes of constituent particles and amount of voids so that chemical reactions in the RPMM can be activated robustly in the presence of the uncertainties in the shock simulation model. The validation process is as follows.

In Section 5.1, an introduction to the discrete particle shock simulation is provided. The purpose and capability of the simulation are discussed. The types of uncertainty associated with the simulations are explained in detail. We argue that the shock simulation-based design problem is **an appropriate example** for validating the RCEM-EMI (Empirical Structural Validation). In Section 5.1.3, the overall procedure of the RCEM-EMI, which is discussed earlier in Chapter 3, is reviewed in terms of the shock simulation example. In Sections 5.3~5.6, details of the RCEM-EMI steps including clarifying the design task, performing DOE, quantifying uncertainty, and searching for a robust ranged set of design specifications are explained in terms of the shock simulation examples. In Section 5.7, we discuss the design results, comparing the solution of the RCEM-EMI with the solutions of other design exploration algorithms. In the last section, we revisit Hypotheses 1 and 2 and argue **the utility of the RCEM-EMI** (Empirical Performance Validation).

5.1. INTRODUCTION TO MICROSCALE DISCRETE PARTICLE SHOCK SIMULATION

In this section, a microscale discrete particle shock simulation model is introduced. This shock simulation model is one of the multiscale computational models incorporated

to predict exothermic reaction response and structural integrity of candidate MESMs as shown in Figure 1.3. The main purpose of this simulation model is to predict shock-induced reaction initiation of a MESM, considering micron or sub-micron size heterogeneous discrete metal particles inside the material, which differs from ordinary continuum field analyses with an homogenous material property assumption. The main purpose of this section is to argue that this simulation-based materials design is a representative materials design problem, addressing the main challenges in Research Questions 1 and 2. Therefore, this example is appropriate for validating Hypotheses 1 and 2 (i.e., the utility of the RCEM-EMI approach).

In Section 5.1.1, the overall procedure of discrete particle shock simulation and the characteristics of the simulation are discussed. In Section 5.1.2, uncertainties associated with the shock simulation are classified and discussed. The appropriateness of the shock simulation example for validating the RCEM-EMI approach is justified.

5.1.1. Discrete Particle Shock Simulation with Reactive Particle Metal Mixtures (RPMM)

We have introduced the microscale discrete particle shock simulation with Reactive Power Metal Mixture in Section 3.2, which is developed by Austin and McDowell (Austin, 2005). In this section, we discuss the procedure of the shock simulation in further detail in order to provide the utility of the example for validating the RCEM-EMI.

As discussed in Section 3.2, the specific RPMM of interest in this simulation is a polymer-bonded thermite system ($Al+Fe_2O_3$), which is shown in Figure 5.2. The left figure of Figure 5.2 is a micrograph of a fracture surface of the RPMM. In the two figures on the right hand side, Al and Fe_2O_3 particles are shown.

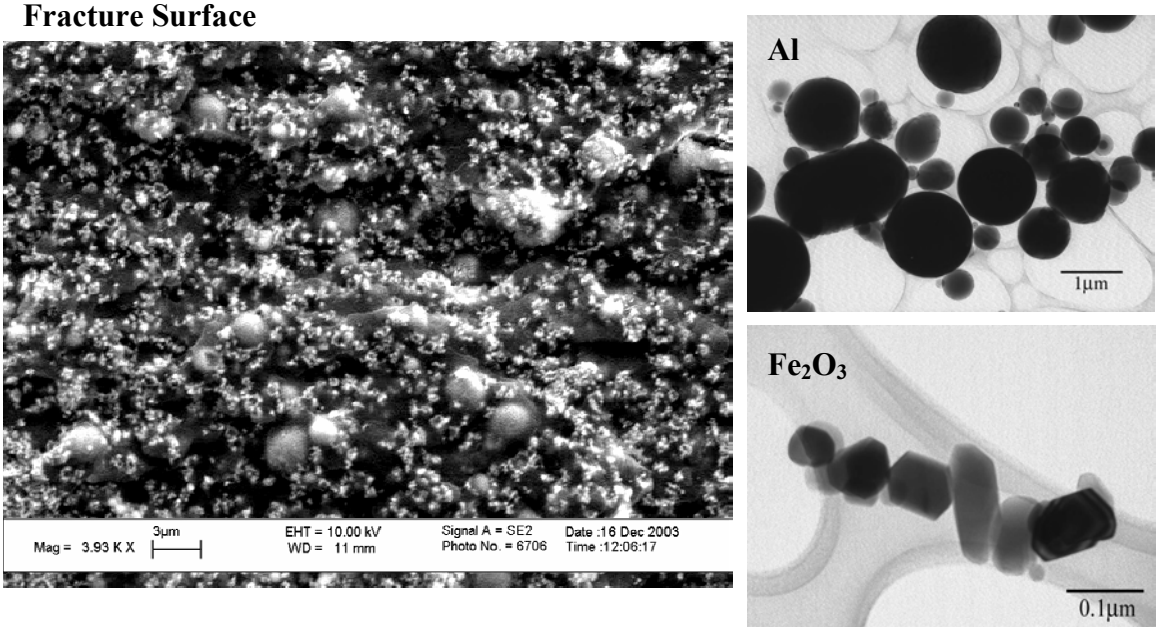

Figure 5.2 Actual microstructure of the RPMM

As a starting point, it is necessary to implement algorithms that generate synthetic microstructures (particle distributions) based on a set of mixture parameters that characterize the morphology of the system. The procedure for generating this microstructure is illustrated in Figure 5.3. The information of the morphology is obtained from the microscopy of a RPMM. The information derived from the micrograph is the size distribution (lognormal distribution) of particles and voids and the first nearest-neighbor distributions of aluminum particles. With diameters conforming to specified lognormal size distributions, discrete sets of micron-scale 'particles' (aluminum particles, iron oxide agglomerates, and voids) are randomly generated. The number of particles generated for each phase is controlled by the prescribed volume fractions of the statistical volume element (SVE). First, aluminum particles are placed within the SVE. Second, the location of the aluminum particles is controlled to reconcile first nearest-neighbor distributions in the aluminum phase to those estimated from experimental microscopy

using simulated annealing technique (Kirkpatrick, 1984). Finally, iron-oxide particles and voids are placed in the gaps. Small amounts of particle overlap are permitted (approximately 5–10% of the particle diameter), meaning the minimum distance between two particle centroids is slightly less than the sum of their radii. Volume fractions of the SVE not occupied by the particles are filled with epoxy (Epon 828). The complexity of the actual microstructure is simplified by assuming a 2-D distribution of circular particles. Particles in the 2-D cross section are considered as cylinders in 3-D, i.e., extended into the plane.

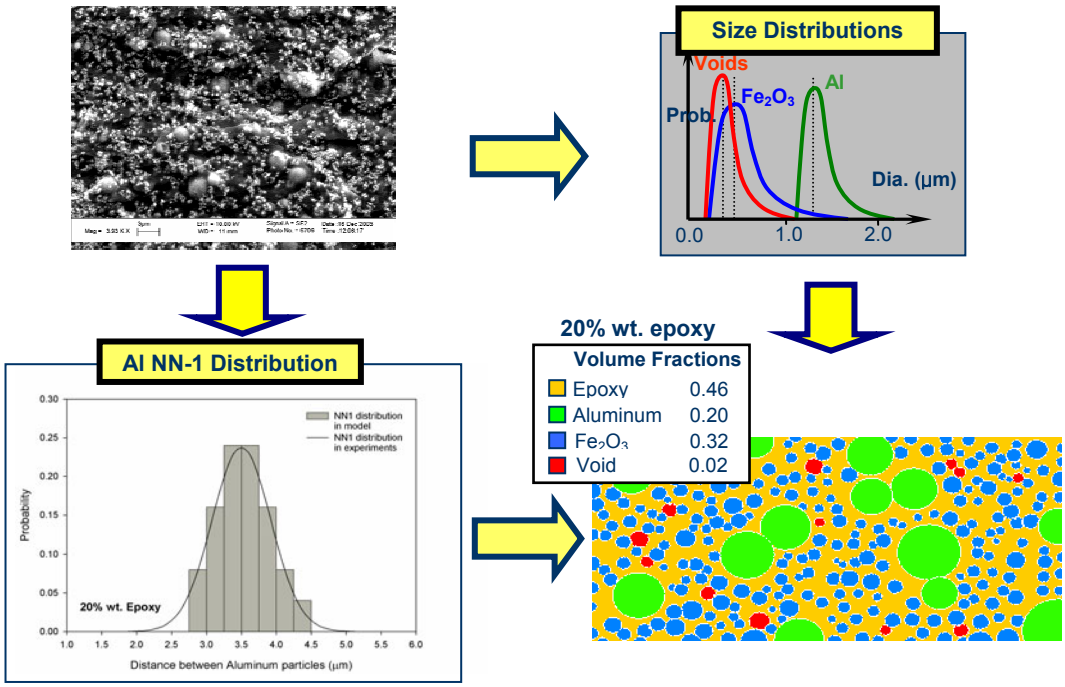

Figure 5.3 A random discrete particle generation procedure (Austin, et al., 2005)

The shock compaction of discrete particle systems has been studied extensively by Benson and co-authors (Benson, 1994; Benson, 1995; Benson, 1995; Benson and Conley, 1999) with numerical techniques. In this simulation, shock waves are propagated through the reactive particle systems in finite element simulations to explore the thermomechanical conditions that lead to microscale reaction initiation. The finite

element simulations are performed in a 2-D multi-material Eulerian hydrocode, Raven (Benson, 1995), developed by Benson. Eulerian formulations are used in these calculations because element distortions are too severe to handle with traditional Lagrangian formulations.

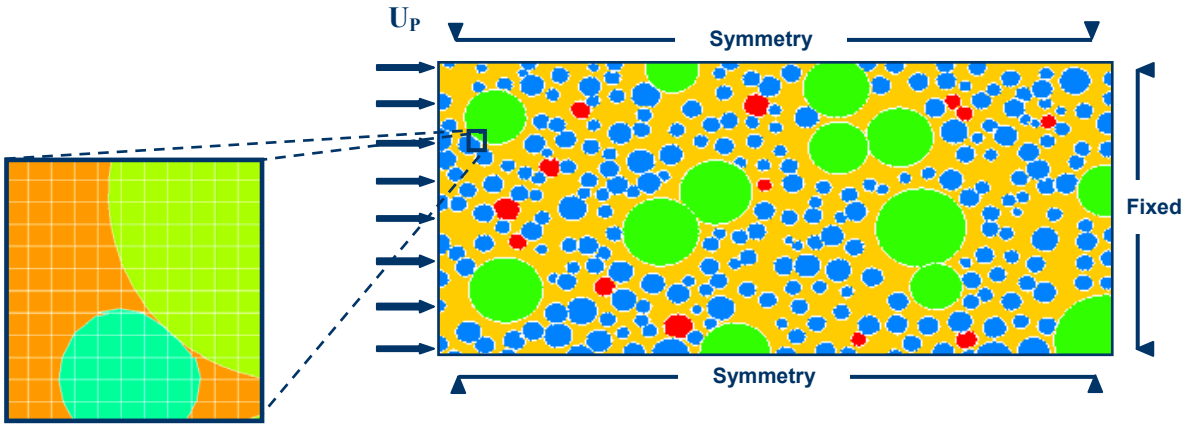

Figure 5.4 Boundary conditions of the discrete particle shock simulation (Austin, et al., 2005)

The shock compaction process is idealized as the passage of a single 1-D shock wave. Here, the plane strain assumption is invoked in order to reduce the true 3-D nature of shock loading to a more tractable 2-D case. The initial boundary value problem, which aims to replicate idealized shock loading, is depicted in Figure 5.4. A compressive shock wave is propagated though the mixture by applying a Lagrangian velocity boundary condition to the left surface of the SVE (here, Up represents the imposed particle velocity). Symmetry planes serve as Lagrangian boundary conditions for the top and bottom surfaces of the model. A fixed Lagrangian boundary condition is imposed on the right surface. The simulation is terminated once the shock wave front has traversed 90–95% of the SVE to avoid wave reflections.

Hydrostatic and deviatoric components of the stress-strain response in each material are distinguished. An equation of state (EOS) is used to calculate pressure and a strength

model is used to calculate deviatoric stress. Discussions of each constitutive model are omitted for brevity; the interested reader may consult the cited references for complete derivations. The Mie-Gruneisen EOS (cf. Ref. (Asay and Shahinpoor, 1993)) is used to model the hydrostatic response of the aluminum and epoxy phases; the Murnaghan EOS (Murnaghan, 1937) is used as the hydrostatic model for the iron oxide phase. A physically-based constitutive model proposed by Klepaczko (Klepaczko, et al., 1993) is used to model the deviatoric stress-strain response of the aluminum phase. The Hasan-Boyce model (Hasan and Boyce, 1995) is used as the strength model for the epoxy phase. Unfortunately, a physically-based constitutive model for iron oxide was not available in the open literature. Therefore, a simple elastic-plastic model has been adopted, consisting of an initial linear elastic response followed by linear isotropic strain-hardening.

Table 5.1 Constitutive models in the discrete particle shock simulation

Material	Epon 828	Al 1100	Iron Oxide
Equation of State	Gruneisen	Gruneisen	Murnaghan
Deviatoric Stress	Hasan-Boyce	MTS (Klepaczko)	Elastic-Plastic (LH)

The performance of a reactive particle system is evaluated based on the number of sites that experience microscale reaction initiation (micro-initiation) during shock wave propagation. The sites that experience micro-initiation are relegated to small volumes of the SVE where the reactants are in intimate contact. Micro-initiation is characterized by the unbounded growth of hot spots that develop at reactant interfaces due to the heat liberated by the exothermic chemical reactions. It should be noted that microscale reaction initiation events are distinctly different from macroscale reaction propagation, which depends on many factors that have not been addressed in these analyses.

The predictions of sites that experience micro-initiation are calculated based on the Merzhanov criterion (Austin, et al., 2005; Merzhanov, 1966). According to the Merzhanov criterion, the thermal explosion of a hot spot occurs when the heat generated from the chemical reaction outpaces the heat conduction to the surroundings. To evaluate the Merzhanov criterion, the following quantities must be determined at a reactant interface: (1) the temperature of the local hot spot, (2) the temperature of the hot spot surroundings, and (3) the size of the hot spot. The aforementioned quantities are calculated during shock wave propagation in the finite element simulations. This provides time histories of the number of micro-initiation sites contained in the SVE. For the purposes of this study, the maximum number of micro-initiation sites during shock wave propagation is taken as the response of the system. This section is described based on the M.S. thesis published by Austin (Austin, 2005).

5.1.2. Empirical Structural Validation: Challenges in RPMM Design Based on the Discrete Particle Shock Simulation

This RPMM design problem is an appropriate example for the RCEM-EMI validation because of the following challenges. One of the challenges in designing an RPMM is that the input variables may have variability caused by natural randomness. For example, the volume fraction of each material, which is a controllable factor (or control factor), could have random variability. Even though a designer determines the volume fraction of Al as a design solution, the real volume fraction of Al may vary from the design specification due to the randomness inherent in material processing. This randomness could produce unexpected performance variation in a manufactured RPMM. Additionally, some input variables cannot be controlled, or are difficult for a material designer to control. Variability in uncontrollable factors (noise factors) effects material performance.

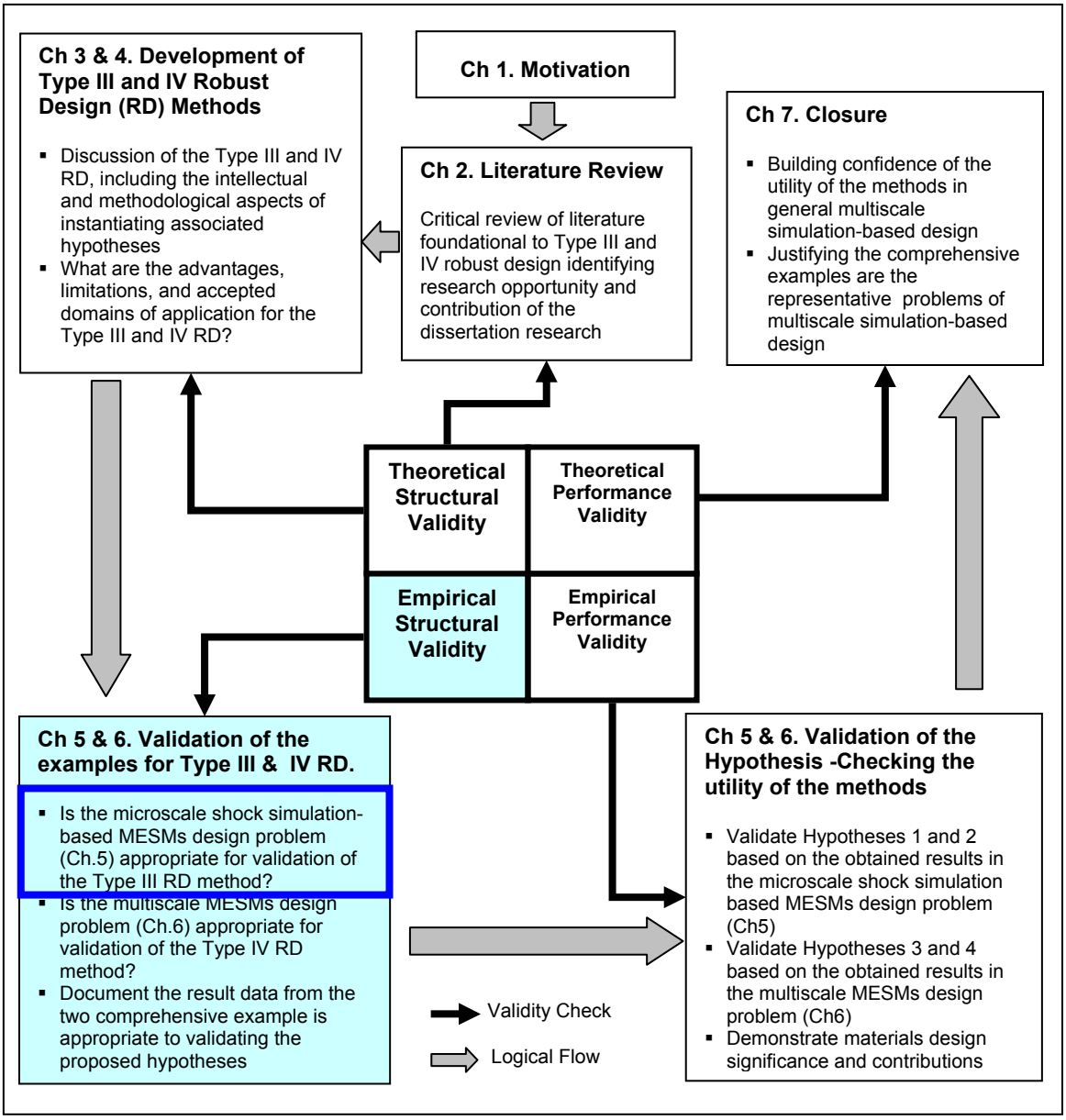

Figure 5.5 Validation square roadmap

For example, the variances of particle size are very hard or expensive for designers to control. In designing a RPMM, it is necessary for a material designer to consider variability in controllable and uncontrollable factors since this variability could cause serious performance defects. Therefore, a robust design method for Type I and II discussed in Section 1.3 and Section 3.4 is needed.

The second challenge in designing RPMMs is that the simulation results, e.g., the estimations of microscale reaction initiation, may contain pseudo-random variability despite a fixed set of input variables. This implies that the system has other noise factors that have not been modeled as input parameters. This is addressed as 'unparameterizable variability' in Section 3.2.1 and will not be repeated here. Due to the unparameterizable variability, it is important to incorporate Type III robust design (see Sections 1.4 and 3.4) as well as Type I and II.

The third challenge in RPMM design is lack of data due to computationally intensive simulations (on the order of an hour for a single run). If a system is deterministic, then material designers need a single simulation to be performed at each evaluation point in a design exploration process. However, if a system is non-deterministic due to unparameterizable variability, then a large number of samples at each evaluation are needed since the accuracy of system's variability estimation depends on the sampling size. The most accurate way of designing a non-deterministic system, considering both unparameterizable variability and variations in control and noise factors, is to perform Monte Carlo simulations for obtaining a statistical distribution of the variability. This approach requires an extremely large number of experiments for an uncertainty analysis at single evaluation point in a design exploration process. Employing this approach is virtually impossible since the finite element simulations incur a significant computational expense. The lack of information causes inaccuracy in creating metamodels for mean and variance of performance, which is one of the main sources of model parameter uncertainty. Therefore, it is required to incorporate Type III robust design (see Sections 1.4 and 3.4) as well as Type I and II.

As mentioned in this section, the RPMM design example based on the non-deterministic microscale particle shock simulation incorporates a variety of uncertainties. These are parameterizable and unparameterizable variability due to inherent randomness and model parameter uncertainty due to lack of simulation data. In addition to the natural uncertainty and model parameter uncertainty, model structure uncertainty is also associated with the simulation due to uncertainty assumptions and idealizations in the simulation model as discussed in Section 3.2.3. This is one of the major uncertainties in estimating reaction initiation capability in this shock simulation, which is discussed in detail in Section 6.1. Consequently, the RPMM design problem based on the microscale discrete particle shock simulation incorporates all types of uncertainty mentioned in Section 3.1 and 3.2 and the uncertainties significantly effect on material performance prediction. Therefore, this example is an appropriate materials design problem for demonstrating the utility of the RCEM-EMI, which is the validation of Hypotheses 1 and 2.

5.1.3. Planning Tasks for Empirical Performance Validation

As discussed in the previous section, this RPMM design problem based on microscale discrete particle shock simulation is an appropriate example for validating Hypotheses 1 and 2. In this section, we plan tasks necessary for empirical performance validation, which is used to build confidence in the utility of the RCEM-EMI discussed in Chapter 3 for this microscale discrete particle shock simulation.

The following three main tasks are necessary for Empirical Performance Validation – validating the utility of the RCEM-EMI for the example problem - in the Validation Square shown in Figure 5.5.

Task 1: *Validate that the integrated estimation of regression model and prediction interval in the RCEM-EMI discussed in Section 3.7 is useful for estimating non-deterministic behavior (i.e., unparameterizable variability) in the shock simulation model in a computationally efficient manner.* The main focus in this validation task is on the efficiency (i.e., sample size) of the approach for capturing the random effects of the simulation comparing with other conventional uncertainty analysis approach (Monte Carlo simulation). Achieved regression model, prediction interval, and obtained samples will be plotted to support the accuracy of the estimation using this approach. This task is the demonstration for validating Hypothesis 2 discussed in Chapter 1.

Task 2: *Find a ranged set of RPMM design specifications robust to Type I, II, and III variability using the RCEM-EMI.* It is argued that the RCEM-EMI is developed for finding ranged set of design specification robust to uncertainty embedded in a model (i.e., unparameterizable variability and model parameter uncertainty) as discussed in Section 3.3 as well as Type I and II variability. This task is planned for demonstrating this capability. Three different design exploration methods are investigated in this task, which are traditional optimization, the RCEM-DCI, and the RCEM-EMI. The design solutions using the three methods are achieved and the uniqueness of the solution found using the RCEM-EMI is discussed and compared with other solutions. Successful results of this task validate Hypothesis 1 discussed in Chapter 1.

Task 3: *Build a confidence to the RCEM-EMI in achieving robust RPMM design solution to model parameter uncertainty due to lack of samples.* As discussed in Section 3.2.2, model parameter uncertainty in a metamodel is due to lack of sampling. In this task, we demonstrate that a design solution found using the RCEM-EMI is robust to model

parameter uncertainty due to lack of sampling. For the demonstration, design solutions are found based on various regression models incorporating from small size samples to large size samples. This solution search is performed using traditional optimization, the RCEM-DCI, and the RCEM-EMI. Using each method, the convergence of design solutions is observed while increasing sample size and the convergence rates of the three methods are compared. Successful validation of the RCEM-EMI is to demonstrate that the solution convergence of the RCEM-EMI is faster and more stable than those of other two design methods. This is the task for validating Hypothesis 1.

In this section, we discuss the plan for empirical performance validation, which is discussed in the following sections. This section is revisited discussing validation results in Section 5.8.

5.2. THE RCEM-EMI FOR DESIGNING RPMMS BASED ON MICROSCALE DISCRETE PARTICLE SHOCK SIMULATION

The overall procedure of the RCEM-EMI is discussed in Section 3.5. In this section, the procedure of the RCEM-EMI for designing RPMMs based on the microscale discrete particle shock simulation is discussed. As shown in Figure 5.6, the procedure of the design task is identical to the procedure described in Section 3.5.

In Section 5.3, the RPMM design task is clarified. Design objectives are established and control and noise factors are defined. Design space of control factors and variance of noise or control factors are defined. Performance requirements and constraints are discussed. The parameters that are assumed and fixed are addressed. Uncertain

assumptions or idealizations are discussed. Finally, the response that is captured as the performance of reaction initiation is defined and explained.

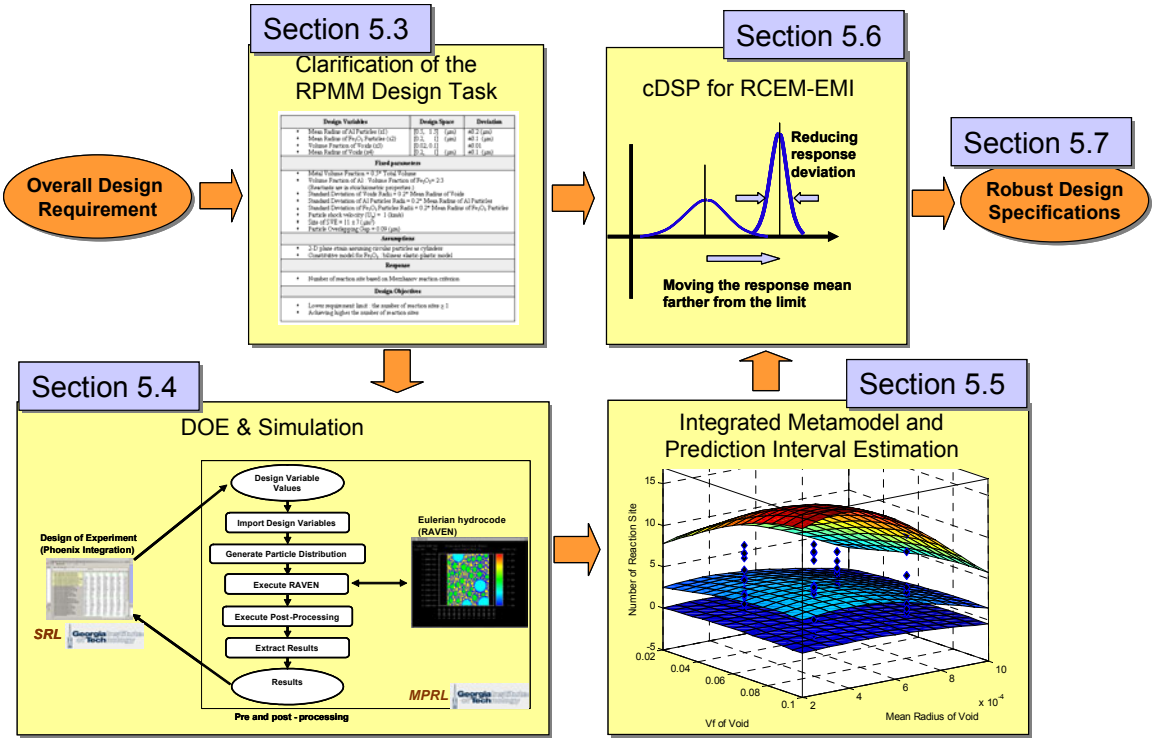

Figure 5.6 The RCEM-EMI for designing an RPMM

In Section 5.4, an infrastructure for DOE and distributed RPMM shock simulation is introduced. The computational interface between the design software, the pre- and post-processing, and the shock simulation package is discussed for automated distributed sequential simulation runs.

In Section 5.5, the mean and prediction interval of the non-deterministic responses (i.e., reaction initiation capability of a RPMM) is modeled using the integrated estimation method discussed in Section 3.7. Response surface models with appropriate link functions (i.e., generalized linear models) are used for modeling the mean and variance of the non-deterministic responses in terms of control and noise factors.

In Section 5.6, a solution search algorithm with compromise Decision Support Problem incorporating Error Margin Indices (EMIs) is used for searching a ranged set of design specifications robust to the variability and uncertainty discussed in Section 5.1.2. The search algorithm finds design specifications that result in robust RPMM reaction initiation under the variability and uncertainty.

In Section 5.7, the design specifications and corresponding responses obtained using the RCEM-EMI are discussed comparing solutions with a method for Type I and II robust design, the Robust Concept Exploration Method with Design Capability Index (RCEM-DCI), and the traditional optimization.

As mentioned above, in the following sections, the steps of the RCEM-EMI for designing RPMMs are explained in detail. Finally, the utility of the RCEM-EMI in designing materials based on non-deterministic simulations is validated and summarized in Section 5.8.

5.3. CLARIFYING THE RPMM DESIGN TASK

The first step for the RCEM-EMI shown in Figure 5.6 is clarifying the design task. The RPMM design objective is to determine the specifications of RPMM that are the mean size of each constituent particle and voids and the volume fraction of voids. The chemical reaction of the designed RPMM should be robustly initiated in the presence of the variability in control and noise factors, the variability in the micro-structure of RPMM, and model parameter uncertainty due to lack of simulation data. The details of the design task are summarized in Table 5.2.

Design variables are the mean radius of aluminum particles (x1), iron-oxide particles (x2), and voids (x3), and the volume fraction of voids (x4). Design spaces of the design variables are determined as shown in the table. The design spaces of particle sizes are specified as wide as the shock simulation allows. The deviations of the design variables are also specified in the table. Even if each mean particle size is accurately measured from the supplier, the true mean size in a small sampled SVE could be different from the supplier's specification. Changes in particle morphology constitute another source of variability discussed in Section 5.1.2.

Some of the parameters are fixed with some assumptions. The volume fraction of metals (aluminum and iron-oxide) is fixed at the maximum level (i.e., 50%) since larger volume fraction of metals will increase the capability of reaction initiation as well as structural integrity. The volumetric ratio between aluminum and iron-oxide is fixed based on the stoichiometric property ratio as shown in Table 5.2.

Table 5.2 A clarification of RPMM design task using the shock simulation.

Clarified Items	Specifications
Design Variables	x_1 : Mean Radius of Al Particles x_2 : Mean Radius of Fe_2O_3 Particles x_3 : Volume Fraction of Voids x_4 : Mean Radius of Voids
Design Space	x_1 = [0.5, 1.5] (μm) x_2 = [0.2, 1] (μm) x_3 = [0.02, 0.1] x_4 = [0.2, 1] (μm)
Deviation of Design Variables	$\Delta x_1 = \pm 0.2$ (μm) $\Delta x_2 = \pm 0.1$ (μm) $\Delta x_3 = \pm 0.01$ $\Delta x_4 = \pm 0.1$ (μm)
Assumptions	▪ Generalized plane strain assuming circular particles as cylinders ▪ Constitutive model for Fe_2O_3 : bilinear elastic-plastic model

Fixed Parameters	▪ Metal Volume Fraction : 50% Volume Fraction ▪ Volume fraction of Al : Volume Fraction of Fe_2O_3= 2:3 (reactants are in stoichiometric properties) ▪ Standard Deviation of Void Radius : 20% of the Mean Radius of Void ▪ Standard Deviation of Al Radius : 20% of the Mean Radius of Al Particles ▪ Standard Deviation of Fe_2O_3 Radius : 20% of the Mean Radius of Fe_2O_3 Particles ▪ Particle Shock Velocity (U_p) : 1 (km/s) ▪ Size of SVE: 14 x 7 (10^{-6} mm^2) ▪ Number of Elements: 250 x 135 ▪ Particle Overlapping: $-0.09*10^{-3}$ (mm)
Response	Number of reaction site based on Merzhanov reaction initiation criterion
Design Objectives	▪ Lower requirement limit: the number of reaction sites ≥ 1 ▪ Achieving higher the number of reaction sites

The standard deviations of the radii of aluminum and iron-oxide particles and voids are assumed to be 20% of the mean radii. The particle velocity (U_p) is also set to 1 (km/s) since higher particle velocity results in better possibility of reaction initiation. The size of SVE is fixed to 14 μm x 7 μm. The shock simulation results of larger SVE size are more accurate, but the computational expense is much higher. For example, the SVE size of 20 μm x 14 μm requires approximately four times longer analysis time than 14 μm x 7 μm. Moreover, the random particle generation process falls into infinite loop more frequently since the particle generation process cannot find the right positions of all particles satisfying given requirements (e.g., volume fractions, means, and standard deviations of particles, etc). Therefore, based on the given shock simulation capability, the window size of SVE is fixed as 14 μm x 7 μm. Larger SVE size should be considered for better accuracy in the future as the simulation capability increases. The particle overlapping is the size of gap between particles. If the gap is set to zero, all particles should not be interfaced. If the gap is set to negative, then particles could overlap. In a manufacturing process, the particles could be overlapped. In addition, as mentioned

above, the particle generation process could fall into an infinite loop when the gap is zero or higher. Therefore, in the simulation, the size of gap is given as 0.09 μm.

The assumptions and idealization in the table are listed based on the discussion in Section 3.2.3 and 5.1.1. As mentioned, in the RCEM-EMI, Type III robust design, the uncertain assumptions of the simulation model are not considered in the design process, but are considered in the Inductive Design Exploration Method, discussed in Chapter 6.

Finally, the response measured for the capability of reaction initiation induced by shock compaction is the number of reaction initiation sites obtained by using the Merzhanov criterion discussed in Section 5.1.1. As discussed in Section 3.2.1, this response varies randomly with the microstructure of a SVE with a fixed set of design variables. It is shown in the simulation results discussed in Section 5.4. The design specification of RPMMs should be robust to the unparameterizable variability. The minimum number of reaction initiation sites for reaction propagation in SVE is set to one, which means at least one reaction site should exist for reaction initiation and propagation in a sampled SVE. A larger density of reaction sites increases the possibility of reaction initiation and propagation.

In this section, the RPMM design tasks are clarified based on information from the shock simulation modeling process and capabilities. The uncertainty and variability, to which the performance of the designed RPMMs should be robust, in the simulation model are defined and summarized. The objectives of the RPMM design task are defined. This information is necessary to DOE and simulation and cDSP for the RCEM-EMI as shown in Figure 5.6.

5.4. DESIGN OF EXPERIMENTS AND SIMULATION

In this section, we discuss the second step of the RCEM-EMI for designing an RPMM shown in Figure 5.6.

5.4.1. Design of Experiments

In this dissertation, the response surface methodology is employed in building empirical models for the shock simulation model. The most commonly used design of experiments (DOE) in second order response surface methodology is Central Composite Design (CCD). CCD is composed of corner points, star points (also called axial points), and center points. The basis of any central composite design is a two-level full or fractional factorial design. The number of corner points is 2^{k-f}, where k denotes the number of factors (i.e., design variables) and f the fraction. This component provides for the estimation of linear main effects and all two-factor interaction effects (Neter, et al., 1996). Corner points have coded coordinates of the form (±1, ±1, ..., ±1). The number of star points is $2k$. These factor level combinations permit the estimation of all quadratic main effects. Star points have coordinates (±α, 0, ... , 0), (0, ±α, ... , 0), etc., where α denotes the distance from a star point to the central points in coded units. The number of the center point is one or may be more than one. The main reason for selecting CCD as DOE for the shock simulation is that the design provides assurance that the precision of the fitted values (i.e., the variance of fitted values) is not affected by the direction; it is affected only by the distance from the center point (Neter, et al., 1996).

In the CCD of the shock simulation, a two-level full factorial design is used for corner points, α is set to 2, and the number of replicates at each experimental point is uniformly set as 20. Therefore, the total number of experiments is 500 as given by

$$n_T = 2^{k-f} n_c + 2kn_s + n_0 \tag{5.1}$$

where the number of factor (k) is 4, the fraction (f) is zero, and the numbers of corner points (n_c), star points (n_s), and center points (n_0) are identically 20.

Table 5.3 The results of central composite design for the discrete particle shock simulation plan

Experimental Trials	x1 (mm)	x2 (mm)	x3	x4 (mm)
1	0.00075	0.0004	0.04	0.0004
2	0.00075	0.0004	0.08	0.0004
3	0.00125	0.0004	0.04	0.0004
4	0.00125	0.0004	0.08	0.0004
5	0.00075	0.0008	0.04	0.0004
6	0.00075	0.0008	0.08	0.0004
7	0.00125	0.0008	0.04	0.0004
8	0.00125	0.0008	0.08	0.0004
9	0.00075	0.0004	0.04	0.0008
10	0.00075	0.0004	0.08	0.0008
11	0.00125	0.0004	0.04	0.0008
12	0.00125	0.0004	0.08	0.0008
13	0.00075	0.0008	0.04	0.0008
14	0.00075	0.0008	0.08	0.0008
15	0.00125	0.0008	0.04	0.0008
16	0.00125	0.0008	0.08	0.0008
17	0.001	0.0006	0.02	0.0006
18	0.001	0.0006	0.1	0.0006
19	0.0005	0.0006	0.06	0.0006
20	0.0015	0.0006	0.06	0.0006
21	0.001	0.0002	0.06	0.0006
22	0.001	0.001	0.06	0.0006
23	0.001	0.0006	0.06	0.0002
24	0.001	0.0006	0.06	0.001
25	0.001	0.0006	0.06	0.0006

In Table 5.3, a set of experiments (i.e., one replicate at each point) is listed with given design spaces of design variables from Table 5.2. As mentioned, the listed simulation points are repeated 20 times resulting in 500 total samples. The simulation time for each simulation takes approximately 30~60 minutes depending on the particle sizes. It is difficult to manually execute such a large number of simulations one by one. Moreover,

the simulation software (i.e., Raven code) is located in a distant place from the execution place. For these reasons, a distributed simulation infrastructure is required for automated serial executions using the remotely placed Raven code. In the next section, a distributed simulation infrastructure for enabling these requirements is discussed in detail.

5.4.2. Automated Parallel and Serial Simulations in a Distributed Computational Infrastructure

The computational infrastructure for the shock simulation of RPMM is composed of three modules, which are the DOE module (Phoenix Integration[5]), the pre- and post-processing module, and the RAVEN simulation module. These modules are placed in two different places, which are Systems Realization Laboratory (SRL) and Mechanical Properties Research Laboratory (MPRL) in the Georgia Institute of Technology. They are seamlessly interfaced together in order to automate the simulation process as shown in Figure 5.7.

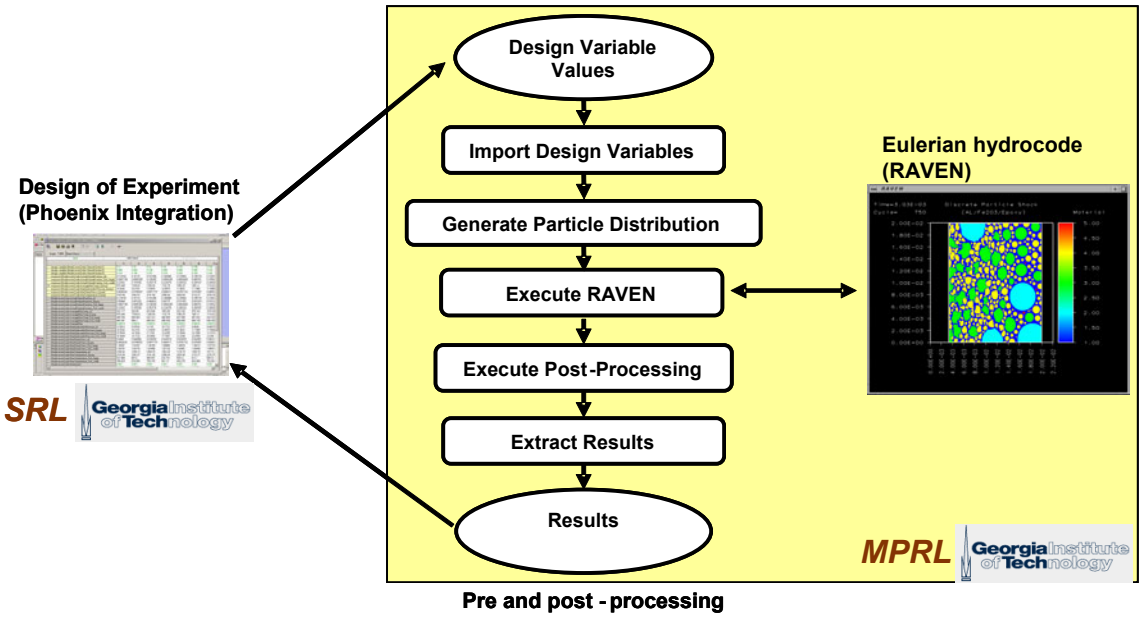

Figure 5.7 Distributed DOE and the shock simulation infrastructure

[5] Design and simulation integration framework (http://www.phoenix-int.com/)

In order to accomplish this goal, an underlying software script written in Perl[6] is used. This script converts file formats, extracts data, and remotely executes the software codes in the appropriate sequence.

The values of the design variables supplied by the DOE module are inserted into the input file used by the software to generate the initial configuration of the SVE. The script then executes the software to generate the initial configuration and extracts the size and placement data for each of the generated particles. This particle data is then inserted into the input file for RAVEN. Upon completion of the RAVEN simulation, a post-processing routine is run to extract the relevant raw data from the simulation output. This data is copied back to the local computer and is processed into a form usable by the DOE module. All of these steps are completely automated; therefore, a large number of simulations designed in the DOE module are executed and collected sequentially without user interaction.

[6] Cross platform programming language (http://www.perl.org/)

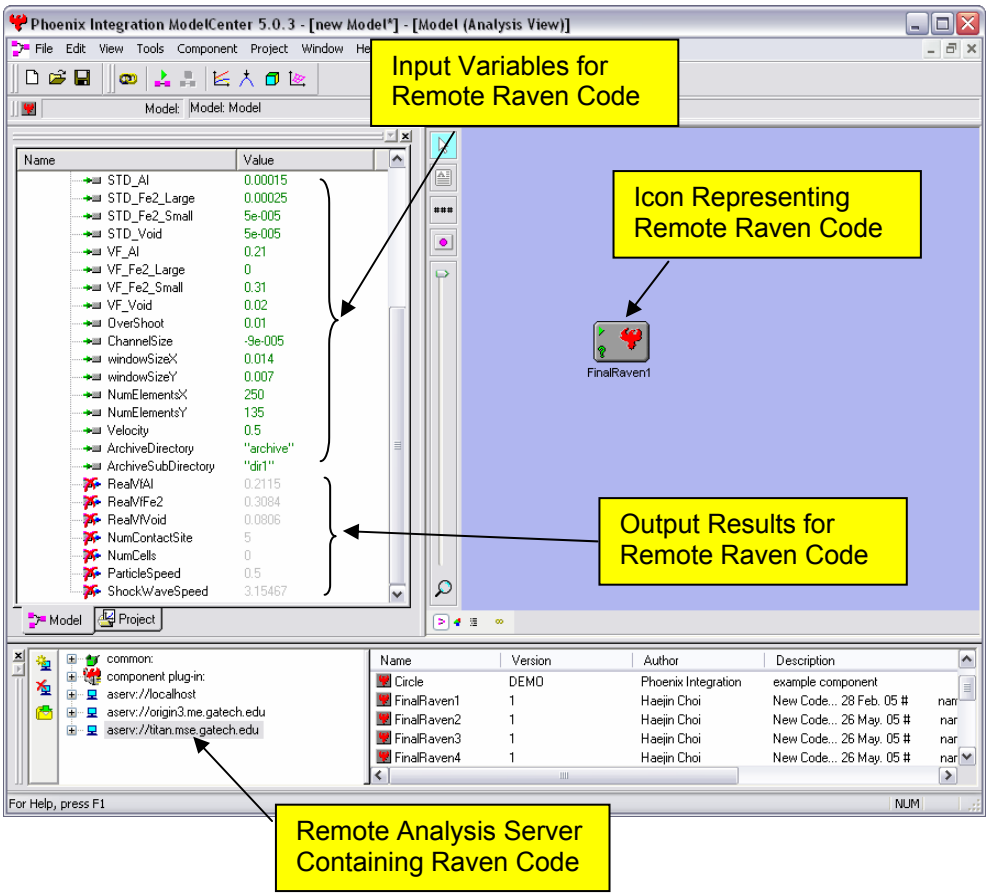

Figure 5.8 Remote raven simulation in the local ModelCenter of Phoenix Integration

In Figure 5.8, ModelCenter, the client software for remote execution, in Phoenix Integration is illustrated showing the remote Raven code placed on a remote server. The Perl script encapsulating pre- and post-processing as well as Raven code is wrapped and published by the Analysis Server, server software for publishing wrapped script via the Internet, in Phoenix Integration. The published remote Perl script including Raven code is shown in the ModelCenter as an Icon. The input parameters for a remote Raven execution can be input in the ModelCenter. Returned simulation results are shown in the ModelCenter after finishing pre-processing, Raven execution, and post-processing in a remote computer.

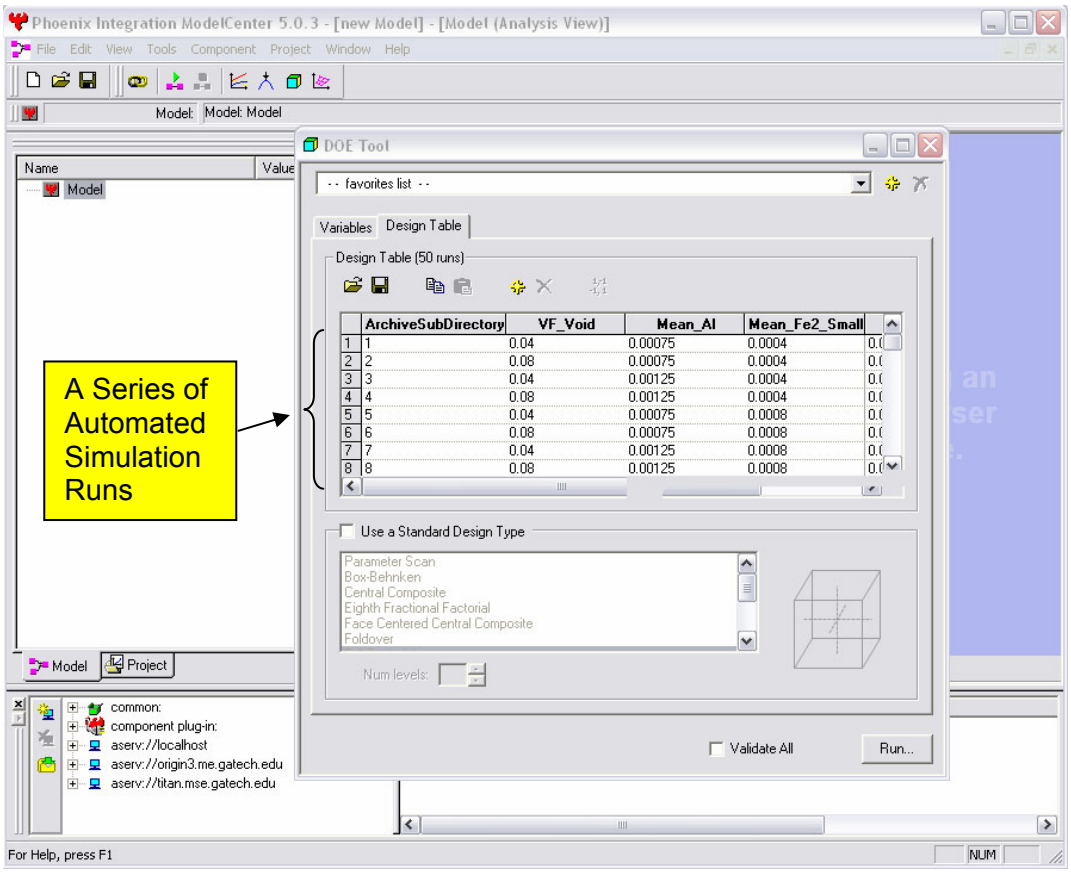

Figure 5.9 An example of a series of automated simulation runs

A list of different input parameters can be specified for sequential automated multiple simulation runs as shown in Figure 5.9. In this shock simulation, the listed experimental points in Table 5.3 are inserted in the table of the ModelCenter for one replicate at each experimental point.

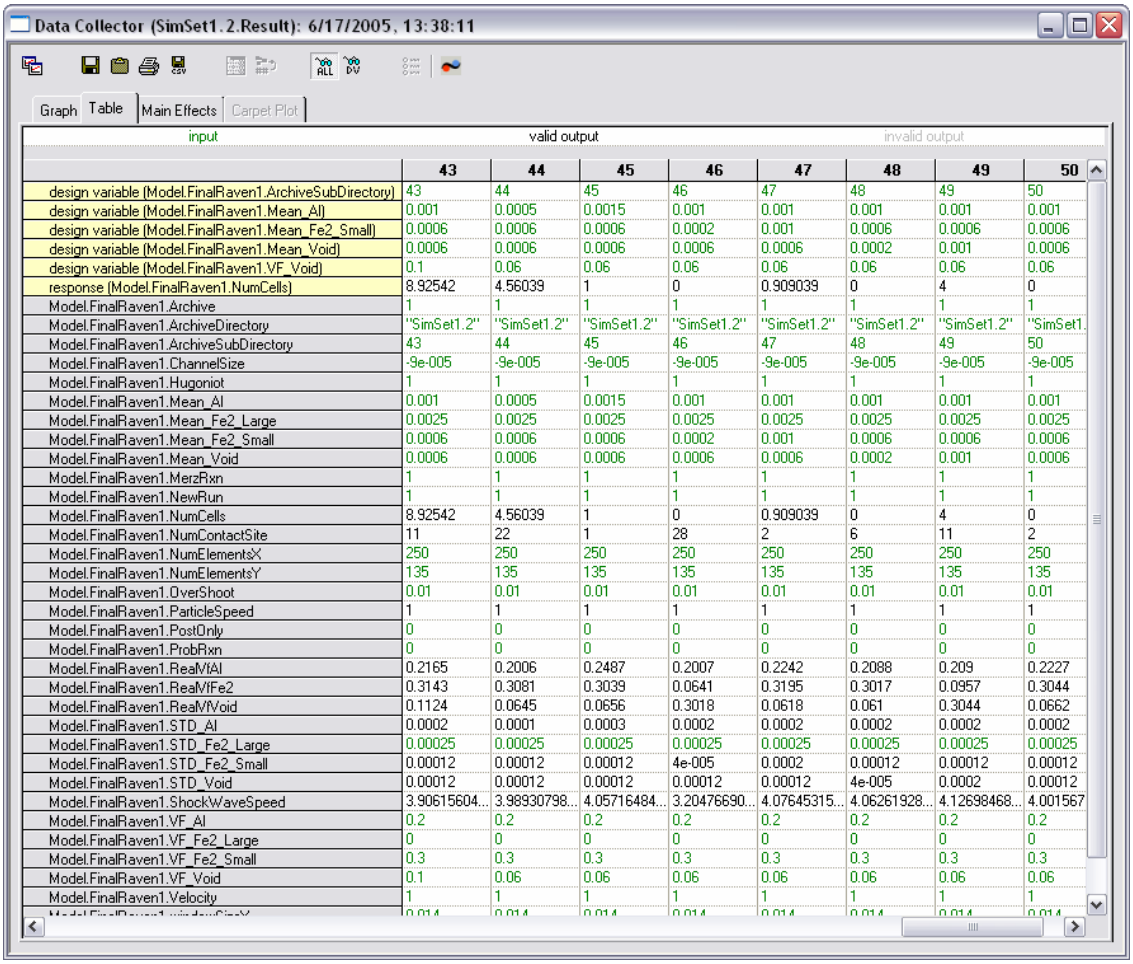

	43	44	45	46	47	48	49	50
design variable (Model.FinalRaven1.ArchiveSubDirectory)	43	44	45	46	47	48	49	50
design variable (Model.FinalRaven1.Mean_Al)	0.001	0.0005	0.0015	0.001	0.001	0.001	0.001	0.001
design variable (Model.FinalRaven1.Mean_Fe2_Small)	0.0006	0.0006	0.0006	0.0002	0.001	0.0006	0.0006	0.0006
design variable (Model.FinalRaven1.Mean_Void)	0.0006	0.0006	0.0006	0.0006	0.0006	0.0002	0.001	0.0006
design variable (Model.FinalRaven1.VF_Void)	0.1	0.06	0.06	0.06	0.06	0.06	0.06	0.06
response (Model.FinalRaven1.NumCells)	8.92542	4.56039	1	0	0.909039	0	4	0
Model.FinalRaven1.Archive	1	1	1	1	1	1	1	1
Model.FinalRaven1.ArchiveDirectory	"SimSet1.2"	"SimSet1.2"	"SimSet1.2"	"SimSet1.2"	"SimSet1.2"	"SimSet1.2"	"SimSet1.2"	"SimSet1.
Model.FinalRaven1.ArchiveSubDirectory	43	44	45	46	47	48	49	50
Model.FinalRaven1.ChannelSize	-9e-005	-9e-005	-9e-005	-9e-005	-9e-005	-9e-005	-9e-005	-9e-005
Model.FinalRaven1.Hugoniot	1	1	1	1	1	1	1	1
Model.FinalRaven1.Mean_Al	0.001	0.0005	0.0015	0.001	0.001	0.001	0.001	0.001
Model.FinalRaven1.Mean_Fe2_Large	0.0025	0.0025	0.0025	0.0025	0.0025	0.0025	0.0025	0.0025
Model.FinalRaven1.Mean_Fe2_Small	0.0006	0.0006	0.0006	0.0002	0.001	0.0006	0.0006	0.0006
Model.FinalRaven1.Mean_Void	0.0006	0.0006	0.0006	0.0006	0.0006	0.0002	0.001	0.0006
Model.FinalRaven1.MerzRxn	1	1	1	1	1	1	1	1
Model.FinalRaven1.NewRun	1	1	1	1	1	1	1	1
Model.FinalRaven1.NumCells	8.92542	4.56039	1	0	0.909039	0	4	0
Model.FinalRaven1.NumContactSite	11	22	1	28	2	6	11	2
Model.FinalRaven1.NumElementsX	250	250	250	250	250	250	250	250
Model.FinalRaven1.NumElementsY	135	135	135	135	135	135	135	135
Model.FinalRaven1.OverShoot	0.01	0.01	0.01	0.01	0.01	0.01	0.01	0.01
Model.FinalRaven1.ParticleSpeed	1	1	1	1	1	1	1	1
Model.FinalRaven1.PostOnly	0	0	0	0	0	0	0	0
Model.FinalRaven1.ProbRxn	0	0	0	0	0	0	0	0
Model.FinalRaven1.RealVfAl	0.2165	0.2006	0.2487	0.2007	0.2242	0.2088	0.209	0.2227
Model.FinalRaven1.RealVfFe2	0.3143	0.3081	0.3039	0.0641	0.3195	0.3017	0.0957	0.3044
Model.FinalRaven1.RealVfVoid	0.1124	0.0645	0.0656	0.3018	0.0618	0.061	0.3044	0.0662
Model.FinalRaven1.STD_Al	0.0002	0.0001	0.0003	0.0002	0.0002	0.0002	0.0002	0.0002
Model.FinalRaven1.STD_Fe2_Large	0.00025	0.00025	0.00025	0.00025	0.00025	0.00025	0.00025	0.00025
Model.FinalRaven1.STD_Fe2_Small	0.00012	0.00012	0.00012	4e-005	0.0002	0.00012	0.00012	0.00012
Model.FinalRaven1.STD_Void	0.00012	0.00012	0.00012	0.00012	0.00012	4e-005	0.0002	0.00012
Model.FinalRaven1.ShockWaveSpeed	3.90615604...	3.98930798...	4.05716484...	3.20476690...	4.07645315...	4.06261928...	4.12698468...	4.001567
Model.FinalRaven1.VF_Al	0.2	0.2	0.2	0.2	0.2	0.2	0.2	0.2
Model.FinalRaven1.VF_Fe2_Large	0	0	0	0	0	0	0	0
Model.FinalRaven1.VF_Fe2_Small	0.3	0.3	0.3	0.3	0.3	0.3	0.3	0.3
Model.FinalRaven1.VF_Void	0.1	0.06	0.06	0.06	0.06	0.06	0.06	0.06
Model.FinalRaven1.Velocity	1	1	1	1	1	1	1	1

Figure 5.10 Results of sequential multiple simulation runs

As shown in Figure 5.10, the results of fifty sequential multiple simulation runs, which are 2 replicates at each experimental point, are collected one by one after a simulation is completed.

Based on the automated computational infrastructure described in this section, 500 samples are collected without human interaction. This computational infrastructure saves a great amount of resources (expense, time, man power, etc.) for gathering a large number of samples with the shock simulation code placed in a remote place. This computational infrastructure is indispensable for designing with computationally intensive simulation and large sample size.

5.5. QUANTIFYING UNCERTAINTY IN SHOCK SIMULATION RESULTS

In this section, we discuss the third step of the RCEM-EMI for designing an RPMM shown in Figure 5.6. Once the design task has been clarified and the samples collected from the shock simulation, the next step is building a mean response model and prediction interval based on the procedure discussed in Section 3.8 in Chapter 3. The procedure illustrated in Figure 5.11 is implemented using MATLAB®.

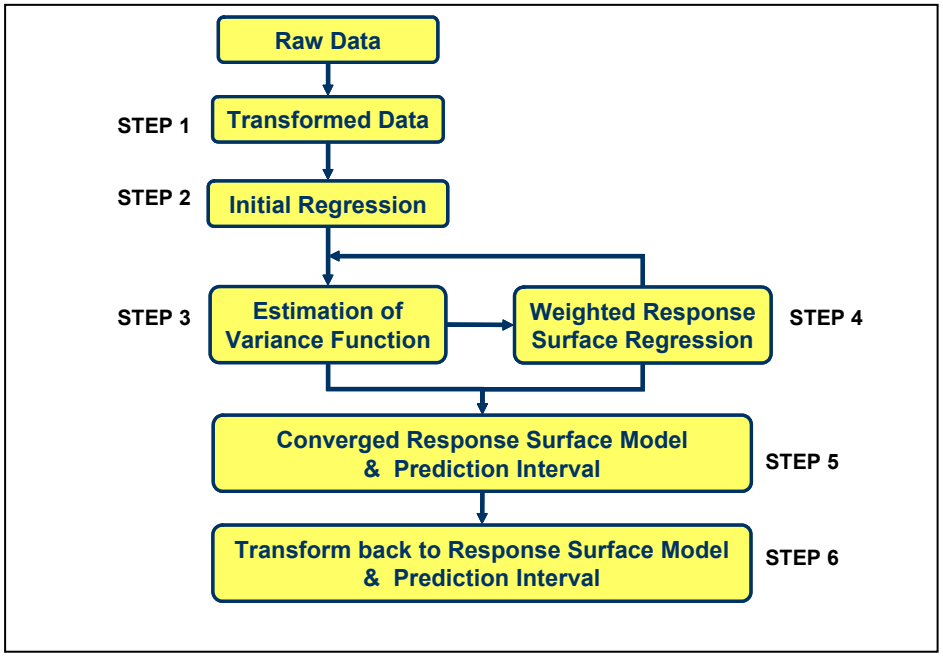

Figure 5.11 A procedure for integrated metamodeling and prediction interval estimation

Quadratic response surface models are employed as the mean response model and an exponential function powered by a quadratic response surface model as the conditional variance model. Therefore, the mean response model is

$$f(\mathbf{x},\boldsymbol{\beta}) = \mathbf{x}\cdot\boldsymbol{\beta}' \tag{5.2}$$

where $\mathbf{x} = [1, x_1, x_2, x_3, x_4, x_1^2, x_2^2, x_3^2, x_4^2, x_1x_2, x_1x_3, x_1x_4, x_2x_3, x_2x_4, x_3x_4]$ and

$\boldsymbol{\beta} = [\beta_0, \beta_1, \beta_2, \beta_3, \beta_4, \beta_{11}, \beta_{22}, \beta_{33}, \beta_{44}, \beta_{12}, \beta_{13}, \beta_{14}, \beta_{23}, \beta_{24}, \beta_{34}]$.

The conditional variance model is

$$\sigma^2 \cdot v^2(\mathbf{x}, \boldsymbol{\beta}, \boldsymbol{\theta}) = \exp(\mathbf{x} \cdot \boldsymbol{\theta}') \tag{5.3}$$

where, $\boldsymbol{\theta} = [\theta_0, \theta_1, \theta_2, \theta_3, \theta_4, \theta_1^2, \theta_2^2, \theta_3^2, \theta_4^2, \theta_{11}, \theta_{22}, \theta_{33}, \theta_{44}, \theta_{12}, \theta_{13}, \theta_{14}, \theta_{23}, \theta_{24}, \theta_{34}]$.

As discussed in the process illustrated in Figure 5.11, designers first investigate the normality of the residuals by fitting raw data a quadratic response surface model and transform the raw data into transformed data (if necessary). In Figure 5.12a, the normal probability plot of the residual obtained by fitting the raw data is skewed, which means the distribution of the residuals is not balanced. The raw data is transformed using $y^{tr} = \ln(y+2)$ and the transformed data is fitted again. Box-Cox transformation (Neter, et al., 1996) is useful for selecting a transformation function. As shown in the Figure 5.12b, the normal probability plot of the residuals with transformed data indicates that the residual is now balanced.

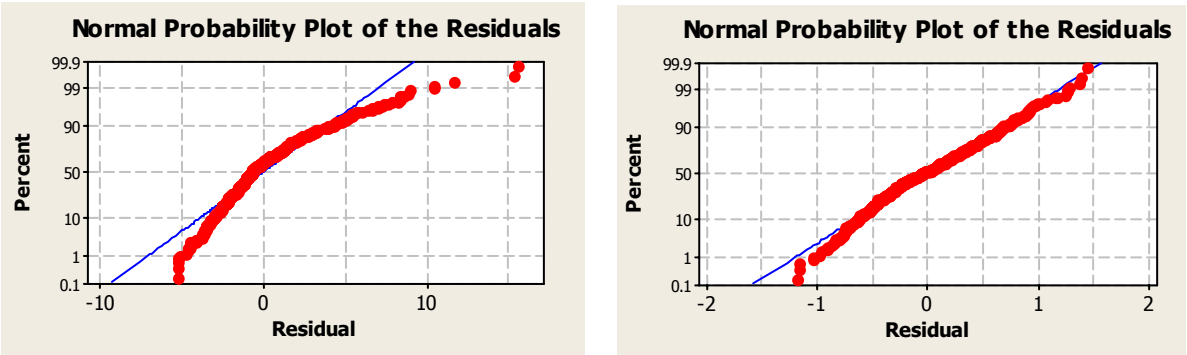

(a) Raw Data (b) Transformed Data

Figure 5.12 Normal probability plot of residuals with raw and transformed response

With transformed data, the second step is an initial regression. The initial regression parameter ($\hat{\boldsymbol{\beta}}_{init}$) for the mean response model is shown in Table 5.4. After getting the initial estimation of the mean response model, iteratively re-weighted regression is performed as described in Step 3 of Figure 3.7. In this example, the maximum pseudolikelihood estimation method in Eq.(3.6) is used for estimating the parameter vector ($\hat{\boldsymbol{\theta}}$) of the conditional variance model. After ten iterations, we have converged parameter vectors, $\hat{\boldsymbol{\beta}}_{converged}$ and $\hat{\boldsymbol{\theta}}_{converged}$, for the mean and conditional variance models as shown in Table 5.4.

Table 5.4 Estimated parameters in mean and variance models

Subscripts	$\hat{\boldsymbol{\beta}}_{init}$	$\hat{\boldsymbol{\beta}}_{converged}$	$\hat{\boldsymbol{\theta}}_{converged}$
0	3.9704e+000	3.9924e+000	6.8363e-001
1	-1.8342e+003	-1.7704e+003	-1.5518e+003
2	-1.3850e+003	-1.4896e+003	4.4727e+002
3	-1.3503e+001	-1.3798e+001	-3.2056e+001
4	-1.2722e+003	-1.2988e+003	-8.4064e+002
11	1.1298e+006	1.1115e+006	-1.2844e+003
22	8.9132e+005	9.2869e+005	-4.4852e+002
33	1.7331e+002	1.7190e+002	8.6503e+001
44	6.8733e+005	6.9570e+005	7.7073e+002
12	-1.0642e+006	-1.0284e+006	-1.3846e+003
13	4.8862e+002	4.0649e+002	2.1635e+004
14	-7.0772e+005	-7.9062e+005	-1.5430e+003
23	-7.2651e+003	-7.3911e+003	-1.2607e+004
24	1.2218e+006	1.2735e+006	-3.9634e+002
34	2.3488e+003	3.3732e+003	1.3293e+004

Based on the converged estimated parameters, the transformed mean response model and prediction interval at new observation ($\boldsymbol{x_0}$) are

$$y^{tr}(\mathbf{x_0}) = \hat{\boldsymbol{\beta}}_{converged} \cdot \mathbf{x_0} \pm t_{N-P,1-\alpha/2} \cdot \exp\left(\frac{\hat{\boldsymbol{\theta}}_{converged} \cdot \mathbf{x_0}'}{2}\right), \tag{5.4}$$

where the number of samples (N) is 500, the total number of predictors (P) is 30, and the confidence level (1-α) is 0.99. Transforming back to original coordinates, the mean

response model $f_0(\mathbf{x_0})$, the upper limit of the prediction interval $f_1(\mathbf{x_0})$, and the lower limit of the prediction interval $f_2(\mathbf{x_0})$ are obtained as

$$
\begin{aligned}
f_0(\mathbf{x_0}) &= \exp\left\{\hat{\boldsymbol{\beta}}_{converged} \cdot \mathbf{x_0}\right\} - 2 \\
f_1(\mathbf{x_0}) &= \exp\left\{\hat{\boldsymbol{\beta}}_{converged} \cdot \mathbf{x_0} + t_{N-P,1-\alpha/2} \cdot \exp\left(\frac{\hat{\boldsymbol{\theta}}_{converged} \cdot \mathbf{x_0}'}{2}\right)\right\} - 2 \\
f_2(\mathbf{x_0}) &= \exp\left\{\hat{\boldsymbol{\beta}}_{converged} \cdot \mathbf{x_0} - t_{N-P,1-\alpha/2} \cdot \exp\left(\frac{\hat{\boldsymbol{\theta}}_{converged} \cdot \mathbf{x_0}'}{2}\right)\right\} - 2
\end{aligned}
\tag{5.5}
$$

The mean response and prediction interval models are plotted in Figure 5.13 using MATLAB®. The models are depicted in terms of the voids' volume fraction and mean radius when the mean radius of Al is 0.00075 (mm) and that of Fe_2O_3 is 0.0004 (mm). As shown in Figure 5.13, the obtained samples' responses are dispersed within the prediction interval limits at fixed design parameters because of the unparameterizable variability (due to the changes in micro-structure of SVE). In this section, we identified the mean response model and prediction interval limit functions. Based on the obtained functions, the next step in the RCEM-EMI is focused on searching for ranged sets of design specifications for the robust reaction initiation of RPMM.

In this section, the mean response model and prediction interval limit functions are identified. Based on the obtained functions, the next step in the RCEM-EMI is searching for ranged set of design specifications for robust reaction initiation of RPMM.

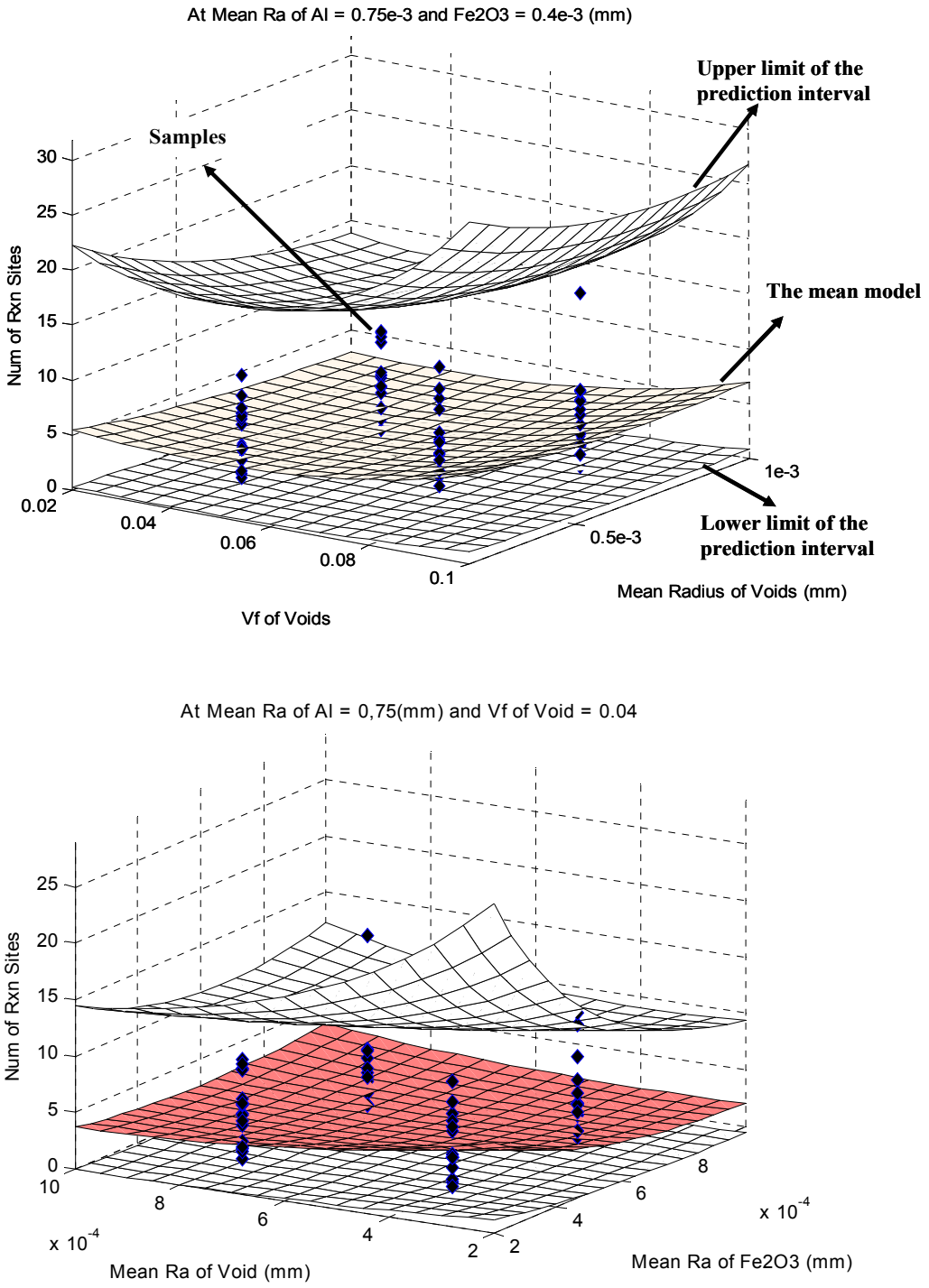

Figure 5.13 The mean response models and prediction intervals for the number of the reaction initiation sites

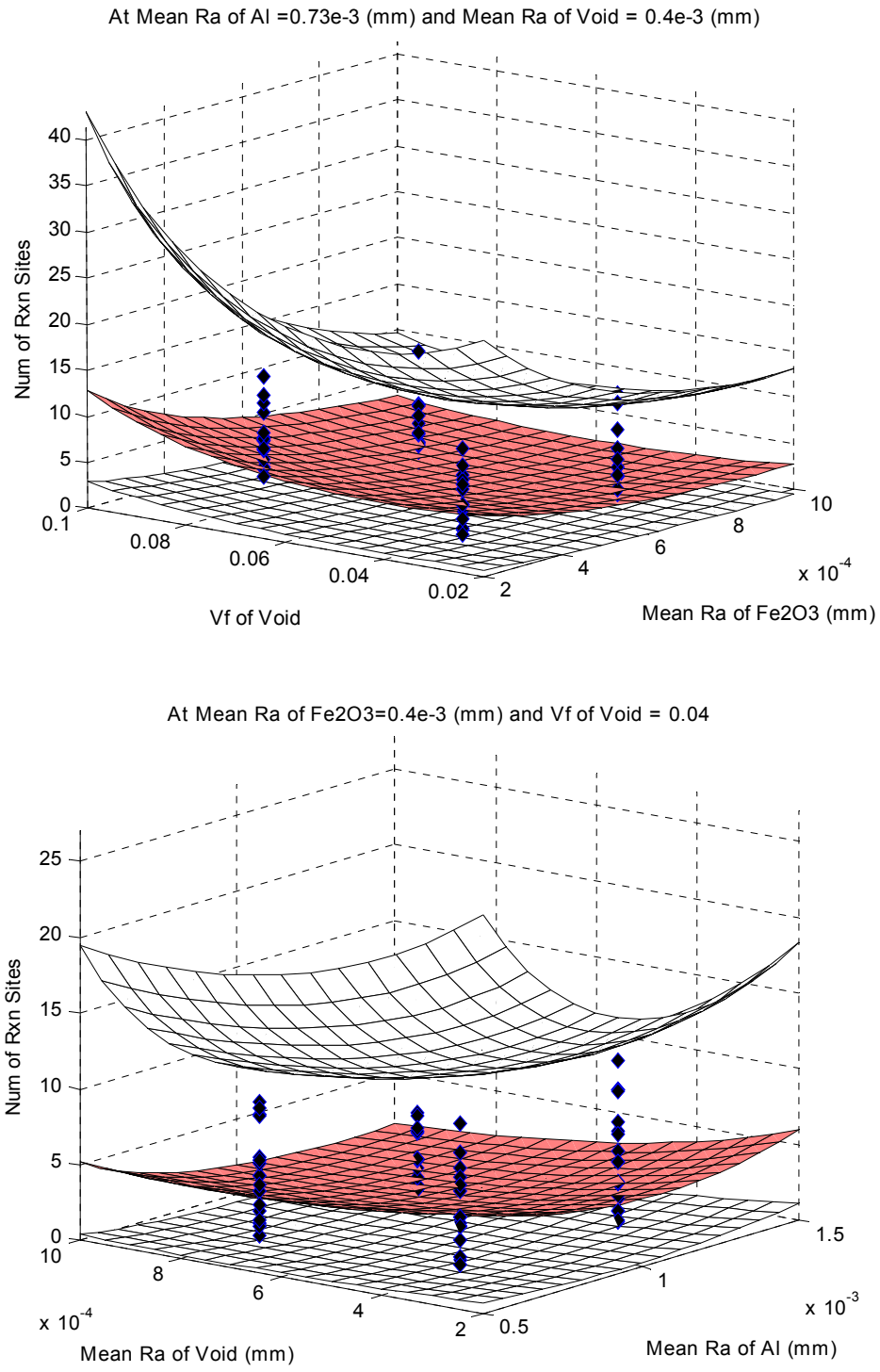

Figure 5.13 is continued.

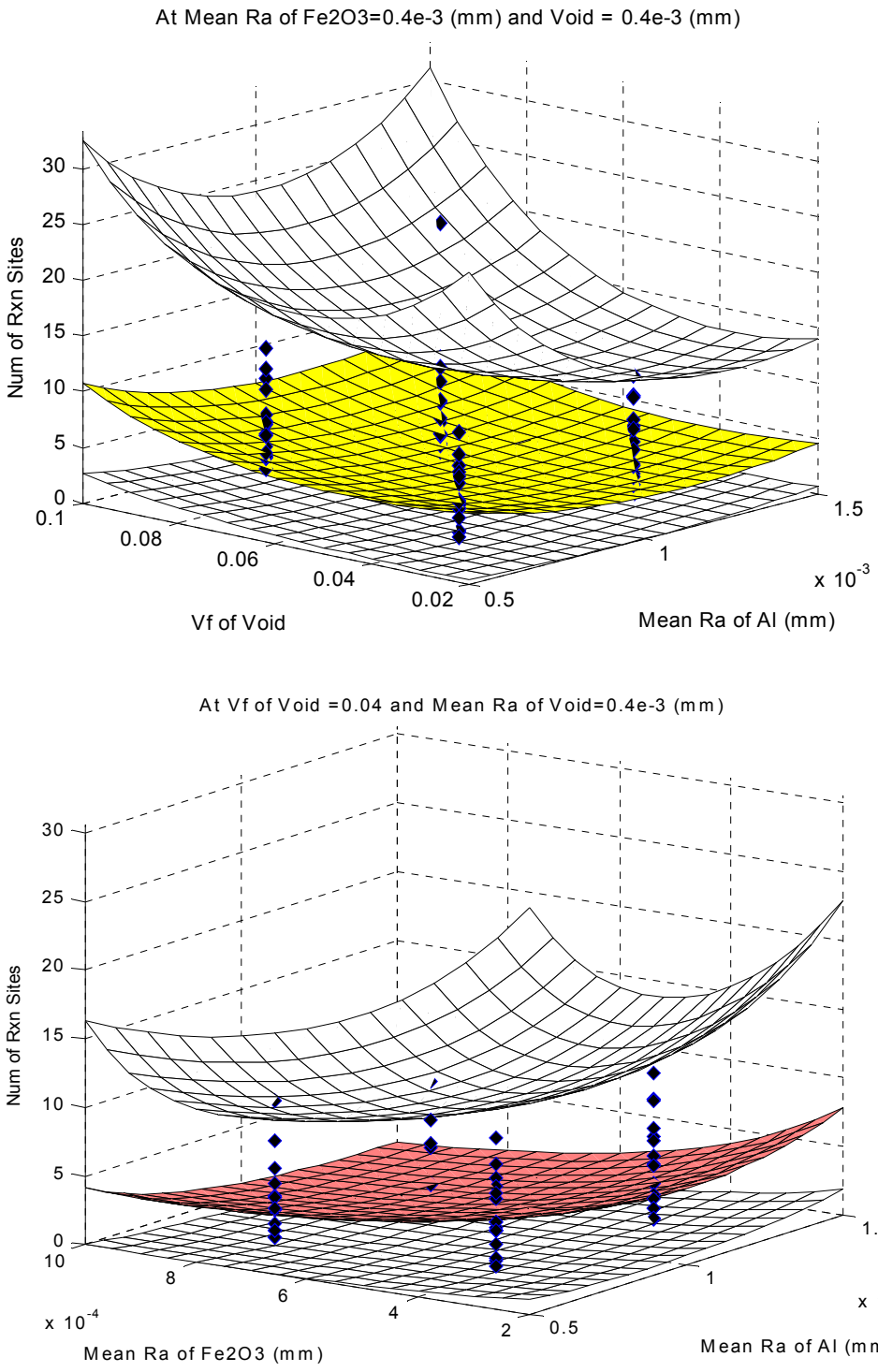

Figure 5.13 is continued.

5.6. FINDING ROBUST MESM SPECIFICATIONS

With the specifications identified in Step (a) in Figure 5.6 and the mean and prediction interval models obtained in Step (c) in Figure 5.6, a cDSP for the RCEM-EMI is formulated incorporating the EMI to achieve robust system responses with ranged sets of design specifications as shown in Table 5.5.

Table 5.5 The cDSP for the RCEM-EMI for identifying a ranged set of robust RPMM design specifications

Methods	Mathematical Form
cDSP for RCEM-EMI	**Given** $\mathbf{x} = \{x_1, x_2, x_3, x_4\}$ (System Variables) $f_0(\mathbf{x})$ (Mean Response Function) $f_1(\mathbf{x})$ (Upper Uncertainty Bound Function) $f_2(\mathbf{x})$ (Lower Uncertainty Bound Function) $LRL = 1$ (Lower Requirement Limit) $EMI_{target} = 10$ (Target EMI) $\Delta\mathbf{x} = [\pm 0.2, \pm 0.1, \pm 0.01, \pm 0.1]$ (Variations in System Variables) **Find** μ_x, (Mean Location of System Variables) d_1^+, d_1^- (Deviation Variables) **Satisfy** Goals: $EMI(\mathbf{x}) / EMI_{target} + d_1^- - d_1^+ = 1$ where $EMI = \{ f_0(\mathbf{x}) - LRL \} / \{ Y_{min} - f_0(\mathbf{x}) \}$ where $Y_{\min} = Min\left\{ \left(f_j(\mathbf{x}) - \sum_{i=1}^{4} \left\lvert \frac{\partial f_j}{\partial x_i} \right\rvert \cdot \Delta x_i \right) \right\}$ $j = 1, 2, 3$ Bounds: $0.5 \le x_1 \le 1.5$, $0.2 \le x_2 \le 1$, $0.02 \le x_3 \le 0.1$, and $0.2 \le x_4 \le 1$ $d_1^-, d_1^+ \ge 0$, $d_1^- \bullet d_1^+ = 0$ **Minimize** $Z = d_1^-$

As shown in Table 5.5, $f_0(\mathbf{x})$, $f_1(\mathbf{x})$ and $f_2(\mathbf{x})$ are determined from the mean response model and the upper and lower prediction interval limits identified in Step (c). Other required inputs are derived from the specifications identified in Step (a). As specified in Table 5.2, the Lower Requirement Limit (LRL) for the response is set to 1, which means

the number of reaction sites should be greater than or equal to 1. The target EMI is set to 10. The deviations of design variables (control variables) are also identified in Step (a). The objective of solving the cDSP is to find the mean location of design variables (x_1,x_2,x_3, *and* x_4) for achieving the target EMI as closely as possible.

The goal formulation centers on a 'larger is better' type response. This means that a larger number of reaction sites are preferred. This is the case in Figure 3.8c. The EMI is formulated based on the mathematical construct discussed in Section 3.9. The bounds of the design variable are derived from the design space identified in Step (a). By minimizing the deviation, d_1^-, under-achievement toward to the target EMI, designers obtain ranged sets of design specifications that are robust to the deviation in design variables, unparameterizable variability, and model parameter uncertainty due to the limited number of samples.

In Table 5.6, mathematical forms of cDSP for RCEM-DCI and optimization for this design problem are illustrated. Comparing with the cDSP for the RCEM-EMI, the cDSP for RCEM-DCI incorporates with only $f_0(\mathbf{x})$. As discussed in Section 3.9, the DCI is calculated based on mathematical constructs in Figure 3.8c and response deviations (ΔY) are obtained by calculating the deviations of $f_0(\mathbf{x})$ due to variations in system variables *without considering* $f_1(\mathbf{x})$ *and* $f_2(\mathbf{x})$. Solutions with the two design exploration methods are also identified for validating the utility of the RCEM-EMI in Section 5.7.

Table 5.6 The cDSP for RCEM-DCI and optimization for searching RPMM design specifications

Methods	Mathematical Form
cDSP for RCEM-DCI	**Given** $\mathbf{x} = \{x_1, x_2, x_3, x_4\}$, $f_0(\mathbf{x})$ (Mean Response Function), $LRL = 1$, $DCI_{target} = 10$, (Target DCI) $\Delta\mathbf{x} = [\pm 0.2, \pm 0.1, \pm 0.01, \pm 0.1]$ **Find** μ_x , d_1^+, d_1^- **Satisfy** Goals: $DCI(\mathbf{x}) / DCI_{target} + d_1^- - d_1^+ = 1$ where $DCI(\mathbf{x}) = \{ f_0(\mathbf{x}) - LRL \} / \Delta Y$ where $\Delta Y = \sum_{i=1}^{4} \left\lvert \frac{\partial f_0}{\partial x_i} \right\rvert \cdot \Delta x_i$ Bounds: $0.5 \le x_1 \le 1.5$, $0.2 \le x_2 \le 1$, $0.02 \le x_3 \le 0.1$, and $0.2 \le x_4 \le 1$ $d_1^-, d_1^+ \ge 0$, $d_1^- \bullet d_1^+ = 0$ **Minimize** $Z = d_1^-$
Optimization	**Given** $f_0(\mathbf{x})$ (Mean Response Function) **Find** $\mathbf{x} = \{x_1, x_2, x_3, x_4\}$ **Satisfy** $0.5 \le x_1 \le 1.5$, $0.2 \le x_2 \le 1$, $0.02 \le x_3 \le 0.1$, and $0.2 \le x_4 \le 1$ **Maximize** $Z = f_0(\mathbf{x})$

5.7. REACTIVE PARTICLE METAL MIXTURES DESIGN RESULTS

5.7.1. Achieving Robustness under Unparameterizable Variability

The design solution using the RCEM-EMI with 500 samples (see Section 5.4.1) is shown in Table 5.7. The RPMM design solution using the RCEM-EMI is compared with

the solutions using RCEM-DCI and traditional optimization. Clearly, all three approaches produce different design solutions. The values in the shaded cells are obtained via the RCEM-EMI approach. The shaded values cannot be achieved using either the optimization or RCEM-DCI method.

Table 5.7 Comparison with Optimal, RCEM-DCI, and RCEM-EMI design solutions

Methods	x_1 (10^{-3}mm)	x_2 (10^{-3}mm)	x_3	x_4 (10^{-3}mm)	EMI	DCI	Est. Mean Num of Rxn Sites	Est. Min. Num of Rxn Sites
Optimi-zation	**1.5**	**0.2**	**0.1**	**0.2**	*1.05*	*1.75*	**21.8**	*1.92*
RCEM -DCI	**0.7**±0.2	**0.2**±0.1	**0.02**±0.01	**0.2**±0.1	*0.91*	**2.74**	8.8	*0.26*
RCEM -EMI	**0.5**±0.2	**0.2**±0.1	**0.1**±0.01	**0.2**±0.1	**1.10**	2.27	18.9	**2.69**

The optimal solution is found on the upper bound of x_1 (mean radius of Al particles) and x_3 (volume fraction of void), and on the lower bound of x_2 (mean radius of Fe_2O_3 particles) and x_4 (mean radius of voids). Using traditional optimization, the maximum performance is determined using only the mean response function. We obtained the maximum mean response (the number of reaction sites) of 21.8 at the upper bounds of x_1 and x_3 and the lower bounds of x_2 and x_4. On the other hand, based on the RCEM-DCI approach, a robust design solution is found at the lower bounds of x_2~x_4 and 0.7 of x_1 by considering deviations in design variables. The RCEM-DCI approach leads to the robust solution using only the mean response function. At the solution, we achieved the maximum DCI, 2.74, over entire design space.

Using the RCEM-EMI approach, we determine a robust design solution at the lower bounds of x_1, x_2, and x_4 and the upper bound of x_3 (volume fraction of voids). At the solution point, the maximum EMI of 1.10 over the entire design space is achieved. The

minimum estimated numbers of reaction sites is 2.69. These are estimated with consideration of the deviation in the design variables, unparameterizable variability, and model parameter uncertainty. In other words, taking into account the deviations in x_1~x_4, unparameterizable variability and 20 replicates, we estimate the minimum number of reaction sites to be 2.69 with a 99% confidence level.

As shown in Table 5.7, the mean performance is the best at the optimal solution and the DCI is the highest at the RCEM-DCI solution. However, if we consider unparameterizable variability, the performance deviation (the interval between the estimated minimum and maximum) at the two solution points is larger than that at the RCEM-EMI solution point as shown in the last two columns of the table. This is due to the optimization and RCEM-DCI approaches not accounting the unparameterizable variability in the system during the design exploration. Additionally, the unparameterizable variability of the results of this shock simulation is quite large. At the RCEM-DCI solution, it cannot be said for certain whether the system performance is satisfactory to the Lower Requirement Limit (at least one reaction site) since the minimum estimated response is 0.26 with a 99% confidence. At the optimal solution, the EMI is 1.05, which indicates the performance deviation due to uncertainty in the model is still satisfactory to the Lower Requirement Limit (LRL). However, a smaller response variation and larger estimated minimum response (2.69) are achieved at the RCEM-EMI solution point, which produce the maximum EMI value (1.10). This result is supported by the plots shown in Figure 5.14.

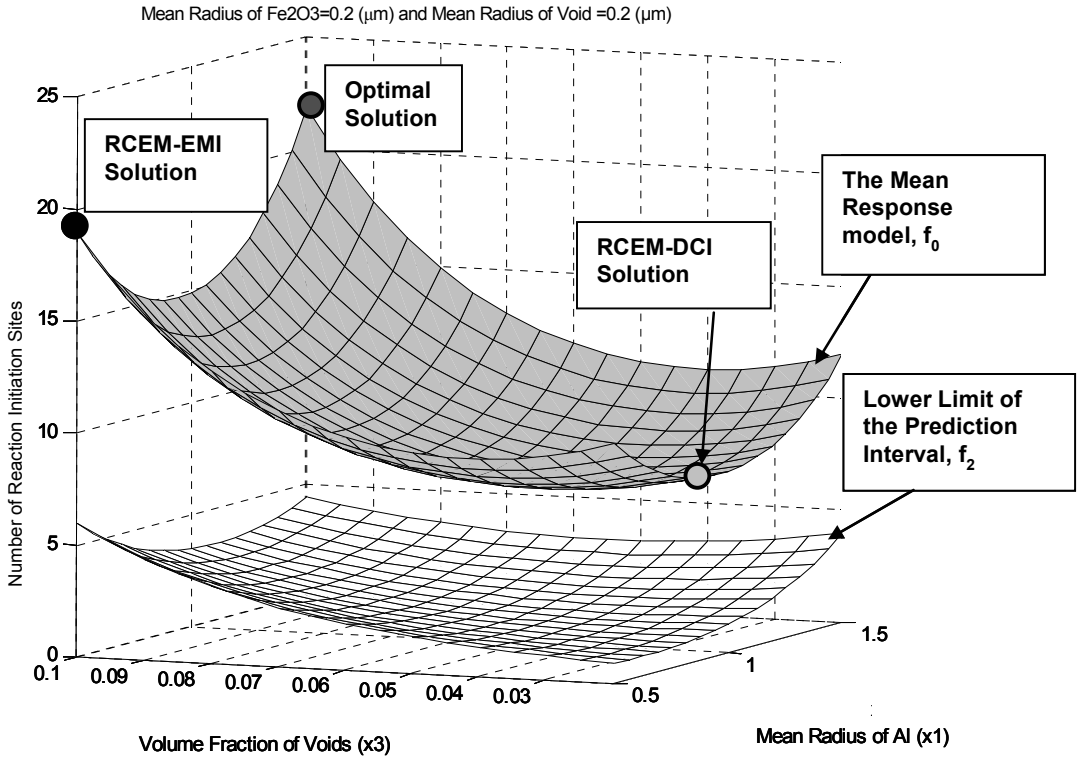

Figure 5.14 The locations of solutions in the mean and lower limit of prediction interval models.

The above plots are the models that estimate the number of reaction sites in terms of x_1 and x_3. The mean radii of Fe_2O_3 and voids are fixed at 0.2 μm since all solutions are predicting this value as the design solution. As we expected, the optimal solution is on the peak of the mean response function and the RCEM-DCI solution is on the flat region of the mean response function. On the other hand, the RCEM-EMI solution is on the other side of the optimal solution. At the RCEM-EMI solution point, the lower limit of the prediction interval is higher than others. Compared with the optimal solution, the response variation due to unparameterizable variability is smaller while mean response is sacrificed somewhat. At the RCEM-DCI solution point, the lower limit of the prediction interval is very low; therefore the response variation might violate the LRL. All solutions

are on either the edge or vertices of the design space, which means the system performances and robustness could be improved further by examining the broader design space. The SVE instances of the obtained design specification based on the three design methods are illustrated in Figure 5.15.

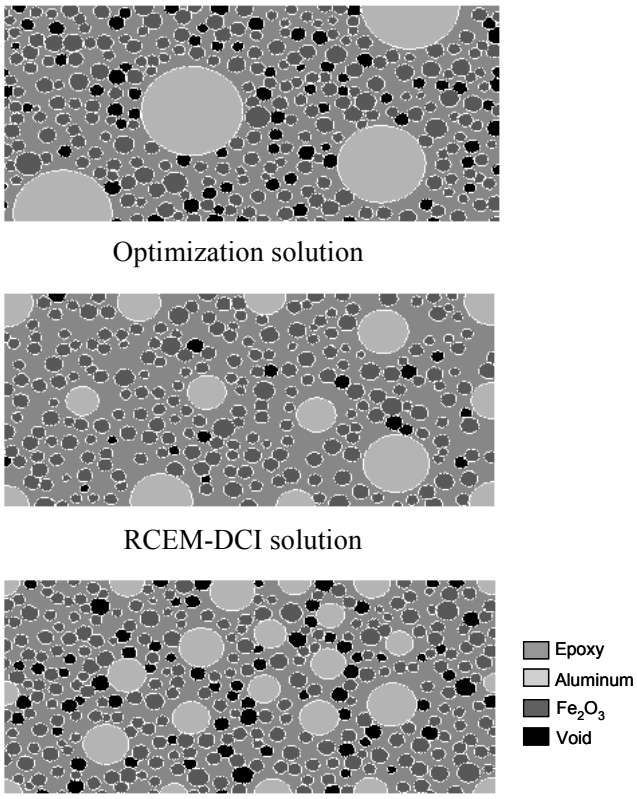

Figure 5.15 Instances of SVE created by the obtained design specifications

In this example, we extend our design space up to the simulation capability limits, such as the limitation of particles' sizes that could be properly analyzed by the Raven simulation code. As the shock simulation capability is extended to incorporate the smaller particles, we may need to redesign our specifications in the broader design space.

As discussed in this section, the RCEM-EMI solution embodies the smallest lower performance deviation (deviation from the estimated mean performance to the estimated

minimum performance). Further, the mean performance is reasonably good when compared to the optimal solution. Therefore, we suggest that the RPMM specifications identified by the RCEM-EMI are more robust (than the optimal solution) to random changes in microstructure (unparameterizable variability), taking the variation in the design variables into account as well.

5.7.2. Achieving Robustness under Model Parameter Uncertainty

In Sections 3.4 and 3.5 in Chapter 3, different types of uncertainty are discussed. It was argued that the RCEM-EMI approach yields solutions that are robust to unparameterizable variability and model parameter uncertainty – Type III robust design. In this section, the RCEM-EMI approach is validated with respect to searching for a solution that is robust to model parameter uncertainty. For the purpose of this demonstration, we proceed from the reduced sample size (11 replicates) to the full sample size (20 replicates). With increasing the sample size, design exploration results based on three different search methods are plotted in Figure 5.16.

While the trend in solution convergence of the RCEM-EMI with increasing sample size is stable, those of other approaches are not. All design solutions of the RCEM-EMI converge and are stabilized at 15 replicates. Using traditional optimization approach, the solutions of x_2, x_3, and x_4 converge at 16 replicates, but the solution of x_1 is still unstable at 20 replicates. Using the RCEM-DCI approach, the solutions of x_1, x_2, and x_4 converge at 15 replicates, but x_3 is still somewhat unstable at 20 replicates. This means that more samples are necessary to achieve converged design solutions for the optimization and RCEM-DCI approaches. Since the mean response model for all methods is obtained using an iteratively re-weighted regression technique, the mean response model is more

robust to large random errors, as discussed in Section 3.8. With a normal regression technique, the convergence of the design solutions using the optimal and RCEM-DCI should be less stable.

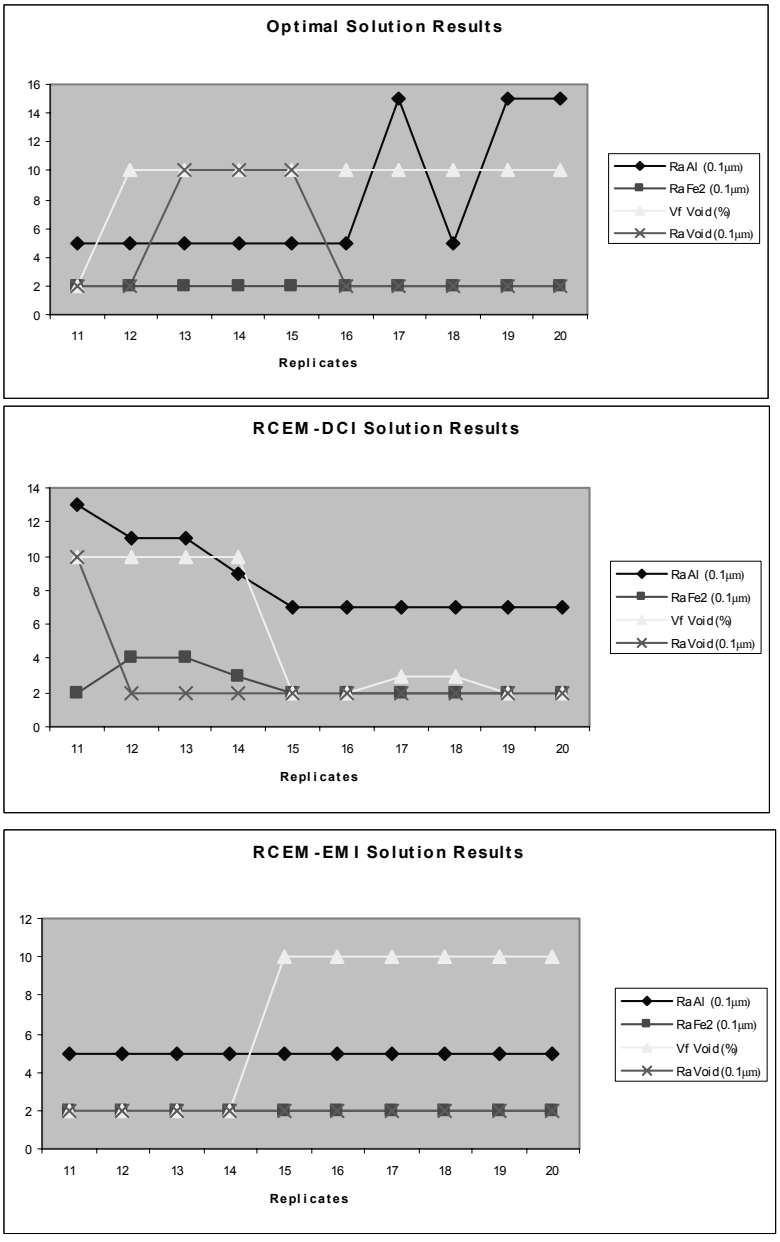

Figure 5.16 Solution convergence of Optimization RCEM-DCI, and RCEM-EMI as increasing sample size

The advantages of the RCEM-EMI identified in this section are (a) the design solution using the RCEM-EMI is the more robust against model parameter uncertainty due to lack of data, and (b) the solution converged at the smaller sample size compared with the traditional solution search algorithms.

5.8. EMPIRICAL PERFORMANCE VALIDATION

In this chapter, the RCEM-EMI is demonstrated based on the microscale shock simulation-based RPMM design problem. In this section, the utility of the RCEM-EMI is argued by validating Hypotheses 1 and 2, which is empirical perforation validation in the validation square shown in Figure 5.17.

Hypothesis 1: The Robust Concept Exploration Method with Error Margin Indices, a method for Type III robust design, provides an effective and efficient mathematical construct to find robust solution range under uncertainty embodied in a model, in which Error Margin Indices are metrics of available margin for potential errors due to uncertainty in models.

Hypothesis 2: Increased uncertainty due to reducing experimental expenses is inevitable; however, we can formulate the bounds of model uncertainty based on mean response and prediction interval approach for later use in robust design exploration.

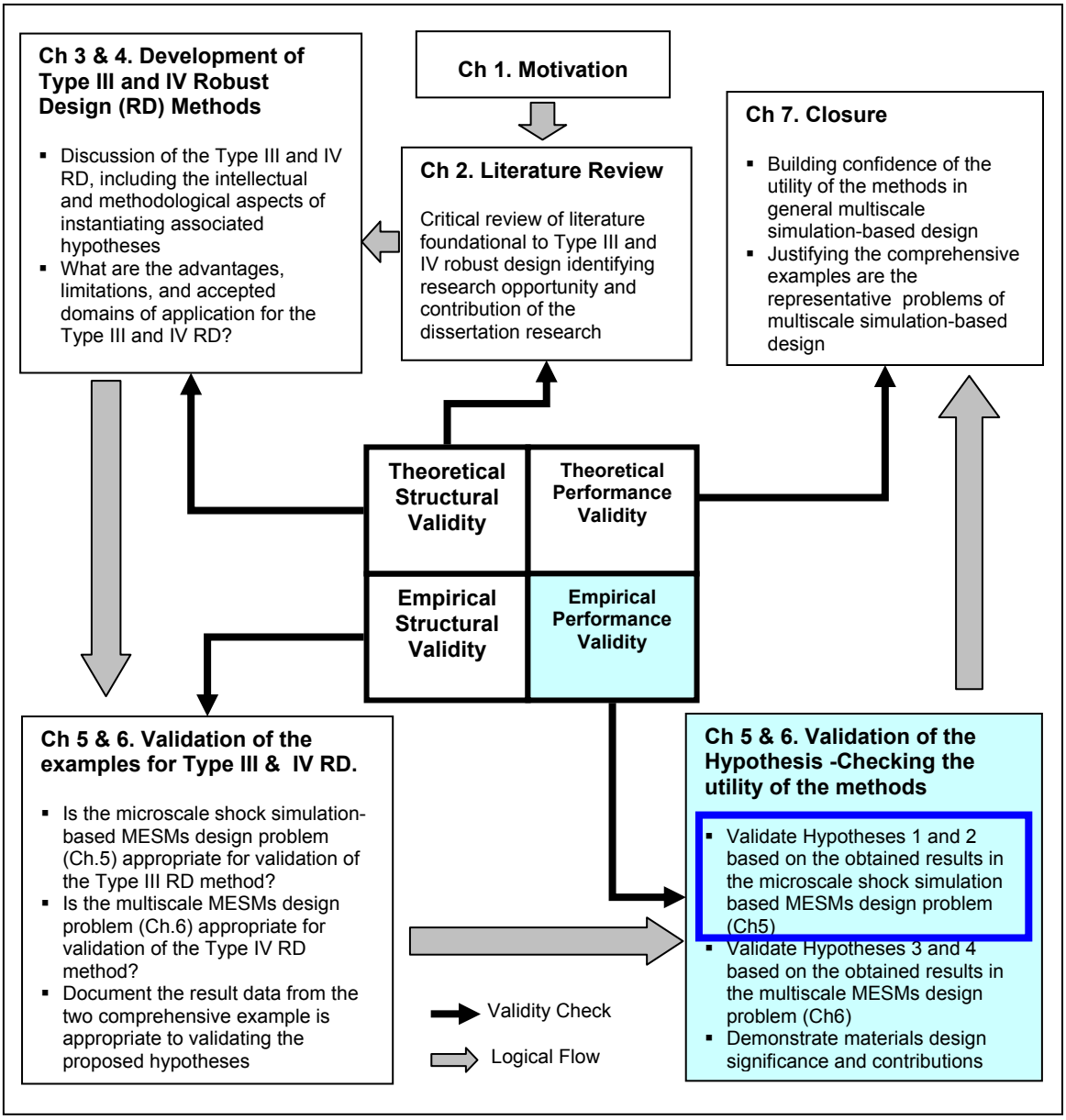

Figure 5.17 Validation square roadmap

- ***Task 1:*** *Validate that the integrated estimation of regression model and prediction interval in the RCEM-EMI discussed in Section 3.7 is useful for estimating non-deterministic behavior (i.e., unparameterizable variability) in the shock simulation model in a computationally efficient manner.*
- ***Results 1:*** In order to minimize the computational load the RCEM-EMI embodies an integrated mean and variance metamodeling approach for

estimating the amount of variability embedded in the system; see Section 5.5. A converged design solution with 375 samples using the RCEM-EMI is illustrated in Figure 5.16. If traditional uncertainty analysis (e.g., Monte Carlo simulation) is invoked in a design exploration process a large amount of sampling is needed to evaluate a single point resulting in a method that is infeasible due to the computational requirements. Herein lies the advantage of the RCEM-EMI; computationally intensive materials analyses and simulations are embodied in the RCEM-EMI.

Based on Result 1, we claim that Hypothesis 2 is correct. Integrated metamodeling and prediction interval estimation method captures uncertainty due to the limitation of sampling size effectively. Based on the uncertainty bounds shown in Figure 5.13, the interval estimation is well established to capture this uncertainty.

- ***Task 2:*** *Find ranged set of RPMM design specification robust to Type I, II, and III variability using the RCEM-EMI.*
- ***Result 2:*** Unparameterizable random changes in a material's micro-structure cause large variations in material performance. A smaller performance deviation at the RCEM-EMI solution point occurs than at the solution points obtained using traditional optimization and RCEM-DCI; see Section 5.7.1. Further, the mean performance at the RCEM-EMI solution point is still reasonably good. Therefore, we suggest that the performance of a material system designed using the RCEM-EMI is more robust to unparameterizable variability than a material system designed using either traditional optimization or RCEM-DCI. Additionally, as shown in Table 5.7, information whether the

material system will satisfy the ranged performance requirements or not with some confidence level is provided by the RCEM-EMI; this information cannot be obtained if other robust design methods are used.

Based on Result 2, we claim that Hypothesis 1 is correct, since the RCEM-EMI is a more ***effective*** method than traditional optimization and RCEM-DCI in order to design an RPMM robust to unparameterizable variability (uncertainty embodied in a model).

- ***Task 3:*** *Build a confidence to the RCEM-EMI in achieving robust RPMM design solution to model parameter uncertainty due to lack of samples*
- ***Result 3:*** As shown in Figure 5.16, using the RCEM-EMI, we obtain stable design solutions with rapid convergence as the sample size is increased. This suggests that the RCEM-EMI design specifications are robust to model parameter uncertainty that arises as a result of a lack of sampling data. Hence, we suggest that a designer can make decisions (that are robust) even if these statistical models are uncertain due to the limitations in sample size.

Based on Result 3, we claim that Hypothesis 1 is correct, since the RCEM-EMI is more ***efficient*** method than traditional optimization and RCEM-DCI.

- ***Results 4:*** In robust design, using traditional optimization, it is often difficult for designers to determine the trade off between performance and performance sensitivity. However, as shown in the mathematical construct of the RCEM-EMI and the RCEM-DCI discussed in Section 3.9, performance and performance sensitivity are formulated into a single index (EMI or DCI) thus circumventing this problem.

Based on Result 4, which is the common advantage of the RCEM-EMI and DCI, we claim that Hypothesis 1 is correct. In the hypothesis, we proposed an effective way of robust design. This result supports the hypothesis since it reduces the complexity of trade off between performance and performance sensitivity. **This simplicity facilitates extending the EMI from a single performance index into a hyper-dimensional index based on an arbitrary shaped constraint boundary in a hyper-dimensional space**; it is discussed in Section 4.7.1. We discuss the advantages and limitations of the EMI in details in Section 7.5.

In summary, it is important to reduce uncertainty in a system by getting more knowledge or data of the system. However, if the system uncertainty cannot be reduced, the RCEM-EMI proposed in this dissertation helps designers pursue robust and reliable solutions despite uncertainty remaining in the system.

5.9. SYNOPSIS OF CHAPTER 5

In this chapter, the utility of RCEM-EMI is validated (Empirical Performance Validation) with an example of the microscale shock simulation-based MESMs design that is validated as an appropriate example (Empirical Structural Validation).

In Section 5.1, an introduction to the microscale discrete particle shock simulation is provided. The purpose and capability of the simulation are discussed. The types of uncertainty associated with the simulation are explained in detail. We argue why the shock simulation-based design problem is an appropriate example for validating the RCEM-EMI (Empirical Structural Validation). In Section 5.1.3, the four tasks for validating the functionality of the RCEM-EMI based on this example are planned.

In Section 5.2, the overall procedure of the RCEM-EMI, which is discussed earlier in Chapter 3, is reviewed in terms of the shock simulation example. In Section 5.3, the first step of the RCEM-EMI, the clarification of the design task, is discussed. The fixed specifications, assumptions, design variables and spaces, uncertainty associated with the simulation, and design objectives are discussed and listed in Table 5.2. In Section 5.4, DOE and the corresponding simulations, the second step, is performed. The automated infrastructure used for the simulation runs is illustrated and discussed as shown in Figure 5.7 though Figure 5.9. The simulation infrastructure saves large amount of time for running serialized multiple simulations and gathering necessary data.

In Section 5.5, unparameterizable variability due to the random microstructure variation is quantified using the integrated metamodeling and prediction interval estimation approach discussed in Chapter 3. The obtained mean response model and the prediction interval are illustrated in Figure 5.13. In Section 5.6, robust ranged set of design specifications are searched. The mathematical formulation of this search algorithm is the cDSP with Error Margin Indices (EMIs). For the purpose of validating the effectiveness of the RCEM-EMI, tradition optimization and Robust Concept Exploration Method with Design Capability Indices (RCEM-DCI) are also employed for searching design solutions.

In Section 5.7, the design exploration results obtained based on the three search algorithms, optimization, RCEM-DCI, and RCEM-EMI, are compared and discussed. The obtained results shown in Figure 5.14 and Figure 5.16 support the argument that the RCEM-EMI solution is more robust to unparameterizable variability and model

parameter uncertainty. In Section 5.8, the validation results are summarized checking the empirical performance validity.

In the next chapter, a multiscale materials design example is employed for the validation of the Inductive Design Exploration Method (IDEM) discussed in Chapter 4.

CHAPTER 6

ROBUST MULTISCALE ENERGETIC STRUCTURAL MATERIALS (MESMS) DESIGN BASED ON MULTI-TIME AND LENGTH SCALE SIMULATIONS

In this chapter, we validate Hypotheses 3 and 4 in Section 1.4.2. In the hypotheses, Type IV robust design is proposed in order to achieve multiple ranged sets of design specifications that are robust to propagated uncertainty along a simulation and analysis chain. The Type IV robust design is instantiated as the Inductive Design Exploration Method (IDEM). In Chapter 4, implementation details including overall procedure and the constituent techniques of the IDEM are discussed. The structural soundness of the method is validated based on a simple example, a clay filled polyethylene cantilever beam design problem, introduced at the end of Chapter 4. In this chapter, a comprehensive example, multiscale (multi- time and length scale) Multifunctional Energetic Structural Materials (MESMs) design example, is employed. Multiscale MESMs simulation and analysis models are logically connected and used for predicting the final response of the MESMs. In this chapter, Al+Fe_2O_3 materials system is chosen as MESMs.

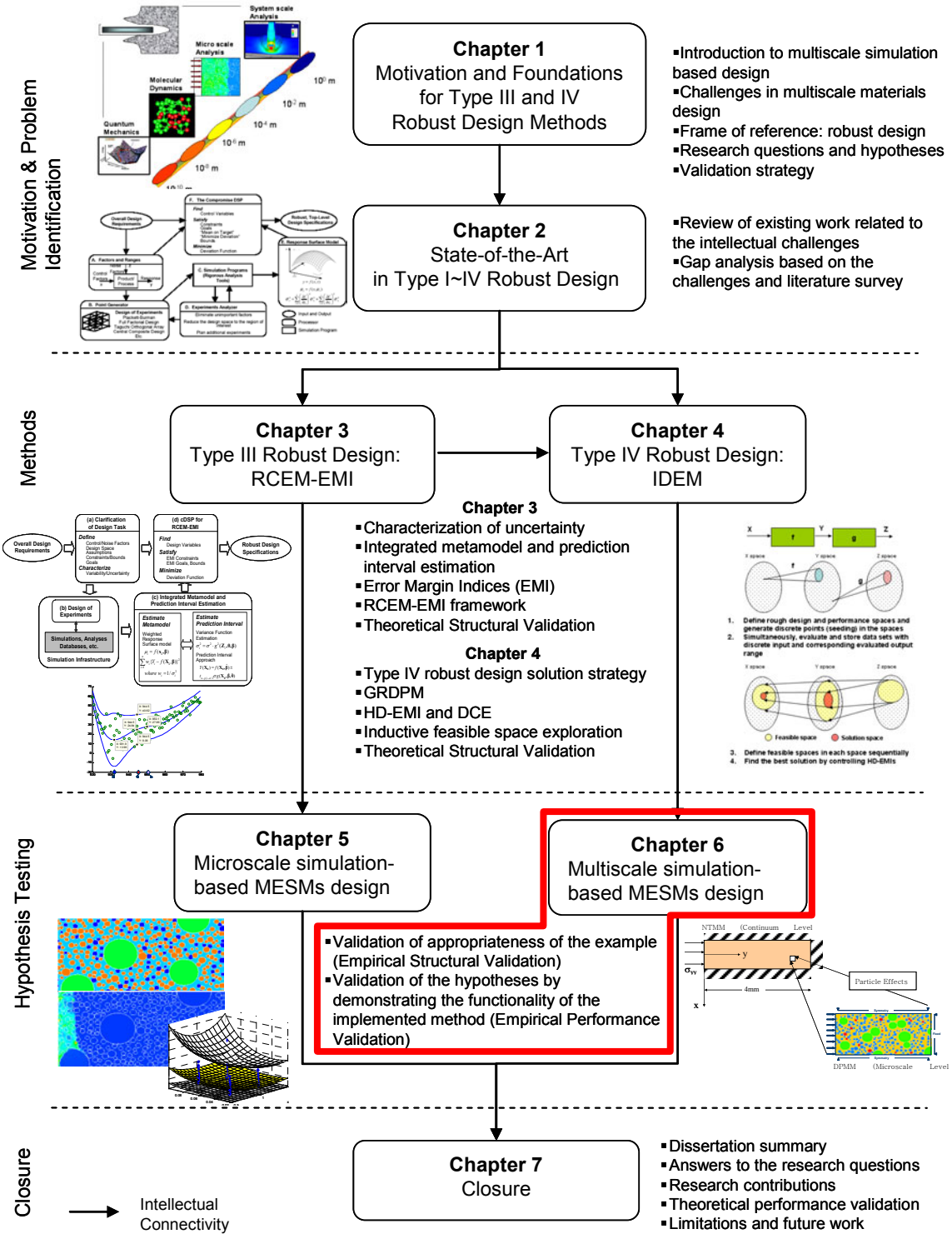

Figure 6.1 Dissertation roadmap

In Section 6.1, the continuum level non-equilibrium thermodynamics mixture model and the microscale discrete particle mixture model are introduced. Those two models are logically interfaced, formulating a simulation chain. In Section 6.2, a multiscale MESMs design problem is addressed, defining information flows in the simulation chain. This design problem is validated as an appropriate example for demonstrating the utility of the IDEM (Empirical Structural Validation). In Section 6.3, the multiscale simulation chain and MESMs design process chain are described using the Graphical Robust Design Process Model (GRDPM) discussed in Chapter 4. In Sections 6.4~6.6, the overall procedure of the IDEM and its details are discussed, identifying robust ranged sets of specifications of the Al+Fe_2O_3 systems. In this discussion, the relationship between Type III and Type IV robust design is also addressed. The MESM design results identified by the IDEM are illustrated and listed. In Section 6.7, the hypotheses are validated by checking whether the IDEM is useful for the multiscale robust MESMs design problem or not (Empirical Performance Validation).

6.1. INTRODUCTION TO MULTISCALE SIMULATION-BASED MULTIFUNCTIONAL ENERGETIC STRUCTURAL MATERIALS DESIGN

In this section, a multiscale simulation-based MESMs design is introduced. This multiscale simulation-based design is composed of the microscale Discrete Particle Mixture (DPM) model employed in Chapter 5 and the continuum level Non-equilibrium Thermo-dynamics Mixture (NTM) model developed by Lu and coauthors (Lu, et al., 2003). In Section 6.1.1, the continuum level NTM model is introduced. This discussion presents the overall capability of the NTM model, its input/output parameters, and some

example results. In Section 6.1.2, the microscale DPM model is reviewed based on the discussion in Chapter 5 highlighting the differences between the DPM model and the homogenized continuum models. In Section 6.1.3, the interface between the DPM and NTM models is discussed in detail. The logic behind the interface of the two models is discussed. This discussion is important for us to establish multiscale simulation-based MESM design tasks and is revisited clarifying the design process model in Section 6.2.

6.1.1. Non-equilibrium Thermodynamics Mixture (NTM) Model - Continuum Level

In this section, the Non-equilibrium Thermodynamics Mixture (NTM) model is briefly introduced. and the details of NTM model are in Ref. (Lu, et al., 2003). In this continuum level analysis, shock-induced chemical reactions in aluminum and iron-oxide mixtures are modeled in the frameworks of non-equilibrium thermodynamics and continuum mechanics, in which both the thermo-chemical and mechano-chemical processes are accommodated. The constitutive model and conservation equation are formulated by introducing a combination of internal state variables and extended irreversible state variables. The internal state variables are mass fractions of reactants and products, and void contents. The extended irreversible state variables include chemical reaction rate, heat flux, and pore collapse flux. The irreversibility of these processes is implied in the nonnegative entropy production rate (i.e., the second law of thermodynamics) and their contribution to the dissipation. The relaxation time due to the duration of the chemical initiation and sustained reactions is in the range of 100-200 nano-seconds. A uniformly blended mixture theory is used to describe the porous mixture. The chemical reaction of the constituents is described as

$$2Al + Fe_2O_3 \rightarrow 2Fe + Al_2O_3 \tag{6.1}$$

The conservation equations, constitutive models, and chemical reaction equation, are described in detail in Ref. (Lu, et al., 2003).

A one dimensional strain problem is implemented in MATLAB®. The example is shown in Figure 6.2.

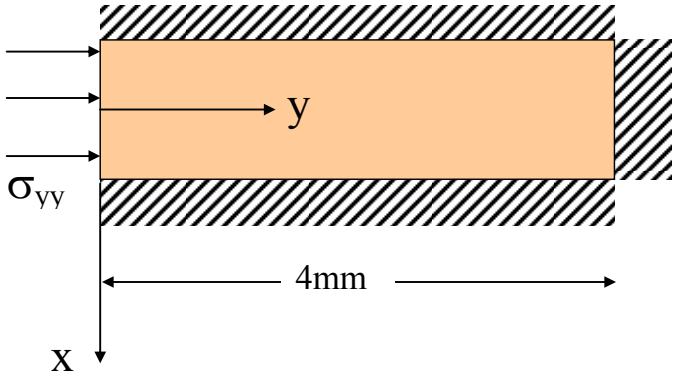

Figure 6.2 One dimensional shock simulation of Non-equilibrium Thermodynamics Mixture

The top, bottom, and right boundary condition are fixed and initial loading (σ_{yy}) is applied on the left boundary. In Table 6.1, the input and output parameters of the NTM model are listed and those variables implemented in the MATLAB® code are listed.

Table 6.1 Input and output parameters in the NTM model

Input Parameters	Output Parameters
▪ Volume fraction of Al: v_al0 ▪ Volume fraction of Fe_2O_3: v_fe2o30 ▪ Volume fraction of Fe: v_fe0 ▪ Volume fraction of Al_2O_3: v_al2o30 ▪ Porosity: alpha0 ▪ Applied loading: σ_{yy} ▪ Initial Temperature: theta0 ▪ Reaction initiation criterion: thetac	▪ Mass fraction of Al: c_al ▪ Mass fraction of Fe_2O_3: c_fe2o3 ▪ Mass fraction of Fe: c_fe ▪ Mass fraction of Al_2O_3: c_al2o3 ▪ Pressure: P ▪ Temperature: theta ▪ Porosity: alpha ▪ Density: rho ▪ Stress: sigmax, sigmay ▪ Velocity :vy ▪ Heat flux :q

The results of a NTM model execution are illustrated in Figure 6.3. The initial conditions are as follows.

- Loading pressure (σ_{yy}) = 15 (GPa)
- Initial porosity (alpha0) = 1.5
- Initial volume fraction of Al (v_al0) = 0.2545
- Initial volume fraction Fe_2O_3 (v_fe2o30) = 0.7455
- Initial volume fraction of Al_2O_3 (v_al2o30) = 0
- Initial volume fraction of Fe (v_fe0) = 0
- Initial temperature (theta0) = 300 (K)
- Reaction initiation criteria (thetac) = 700 (K)

The results shown in Figure 6.3 are the distributions of pressure, temperature, and mass fraction of Fe at the time frame of 300 nano-seconds after the initial loading.

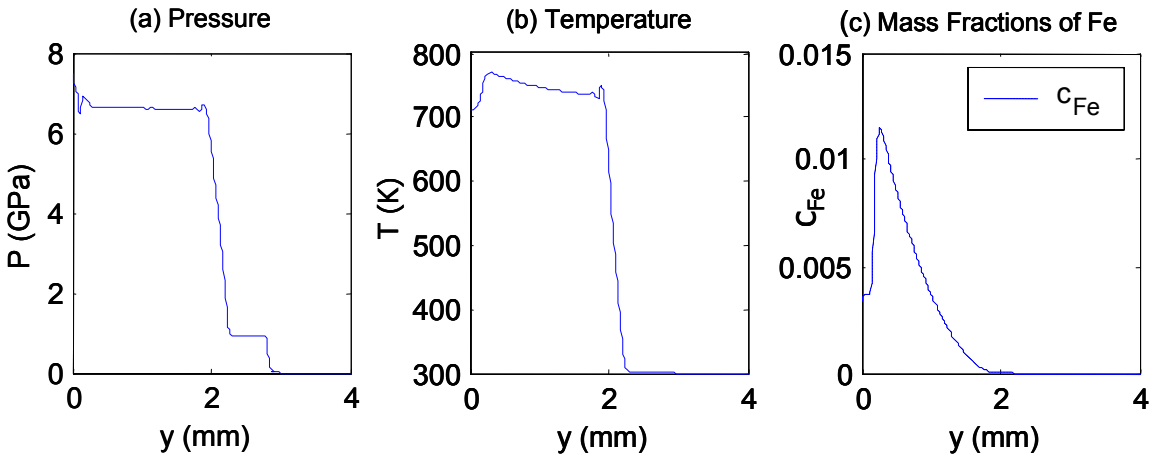

Figure 6.3 An example of NTM model execution

The output that we need to focus on in this analysis is the amount of chemical reaction in the material system. In order to assess the amount of chemical reaction, the mass fraction of Fe is the parameter to be captured since it is the product of the chemical

reaction as shown in Eq. (6.1). In this study, we calculate the sum of the predicted mass fraction of Fe at all nodes in the finite difference meshes in the NTM model at 300 nano-seconds after the initial loading. This parameter is called the accumulated mass fraction of Fe (*acFe*) in this dissertation.

In summary, the NTM model is a non-equilibrium thermodynamic model incorporating shock-induced chemical reactions. In this model, void collapse flux, chemical reaction flux and heat flux and associated relaxation times in the constitutive models are included, which explains the delayed initiation and sustained chemical reaction. However, the reaction initiation conditions in NTM model are assumed and these reaction initiation criteria need to be obtained from the lower scale model, the microscale Discrete Particle Mixture (DPM) model, to predict simulation results more accurately. For this reason, we need to formulate a multiscale analysis chain incorporating the microscale DPM model and the continuum NTM model in order to provide accurate reaction behavior of the Al and Fe_2O_3 mixture system. A detailed discussion of the NTM model are beyond the scope of this dissertation and are found in Ref. (Lu, et al., 2003).

6.1.2. Discrete Particle Mixture (DPM) Model– Microscale Level

The microscale Discrete Particle Mixture (DPM) model is introduced and discussed in detail in Section 5.1. In this section, we discuss the differences between the microscale DPM model and the continuum NTM model.

As discussed in Section 5.1, the microscale DPM model includes sub- or several-micron sized discrete particles of aluminum and iron-oxide. Heterogeneity in the micro-structure of the material due to the discrete particles in statistical volume element is

explicitly considered in the shock simulation. This is different from the continuum NTM model, in which we usually assume homogenous material distribution. As discussed in the previous section, the continuum NTM model employs the mixture theory (e.g., uniformly blended mixture theory). In other words, the heterogeneity of the micro-structure is ignored in the NTM model. Therefore, the results of the DPM model should be more accurate than the results of the NTM model. From this perspective, it is more accurate to incorporate a smaller scale level of the DPM model results in estimating materials performance for better accuracy. However, it is virtually impossible to incorporate the microscale DPM model in system scale models because of the complexity and heavy computational load.

The model implemented and discussed in Chapter 5 is used again in this multiscale simulation-based MESMs design problem. The input parameters are the volume fraction of metals (Al and Fe_2O_3), the mean diameters of metal particles, the volume fraction of void, and the mean diameter of voids. However, the response (i.e., reaction initiation sites based on the Merzhanov criterion) used in Chapter 5 from the DPM model should be modified so that the response of DPM model could be interfaced to the NTM model to estimate more accurately the material performance in the continuum level analysis. In the next section, the interfaced parameters between the DPM model and the NTM model, which are the responses of the DPM model as well as the input parameters of the NTM model, are identified discussing logical reasoning behind the interface.

6.1.3. Logical Interface between Discrete Particle Mixture Model and Non-equilibrium Thermodynamic Mixture Model

The objective of this section is to establish a logical interface, a mapping between the NTM and DPM models, in order to include the discrete particle effects of the microscale

level DPM model in the continuum level NTM model. As discussed, the heterogeneity of discrete particles is ignored in the NTM model. It is too computationally intensive to include those discrete particles in the large domain (i.e., continuum scale domain). Therefore, the NTM model incorporates uniformly blended mixture theory ignoring the details. Comparing the scales of the two models, a SVE of the DPM model could be represented as a dot in the domain of the NTM model as shown in Figure 6.4, since the length of the NTM model specimen is 4 mm and the length of the SVE of the DPM model is 22 μm.

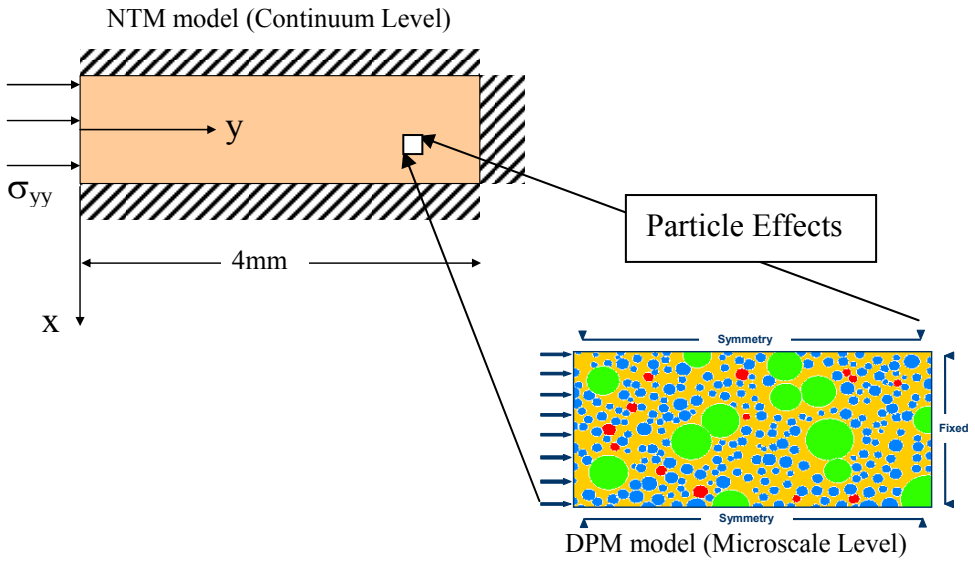

Figure 6.4 Multiscale MESMs analysis models

To establish a logical interface, the first task is to identify a simulation outcome of the DPM model that cannot be achieved in the NTM model, and an analysis outcome of the NTM model that is not achievable in DPM model. In the DPM model, we can obtain the sizes and temperatures of local hot spots where chemical reactions are initiated. However, the temperature distribution after the first reaction initiation cannot be obtained in the DPM model since the DPM model includes the temperature rise due to a mechanical

shock but not due to the chemical reaction and reaction propagation. On the other hand, it is not possible to estimate the condition for first reaction initiation in the NTM model, since the first reaction initiation usually occurs at local contact points between the metal particles.

The logic for the interface between the NTM model and DPM model is to capture local reaction initiation conditions at the DPM model and input the identified reaction initiation condition in the NTM model. In this multiscale modeling, it is assumed that the main criterion for determining chemical reaction initiation is temperature. In Figure 6.5, hot spots where reaction is initiated are illustrated in a temperature distribution profile at the time when the first reaction starts. For example, the temperature profile shown in Figure 6.5 is captured at 0.66 nano-seconds when the first reaction initiation hot spots (i.e., three spots) appear. The critical temperature at which chemical reaction will be initiated is the average of the hot spot temperatures with weighting by the spot sizes; this weighted average temperature is the input parameter in the NTM model as the reaction initiation condition. The weighted average of temperatures of local hot spots at a first reaction initiation (T_{ignit}) is

$$T_{ignit} = \frac{\sum_{i=1}^{n} A_i \cdot T_i}{\sum_{i=1}^{n} A_i}, \tag{6.2}$$

where n is the number of hot spots, T is the temperature of a hot spot, and A is the size of a hot spot.

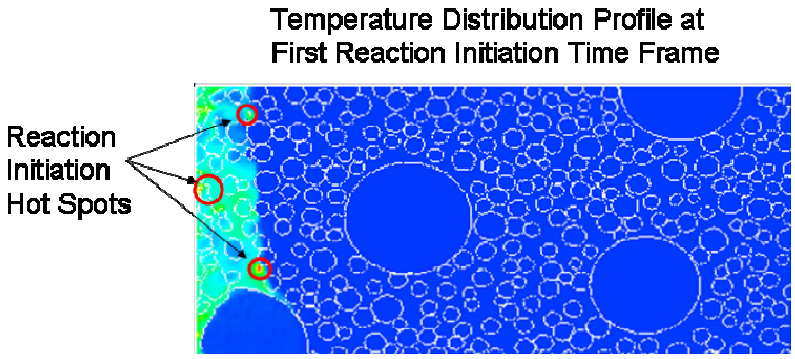

Figure 6.5 Local hot spots at a first reaction initiation time frame in the DPM model

The obtained T_{ignit} in the DPM model is then used as the reaction initiation criterion (i.e., thetac in Table 6.1) in the NTM model as shown Figure 6.6.

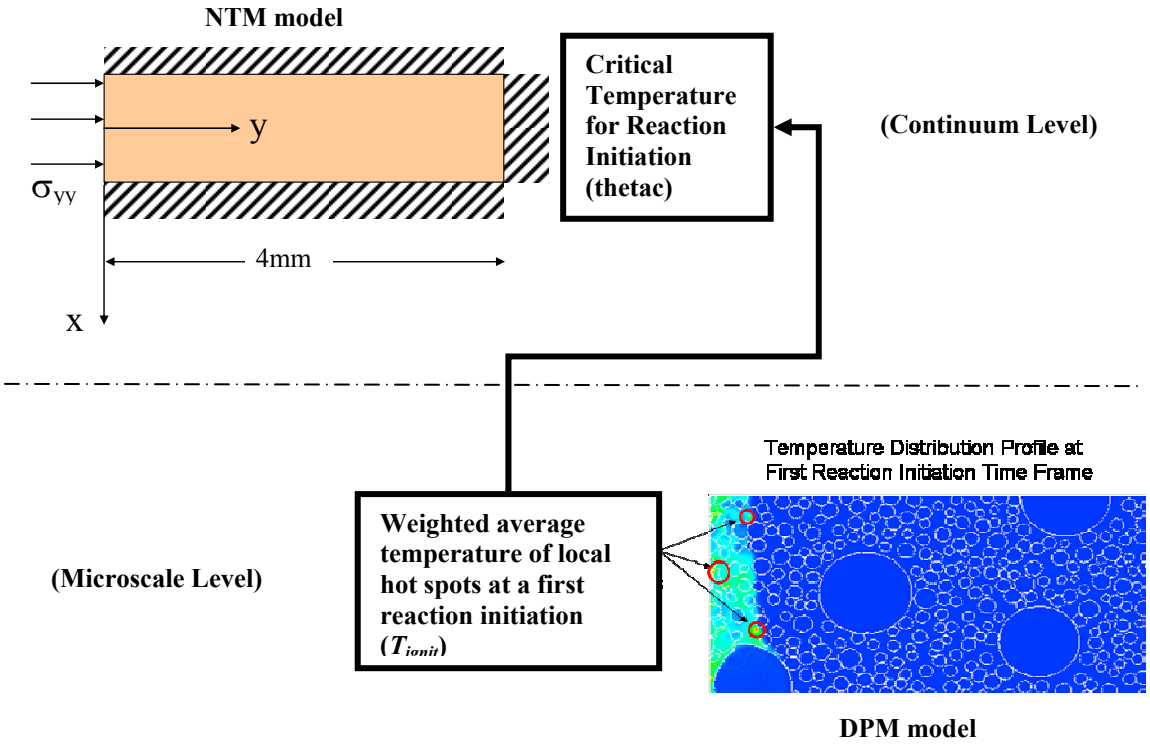

Figure 6.6 Connecting the NTM model and the DPM model

In this section, the logical interface between the multiscale models, the NTM model and the DPM model, is established. Based on this logical interface, a multiscale MESMs design problem is formulated in Section 6.2.

6.2. FORMULATION OF MULTISCALE MESMS DESIGN PROBLEM

In this section, a multiscale MESM design problem, including the NTM model and the DPM model, is formulated based on the logical interface discussed in Section 6.1.3. Information flow in the multiscale simulation models is introduced in Section 6.2.1. The inputs and outputs of each model and the interdependent variables (i.e., connecting parameters) are defined in this section. In Section 6.2.2, the empirical structural validity in the validation square is checked. The appropriateness of this multiscale problem is validated by discussing the uncertainties associated in the NTM model and propagated uncertainty from the DPM model through the NTM model to the final estimation of MESM's performance. In Section 6.2.3, empirical performance validation is planned by identifying tasks that must be performed for validating associated hypotheses (i.e., Hypotheses 3 and 4).

6.2.1. Information Flow of the Multiscale Simulation

Based on the logical interface discussed in Section 6.1.3, the information flow for designing MESMs based on the multiscale models (i.e., NTM model and DPM model) is discussed in this section. The first task to identify the information flow is defining inputs and outputs of each model.

At the microscale DPM model, the input variables are identical to those in the case study example in Chapter 5. As introduced in Section 5.3, the input variables are the mean radius of Al particles, the mean radius of Fe_2O_3 particles, the volume fraction of voids, and the mean radius of voids. The output (i.e., response) of the DPM model is the weighted average of the temperatures of local hot spots at first reaction initiation (T_{ignit}) as discussed in Section 6.1.3. The simulation software is the Raven code used in Chapter 5. In summary, the DPM model is the same model but produces different responses (T_{ignit}). A separate post-processing code is implemented using Java to capture T_{ignit} from the temperature profile database, the archived results of the simulations.

At the continuum NTM model, input variables are a critical temperature for chemical reaction initiation, which is also the output of the DPM model (T_{ignit}), and the volume fraction of voids. Since this is a continuum model, particle size effects, such as the mean radius of Al, etc., cannot be considered. The response that we capture from the NTM model is the accumulated mass fraction of Fe (*acFe*) over the entire one-dimensional specimen at 300 nano-seconds, which is the summation of the mass fractions at all nodes in the graph of Figure 6.3.c. Since Fe is the product of the chemical reaction, the accumulated mass fraction of Fe indicates the amount of chemical reaction.

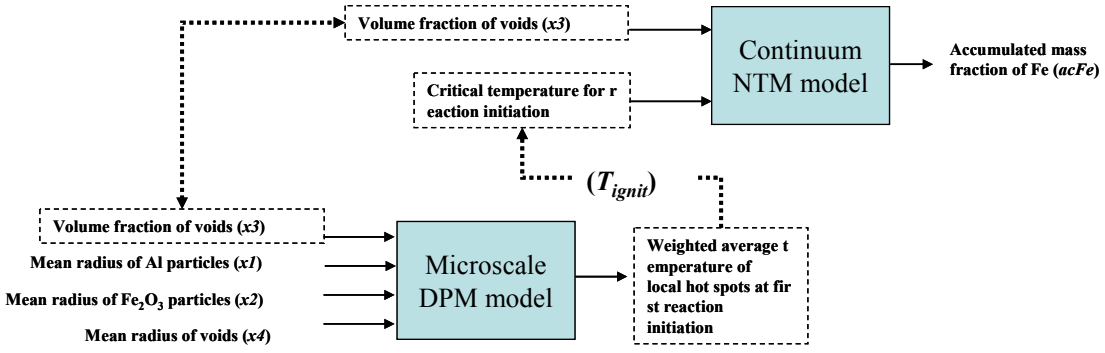

Figure 6.7 Information interface map between DPM model and NTM model

The information interface map between the DPM model and NTM model is illustrated in Figure 6.7. The symbols for the variables are listed as follows:

- x_1 : Mean radius of Al particles (mm)
- x_2 : Mean radius of Fe_2O_3 particles (mm)
- x_3 : Volume fraction of voids
- x_4 : Mean radius of voids (mm)
- T_{ignit} : Weighted average temperature of local hot spots at a first reaction initiation and critical temperature for reaction initiation (K)
- *acFe* : Accumulated mass fraction of Fe at 300 nano-seconds after the initial loading

The microscale DPM model includes four input variables (i.e., x_1~x_4) and one output (i.e., T_{ignit}) as discussed previously, and the continuum NTM model does two inputs (i.e., x_3 and T_{ignit}) and one output (*acFe*). As shown in the figure, common variables in the two models are wrapped in dotted boxes. The volume fraction of voids is the shared input variable (control factor) by the two models. As discussed, the output of the DPM model, weighted average temperature of local hot spots at a first reaction initiation, is one of the inputs of the NTM model, critical temperature for reaction initiation, which is the interdependent variable.

In this section, the information flow between DPM model and NTM model is formulated, resulting in an instance of the information flow of a complex design process illustrated in Figure 1.10. This information flow is the definition of the simulation chain, which is used for designing MESMs ($Al+Fe_2O_3$) system in this chapter. In the next section, the model structural uncertainty and propagated uncertainty in this simulation chain are discussed to check the empirical structural validity of this example.

6.2.2. Empirical Structural Validation: Propagated Uncertainty and Model Structural Uncertainty in DPM model and NTM model

In this section, the empirical structural validity of this example for demonstrating the utility of the IDEM is checked. As discussed in Section 1.5, we check if the example problem, multiscale simulation-based MESM design, is appropriate for validating the functionality of the IDEM. The validation square roadmap is shown in Figure 6.8.

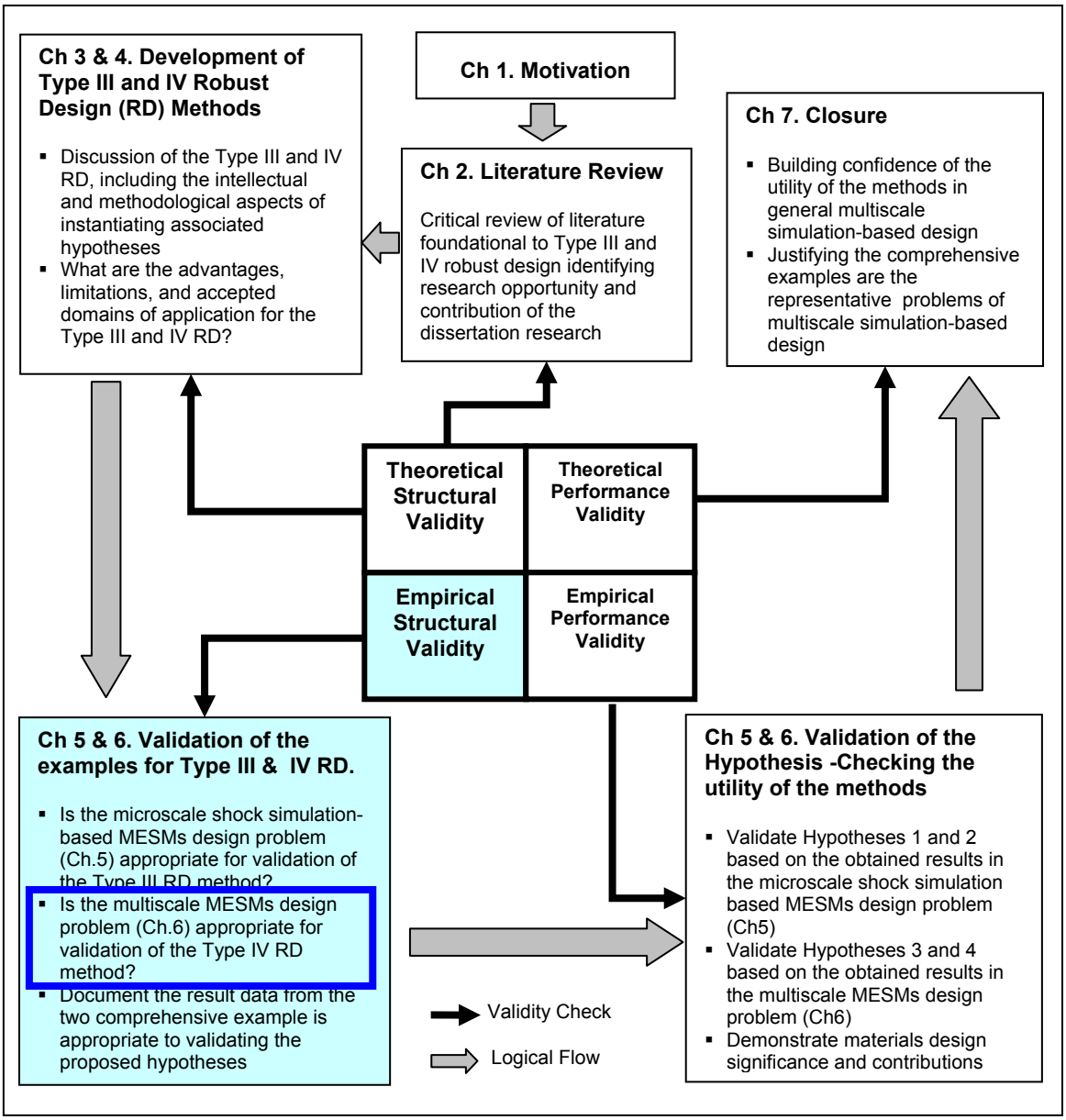

Figure 6.8 Validation square roadmap

An appropriate example should include propagated uncertainty in a simulation and analysis chain, which is related to Hypotheses 3 and 4. In the multiscale MESM design problem discussed in Section 6.1, the continuum NTM model and the microscale DPM model interface with each other. Uncertainty propagation along this multiscale simulation chain is illustrated in Figure 6.9.

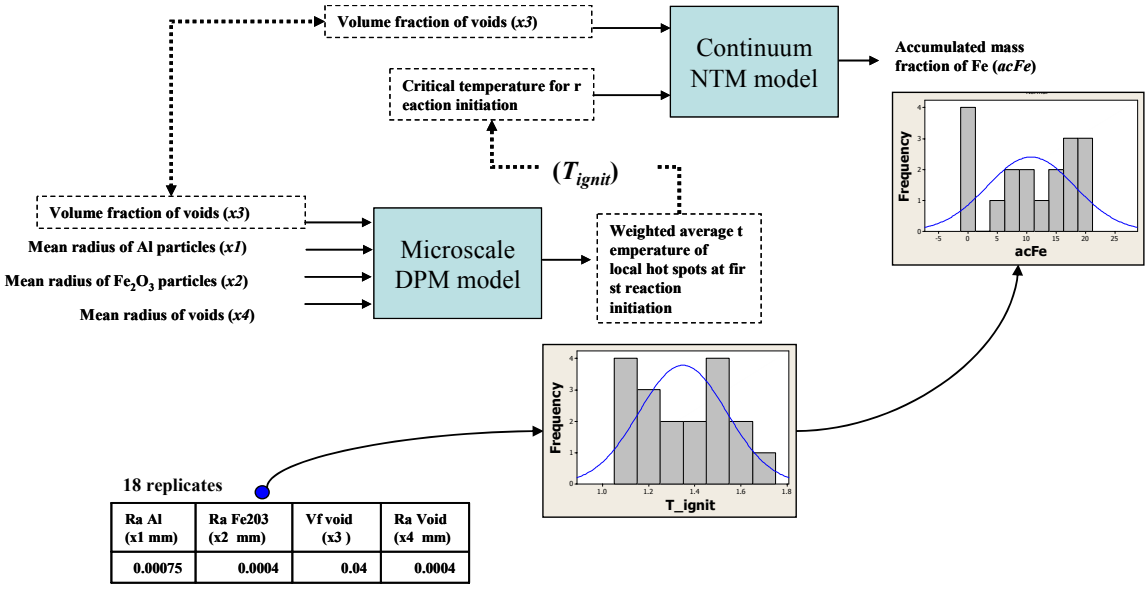

Figure 6.9 An illustration of propagated uncertainty in multiscale simulation-based MESMs design

As shown in Figure 6.9, eighteen replicates at a single input point are simulated in the microscale DPM model. A histogram of the outputs (T_{ignit}) of the replicated simulation is illustrated in the figure. As expected, replication of a single input generates a distribution of varied outputs. The interval of the variation is from 1078K to 1697K, which is quite large. Each of these outputs of the microscale DPM model becomes a set of inputs to the analysis of continuum NTM model. Another histogram of the outputs (*acFe*) of the continuum NTM model analysis is illustrated in this figure. The deviation of the *acFe* is from 0 to 20.076, which means a reaction could be initiated or not. Refer to Table A.1 for the simulation results. Based on this observation, unfortunately, we cannot decide that the

set of input parameters is good enough for reaction initiation at the continuum level. This demonstrates that uncertainty in a simulation or analysis model is propagated through the multiscale simulation chains and the variance of the distribution become larger at the end of the chain. In this demonstration, the variances in design variables (*x1~x4*) are not considered. If these are included in this uncertainty propagation demonstration, then the propagated uncertainty should become even more significant. The normal distributions shown in the histograms are for the purpose of illustration.

In addition to the propagated uncertainty, the microscale DPM model and the continuum NTM model are associated with model structure uncertainty discussed in Section 3.2.3. The model structure uncertainty in the microscale DPM model is discussed in Section 5.1.2, particularly the assumptions made due to an uncertain constitutive model for iron-oxide and idealization from 3D particles to 2D cylinders. The response employed in this multiscale MESM problem is a weighted average of the hot spot temperatures at the first reaction initiation. However, it is not fully validated that the average temperature in the DPM model is equivalent to the critical temperature for the chemical reaction initiation in the NTM model. The criteria for chemical reaction initiation derived from the microscale DPM model need to be further investigated in order to include the delay in the chemical reaction. For example, the hot spots should be sustained longer than the reaction delay time interval. Therefore, we have additional potential uncertainty in the DPM model in the multiscale simulation chain.

The major assumption in the continuum NTM model is the uniformly blended mixture theory used for describing discrete particles and porous mixtures, which is a simplification for enabling numerical calculation in a larger scale continuous medium.

This assumption is common in continuum level simulation or analysis; however it could produce some unquantifiable uncertainty in responses. This uncertainty requires a model calibration process based on real experimental results. The constitutive models (Lu, et al., 2003) of void collapse flux, heat flux, and mass diffusion flux are still immature; therefore, there could be some uncertainties in the predicted responses of *acFe*. These are the sources of model structure uncertainty discussed in Section 3.2.3.

As discussed in this section, the multiscale simulation-based MESM design task is associated with the accumulated and propagated uncertainty in the simulation chain of the microscale DPM model and the continuum NTM model. This design problem is also associated with the model structure uncertainty in each of the models in the chain. Therefore, this example problem is an appropriate case study for validating Hypotheses 3 and 4. Based on the confidence in this example, we plan detailed validation tasks in the next section.

6.2.3. Planning Tasks for Empirical Performance Validation

In the previous section, it is validated that this multiscale simulation-based MESMs design problem is an appropriate example for validating Hypotheses 3 and 4. In this section, we plan tasks necessary for empirical performance validation, which is used to build confidence in the utility of the Graphical Robust Design Process Model (GRDPM) discussed in Section 4.4 and the Inductive Design Exploration Methods discussed in Section 4.5~4.8 for this multiscale simulation-based MESMs design problem.

Task 1*: Demonstrate the GRDPM represents the robust MESM design process better than other process representation protocols.* In this task, GRDPM is used for describing a process for robust design of MESMs based on the DPM model and NTM model. The

MESMs design process is formulated based on the analysis chain in Figure 6.7. The IDEF0 process model reviewed in Section 2.5.1 is employed to demonstrate the utility of the GRDPM. Comparing those two process models, we argue the utility of GRDPM, which is the validation of Hypothesis 3

Task 2*: Identify ranged sets of design specifications instead of a point solution range with given ranged performance requirement.* One of the main advantages of the Inductive Design Exploration Method (IDEM) is to find multiple ranged sets of design specifications with given performance requirement ranges, which is mentioned in Hypothesis 4. In this chapter, we demonstrate that designers may find ranged sets of feasible design specifications based on the IDEM.

Task 3*: Identify robust ranged sets of solutions for propagated uncertainty in the multiscale MESMs simulation and analysis chain.* As discussed in the previous section, the uncertainty in the DPM model propagates through the NTM model and is expanded at the final performance estimation. In this task, we compare the robust solution found using the IDEM at Task 2 with other specifications to demonstrate its ability to find a robust solution against propagated uncertainty in multiscale simulation/analysis chain.

Task 4*: Identify the best robust solution considering model structure uncertainty in the microscale DPM model and/or in the continuum NTM model.* As discussed in the previous section, the two models in the multiscale simulation chain have model structure uncertainty. In this task, the best robust solution is identified among the feasible ranged sets of design specifications obtained in Task 3. The best solution is identified by trading off achieved HD-EMIs.

The results of these four tasks are discussed in Section 6.7 and summarized in Section 6.7 revisiting Hypotheses 3 and 4.

6.3. PROCESS MODELS FOR REPRESENTING THE ROBUST MULTISCALE MESMS DESIGN PROCESS

In this section, Task 1, discussed in Section 6.2.3, is performed to demonstrate the utility of the Graphical Robust Design Process Model (GRDPM). The multiscale MESM simulation chain is described using the IDEF0 process model in Section 6.3.1. The GRDPM for MESM design is discussed in Section 6.3.2. The two process description models are compared in order to validate Hypothesis 3, highlighting the utility of the GRDPM.

6.3.1. The IDEF0 Process Model Describing the Multiscale MESMs Analysis Chain and Design Process

In Chapter 2, we review the IDEF0 Process Model. This semantic process model is for describing processes, which include design, simulation, and manufacturing processes. The multiscale MESM simulation chain is represented using the IDEF0 model in Figure 6.10.

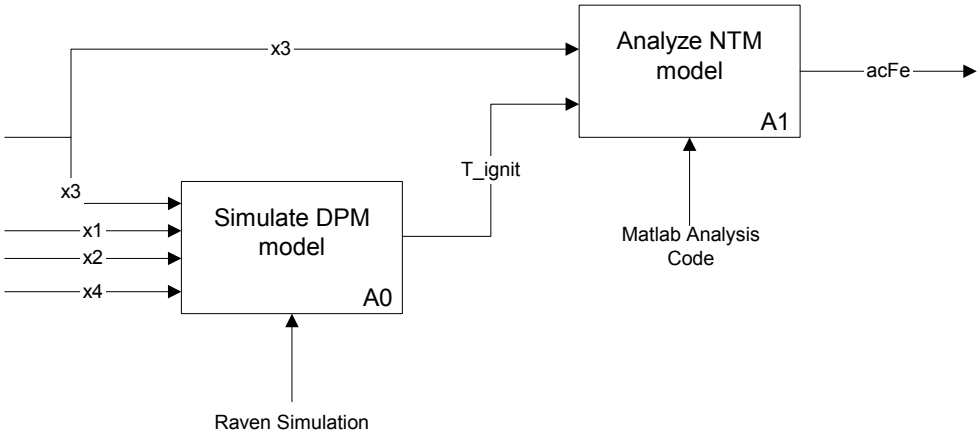

Figure 6.10 IDEF0 process model for multiscale MESM analysis chain

The multiscale simulation process starts with the task 'Simulate DPM model' using the Raven simulation tool as discussed in Chapter 5. The input of the DPM model is *x1~x4*, which are the mean radius of aluminum particles, the mean radius of iron-oxide, the volume fraction of voids, and the mean radius of voids, respectively. The output of the DPM model of critical temperature for chemical reaction initiation becomes the input of the task 'Analyze NTM model' with the shared design variable *x3* (i.e., the volume fraction of voids). The task 'Analyze NTM model' is supported by the MATLAB® analysis code (Lu, et al., 2003). The output, which is the response of this multiscale simulation and analysis chain, is the accumulated mass fraction of Fe (*acFe*) as discussed in Section 6.1.1.

The process described in Figure 6.10 is the simulation and analysis process for predicting the chemical reaction of the aluminum and iron-oxide mixture system; it is a bottom up approach. However, the design process in the IDEM is the inverse process of the simulation and analysis process chain, which is represented using the IDEF0 model in Figure 6.11.

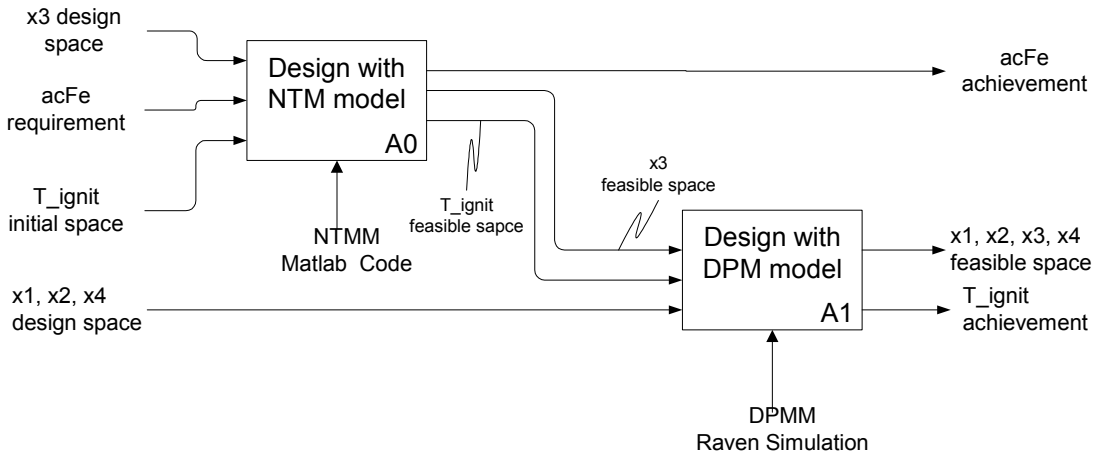

Figure 6.11 The IDEF0 process model of the IDEM for the multiscale MESMs design

The design process starts with defining the design space (i.e., the space of T_{ignit} and *x3*) in the task of 'Design with NTM model', which is defining the space of T_{ignit} and *x3*. The required range of the performance (*acFe*) should be given for this design task. The task, 'Design with NTM model' is supported by the MATLAB analysis code for predicting the amount of *acFe.* The outputs of this design task are the achieved *acFe* and the feasible space of T_{ignit} and *x3.* The feasible space of *x3* becomes the design space of *x3* and the feasible space of T_{ignit} does the performance requirement range for the microscale design task, 'Design with DPM model'. The design space of other design variables (*x1, x2,* and *x4*) should be given also for this microscale design task, which is supported by the microscale Raven simulation code for predicting average hot spot temperature at the first reaction initiation (i.e., T_{ignit}). Finally, the feasible design space of all design variables is identified with corresponding performance ranges (i.e., the ranges of *acFe* and T_{ignit}).

In this section, we investigate the multiscale simulation and analysis based MESM design process described with the IDEF0 model. The IDEF0 model is effective for describing a series of tasks; however, it cannot describe the uncertainty characteristics associated with design tasks of each scale. In the next section, we describe the robust design process using the GRDPM.

6.3.2. The Graphical Robust Design Process Model (GRDPM) for the Robust Multiscale MESMs Design Process

Based on the analysis process and the IDEM described in the previous section, we discuss the GRDPM, depicting a robust multiscale MESM design process in this section. As discussed, the uncertainties associated with the supporting model, computing code or programs, input parameter, corresponding output parameter, and responses cannot be described in an IDEF0 model, though it is the most important information in robust

design tasks. Using the GRDPM, those uncertainty characteristics associated with multiscale robust MESM design tasks can be explicitly depicted with the semantically rich graphical entities discussed in Section 4.4.1. The GRDPM for the robust multiscale MESM design process is depicted in Figure 6.12.

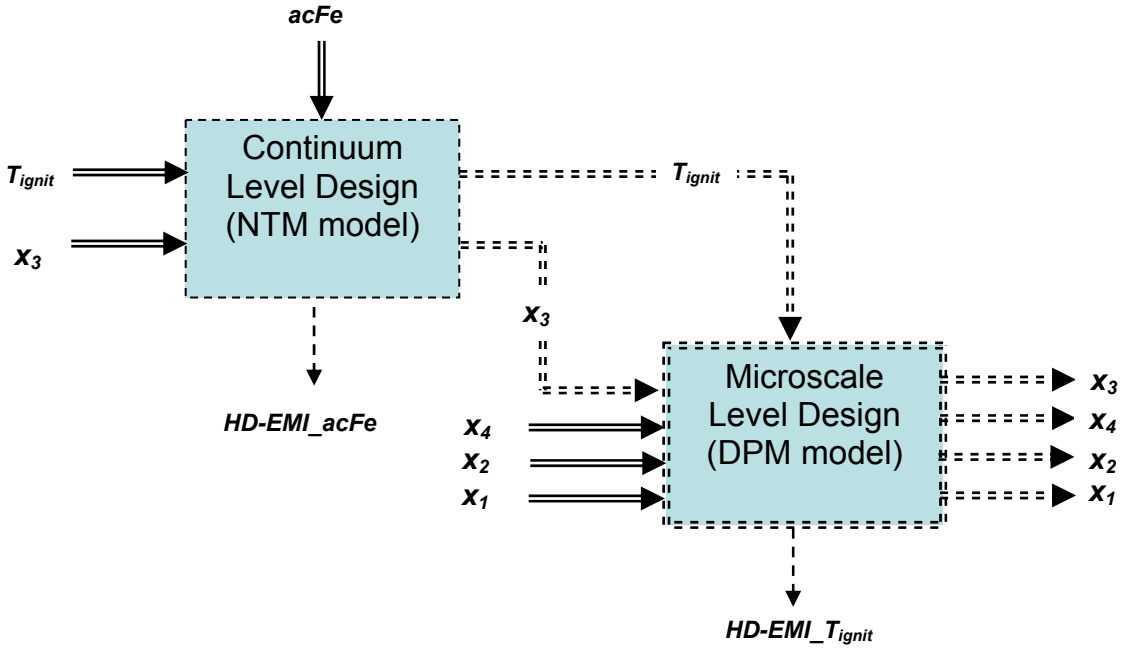

Figure 6.12 The GRDPM of the IDEM for the multiscale simulation-based MESMs design

The IDEM design process for the multiscale robust MESM design process is discussed in the previous section as shown in Figure 6.11. In addition to the information displayed in the IDEF0 model, the GRDPM includes the uncertainty aspects of the design tasks. The 'Continuum Level Design" task with NTM model is depicted as a single dotted box, which illustrates that the design task is performed based on a uncertain analysis model. Since it is a single (i.e., discrete) dotted (i.e., uncertain) box (i.e., task or function), it represents that the uncertainty in the analysis model associated with this task is unquantifiable (i.e., model structure uncertainty). The given required range of performance (i.e., range of *acFe*) is illustrated as a double line since it is a certain ranged

value. The design spaces of T_{ignit} and *x3* for this continuum level design task are also double lines since those are ranged certain values. As the output of the decision in this task, the design task produces the feasible ranges out of the design spaces of T_{ignit} and *x3* with corresponding decision criterion, which is the achieved HD-EMI of *acFe.* Since these values (i.e., T_{ignit}, *x3,* and HD-EMI of *acFe*) are obtained based on the uncertain analysis model, those outputs are illustrated as dotted double lines.

The obtained uncertain ranges of outputs (i.e., T_{ignit} and *x3*) from the task of 'Continuum Level Design' become input ranges of the 'Microscale Level Design' task that is supported by the microscale DPM model shock simulation. The obtained uncertain range of T_{ignit} from the 'Continuum Level Design' task becomes the uncertain bound of required performance for the 'Microscale Level Design' task. Similarly, the uncertain range of *x3* becomes the uncertain design space of *x3.* With the design spaces of *x1, x2,* and *x4,* the 'Microscale Level Design' task is performed. Since this design task is supported by the DPM model shock simulation with quantifiable uncertainty (i.e., unparameterizable variability in the RPMM systems), this design task is illustrated as a double (i.e., ranged) dotted line (i.e., uncertain) box (i.e., task or function). The outputs of this task, which are the feasible space of *x1~x4* and HD-EMI for $T_{ignit,}$ are uncertain since the supporting simulation model, the given performance range, and one of the design spaces are uncertain. Therefore, the feasible range of *x1~x4* are depicted as double dotted lines and the obtained HD-EMI for T_{ignit} is a single dotted line.

As described in this GRDPM, the uncertainties associated with the design tasks are explicitly represented conveying their types. Compared with the IDEF0 model, the information flows of the decision process are efficiently represented in the GRDPM. The

information of the design variables flows from the left to the right along the design process, and the information of the corresponding performance from the top to the bottom of the boxes. Since the ranged and discrete value of a parameter is described as a double or a single line, respectively, we may easily estimate whether the design results still have design freedom for more adjustment or not. Moreover, the decision-making criteria (the HD-EMIs in the IDEM) are depicted in the model so that the reliability of the decision in the tasks under uncertainty can be easily identified by designers. We discuss the advantages of the GRDPM describing a robust multidisciplinary design task in detail in Section 6.7. In the next section, we discuss the procedure of the multiscale simulation-based MESMs design using the IDEM in detail.

6.4. THE PROCEDURE OF THE MULTISCALE MESMS DESIGN USING INDUCTIVE DESIGN EXPLORATION METHOD

In the previous section, we discuss the overall procedure for designing MESMs that are robust to uncertainty in the simulation and analysis chain based on the IDEM. The details of each scale level design task are described in Figure 6.13. As shown in the figure, multiscale design tasks require the same procedure at each scale level. The procedure at the individual design task is similar to the overall process of the RCEM-EMI; however, it includes the Discrete Constraints Evaluation (DCE) process instead of the cDSP for RCEM-EMI. The individual design procedure starts with given performance requirements and constraints and an initial design space. Based on the given information, designers clarify the control and noise factors, the uncertainty in the factors and the analysis or simulation model, and system constraints.

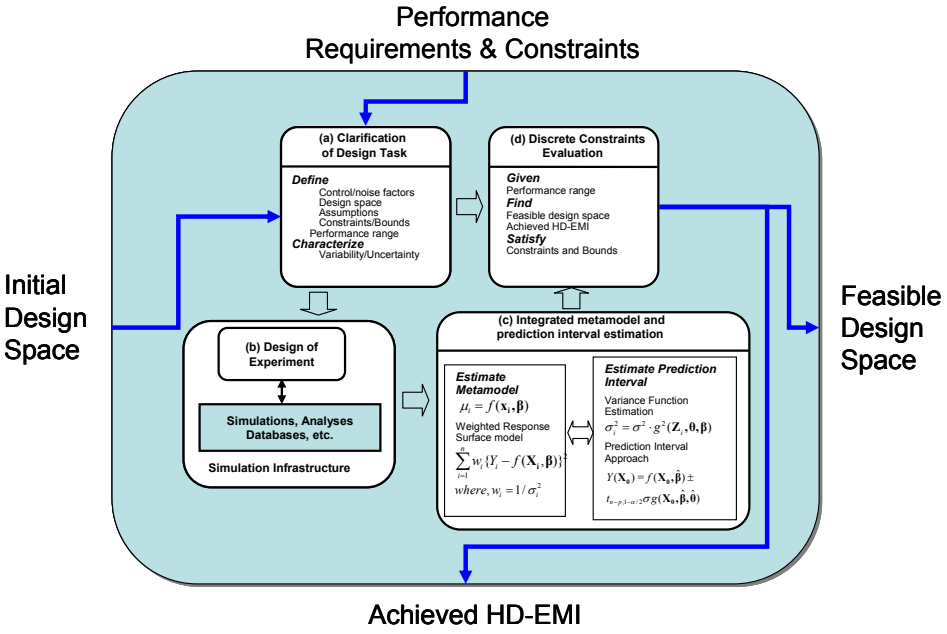

Figure 6.13 The generalized process at each scale level design task

The next step is designing experiments and collecting experimental data using simulation infrastructure or experiment sets. Based on the collected data, designers generate a metamodel for the most probable response. If the simulation, analysis, or experiments are non-deterministic, then the integrated metamodel and prediction interval estimation method discussed in Chapter 3 are required to quantify the unparameterizable variability. Up to this point in the process, the tasks are identical to the tasks in the overall RCEM-EMI construct described in Figure 3.6. However, the last step is different from the RCEM-EMI framework. In the RCEM-EMI, designers search for a robust ranged set of design specifications based on the given performance requirement, which is the single best solution with tolerance inside. The DCE process is an algorithm for finding all feasible space in the design space that satisfies the given required performance range. Therefore the results are multiple sets of all feasible solutions, taking into account

the variability and uncertainty in the model. The DCE process also provides the achieved HD-EMIs of each feasible solution set.

The task procedure of the individual design task is illustrated in Figure 6.13. The generalized task procedure identifies feasible ranged sets of design specifications and corresponding achieved HD-EMIs with given performance range and design space. This procedure is identical to the procedure used at all levels of design tasks in multiscale simulation-based design process. A multiscale simulation-based design process is composed of a number of these instances.

As discussed in Section 4.5, the IDEM is a top-down design process sequentially identifying feasible design spaces from the highest level requirements to the lowest level design space. The generalized procedure of each level design task above is used at each scale level task of the IDEM for the multiscale robust MESMs design as illustrated in Figure 6.14.

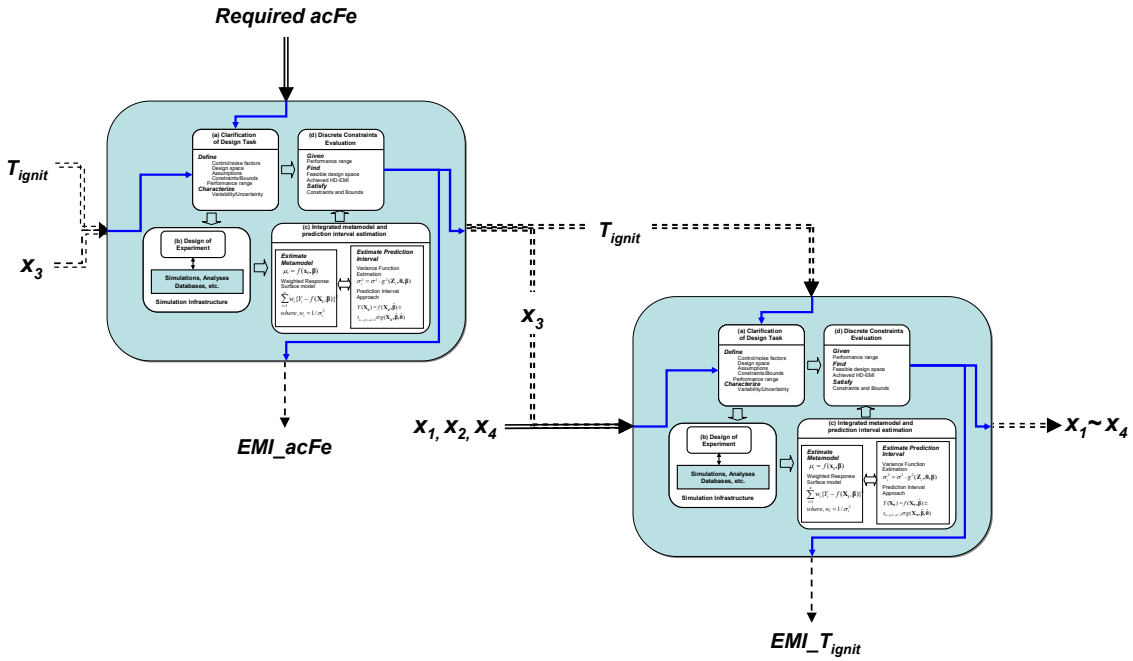

Figure 6.14 Multiscale robust MESMs design based on the IDEM

As discussed in Section 6.3.2, this design process starts with 'Continuum Level Design' task. In this design task, the range of *acFe* is given as a required performance range and the design space of T_{ignit} and *x3* is also given. Based on the given design space, we plan the simulation runs (DOE) using the MATLAB® analysis code of NTM model. With the obtained results, the next step is building a metamodel. Since this analysis code is a deterministic model and includes model structure uncertainty, we do not include the prediction interval estimation approach but estimate only the most probable model. Based on the obtained metamodel, we identify the feasible space of T_{ignit} and *x3* that is satisfactory to the required *acFe* within the given design space of T_{ignit} and *x3* using the DCE process.

The 'Continuum Level Design' task is followed by the task of 'Microscale Level Design". In this design task, the design spaces of *x1, x2,* and *x4* are given and the design space of *x3* is passed from the 'Continuum Level Design' task as a feasible region. The required performance range (i.e., the feasible range of T_{ignit}) is also passed from the previous design task. As discussed above, the ranges of T_{ignit} and *x3* that are passed to 'Microscale Level Design' include uncertainty inside; therefore, they are represented as double (i.e., ranged) dotted (i.e., uncertain) lines (i.e., values). Since the range of T_{ignit} is performance bounds for this design task, the arrow comes from the top to the box. The range of *x3* is the design space for this design task; therefore, the arrow comes from the left to the box. The box (i.e., a design task) is represented by double dotted lines since the microscale DPM model incorporated in this task includes ranged uncertainty (i.e., model parameter uncertainty) due to the unparameterizable variability.

The procedure in the 'Microscale Level Design' task is similar to the procedure in the 'Continuum Level Design' task. Based on the inputs (design space, feasible space, and performance requirement) from the previous task, the given microscale DPM model, and the Raven simulation code, designers clarify the design tasks identifying the characteristics of uncertainty, system constraints, control and noise factors, etc. The DOE and simulation follow the design task clarification. This is discussed in detail in Section 5.4. Based on the obtained data in the DOE and simulation task, designers generate a metamodel and prediction interval for T_{ignit}. The detailed procedure is identical to the procedure described in Section 5.5. Once designers obtain a metamodel and its prediction interval, they search for feasible regions that satisfy the passed T_{ignit} requirement within the design space of *x1, x2, and x4* and the feasible space of *x3* using the DCE. The function evaluation calculates the mean, upper, and lower deviation of performance based on the metamodel, the prediction interval limits (i.e., upper and lower bounds), and the variations in control and noise factors using Eq. (3.16). The results of the DCE are feasible solution sets of design specifications.

In this section, we discuss the overall inductive design process for multiscale robust MESMs design using the IDEM. The design task in each scale level is represented as a generalized task procedure shown in Figure 6.13, which is reusable for any level of design task. In the following two sections, the details of the procedures performed at each scale level for the multiscale robust MESMs design are discussed.

6.5. MULTISCALE MESMS DESIGN USING THE INDUCTIVE DESIGN EXPLORATION METHOD

In this section, we follow the IDEM discussed in Chapter 4 for robust multiscale MESMs design under uncertainty in simulation and analysis models and its propagation in the simulation chain. According to the design task flow discussed in Section 6.4, the details of IDEM are discussed. In Section 6.5.1, the continuum level MESMs design task is clarified. The clarified design task is followed by the DOE, achieving analysis results, and building a metamodel in Section 6.5.2. The microscale level MESMs design task is clarified in Section 6.5.3, which is followed by the DOE, simulation data, and building a metamodel and prediction interval in Section 6.5.4. Finally, based on the previous steps, inductive design exploration for obtaining feasible range sets of robust design specifications is discussed in detail in Section 6.5.5.

6.5.1. Clarifying Continuum Level MESMs Design Task

In this section, the continuum level MESMs design task is clarified. As shown in Table 6.2, the design variables (T_{ignit} and *x3*) and design space are defined as shown in the table. The response of this design task is defined as *acFe,* which is the accumulated mass fraction of Fe at 300 nano seconds. The purpose of the continuum level design task is to identify the feasible space of T_{ignit} and *x3* while achieving at least 5 of *acFe.* One of the important items in this clarification is to identify uncertainties in this design task. The design variable (i.e., control factor), *x3*, has a deviation of 0.01. This means the volume fraction of void could have deviation of 0.01 from a designer's decision in real case due to manufacturing variance. The main assumption in this calculation is the uniformly blended mixture theory discussed in Section 6.1.1. Another idealization is that one

dimensional shock is imposed for this NTM model analysis, which is an ideal case of real shock simulation. This assumption is made for computational efficiency. Since the NTM model is a specific model for one dimensional shock problems, the mesh and calculation (finite difference analysis) are one dimensional. A 4 (mm) sized 1-D specimen is discretized by 401 nodes.

Table 6.2 Clarification of the continuum level design task

Clarified Items	Specifications
Design variables and space	▪ T_{ignit}: Critical temperature for chemical reaction initiation ▪ *x3*: Volume fraction of voids ▪ T_{ignit} = [1, 1.6] (1000 K) ▪ *x3* = [0.02, 0.1]
Response	▪ *acFe*: Accumulated mass fraction of Fe
Uncertainty & Assumption	▪ Variability in the volume fraction of voids: $\Delta x3=0.01$ ▪ Uniformly blended mixture theory ▪ One dimensional shock simulation ▪ One dimensional finite difference approximation
Fixed parameters	▪ Metal volume fraction : 50% Volume Fraction ▪ Volume fraction of Al : Volume fraction of Fe_2O_3= 2:3 (reactants are in stoichiometric properties) ▪ Left boundary velocity : 1000 (m/s) ▪ Length of specimen: $4x10^{-3}$ (m) ▪ Mesh length : $10x10^{-6}$ (m) ▪ Time interval for calculation : 0 ~ $300x10^{-9}$ (seconds)
Objectives	▪ Achieve $acFe \geq 5$ with consideration of uncertainty in NTM model ▪ Identify feasible space of T_{ignit} and *x3*
Analysis and simulation tool	▪ Non-equilibrium thermodynamics mixture model implemented in MATLAB®

Some parameters in this design task are fixed in order to reduce the scope of the design problem. This is important for computational efficiency and for reducing design lead time. In this design task, the volume fraction of metal constituents (Al and Fe_2O_3) is fixed in order to study the particle size effect in the microscale simulation. The ratio of Al

and Fe_2O_3 is also set to the stoichiometric ratio, which is the same as that in the microscale shock simulation discussed in Chapter 5. The left boundary condition is set as 1000 (m/s) and the time interval for shock propagation calculation is from zero to 300 nano seconds after the initial shock loading. As discussed above, this is a one dimensional shock analysis model; therefore, the length of specimen is set to $4x10^{-3}$ (m) and the element length is 10 (μm) with 401 nodes.

In this section, the continuum level design task using NTM model analysis code is clarified. Based on this clarification, the next step is designing experiments, collecting analysis data, and building metamodels.

6.5.2. Design of Experiments, Analysis Results, and Response Surface Model for the Continuum Level MESMs Design Task

The MATLAB® analysis code for the NTM model is not computationally intensive; it takes on the order several minutes for a single calculation. However, in this dissertation, we adopt a metamodeling approach instead of direct use of the simulation for the function evaluation for the following reasons. First, the analysis of uncertainty in response due to the variability in control factors requires a large amount of analysis data during the search for feasible regions. Second, the solution search algorithm requires large numbers of function evaluations that include the aforementioned uncertainty analysis. Finally, the NTM model analysis code is in a remote place, which makes the acquisition of large amount of data more difficult. In these worst cases of the design task, we recommend using a metamodel rather than directly computing the results.

For achieving an accurate response surface model, a central composite design with two factors is employed in this study. The experimental points and the NTM model analysis data are listed in Table 6.3.

Table 6.3 Experimental points and obtained data using continuum NTM model code

Volume Fraction of Voids (*x3*)	T_{ignit} (1000 K)	acFe (responses)
0.032	1.088	19.452
0.088	1.088	21.615
0.032	1.512	0
0.088	1.512	8.975
0.020	1.300	12.892
0.100	1.300	16.776
0.060	1.000	22.054
0.060	1.600	0
0.060	1.300	15.004

As shown in Figure 6.15, the regression parameters of a full quadratic response surface model of *acFe* versus *x3* (volume fraction of voids) and T_{ignit} are estimated using MINITAB®. The full quadratic response surface model fits well with the obtained data (R^2 =99.2%). The constant and the second order of *x3* terms have high p-value, which means those coefficients are more likely zeros. Therefore, we can say that the relationship between *x3* and *acFe* is linear. This relationship is also shown in the surface plot of this response surface model.

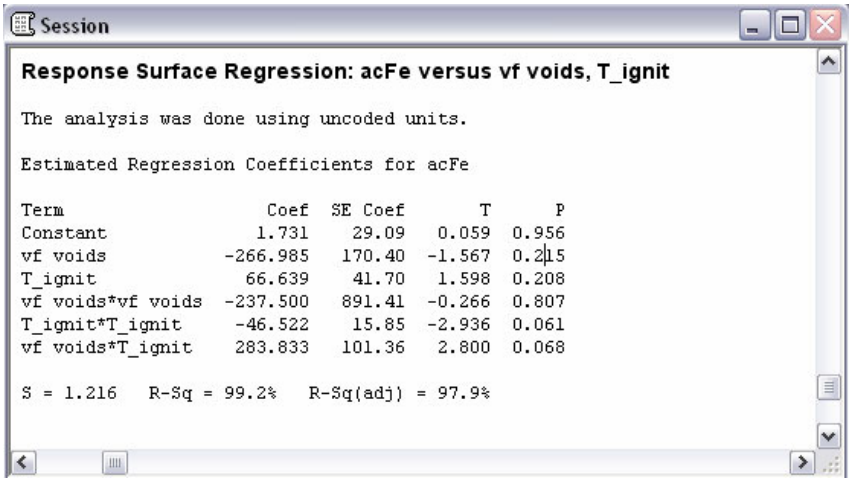

Figure 6.15 Estimation of the regression parameters in response surface model

The estimated response surface and contour plots are plotted in Figure 6.16. The range of responses is from 0 to about 25. As expected, the relationship between *acFe* and *x3* shows linear behavior. There are some interaction factors between *x3* and $T_{ignit,}$ which is also shown in the estimated parameters in Figure 6.15. The effect of *x3* is small at the low level of T_{ignit}, but large at the high level. On the other hand, the effect of T_{ignit} on the response is significant and shows quadratic behavior.

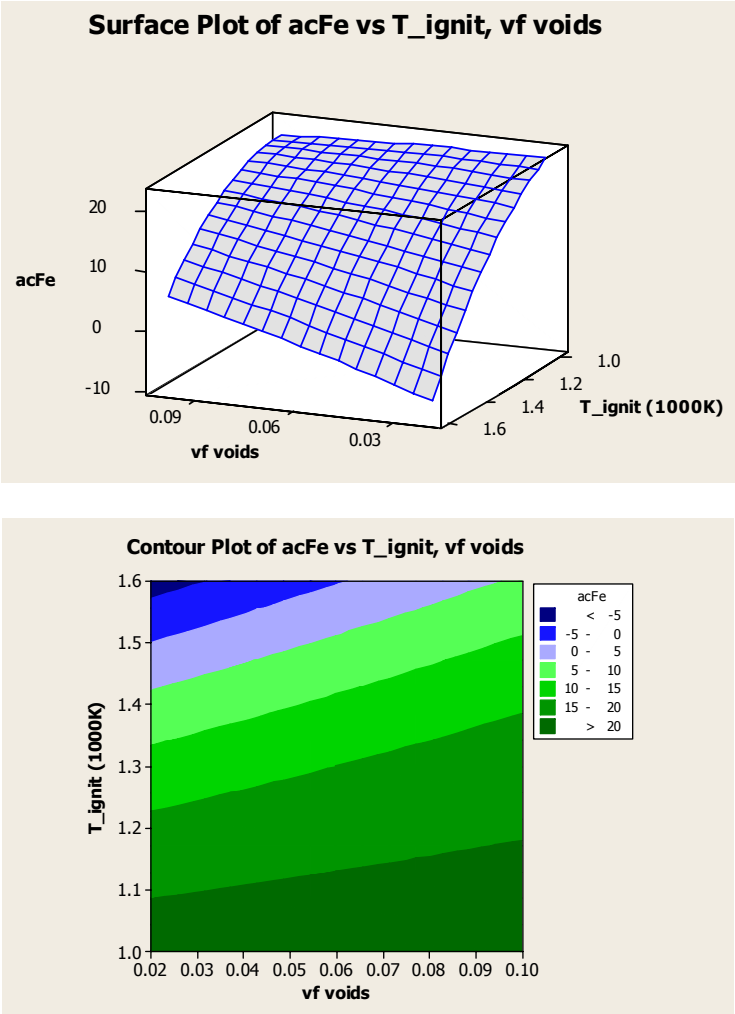

Figure 6.16 The estimated response surface and contour plots of *acFe* versus *x3* and T_{ignit}

Once a response surface model for estimating *acFe* is obtained, then we formulate the mathematical functions for estimating mean, minimum, and maximum responses based on Eq. (3.14). The mean of the response is obtained using the estimated response surface model as

$$acFe_{\text{mean}} = f_0(x_3, T_{ignit}) \text{ : Response Surface Model} \tag{6.2}$$

where $f_0(x_3, T_{ignit}) = 1.73 - 267 \cdot x_3 + 66.6 \cdot T_{ignit} + 237.5 \cdot x_3^2 - 46.5 \cdot T_{ignit}^2 + 284 \cdot x_3 T_{ignit}$

As shown in Eq. (6.3), the minimum and maximum responses due to the variations in control factors are obtained based on the worst case scenario. As discussed in Section 6.5.1, the worst case scenario is a conservative approximation technique for estimating response deviation; however, it could be derived using other uncertainty analysis technique discussed in Section 2.2.1.

$$\begin{aligned} acFe_{\text{min}} &= acFe_{\text{mean}} - \Delta acFe \\ acFe_{\text{max}} &= acFe_{\text{mean}} + \Delta acFe \end{aligned} \tag{6.3}$$

where $\Delta acFe(x_3, T_{ignit}) = \left|\frac{\partial f_0}{\partial x_3}\right| \cdot \Delta x_3 + \left|\frac{\partial f_0}{\partial T_{ignit}}\right| \cdot \Delta T_{ignit}$

The deviation of x3 (Δx_3) is 0.01 as discussed in Section 6.5.1. The deviation of T_{ignit} (ΔT_{ignit}) is set to 0.005 which is the resolution of discretization for the DCE (Discrete Constraints Evaluation) since T_{ignit} does not have a given tolerance from the clarification of task; T_{ignit} is an interdependent variable. Based on these mathematical formulations, designers get the mean, minimum, and maximum responses for Inductive Discrete Constraints Evaluation (IDCE) process along the robust MESMs design process chain.

6.5.3. Clarifying Microscale Level Design Task

In this section, we discuss the next step, which is clarifying the microscale level design task based on the microscale DPM model shock simulation discussed in Section 6.1.2. The specifications in this design task are similar to those in the design task discussed in Section 5.3. In this section, this clarification is discussed focusing on the differences with the design task discussed in Section 5.3. This clarification task is summarized in Table 6.4.

The design variables are identical to those in Section 5.3. The design spaces of the design variables except *x3* are also identical. The design space of *x3* is the feasible space passed down from the continuum level design task. The response of this design task is T_{ignit}, which is the weighted average temperature of local hot spots at the first reaction initiation. This parameter is equivalent to the critical temperature in the NTM model, as it is the interdependent variable linking the two levels of design tasks.

The uncertainty and variability in this design task are identical to those listed in Section 5.3. Among the fixed parameters, the size of SVE has been increased from 14 μm x 7 μm to 22 μm x 11 μm. This change reduces unparameterizable variability while sacrificing computational performance for the simulation. Therefore, the runs in this design task require approximately four times more computational time than the runs in Chapter 5. The objective of this design task is to identify feasible spaces of *x1~x4, satisfying* the feasible range of T_{ignit} identified in the continuum NTM model design task with consideration of uncertainty in DPM model.

Table 6.4 Clarification of the microscale level design task

Clarified Items	Specifications
Design variables and space	▪ *x1* : Mean Radius of Al Particles ▪ *x2* : Mean Radius of Fe_2O_3 Particles ▪ *x3* : Volume Fraction of Voids ▪ *x4* : Mean Radius of Voids ▪ *x1* = [0.0005, 0.0015] (mm) ▪ *x2* = [0.0002, 0.001] (mm) ▪ ***x3* space = the feasible range obtained from continuum level design task** ▪ *x4* = [0.0002, 0.001] (mm)
Response	▪ T_{ignit} : Weighted average temperature of local hot spots at a first reaction initiation (equivalent to critical temperature in NTM model)
Uncertainty & Assumption	▪ $\Delta x_1 = \pm 0.0002$ (mm) ▪ $\Delta x_2 = \pm 0.0001$ (mm) ▪ $\Delta x_3 = \pm 0.01$ ▪ $\Delta x_4 = \pm 0.0001$ (mm) ▪ Generalized plane strain assuming circular particles as cylinders ▪ Constitutive model for Fe_2O_3 : bilinear elastic-plastic model
Fixed parameters	▪ Metal Volume Fraction : 50% Volume Fraction ▪ Volume fraction of Al : Volume Fraction of Fe_2O_3= 2:3 (reactants are in stoichiometric properties) ▪ Standard Deviation of Void Radius : 20% of the Mean Radius of Void ▪ Standard Deviation of Al Radius : 20% of the Mean Radius of Al Particles ▪ Standard Deviation of Fe_2O_3 Radius : 20% of the Mean Radius of Fe_2O_3 Particles ▪ Particle Shock Velocity (U_p) : 1 (km/s) ▪ Size of SVE: 22 x 11 (10^{-6} mm^2) ▪ Number of Elements: 380 x 200 ▪ Particle Overlapping: -0.09×10^{-3} (mm)
Objectives	▪ Satisfy **the feasible range of T_{ignit} identified in continuum level MESMs design task** with consideration of uncertainty in DPM model ▪ Identify feasible space of *x1~x4*
Analysis and simulation tool	▪ Microscale discrete particles (Al+Fe_2O_3) shock simulation implemented in Raven

In this section, the microscale level design task using the DPM model Raven shock simulation is clarified. Based on this task clarification, the next step is designing experiments, collecting analysis data, and building metamodels.

6.5.4. Design of Experiments, Simulation Results, Regression model, and Prediction Interval for Microscale Level MESMs Design Task

In this section, we discuss a procedure for obtaining a metamodel and prediction interval in order to empirically estimate the response, weighted average hot-spot temperature at the first reaction initiation. This procedure is similar to that discussed in Section 5.4 and 5.5.

Since the design variables and spaces of this design task are the same as those of the design task discussed in Section 5.4.1. The DOE in this design task is exactly same as the DOE in the design task in Section 5.4.1. Based on the designed experimental points, 360 simulation data points are collected using the simulation infrastructure discussed in Section 5.4.2. A new post-processing code is developed in order to retrieve the response from a raw database of simulation results. The simulation data include about 15 replicates at each experimental point**.** We cannot collect the responses from all performed simulations since the response is obtainable only when a shock induced reaction is initiated; such a reaction is not initiated in some of the simulations.

The next step is building a metamodel and prediction interval using the exact same procedure described in Figure 3.7 with different response data. First, it is necessary to check if we need to transform the raw response data. As shown in Figure 6.17, the normal probability plot (a) is skewed. However, the plot (b) is balanced after the transformation. The function employed in this transformation is

$$y^{tr} = 1/(y+2)^3 \tag{6.4}$$

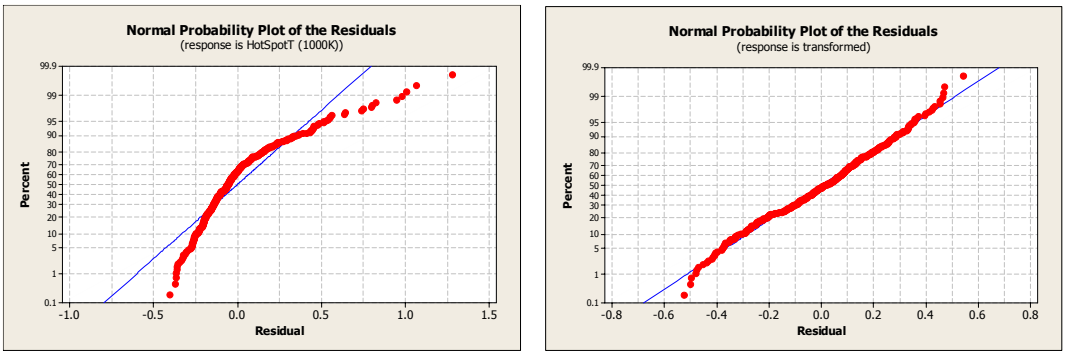

(a) (b)

Figure 6.17 Normal probability plots of the residuals: (a) Raw data, (b) Transformed data

With the transformed data, we develop regression models. A quadratic response surface model is also employed as the mean response model and an exponential function powered by a quadratic response surface model is employed as the conditional variance model. As discussed, the mean response model is

$$y^{tr} = \mathbf{x} \cdot \boldsymbol{\beta}' \tag{6.5}$$

where $\mathbf{x} = [1, x_1, x_2, x_3, x_4, x_1^2, x_2^2, x_3^2, x_4^2, x_1x_2, x_1x_3, x_1x_4, x_2x_3, x_2x_4, x_3x_4]$ and

$\boldsymbol{\beta} = [\beta_0, \beta_1, \beta_2, \beta_3, \beta_4, \beta_{11}, \beta_{22}, \beta_{33}, \beta_{44}, \beta_{12}, \beta_{13}, \beta_{14}, \beta_{23}, \beta_{24}, \beta_{34}]$.

The conditional variance model is

$$\sigma^2 \cdot v^2(\mathbf{x}, \boldsymbol{\beta}, \boldsymbol{\theta}) = \exp(\mathbf{x} \cdot \boldsymbol{\theta}') \tag{6.6}$$

where, $\boldsymbol{\theta} = [\theta_0, \theta_1, \theta_2, \theta_3, \theta_4, \theta_1^2, \theta_2^2, \theta_3^2, \theta_4^2, \theta_{11}, \theta_{22}, \theta_{33}, \theta_{44}, \theta_{12}, \theta_{13}, \theta_{14}, \theta_{23}, \theta_{24}, \theta_{34}]$.

The variances of the random errors in the response are not constant in the design space (i.e., heteroscadastic) in this case, either. Therefore, the integrated metamodeling and prediction interval approach discussed in Section 3.7 is required for this problem. The maximum log likelihood estimator in Eq. (3.5) is used for estimating the regression parameters, $\boldsymbol{\beta}$ and $\boldsymbol{\theta}$.

After four iterations, $\hat{\boldsymbol{\beta}}_{converged}$ and $\hat{\boldsymbol{\theta}}_{converged}$ are obtained as shown in Table 6.5.

Table 6.5 Converged regression parameters for the mean response model and the conditional variance model

Subscripts	$\hat{\boldsymbol{\beta}}_{init}$	$\hat{\boldsymbol{\beta}}_{converged}$	$\hat{\boldsymbol{\theta}}_{converged}$
0	0.06058	0.057632	-12.886
1	-1.9166	1.0566	98.022
2	-40.652	-41.796	1987
3	-0.28531	-0.28438	34.052
4	-39.322	-33.785	59.154
11	1561.6	986.21	5.0938
22	28269	29929	2.9957
33	2.0132	1.9563	-231.05
44	13860	13711	3.6701
12	1860.9	2270	4.9126
13	-67.951	-74.761	60.629
14	4134.4	1351.5	3.8467
23	-80.364	-55.384	101.99
24	14434	10091	4.6436
34	195.05	195.5	-30.84

After transforming back to the original coordinates, the estimated mean response model (y_{mean}) and the upper and lower bound of the prediction interval (y_{upper} and y_{lower}) are

$$y_{mean} = \left(\hat{\boldsymbol{\beta}}_{converged} \cdot \mathbf{x}'\right)^{-1/3} - 2$$

$$y_{upper} = \left\{\hat{\boldsymbol{\beta}}_{converged} \cdot \mathbf{x}' - t_{N-P,1-\alpha/2} \cdot \exp\left(\frac{\hat{\boldsymbol{\beta}}_{converged} \cdot \mathbf{x}'}{2}\right)\right\}^{-1/3} - 2 \tag{6.7}$$

$$y_{lower} = \left\{\hat{\boldsymbol{\beta}}_{converged} \cdot \mathbf{x}' + t_{N-P,1-\alpha/2} \cdot \exp\left(\frac{\hat{\boldsymbol{\beta}}_{converged} \cdot \mathbf{x}'}{2}\right)\right\}^{-1/3} - 2$$

where the number of samples (*N*) is 360, the total number of predictors (*P*) is 30, and the confidence level (1-α) is 0.99. The estimated models are illustrated in Figure 6.18.

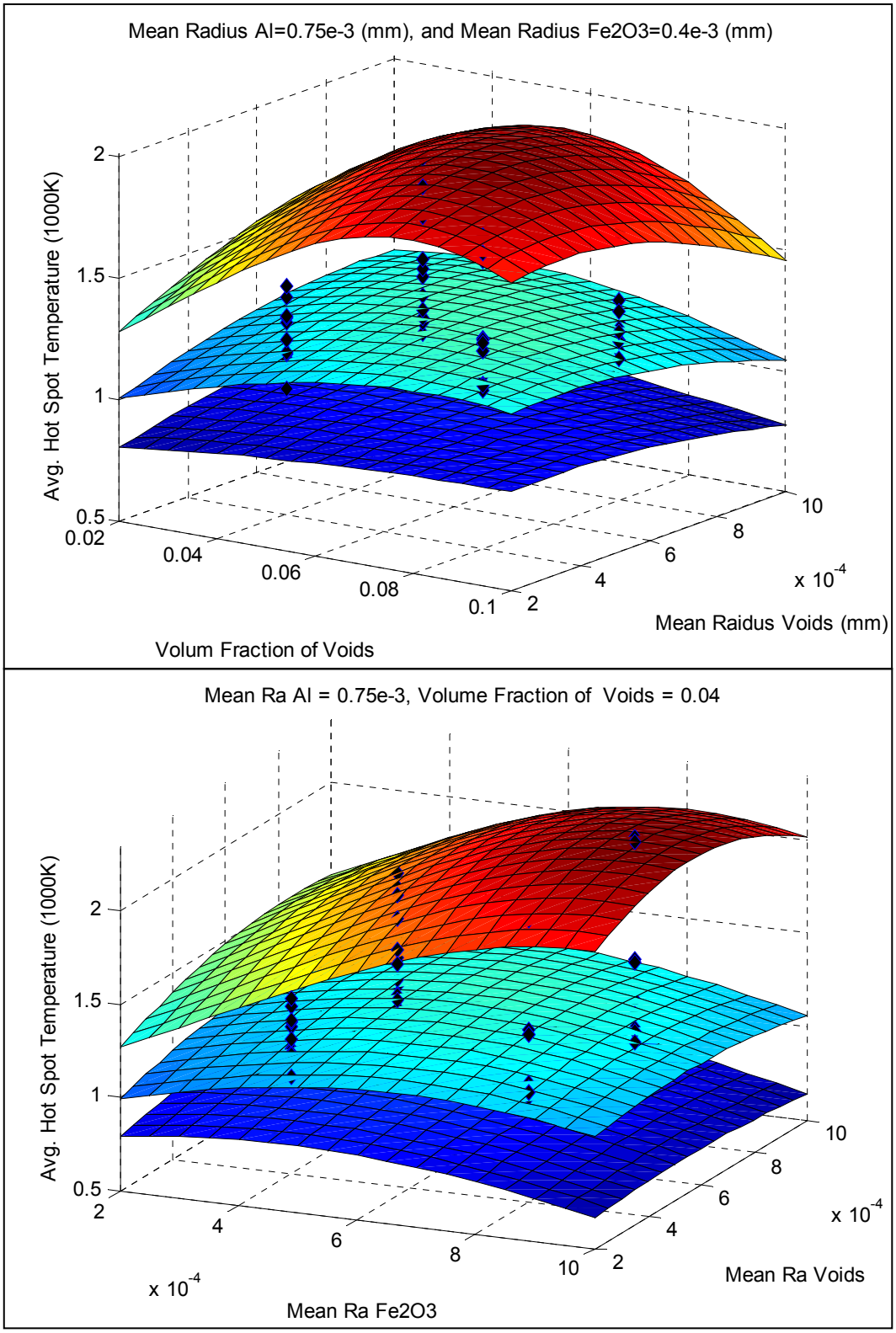

Figure 6.18 Estimated mean response model and upper/lower bounds of the prediction interval

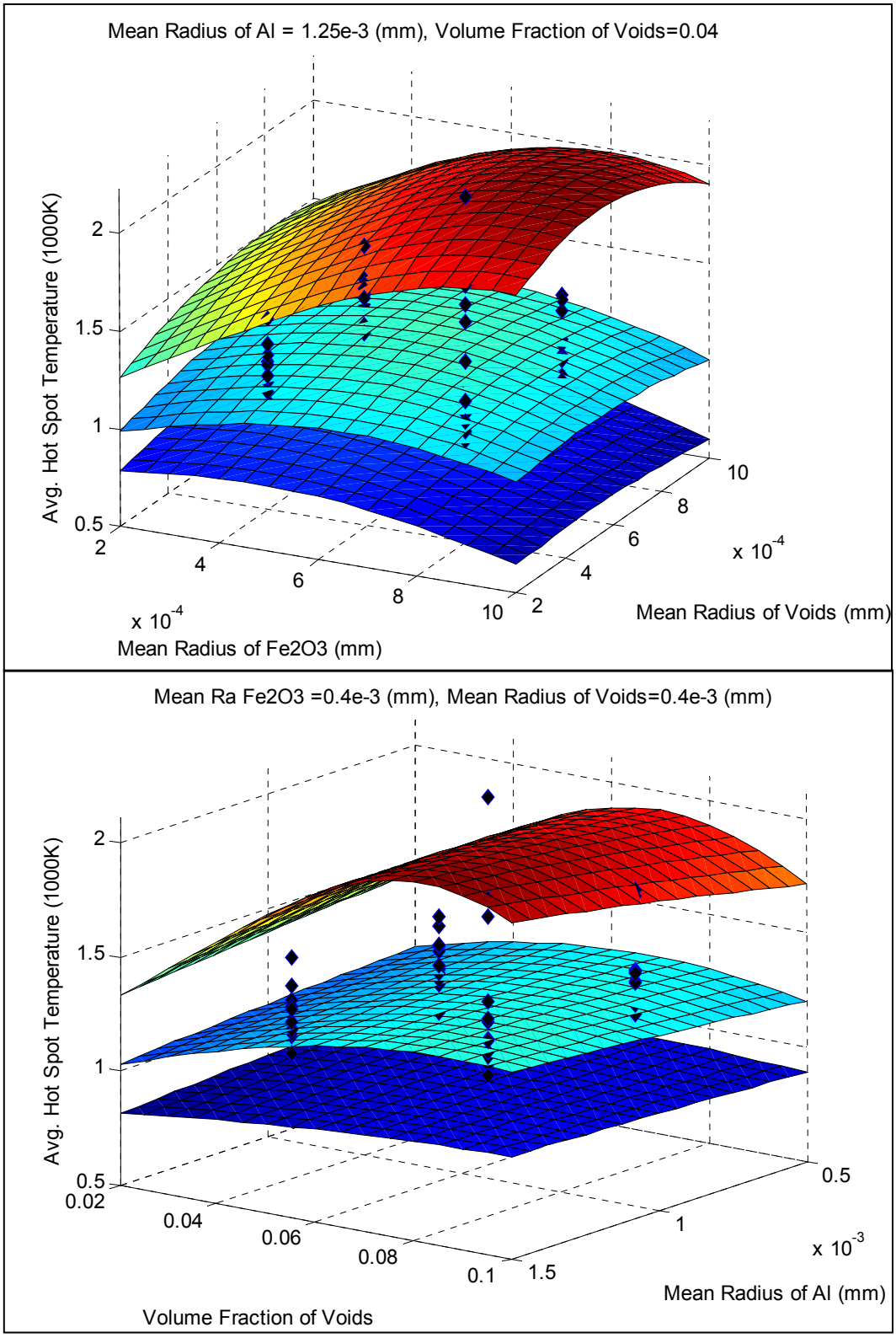

Figure 6.18 is continued

Now, the metamodel and the prediction interval are obtained based on DOE and simulation data quantifying unparameterizable variability. Now, designers may use the metamodels in Eq. (6.7) instead of directly using the computationally intensive Raven shock simulation for estimating mean and variation of T_{ignit} at a given point.

The next step is to calculate the maximum and minimum responses at a point due to the variations in design variables with consideration of the unparameterizable variability. These responses are calculated based on Eq. (3.16). Therefore, the maximum minimum responses at a point ($\mathbf{x}$) in the design space are:

$$y_{\text{minimum}} = \text{Min}\left\{\left(y_{mean}(\mathbf{x}) - \sum_{i=1}^{4}\left|\frac{\partial y_{mean}}{\partial x_i}\right|\cdot\Delta x_i\right), \left(y_{upper}(\mathbf{x}) - \sum_{i=1}^{4}\left|\frac{\partial y_{upper}}{\partial x_i}\right|\cdot\Delta x_i\right), \left(y_{lower}(\mathbf{x}) - \sum_{i=1}^{4}\left|\frac{\partial y_{lower}}{\partial x_i}\right|\cdot\Delta x_i\right)\right\} \quad (6.8)$$

$$y_{\text{maximum}} = \text{Max}\left\{\left(y_{mean}(\mathbf{x}) + \sum_{i=1}^{4}\left|\frac{\partial y_{mean}}{\partial x_i}\right|\cdot\Delta x_i\right), \left(y_{upper}(\mathbf{x}) + \sum_{i=1}^{4}\left|\frac{\partial y_{upper}}{\partial x_i}\right|\cdot\Delta x_i\right), \left(y_{lower}(\mathbf{x}) + \sum_{i=1}^{4}\left|\frac{\partial y_{lower}}{\partial x_i}\right|\cdot\Delta x_i\right)\right\}$$

In this section, the metamodel and prediction intervals are formulated based on the integrated estimation technique. Based on the obtained metamodels, mean, maximum, and minimum performances at a given point are achieved considering variations in design variables (*x1~x4*) and unparameterizable variability due to the random microstructure changes.

Now, all multiscale models (the response surface model for NTM model and the generalized linear model and prediction interval for DPM model) are ready for providing mean, maximum, and minimum performances at a given input point with tolerance. In the next section, we explore a given design space for achieving feasible design space in an inductive (top-down) manner.

6.5.5. Inductive Feasible Solution Space Search for Designing Robust MESM under Uncertainty

In this section, we search for feasible solution spaces using the IDEM discussed in Section 4.5. The resolution of discrete seeds in interdependent variables (T_{ignit}) is set to 10 K and the resolutions of discrete seeds in design variables ($x1$~$x3$) are set to the value of variation. For more accurate results, the designer may discretize into finer seeds in design spaces. When the minimum required HD-EMI at the continuum level is one, the feasible region of Tignit and x3 found by DCE is shown in Figure 6.19.

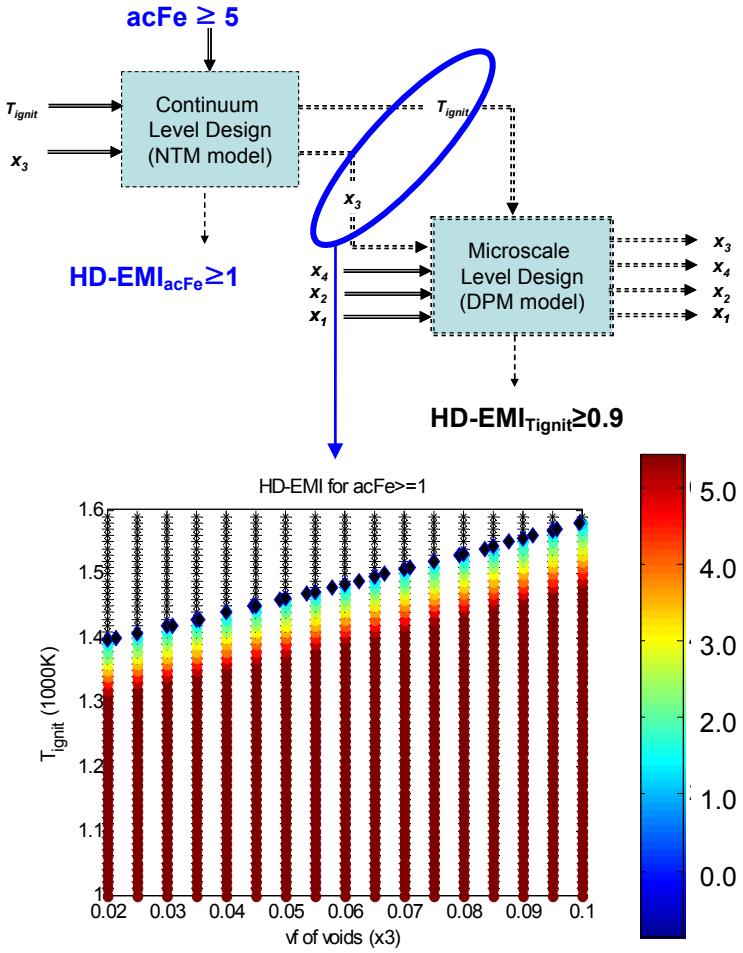

Figure 6.19 Obtained feasible range in T_{ignit} and $x3$ space using DCE.

In Figure 6.19, the exact boundary points (diamond points) are also found and HD-EMIs are indicated as a color map. Comparing the figure with the contour plot of the response surface model in Figure 6.16, the trend accurately matches. However, the boundary points in Figure 6.19 are more conservative (i.e., estimating smaller area) than the boundary (*acFe*=5) of the contour plot, since we consider response deviation due to the variation in *x3*. Based on the obtained feasible space (i.e., discrete feasible points) of T_{ignit} and *x3,* we identify the feasible space of design variables (*x1~x4*).

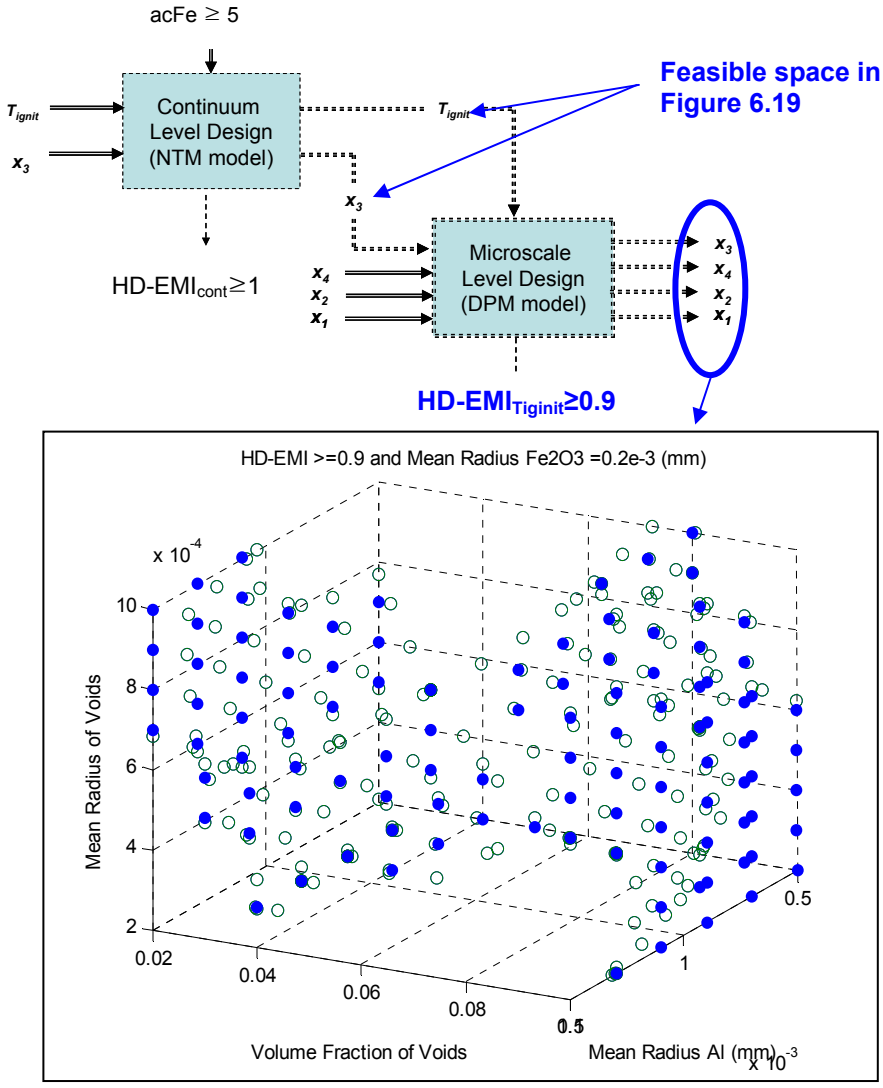

Figure 6.20 Feasible discrete points in x1, x3, and x4 space (x2=0.0002mm)

The discrete feasible points are illustrated as filled circles and the boundary points as void circles. The feasible discrete points and boundary points are illustrated in Figure 6.20; the space is depicted at *x2* (mean radius of Fe_2O_3) = 0.0002 (mm). From the boundary points and feasible points, we may estimate the approximate feasible space. All feasible points satisfying HD-EMI$_{Tignit}$ ≥0.9 are listed in Table A.2. By increasing required minimum HD-EMI, the smaller feasible region can be obtained. As shown in Figure 6.21, the number of feasible points decreases as the required HD-EMI of T_{ignit} increases, leaving only the more reliable (i.e., higher HD-EMI) design solutions.

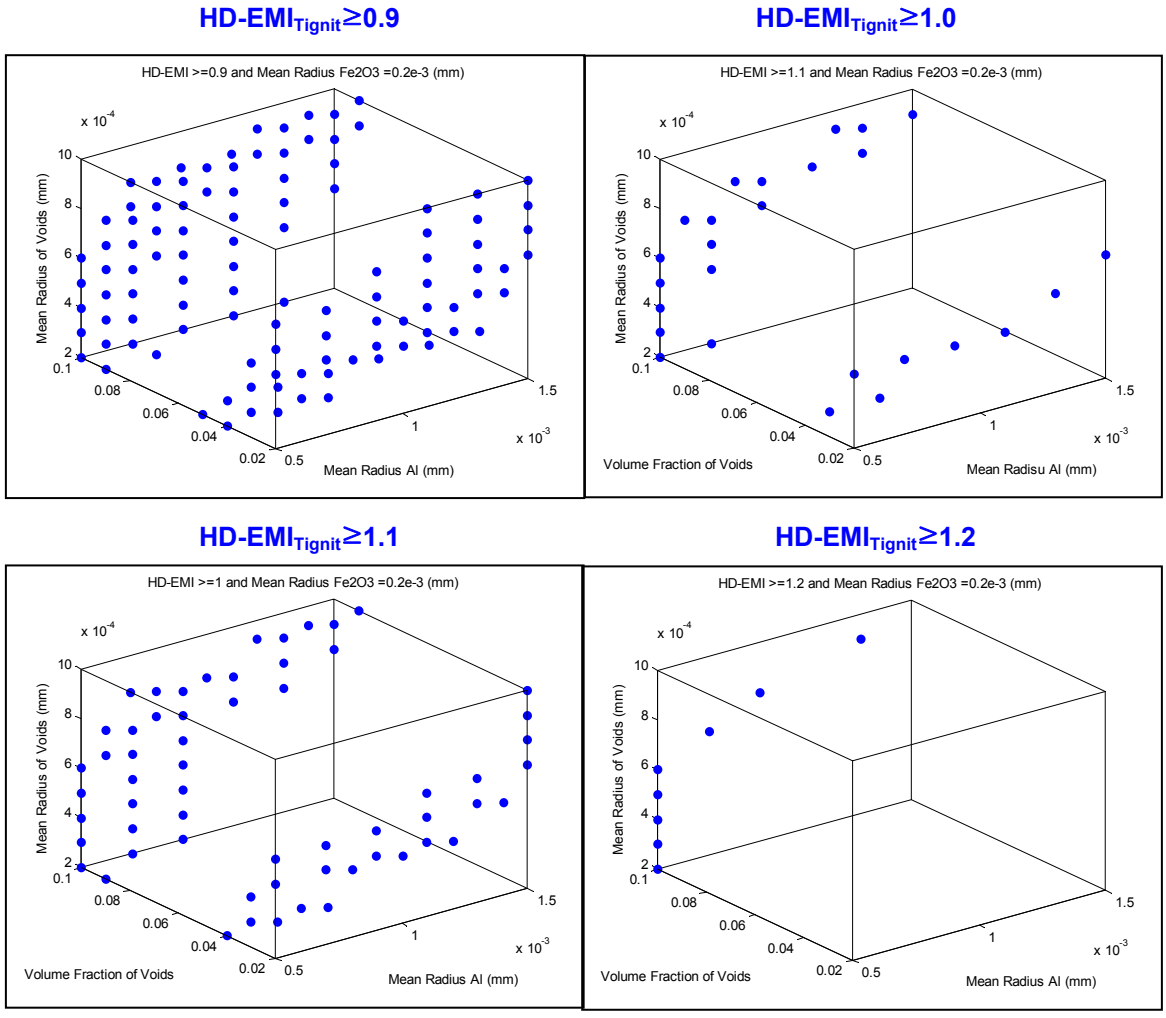

Figure 6.21 Reduced feasible region by increasing the required minimum HD-EMI for T_{ignit}

The reduced feasible points that satisfy HD-EMI$_{Tignit}$ ≥1.2 are listed in Table 6.6. As discussed in Section 4.7.3, higher HD-EMIs indicate better robustness against uncertainties in a model and variation in design variables. From the table, higher HD-EMIs (i.e., larger than 1.2) are achieved when mean radius of Fe_2O_3 is 0.0002 (mm) and volume fraction of voids is 0.1. Therefore, we may estimate robust (flat) region and smaller upper and lower variability limits at these values.

Table 6.6 Feasible discrete points at HD-EMI $_{acFe}$ ≥ 1, HD-EMI $_{Tignit}$ ≥ 1.2

Mean Radius of Al (x1) (mm)	Mean Radius of Fe_2O_3 (x2) (mm)	Volume Fraction of Voids (x3)	Mean Radius of Voids (x4) (mm)	HD-EMI$_{Tignit}$
0.0005	0.0002	0.1	0.0002	1.23
0.0005	0.0002	0.1	0.0003	1.20
0.0005	0.0002	0.1	0.0004	1.20
0.0005	0.0002	0.1	0.0005	1.22
0.0005	**0.0002**	**0.1**	**0.0006**	**1.27**
0.0007	0.0002	0.1	0.0007	1.23
0.0009	0.0002	0.1	0.0008	1.24
0.0013	0.0002	0.1	0.0009	1.23

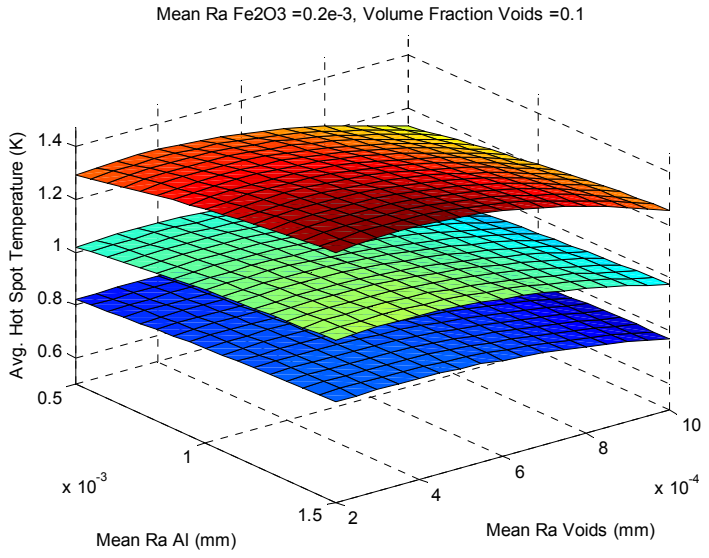

Figure 6.22 Plots of mean response functions and upper/lower limit functions at x2=00002 and x3=0.1

This estimation is validated by the plots of mean response function and upper/lower limit functions in Figure 6.22. Compared with the plots in Figure 6.18, the plots in this figure

are relatively flat and the intervals between upper and lower limit functions are also relatively small through out the entire space of *x1* and *x4*.

In order to validate the utility of the IDEM, the robust solution obtained in this section and the optimal solution based on the mathematical construct shown in the following table are compared. As shown in Table 6.7, the mathematical models for the optimization are the response surface model of the continuum NTM model obtained in Section 6.5.2 and the mean response function of the microscale DPM model in Section 6.5.4.

Table 6.7 The mathematical form for an optimization based on the obtained metamodels of the NTM model and DPM model

Given

$$acFe = 1.73 - 267 \cdot x_3 + 66.6 \cdot T_{ignit} + 237.5 \cdot x_3^2 - 46.5 \cdot T_{ignit}^2 + 284 \cdot x_3 T_{ignit}$$

where $T_{ignit} = \left(\hat{\boldsymbol{\beta}}_{converged} \cdot \mathbf{x}'\right)^{-1/3} - 2$ (see Table 6.5 for $\hat{\boldsymbol{\beta}}_{converged}$)

Find

$$\mathbf{x} = \{x_1, x_2, x_3, x_4\}$$

Satisfy

$$0.0005 \le x_1 \le 0.0015,\ 0.0002 \le x_2 \le 0.001,$$
$$0.02 \le x_3 \le 0.1, \text{ and } 0.0002 \le x_4 \le 0.001$$

Maximize

Z= acFe

In this optimization process, Type I~IV robust design concepts are not employed. The exploration results of optimization with only the mean models and those of the IDEM obtained in this section are compared. The obtained results are totally different from each other as listed in Table 6.8. The optimal solution finds the largest mean radii of Al and Fe_2O_3 particles within the design space. The solutions for the volume fraction of voids and mean radius of voids are on the lower bound of the design space.

Table 6.8 A comparison of the design solutions using optimization and the IDEM

Methods	*x1* (mm)	*x2* (mm)	*x3*	*x4* (mm)	Estimated T_{ignit} Minimum Mean Maximum	Estimated *acFe* Minimum Mean Maximum
Optimal solution with mean models	0.0015	0.001	0.02	0.0002	540.4 884.9 1596	-9.8 23.86 24.16
Type I~IV Robust solution using IDEM	0.0005	0.0002	0.1	0.0006	744.2 1002 1466	10.8 21.17 21.5

The estimated mean of T_{ignit} at the optimal solution is 884.9 K and the final response, estimated *acFe,* is 23.86, which is the highest estimated *acFe* in the design space. However, the lower and upper deviations of the estimated T_{ignit} are very large at the optimal solution. Specifically, the upper limit of the estimated T_{ignit} range is 1596 K, which is a very high temperature. This large variability of the estimated T_{ignit} is propagated through the continuum NTM model and expanded into the much larger variability range of the estimated *acFe,* which is -9.8 as minimum and 24.16 as maximum. This means there is much less chance of chemical reaction initiation since the negative *acFe* means no chemical reaction at all. In the optimization process, the possibility of the large performance deviation cannot be expected since the propagated uncertainty is not considered while exploring the design space.

On the other hand, performance deviations at the best solution points obtained by the IDEM are smaller than those at the optimal solution. Specifically, the estimated lower limit (10.8) of *acFe* is much higher than that at the optimal solution and satisfies the lower requirement limits (acFe≥5). The mean *acFe* (21.17) at the IDEM solution is lower than that (23.86) at the optimal solution; however, the performance at the IDEM solution is still good enough since the difference between them is only about 2.7.

6.6. STRATEGIC DECISION-MAKING UNDER UNQUANTIFIABLE UNCERTAINTY IN SIMULATION MODELS

In Section 4.8, we discuss the strategic decision-making in order to get the most reliable solution against the model structure uncertainties in the DPM model and NTM model. In the previous section, we set HD-EMI $_{acFe} \geq 1$ and increase the HD-EMI$_{Tignit}$ as much as possible. The best solution obtained is 0.0005, 0.0002, 0.1, and 0.0006 for *x1, x2, x3* and *x4*, respectively as listed in Table 6.8. The best solution is selected by searching the highest HD-EMI$_{Tignit}$ among the feasible solutions obtained by setting all required HD-EMIs to 1. This means we searched for the best solution that is the most reliable against model structure uncertainty in the microscale DPM model.

In this section, we set HD-EMI$_{Tignit} \geq 1$ and increase HD-EMI $_{acFe}$ as much as possible. First, we set HD-EMI$_{acFe} \geq 5$ remaining the required HD-EMI for T_{ignit} as 1. The obtained feasible solutions are listed in Table 6.9.

Table 6.9 Feasible discrete points at HD-EMI of *acFe* ≥ 5, HD-EMI of $T_{ignit} \geq 1$

Mean Radius of Al (x1) (mm)	Mean Radius of Fe_2O_3 (x2) (mm)	Volume Fraction of Voids (x3)	Mean Radius of Voids (x4) (mm)	HD-EMI_T_{ignit}
0.0005	0.0002	0.1	0.0002	1.009
0.0005	0.0002	0.1	0.0005	1.005
0.0005	0.0002	0.1	0.0006	1.048
0.0007	0.0002	0.1	0.0007	1.017
0.0009	0.0002	0.1	0.0008	1.023
0.0013	0.0002	0.1	0.0009	1.014

All feasible solution points listed in this table is also listed in Table 6.6. This means the robust feasible solution sets to the model structure uncertainty in the continuum NTM model are also robust to the model structure uncertainty in the microscale DPM model. Further increasing the required HD-EMI for *acFe* up to 6.05, we obtain the best solution

(i.e., the most reliable solution under the potential uncertainty in the continuum NTM model) that is same to the solution obtained by increasing the HD-EMI for $T_{ignit.}$

The reason why the best solutions of the two different scenarios are identical is that the response behavior of the NTM model is not sufficiently nonlinear to produce a different shape of constraints boundary when increasing the required HD-EMI for *acFe*. As shown in Figure 6.23, the boundary shape of the feasible space is very similar to the one shown in Figure 6.19. For this reason, the rank of the highest HD-EMIs for T_{ignit} of feasible solutions is not altered by increasing the required HD-EMI for *acFe*. In other words, the solution with the highest HD-EMI is the same for the two scenarios.

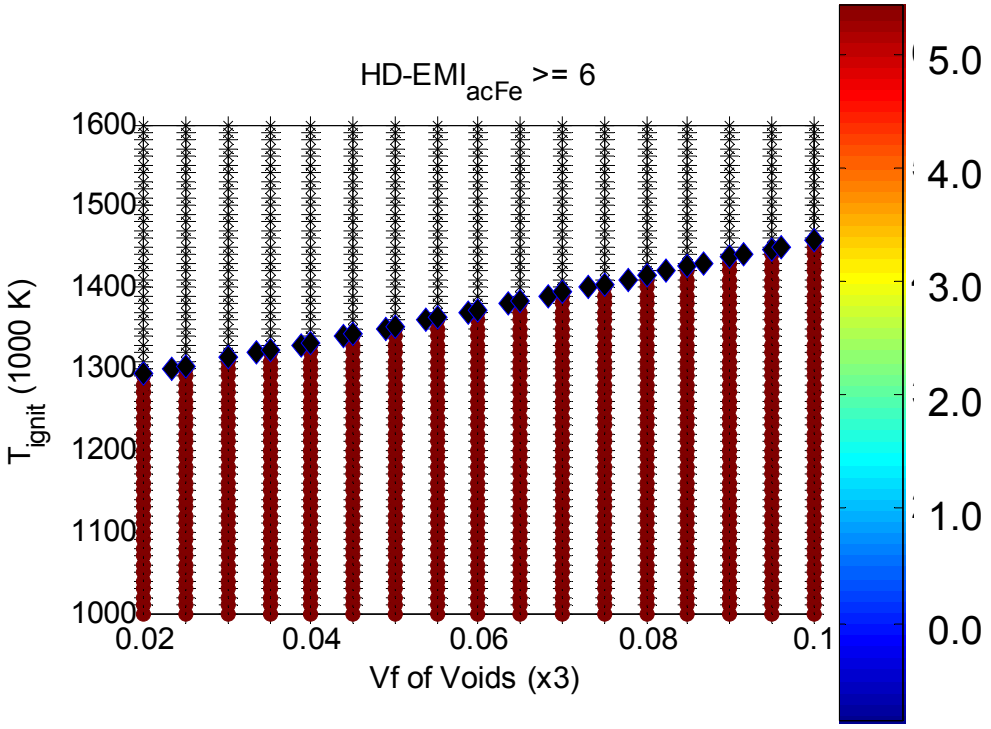

Figure 6.23 Obtained feasible range when the required HD-EMI for *acFe* is 6

In this section, the best MESM design solution among the feasible solutions is identified taking into account the model structure uncertainty (potential uncertainty) in multiscale models. We suggest this strategic selection should be performed among only

the robust feasible design solution sets that satisfy all the required HD-EMIs (mostly, HD-EMIs = 1). The reason is that the HD-EMI is the index of robustness based on quantified uncertainty and the first priority of a robust design should be achieving robustness against the quantified uncertainty. **Only when the robustness against quantified uncertainty is fully satisfied and designers still have design freedom (multiple feasible solution sets), should this strategic selection be performed for achieving robustness against model structure uncertainty.** In the next section, the design example results discussed are summarized and the utility of the IDEM is clarified validating the hypotheses discussed in Section 1.4.3.

6.7. EMPIRICAL PERFORMANCE VALIDATION

In this section, the empirical performance validity of the IDEM is checked. As shown in the validation square roadmap, Hypotheses 3 and 4 are validated by checking the utility of the IDEM based on the results obtained from the multiscale simulation-based robust MESMs design example.

Hypothesis 3: *A graphical robust design process model associated with Error Margin Indices is an effective protocol for designers to identify a complex robust design process chain.*

Hypothesis 4: *The Inductive Design Exploration Method for Type IV robust design provides an effective mean to find robust multiple ranged sets of design specifications in an inductive manner in a distributed, multidisciplinary systems design problem.*

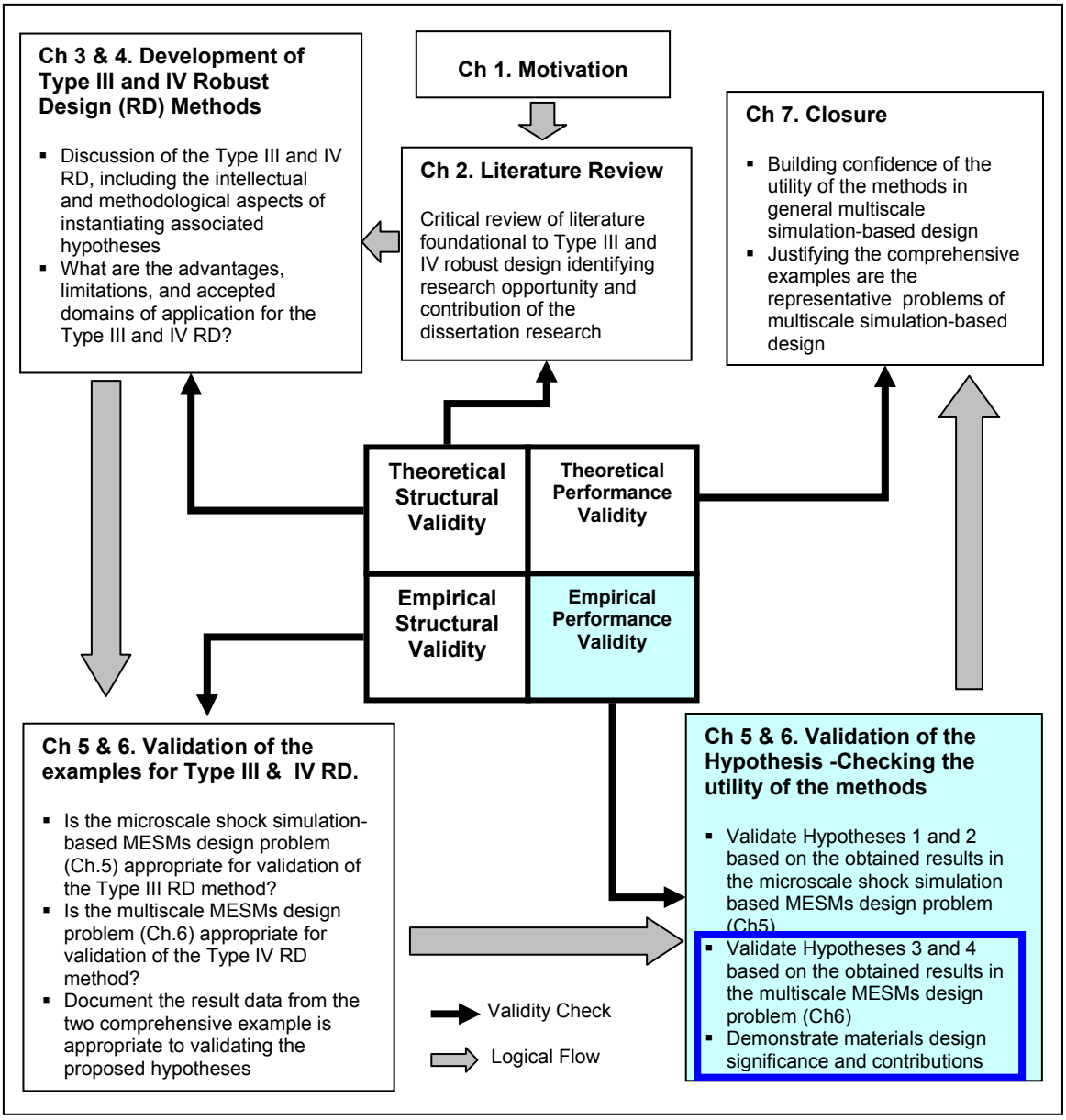

Figure 6.24 Validation square roadmap

For validating the utility of the IDEM, we discuss the results of the tasks planned in Section 6.2.3 as follows.

Task 1: *Demonstrate GRDPM represents robust design process better than other process representation protocols.*

Result 1: In Figure 6.12, the multiscale MESMs design process is described using the GRDPM. In the figure, the uncertainties associated with the design task are explicitly

represented conveying their types. Comparing the IDEF0 model, the information flows of the decision process are efficiently represented in the GRDPM. The information of the design variables flows from the left to the right along the design process, and the information of the corresponding performance from the top to the bottom of the boxes. Since the ranged and discrete value of a parameter are described as double or single lines, respectively, we may easily estimate if the design results still have design freedom for more adjustment or not. Moreover, the decision criteria (the HD-EMIs in the IDEM) are depicted in the model so that the reliability of the decision in the tasks under uncertainty can be easily identified by designers. These results support Hypothesis 3.

Task 2*: Identify ranged sets of design specifications instead of a point solution range given ranged performance requirement.*

Result 2: As shown in Figure 6.20 and Figure 6.21, designers may find multiple ranged sets of robust feasible solutions instead of a single robust or optimal solution employing the IDEM. The feasible region is represented accurately by finding the exact boundary points in between discrete feasible and infeasible points based on root finding methods as illustrated in Figure 6.20. Since all discrete points in the input spaces are evaluated separately using the DCE technique, any types of feasible region (such as isolated multiple feasible region) may be obtained by the IDEM. As shown in Figure 6.21, designers may expand or reduce the feasible region by reducing or increasing the required HD-EMIs, respectively. This capability is the uniqueness of the IDEM that cannot be found in other design exploration methods, such as RCEM, optimization, RCEM-EMI, robust optimization, Taguchi methods, etc. In the RCEM, the range of a design solution is limited to only the range of deviations (i.e., tolerance) in design

variables. In addition, designers may find feasible solution ranges in all intermediate spaces in the series of sequential or parallel design process as shown in Figure 6.19 and Figure 6.20. This capability is essential for finding robust design solutions based on a multidisciplinary, complex, coupled simulations and analyses processes. If one of the simulation and analysis models in the complex process is updated, then designers should explore all design and interdependent variable spaces in order to find new solutions based on the updated models. However, using the IDEM, designers need to explore only the input space corresponding to the modified model. These results support Hypothesis 4 in this dissertation.

Task 3*: Identify robust ranged sets of solution for propagated uncertainty in the multiscale MESMs simulation and analysis chain.*

Result 3: As discussed in Chapter 1, Type IV robust design is to design an insensitive system to the propagated uncertainty in a simulation or analysis chain. As shown in Section 6.2.2, the multiscale MESMs design problem incorporates with two different scales of simulation models. In Figure 6.9, the uncertainty propagation though the DPM model and NTM model chain is illustrated. Based on the IDEM, ranged sets of robust design solutions are obtained as shown in Figure 6.20 and Figure 6.21. Those solutions are achieved taking the propagated uncertainty into account in a top-down (inductive) manner. One of the robust solution sets obtained based on the IDEM is compared with an optimal solution identified based on the traditional optimization process illustrated in Table 6.7. Those two solutions and the corresponding performance ranges are listed in Table 6.8. The performance (*acFe*) deviation at the IDEM solution point is even smaller than that at the optimal solution while the mean of the performance distribution is

maintained as reasonably good. Therefore, we predict that the tailored MESM as the IDEM solution point should robustly reacts in the presence of the accumulated uncertainty through the multiscale simulation and analysis chain. This multiscale robust MESM design result supports for answering Research Question 4 and Hypothesis 4 (Type IV robust design).

Task 4*: Identify a robust solution considering model structure uncertainty in the microscale DPM model and/or in the continuum NTM model.*

Result 4: In Section 6.6, we present a strategic selection technique that is robust to model structure uncertainty in simulation and analysis models. The most promising solution sets that are robust to the model structure uncertainty in the microscale DPM model are listed in Table 6.6. These solutions are identified among the feasible solution sets satisfying all the required HD-EMIs (HD-EMIs $\geq$ 1). In Table 6.9, the identified robust solution sets are listed with the same procedure above with emphasis on the model structure uncertainty in the continuum NTM model. As shown in the two tables, the robust solution sets are almost identical and the best solution among them is the same value. This means, in this example, that the robust solution against the model structure uncertainty of the microscale DPM model is also robust to that of the continuum NTM model. The reason for an identical robust solution for the two different scenarios is discussed in Section 6.6.

As discussed in this section, the IDEM is successfully validated, checking the empirical performance validity in the Validation Square. In the next section, the discussion of this chapter is summarized.

6.8. SYNOPSIS OF CHAPTER 6

In this chapter, the Graphical Robust Design Process Model (GRDPM) and the Inductive Design Exploration Method (IDEM) are tested on the multiscale simulation-based Multifunctional Energetic Structural Materials (MESMs) design example. This test validates Hypotheses 3 and 4. The multiscale simulation models employed for the MESMs design are the continuum level Non-equilibrium Thermodynamic Mixture Model (NTM model) and the microscale Discrete Particle Mixture Model (DPM model).

In Section 6.1, the NTM model and DPM model are introduced. The NTM model is a one dimensional continuum analysis code that predicts the amount of chemical reaction considering various fluxes in its constitutive model. The DPM model is the same model employed in Chapter 5, but it produces a different response. The output of DPM model is defined to be logically interfaced to one of the inputs of NTM model in Section 6.1.3. In Section 6.2, the multiscale MESMs design problem is formulated defining information flow in the simulation chain of the NTM model and DPM model. Uncertainty propagation through these two models is illustrated in Figure 6.9 validating that this example is appropriate for demonstrating the IDEM.

In Section 6.3, the multiscale simulation chain and MESMs design process are described using the Graphical Robust Design Process Model (GRDPM) discussed in Chapter 4. The IDEF0 and GRDPM of the multiscale MESMs design process are compared with each other highlighting the advantages of GRDPM in representing uncertainty associated with the design process.

In Section 6.4, the overall procedure of the IDEM for this example is discussed. In each design task of the inductive (top-down) design process, there is a generalized design

procedure similar to the RCEM-EMI construct discussed in Section 3.4. Therefore, the IDEM includes part of the RCEM-EMI construct. The IDEM for the multiscale MESMs design is described in detail in Section 6.5. This procedure includes clarification of design task, DOE, simulation runs, and metamodel creation at each level of tasks. After the tasks at each level are done, inductive search algorithm is performed in order to identify the feasible ranged sets of robust design specification. The multiscale MESM design results identified by the IDEM are illustrated and listed in Section 6.5.5.

In Section 6.6, the best solution among the multiple feasible solutions is identified by controlling the HD-EMIs. A more reliable solution is obtained by increasing the HD-EMI of which simulation model includes higher degree of Model Structure Uncertainty. In Section 6.7, Hypotheses 3 and 4 are validated by checking the utility of the IDEM in the multiscale robust MESMs design problem.

CHAPTER 7

CLOSURE

The principal goal in this dissertation is to address Type III and IV robust design paradigm and establish methods for identifying robust, multifunctional materials design based on a multiscale non-deterministic analysis and simulation chain.

The motivation for establishing the methods, the details of the methods themselves, and the results obtained by applying it to multiscale Multifunctional Energetic Structural Materials (MESMs) design problems are summarized in Section 7.1. In Section 7.2, the research questions and hypotheses posed in Chapter 1 are revisited and critically evaluated with a special emphasis on the validity of the research hypotheses beyond the example problems described in this dissertation. Based on the summary and critical review, the achievements and research contributions reported in this dissertation are presented in Section 7.4, followed in Section 7.5 by opportunities for future work.

7.1. A SUMMARY OF THIS DISSERTATION

One of the important factors to be considered in designing an engineering system is uncertainty, which emanates from natural randomness, limited data, or limited knowledge of systems. In this study, a new robust design methodology is established in order to design multifunctional materials by employing multi-time and length scale analyses as shown in Figure 7.1. The method involves the integration of robust design techniques,

design of experiments, multiscale material simulations, metamodeling, uncertainty analysis and estimation, multiobjective decision-making and collaborative, distributed design.

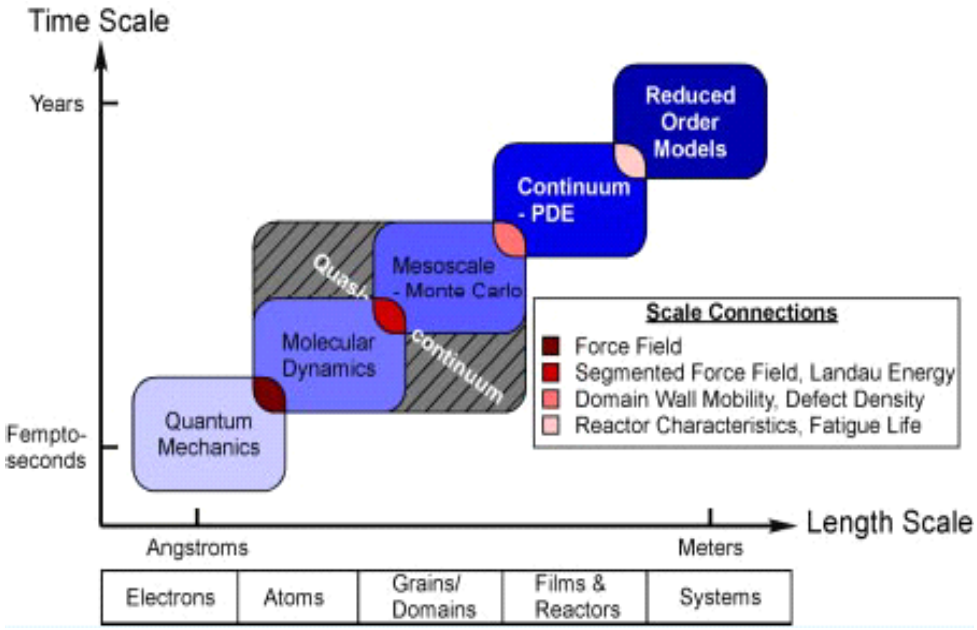

Figure 7.1 Hierarchical Materials Design

The Robust Concept Exploration Method with Error Margin Index (RCEM-EMI) is proposed for decision-making with consideration of non-deterministic system behavior. Following the steps in the RCEM-EMI, a designer may search for a solution that is robust to the uncertainty embedded in a system as well as to the uncertainty in system parameters. The Inductive Design Exploration Method (IDEM) is proposed to facilitate distributed, robust decision-making under propagated uncertainty in a series of analyses or simulations. In the IDEM, the propagated uncertainty is mitigated by passing ranged sets of robust design specifications in a top-down manner.

These methods are verified in the context of 'Design of Multifunctional Energetic Structural Materials (MESMs)'. The MESMs are being developed to replace the large

amount of steel reinforcement in a missile penetrator with a material that has light weight, high energy release, and structural integrity with appropriate reinforcements. In this example, the methods facilitate following state-of-the-art design capabilities, designing robust MESMs under (a) random microstructure changes and (b) propagated uncertainty in a multiscale analysis chain. The methods are established to facilitate effective and efficient materials design; however, they are generalized to be applicable to any complex engineering systems design that incorporates computationally intensive simulations or expensive experiments, non-deterministic models, accumulated uncertainty in multidisciplinary analyses, and distributed, collaborative decision-making.

7.1.1. Robust design of MESMs for non-deterministic random morphology variability in Reactive Powder Metal Mixtures (RPMMs)

The MESMs, composed of Reactive Powder Metal Mixtures (RPMMs), can deliver superior energetic performance, and are unique in that the components serve the dual purpose of providing both energetic fuel and structural integrity to a reactive system. The development of MESMs employs computational, experimental, and analytical tools to design MESMs from the nano-scale to macroscopic length scales and to compare their performance over parametric ranges of the Al and Fe_2O_3 mixture composition and phase morphology.

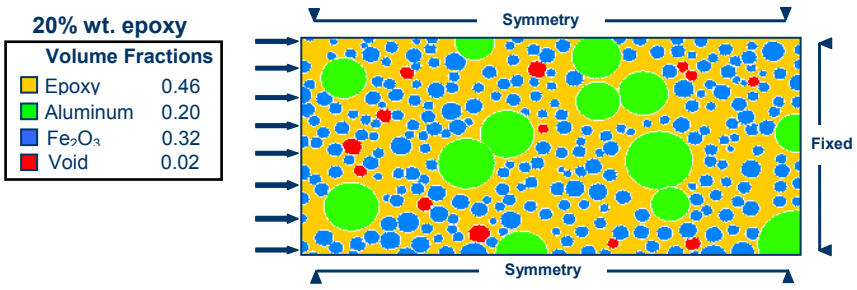

Figure 7.2 A statistical volume element of Al and Fe_2O_3 mixture

In Figure 7.2, a Statistical Volume Element (SVE) in a simulation for analyzing shock induced reaction initiation is illustrated. The components of the SVE include Fe_2O_3 and aluminum particles, epoxy binder, and voids. Each of these has a particle diameter mean, its variance and a volume fraction. However, during the simulation each instantiation of the SVE for purposes of analysis incorporates random assignment of particulate positions. Because of this randomness in the phase morphology, the system response has large random variability even with a fixed set of input parameters. It implies that the system has non-parametric variability that cannot be modeled numerically. This variability is defined as "unparameterizable variability". Unparameterizable variability usually exists in high fidelity analysis models at extremely small scale and results in uncertainty in the simulation or metamodels incorporated with design exploration. This may lead a designer to make a wrong decision. However, this problem cannot be solved by existing robust design methods since the methods focus on parametric variability in noise and control factors.

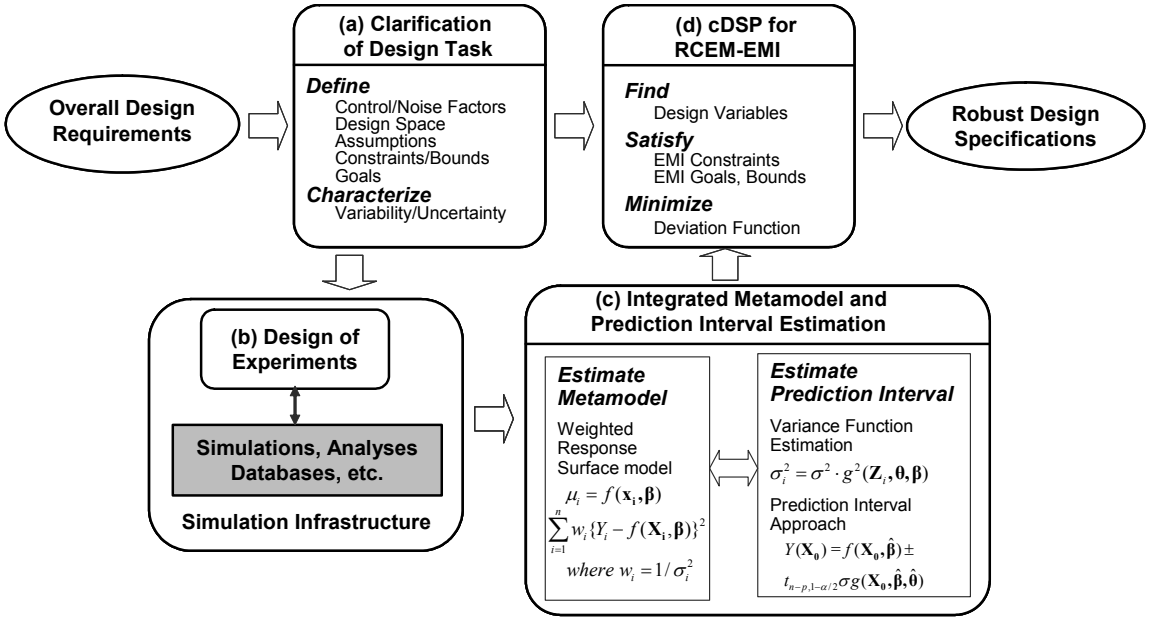

Figure 7.3 Procedure of the RCEM-EMI for robust design under model uncertainty

To consider unparameterizable variability as well as parametric variability in noise and control factors for robust decision making, we proposed a method, the Robust Concept Exploration Method with Error Margin Indices (RCEM-EMI), in which the Error Margin Index (EMI) is a mathematical construct that represents a metric of margin for stochastic variability in the model. A higher EMI allows more margins for the uncertainty in a model, which makes the designed system more reliable. The RCEM-EMI produces robust design specifications given overall design requirement as shown in Figure 7.3. The RCEM-EMI has four steps, which are (a) clarification of design task, (b) design of experiments (DOE) and simulation, (c) integrated metamodel and prediction interval estimation, and (d) compromise Decision Support Problem (cDSP) with EMI. At each evaluation point during the design exploration, an EMI is calculated based on the metamodel and upper/lower bounds around the model. By maximizing EMI in single objective problem or trading off among multiple EMIs in multi-objectives problem, designers can find the best robust solution against the two types of non-parametric and parametric uncertainty. The RCEM-EMI construct is developed and demonstrated on the MESMs design example.

7.1.2. MESMs design for robust reaction initiation against propagated uncertainty in series of multiscale analyses

The research is motivated by the interest in materials design that incorporates serialized (process-structure-property-performance) analyses in multiple time and length scales (from quantum to system scale). These analyses are mutually interfaced to estimate the dual functionality – energetic fuel and structural integrity - of MESMs by passing analysis results to other analyses as input parameters. A critical temperature that initiates chemical reaction in intermediate contact region between Fe_2O_3 and Al particles

are evaluated in order to analyze the energetic behavior of MESMs. The critical temperature for a chemical reaction initiation obtained at the microscale level discrete particle shock simulation of RPMMs is then passed to the continuum level non-equilibrium thermodynamic mixture model in order to estimate the portion of a specimen undergoing chemical reaction under a shock loading. The critical problem in this interfaced analyses chain is that uncertainty in the analysis and simulation is accumulated via the interdependent variables (i.e., the critical temperature for reaction initiation) and may result in a large error in the final response (the amount of chemical reaction).

In previous approaches, the accumulated uncertainty in a series of models has been estimated based on sequential uncertainty propagation. Those approaches required a considerable amount of sampling, and the sampling points should be decided sequentially while propagating variability. Furthermore, the uncertainty analyses and the design exploration (or optimization) processes are completely coupled so that a computing infrastructure for seamless (interoperable) integration between them is indispensable.

In this dissertation, the Inductive Design Exploration Method (IDEM) is proposed in order to overcome these challenges by using modular uncertainty analyses, finding robust and feasible design spaces based on a simulation model, and passing the solution space to the next designer task. Using the IDEM, designers may considerably reduce design lead-time by decoupling the sequential uncertainty propagation into independent modular uncertainty analyses and employing parallel computing techniques. Based on the data obtained from concurrent modular uncertainty analyses, designers find sets of robust solutions that meet given final performance requirements by a top-down synthesis technique, called Discrete Constraints Evaluation (DCE). The DCE is a technique for

sequentially finding feasible regions in intermediate linking variables' and design variables' spaces in an inverse way (from the final performance via linking variables' space to the design variables' space). The procedure of the IDEM is illustrated in Figure 7.4.

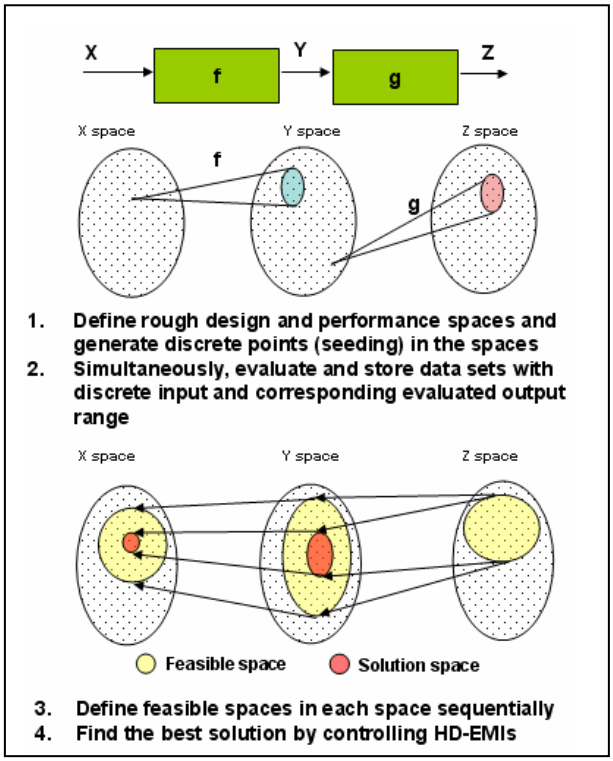

Figure 7.4 Procedure of the IDEM for robust design under propagated uncertainty

The objective is to find the best ranged set of design specifications in the space X considering uncertainty in mapping functions f and g and the propagated uncertainty through a design process. First, rough design and performance spaces (X, Y, and Z spaces) are defined and then discrete points in each space are generated. Second, at each discrete point, the mapping functions (f and g) are simultaneously evaluated and data sets composed of discrete input and ranged output are stored in a database. Third, feasible ranges in Y and X spaces are sequentially defined with a given final performance range

in the Z space. Finally, the best solution range is specified by controlling the HD-EMIs (extended EMI into hyper dimensional space) in X and Y spaces while trading off reliability against the uncertainty in mapping functions, f and g.

In this dissertation, the IDEM is validated in a MESMs design problem based on microscale discrete particle shock simulation and continuum level non-equilibrium thermodynamic mixture analysis. Using the IDEM, designers may find a robust ranged set of specifications in all types (sequential, parallel, and hierarchical) of subsystem networks.

7.2. ANSWERING THE RESEARCH QUESTIONS AND VALIDATING THE HYPOTHESES

As stated in Section 1.4, the principal objective in this dissertation is to establish a methodology to design complex engineering systems that are robust to uncertainty embedded in a system model and propagated uncertainty. The primary interest of the complex engineering system is 'materials' to be designed based on a chain of simulation and analysis models implementing multiscale phenomena. The concept of this new robust design methodology is exploited in the context of the primary research question in Section 1.4.

Primary Research Question

How can we design complex engineered systems in the presence of uncertainties embodied in modeling of phenomena and in the design and analysis process chain?

Hypothesis for the Primary Research Question

The development of Type III and IV robust design will allow a designer (design team) to maximize ranges of values for design variables and maintain the bound of performance parameters in infeasible ranges considering uncertainties embodied in models and process chains.

In Sections 1.4.1 and 1.4.2, the primary hypotheses, Type III and IV robust design, are presented and four research questions are posted in conjunction with the primary research question. Research Questions 1 and 2 are for Type III robust design and Research Question 2 is a support for Research Question 1. Research Questions 3 and 4 are for Type IV robust design and Research Question 3 is a support for Research Question 4.

Research Question 1

How can we get a ranged set of design specifications that are robust to the uncertainty embedded in a model?

Research Question 2

How can we estimate the amount of variability in the response of a non-deterministic model with variability in input variables in a computationally efficient manner?

Research Question 3

How can we represent complex multidisciplinary robust design process chains and their associated uncertainties in a way that is easily identifiable to designers?

Research Question 4

How can we achieve robustness in designing a multi-disciplinary complex system in

which uncertainty is propagated and expanded by exchanging uncertain information between subsystem models in a design and analysis process chain?

In order to answer these research questions, hypotheses were identified in support of achieving the principal objective for the dissertation. The end results are the Robust Concept Exploration Method with Error Margin Index (RCEM-EMI) and the Inductive Design Exploration Method (IDEM). Validations of the hypotheses for answering the research questions are discussed in detail at each chapter with a validation road map. However, in this section those validations are revisited and summarized. Validations of hypotheses are listed in Table 7.1 and discussed in detail in the following sections.

Table 7.1 Summary of validation of the hypotheses

Hypothesis	Validation	Details
Hypothesis 1 The Robust Concept Exploration Method with Error Margin Indices, a method for Type III robust design, provides an effective and efficient mathematical construct to find robust solution range under uncertainty embodied in a model, in which Error Margin Indices are metrics of available margin for potential errors due to uncertainty in models.	***Theoretical Structural Validation***	
	▪ Uncertainty problems in multiscale simulation-based materials design are identified.	§1.2, §3.1, §3.2
	▪ Existing robust design methods are reviewed and research opportunities are identified.	§1.3, §2.3
	▪ Type III robust design is proposed.	§1.4.1, §3.3
	▪ Overall procedure of the RCEM-EMI, an Instantiation of Type III robust design, is discussed in detail.	§3.4, Figure 3.6
	▪ Mathematical construct of EMI is established and discussed in detail.	§3.8, Eqs. (3.16) and (3.17)
	▪ Compromise Decision Support Problem is employed for searching ranged set of design specifications based on EMI.	§3.9, Table 3.2
	▪ A simple example, a randomized ninth order polynomial function, is solved for validating overall procedure and mathematical construct of the RCEM-EMI.	§3.10,Figure 3.11, Figure 3.12, Figure 3.13,Table 3.6
	Empirical Structural Validation	
	▪ Non-deterministic microscale discrete particle shock simulation incorporates unparameterizable variability due to the randomness in microstructure.	§ 5.1.1, §5.1.2
	▪ Non-linear dynamic shock simulation needs large amount of resources resulting in lack of simulation data.	§ 5.1.1, §5.1.2
	▪ Randomness in microstructure and lack of simulation data result in model parameter uncertainty in a metamodel of the material system response.	§ 5.1.1, §5.1.2
	Empirical Performance Validation	
	▪ Two tasks are planed for validation of the utility of the RCEM-EMI.	§5.1.3
	▪ The RCEM-EMI is followed for designing RPMM (an instance of MESMs) based on microscale shock simulation.	§5.2~§5.6; Figure 5.6, Table 5.2~Table 5.6
	▪ Using the RCEM-EMI, designers may find ranged sets of design specifications robust to unparameterizable variability.	§5.7.1,Table 5.7, Figure 5.14, §5.8
	▪ Using the RCEM-EMI, designers may find a robust solution under the uncertainty in the parameters of a system model (i.e., the robust solution found by the RCEM-EMI converges fast while increasing sample size).	§5.7.2, Figure 5.16, § 5.8

Table 7.1 is continued

Hypothesis	Validation	Details
Hypothesis 2 Increased uncertainty due to reducing experimental expenses is inevitable; however, we can formulate the bounds of model uncertainty based on mean response and prediction interval approach for later use in robust design exploration.	***Theoretical Structural Validation***	
	▪ Various types of uncertainty in multiscale simulation-based materials design are discussed.	§1.2.4
	▪ Formulation of those uncertainties in system design perspective is discussed.	§1.4.1
	▪ Various classifications of uncertainty types are discussed.	§2.1
	▪ Existing uncertainty analysis methods are critically reviewed and research opportunities for quantifying uncertainty in computationally efficient manner are identified.	§2.2; Table 2.1 §2.6
	▪ Uncertainties in modeling and simulation of materials are defined; parameterizable and unparameterizable variability, model parameter uncertainty, and model structure uncertainty are defined.	§3.2
	▪ Design of Experiments and automated simulation infrastructure are discussed.	§3.6
	▪ Procedure and Mathematical construct of integrated regression model and prediction interval estimation technique are discussed in detail.	§3.7; Figure 3.7, Eqs. (3.1)~(3.13)
	▪ Validation of the mathematical construct based on a randomized ninth order polynomial function.	§3.10.4; Figure 3.11, Figure 3.12
	Empirical Structural Validation	
	▪ Non-deterministic microscale discrete particle shock simulation incorporates unparameterizable variability due to the randomness in microstructure.	§5.1.1, §5.1.2
	▪ Randomness in microstructure and lack of simulation data result in model parameter uncertainty in a metamodel of the material system response.	§5.1.1, §5.1.2
	▪ A distributed environment for the discrete particle shock simulation is discussed.	§5.4.1
	Empirical Performance Validation	
	▪ Design of Experiments and automated simulation infrastructure for obtaining RPMM shock simulation data is discussed and illustrated.	§5.4.2;Figure 5.7~ Figure 5.10
	▪ Designers may capture the regression model (the most probable model) and prediction interval (upper and lower limits around a regression model) in a computationally efficient manner.	§5.5; Table 5.4, Figure 5.12, Figure 5.13, Eq.(5.5)
	▪ Using RCEM-EMI, incorporating integrated regression model and prediction interval estimation technique, designers may find ranged sets of design specification robust to unparameterizable variability and model parameter uncertainty.	§5.7.1,Table 5.7, Figure 5.14, §5.8 §5.7.2, Figure 5.16, §5.8

Table 7.1 is continued

Hypothesis	Validation	Details
Hypothesis 3 A graphical robust design process model associated with Error Margin Indices is an effective protocol for designers to identify a complex robust design process chain.	***Theoretical Structural Validation***	
	▪ Propagated uncertainty problems in multiscale simulation-based materials design are identified.	§1.4.2, §4.1, §6.2.2
	▪ Type IV robust design is defined.	§1.4.2, §4.2
	▪ P-diagram and IDEF0 process model are reviewed.	§2.5
	▪ Research opportunity for establishing robust design process model is identified.	§2.6
	▪ Graphical entities in order to represent design activities in a robust design process incorporating uncertainties in parameters and models are established.	§4.4; Table 4.2, Figure 4.6
	▪ Graphical Robust Design Process Model (GRDPM) for a complex multi-level simulation-based design is illustrated.	§4.4.2; Figure 4.8
	▪ Material and product design integration for clay-filled polyethylene cantilever beam design is illustrated using GRDPM.	§4.9; Figure 4.20, Table 4.5
	Empirical Structural Validation	
	▪ Multiscale simulation-based MESMs design process is identified.	§6.1
	▪ Information flow between microscale level and continuum level simulation for designing MESMs is established.	§6.2; Figure 6.6, Figure 6.7
	▪ Uncertainty and its propagation in the MESM multiscale simulation chain are identified.	§6.2.2
	▪ The limitations of IDEF0 process model for describing multiscale simulation-based MESM design process are identified.	§6.3.1
	Empirical Performance Validation	
	▪ The GRDPM is employed in order to represent multiscale simulation-based robust MESMs design.	§6.3.2, Figure 6.12
	▪ GRDPM associated with HD-EMIs are illustrated in order to show the robustness under propagated uncertainty in a decision making.	§6.3.2, §6.4, Figure 6.19, Figure 6.20
	▪ The utility of the GRDPM is discussed comparing with the IDEF0 process model.	§6.3.1, §6.3.2, §6.7

Table 7.1 is continued

Hypothesis	Validation	Details
Hypothesis 4 The Inductive Design Exploration Method for Type IV robust design provides an effective mean to find robust multiple ranged sets of design specifications in an inductive manner in a distributed, multidisciplinary systems design problem.	***Theoretical Structural Validation***	
	▪ Propagated uncertainty problems in multiscale simulation-based materials design are identified.	§1.2.4, §4.1, §6.2.2
	▪ Existing multidisciplinary robust design methods are reviewed and research opportunities are identified.	§2.4, §2.6
	▪ Type IV robust design is proposed.	§1.4.2, §4.2
	▪ Overall procedure of the IDEM, an Instantiation of Type IV robust design, is discussed in detail.	§4.5; Figure 4.9
	▪ Inductive Discrete Constraints Evaluation (IDCE) technique is defined and explained in detail.	§4.7
	▪ Mathematical construct of HD-EMI is established and discussed in detail.	§4.7; Figure 4.13
	▪ Compromise Decision Support Problem is employed for searching the best solution set against model structure uncertainty (potential errors).	§4.8; Table 4.3
	▪ Clay-filled polyethylene cantilever beam design is employed and the construct of the IDEM is validated.	§4.9; Figure 4.21
	Empirical Structural Validation	
	▪ Multiscale simulation-based MESMs design process is identified.	§6.1
	▪ The logical interface between the multiscale simulation models is identified.	§6.1.3
	▪ Uncertainty and its propagation in the MESM multiscale simulation chain are identified.	§6.2.2
	▪ Assumptions and Idealizations in developing computation models in the multiscale MESMs simulation and analysis are identified.	§6.2.2, Table 6.2, Table 6.4
	Empirical Performance Validation	
	▪ The IDEM is successfully employed for finding ranged sets of feasible design specification based on Type I-IV robust design concepts.	§6.4,§6.5,§6.5.5 Figure 6.19, Figure 6.20, Figure 6.22
	▪ The solution obtained using the IDEM is robust to the propagated uncertainty in the multiscale MESMs simulation and analysis chain.	§6.2.2,§6.5.5, Table 6.7, Table 6.8,
	▪ A designer may strategically select the best robust solution among feasible solutions by increasing required HD-EMIs	§6.6, Table 6.9, Figure 6.23

7.2.1. Hypothesis 1: Type III Robust Design

In this section, we discuss the validation of Hypothesis 1 for answering Research Question 1. Hypothesis 1 is embodied as the RCEM-EMI in Chapter 3.

Hypothesis 1

The Robust Concept Exploration Method with Error Margin Indices, a method for Type III robust design, provides an effective and efficient mathematical construct to find robust solution range under uncertainty embodied in a model, in which Error Margin Indices are metrics of available margin for potential errors due to uncertainty in models.

Theoretical Structural Validation: Based on characterized uncertainties in engineering systems, specifically in materials systems, in Section 3.2, we identify a need for new robust design, called Type III robust design in Section 3.3. As discussed in the section, the parameterizable variability has been considered in Type I and II robust design; however, unparameterizable variability and model parameter uncertainty among quantifiable uncertainty has not been considered in the existing robust design method. We identified this limitation based on the literature reviews in Section 2.3. Type III robust design focuses on obtaining design solutions that are insensitive to variability or uncertainty embedded within the model used. This embedded uncertainty typically differs from uncertainty in noise and control factors because variability or uncertainty may exist in the parameters of constraints, metamodels, and equations. In Sections 3.4~3.9, implementation details of the RCEM-EMI are discussed. The RCEM-EMI is a procedural framework for identifying a ranged set of design specifications robust to unparameterizable variability and model parameter uncertainty. Error Margin Indices

(EMIs) are developed as metrics indicating the degree of reliability of a decision that satisfies system constraints or bounds. The EMIs are used in search algorithms to find ranged sets of design specifications that meet a range of system requirements. Mathematical constructs for EMIs with given uncertainty bounds are introduced in Figure 3.9 in conjunction with Eqs. (3.16) and (3.17) for identifying upper and lower response deviations. In Section 3.9, the compromise Decision Support Problem (see Table 3.2) is employed as a mathematical construct for searching ranged sets of design specifications using EMIs. The formulated RCEM-EMI construct is approved by a randomized ninth order polynomial function. The randomized variability (i.e., unparameterizable variability) in response is quantified using an integrated regression model and prediction interval as shown in Figure 3.11, Figure 3.12, and Figure 3.13. The design exploration results are shown in Table 3.6 and discussed in Section 3.10.6. As shown in Table 3.6, the mean performance is the best at the optimal and RCEM-DCI solution; however, if designers consider unparameterizable variability, the performance deviations (the interval between estimated minimum and maximum) at the two solution points are larger than that at the RCEM-EMI solution point. Based on the results, it is validated that a ranged set of design specifications robust to the random variability in the function is identified using the RCEM-EMI; therefore, the mathematical construct of the RCEM-EMI is proven to be sound.

Empirical Structural Validation: Non-deterministic microscale discrete particle shock simulation is reviewed in Section 5.1.1 and its value as a comprehensive example is argued in Section 5.1.2. The shock simulation incorporate pseudo random morphology changes in microstructure, and those changes give significant effects on the material

performance, which is a perfect example for unparameterizable variability since the morphology changes are difficult for us to parameterize as numeric numbers. Moreover, this shock simulation is a non-linear dynamic analysis; therefore, it requires a large amount of computing resources, which results in lack of simulation data for complete uncertainty analysis, such as Monte Carlo simulation. Lack of data and unparameterizable variability produces large amount of model parameter uncertainty in a metamodel that we employ for characterizing material system responses. These aspects make this microscale shock simulation-based MESMs design problem be a good example for validating Hypothesis 1, Type III robust design.

Empirical Performance Validation: Two tasks are planned for checking the Empirical Performance Validity of the RCEM-EMI, a method for Type III robust design. Those are; (a) finding a ranged set of RPMM (an instance of MESMs) design specifications robust to Type I, II, and III variability using the RCEM-EMI, and (b) building a confidence that the RCEM-EMI achieves RPMM design specifications that are robust to model parameter uncertainty due to lack of samples. Traditional optimization, the RCEM-DCI, and the RCEM-EMI solutions are compared with each other in order to demonstrate the utility of the RCEM-EMI for this shock simulation-based RPMM design. The overall procedure of the RCEM-EMI for designing robust RPMM is discussed in Section 5.2 and is illustrated in Figure 5.6. The RPMM design tasks are clarified in Table 5.2, which identifies the design space, associated uncertainties, and design goals. The cDSP formulation for the RCEM-EMI solution finding process is illustrated in Table 5.5. The cDSP forms for traditional optimization and the RCEM-DCI are illustrated in Table 5.6. The performance of the RCEM-EMI is demonstrated based on the tasks mentioned

above. In Section 5.7.1 (see Table 5.7), the solutions found by the three solution search algorithms are compared and discussed. The solution found using the RCEM-EMI is the most robust against unparameterizable variability as well as the variability in control factors. This result is also supported by the plots of regression model and prediction interval shown in Figure 5.14. Using larger sample size for building the metamodel, solution convergences of the three solution search algorithms are compared in Section 5.7.2. As shown in Figure 5.16, the solutions using the RCEM-EMI converge faster and are more stable than those of optimization and the RCEM-DCI. It is important to reduce uncertainty in a system by getting more knowledge or data of the system. However, if the system uncertainty cannot be reduced, the RCEM-EMI developed in this dissertation helps designers pursue robust and reliable solutions despite uncertainty remaining in the system. Therefore, Hypothesis 1 is validated.

7.2.2. Hypothesis 2: Integrated Regression Model and Prediction Interval Estimation

The hypothesis for Research Question 2 is proposed in Chapter 1 as shown below.

Hypothesis 2

Increased uncertainty due to reducing experimental expenses is inevitable; however, we can formulate the bounds of model uncertainty based on mean response and prediction interval approach for later use in robust design exploration.

Hypothesis 2 is embodied in the third step, integrated regression model and prediction interval estimation of the RCEM-EMI, as presented in Chapter 3. In the hypothesis, we assumed that we formulate the uncertainty bound considering lack of data due to

computational expenses and unparameterizable variability using the integrated regression model and prediction interval estimation technique.

Theoretical Structural Validation: Hypothesis 2 is an important step in Type III robust design, since a robust design starts with accurate uncertainty analyses (i.e., quantifying amount of uncertainty). For establishing an uncertainty analysis technique, this dissertation starts with defining sorts of uncertainties since an uncertainty quantification method should be different depending on the types of uncertainties to quantify. In Section 1.2.4, types of uncertainty in multiscale simulation-based materials design are discussed. These examples are followed by a discussion of the uncertainties in the system-based design formulation in Section 1.4.1. Uncertainty classifications defined by various researchers are discussed in Section 2.1, and existing methods for uncertainty analysis are critically reviewed in Section 2.2. Based on the types of uncertainty and the available uncertainty analysis method, the research opportunity for quantifying uncertainty in a computationally efficient manner is identified in Section 2.6 (see Table 2.1). Executing simulations or analyses and gathering results are more difficult when the computing resources, such software, hardware, and operators, are geographically distributed. we discuss an automated simulation infrastructure for executing large numbers of simulations and collecting the results in Section 3.6. An overall procedure for the integrated regression model and prediction interval estimation is discussed in Section 3.7 and embodied by mathematical constructs in Eqs.(3.1)~(3.11). The integrated regression model and prediction interval estimation technique is approved as structurally sound by demonstrating a randomized ninth order polynomial function in Section 3.10.4. The results of the quantification are illustrated in Figure 3.11 and Figure 3.12.

Empirical Structural Validation: Since Hypothesis 2 is one of the steps in the RCEM-EMI, the same example problem, microscale shock simulation-based RPMM design, is employed for validation. As discussed in Section 7.2.1, the RPMM design problem is associated with a random generation of microstructure, and its effect on materials performance prediction is significant. The simulation requires a large amount of computing resources. Therefore, this problem incorporates unparameterizable variability and model parameter uncertainty in a metamodel, which is appropriate for validating the utility of the integrated regression model and prediction estimation technique. Moreover, the simulation (i.e., analyzers) and design tools (i.e., designers) are placed in distributed places; therefore, a distributed computational framework is required for efficient sampling as discussed in Section 5.4.1.

Empirical Performance Validation: As mentioned in the Empirical Performance Validation for Hypothesis 1, two other tasks associated with the RCEM-EMI are planned for validating both Hypotheses 1 and 2. A task, specifically planned for validating Hypothesis 2, is to validate that the integrated metamodel and prediction interval estimation in the RCEM-EMI discussed in Section 3.7 is useful for estimating non-deterministic behavior (i.e., unparameterizable variability) in the shock simulation model in a computationally efficient manner. The automated simulation infrastructure, composed on automated pre- and post-processing modules, Raven shock simulation software, and automated sequential execution and data collection using ModelCenter®, is demonstrated and approved to be efficient for gathering a large amount of data in a distributed environment as shown in Figure 5.7~Figure 5.10. In Section 5.5, it is discussed that designers may estimate a regression model (i.e., the most probable model)

and a prediction interval based on the obtained sample size. The sample size is not the limitation for building metamodels; however, more accuracy could be acquired by increasing sample size. Based on the 500 samples (i.e., 20 replicates at each experimental point), an accurate regression model and prediction interval across entire design space are obtained as shown in Figure 5.12and Figure 5.13. The details are discussed in Section 5.5. Using the metamodels obtained by the integrated regression model and prediction interval estimation technique, the RCEM-EMI solution search algorithm is formulated using cDSP. The solutions incorporating the prediction interval as well as the regression model (i.e., the RCEM-EMI solutions) are more robust under unparameterizable variability as shown in Figure 5.14 and Table 5.7. Moreover, the solutions incorporating the prediction interval converge to the estimated true solution at smaller sample size than other solutions that do not incorporate the prediction interval. This means that incorporating the estimated prediction interval with the search design solution actually reduces the required computational resource (i.e., sample size) for the right decision. This solution convergence is illustrated in Figure 5.16 and discussed in detail in Section 5.7.2. Therefore, we claim that the integrated metamodeling and prediction interval estimation method captures uncertainty due to the limitation of sampling size effectively, which enables robust design approach with computationally intensive simulations or expensive experiments. We are confident to claim that Hypothesis 2 is correct.

7.2.3. Hypothesis 3: Graphical Robust Design Process Model

Hypothesis 3 for answering Research Question 3 is embodied in the first step of the Inductive Design Exploration Method (IDEM), presented in Chapter 4.

Hypothesis 3

A graphical robust design process model associated with Error Margin Indices is an effective protocol for designers to identify a complex robust design process chain.

The Graphical Robust Design Process Model (GRDPM) is proposed to represent design process including associated uncertainties in control/noise factors and the model itself. GRDPM should facilitate efficient design process modeling and illustrate a complex design process and propagated uncertainty in a multi-level or multiscale model chain. GRDPM is the first step of the DEM since designers are required to identify their design process before identifying design solutions in a complex design process with multi-level decision making.

Theoretical Structural Validation: One of the challenges in multiscale simulation-based design is a complex model chain in which multiscale simulation or analysis models interface with each other. Uncertainty in a model in the chain could be propagated through and large amount of errors could exist in the final performance estimation. In Section 1.2.4, propagated uncertainty problems in multiscale simulation-based materials design are discussed. For mitigating this propagated uncertainty in a model chain, Type IV robust design is proposed in Section 1.4.2. In this section, as the first step of Type IV robust design, we identified that a graphical representation of a design process is required for efficiently representing a complex design process incorporating multiscale simulation and analysis model chains. The P-diagram and the IDEF0 process model are critically evaluated in Section 2.5 and research opportunities are identified in Section 2.6. The existing process models are unable to represent uncertainty associated with a model (or process) chain, or to illustrate decision making and design freedom in a design process.

Therefore, it is approved that Research Question 3 and Hypothesis 3 are appropriately formulated in order to facilitate those requirements in multiscale simulation-based design. In Section 4.4, graphical entities in GRDPM are defined and some examples of combined graphical entities are illustrated (see Table 4.2 and Figure 4.6). In Section 4.4.2, a complex simulation-based design process is illustrated based on GRDPM in Figure 4.8 and compared with the design process model using the P-Diagram depicted in Figure 4.7. An integrated material and product design example, a clay-filled polyethylene cantilever beam design problem, is employed for validating the structure of GRDPM. The GRDPM of this design process is illustrated in Figure 4.20.

Empirical Structural Validation: In Section 6.1, multiscale simulation-based MESMs design is introduced. In this multiscale simulation chain, two different scale models are interfaced. Those are continuum level Non-equilibrium Thermodynamic Mixture Model (NTM model) and microscale Discrete Particle Mixture Model (DPM model) employed for validation of the RCEM-EMI in Chapter 5. The logical interface between NTM model and DPM model is established connecting the average temperature of reaction initiation hot spots in DPM model and the critical temperature for chemical reaction in NTM model. In Section 0, information flow between DPM model and NTM model is established (see Figure 6.6). The associated design variables and parameters of the two models are incorporated with the information flow map as shown in Figure 6.7. In Section 6.3.1, we identify the requirements of the GRDPM based on the limitation of the IDEF0 process model for describing this simulation chain.

Empirical Performance Validation: In Section 6.3.2, the robust multiscale MESM design process is described using the GRDPM. The utility of the GRDPM is discussed in

comparison with the IDEF0 process model illustrated in Section 6.3.1. The main contribution of the GRDPM is that this semantic process model may represent the uncertainties in multiscale (or distributed multidisciplinary) design tasks and the degree of robustness in decision-making. As shown in Figure 6.12, designers may easily identify the uncertainty in the design tasks associated with the continuum NTM model and the microscale DPM model. As illustrated in Figure 6.14, each box of the GRDPM includes a generalized design sub-process applicable to all scale level design task. As shown in Figure 6.19 and Figure 6.20, designers may easily identify the decision-making process in the robust multiscale MESMs design tasks. As shown in the results, the uncertainties associated with the design task are explicitly represented using the GRDPM. The information of the design variables flows from the left to the right along the design process, and the information of the corresponding performance from the top to the bottom of the boxes. Since the ranged and discrete value of a parameter are described as double or single lines, respectively, designers may easily estimate if the design results still have design freedom for more adjustment or not. Moreover, the decision criteria (the HD-EMIs in the IDEM) are depicted in the model so that the reliability of the decision in the tasks under uncertainty can be easily identified by designers. Therefore, we claim that the GRDPM associated with the HD-EMI provides an effective mean for designers to identify changes in design freedom and uncertainty propagation within a robust design process chain; which supports Hypothesis 3.

7.2.4. Hypothesis 4: Type IV Robust Design

Hypothesis 4 is formulated for answering Research Question 4 and is embodied in Chapter 4. In this hypothesis, we propose the Inductive Design Exploration Method

(IDEM) for robust decision-making under propagated uncertainty and model structure uncertainty. The IDEM includes GRDPM discussed in the previous section as the first step of its procedure. One of the main focuses in the IDEM is finding multiple sets of ranged design specifications that are satisfactory to required bounds in performance while considering propagated uncertainty in a model chain. Therefore, it is quite different from other multidisciplinary robust design techniques, which search for a single robust solution.

Hypothesis 4

The Inductive Design Exploration Method for Type IV robust design provides an effective mean to find robust multiple ranged sets of design specifications in an inductive manner in a distributed, multidisciplinary systems design problem.

Theoretical Structural Validation: As discussed in the theoretical structural validation for Hypothesis 3, Hypothesis 4 is proposed for facilitating robust design based on a multiscale model chain. One of the main concerns for designing based on a model chain is propagated uncertainty as discussed in Section 1.2.4. Type IV robust design is proposed in Section 1.4.2. in order to deal with the propagated and model structure uncertainty. Existing multidisciplinary robust design methods related to the concept of Type IV robust design are critically reviewed in Section 2.4. Based on this review, in Section 2.6, we identified the research opportunity in Type IV robust design that must be established for the multiscale simulation-based materials design. It is validated that Hypothesis 4 is appropriately proposed including the identified requirements. In Chapter 4, the construct of the IDEM including GRDPM is discussed in detail. The overall procedure of the IDEM is illustrated in Figure 4.9 and discussed in Section 4.5. The Inductive Discrete Constraint Evaluation (IDCE) technique in the IDEM is discussed in

Section 4.7 followed by a discussion of HD-EMI, which is an extension of EMI, in Figure 4.13. In the IDCE technique, HD-EMIs are used as metrics for the evaluation of discrete points. The final results of IDCE in a top-down design process are multiple feasible sets of discrete solution points robust to propagated uncertainty in a bottom-up model chain. Among the multiple feasible sets of discrete solution sets, the best solution among feasible multiple solution sets is searched considering model structure uncertainty. As discussed in Section 4.8, compromise Decision Support Problem (cDSP) is employed and HD-EMI is used as an index for robustness against model structure uncertainty during searches for the best solution. The mathematical formulation of the cDSP is illustrated in Table 4.3. The construct of the IDEM is approved by a concept proof example, a clay-filled polyethylene cantilever beam design in Section 4.9. The feasible space in the interdependent variable spaces between material and product design is illustrated in Figure 4.21. The best solutions for four different model structure uncertainty scenarios are found using the IDEM as listed in Table 4.4.

Empirical Structural Validation: In Section 6.1, the logical interface between the microscale DPM model and the continuum NTM model is established as shown in Figure 6.6. The multiscale simulation and analysis chain is identified with the definition of the input parameters, the interdependent parameter, and the output parameters for estimating the performance of the MESMs system.

In Section 6.2.2, the multiscale simulation-based MESMs design example is validated as a representative multiscale materials design example and this example is appropriate for testing the utility of the IDEM. In Figure 6.9, an example of propagated uncertainty across the two multiscale (continuum and microscale) simulation models is illustrated. As

expected, the uncertainty (unparameterizable variability) in the microscale DPM model is expanded via the interdependent variable (T_{ignit}) to the continuum NTM model and the distribution of the final estimated response (*acFe*) has a large amount of variation.

In addition to this propagated uncertainty, those two scale models include model structure uncertainty (unquantifiable uncertainty) due to uncertain assumptions and idealizations for efficient computation. The model structure uncertainty in the microscale DPM model is discussed in Section 5.1.2. The model structure uncertainty in the continuum NTM model is introduced in Section 6.2.2 and summarized in Table 6.2 clarifying the design task.

Empirical Performance Validation: In Section 6.2.3, three validation tasks are planned in order to build confidence in the utility of the IDEM. The first task is planned for validating the utility of the GRDPM. The first task, which is finding ranged sets of robust design specification, is validated in Section 6.5 and 6.5.5. The modular design tasks at each level are performed in Section 6.5. Based on the modular design tasks processed at each level, the feasible regions in the design space and interdependent variable space are identified in an inductive manner in Section 6.5.5. The results are illustrated in Figure 6.19 and Figure 6.20, and the obtained specifications with consideration of all types of uncertainty (Type I~IV) are listed in Table 6.6. The second validation task, which is achieving robust design specifications against the propagated uncertainty, is discussed in Section 6.5.5. In Table 6.8, the design solutions identified based on traditional optimization (see Table 6.7 for the mathematical formulation) and the IDEM are compared each other. From the result, it is validated that the IDEM solution is more insensitive to the propagated uncertainty than the optimal solution. The

last validation task for the IDEM, obtaining a solution robust to model structure uncertainty, is validated in Section 6.6. In this section, the best robust solution among the feasible ranged solutions obtained in Section 6.5.5 (see Figure 6.21) is achieved by strategically selecting HD-EMIs. The robust solution ranges obtained with the two difference scenarios (i.e., emphasizing either the model structure uncertainty in the NTM model or DPM model) are obtained as shown in Table 6.6 and Table 6.9. Therefore, it is validated that, using the IDEM, designers may find ranged multiple sets of design specifications that cannot be achieved by other method. The IDEM is validated as an effective method for finding design specifications robust to propagated uncertainty that is an important issue in multiscale materials design. These results support Hypothesis 4.

From Section 7.2.1 to 0, the validation results for the four hypotheses are summarized answering research questions posted in Chapter 1. It is identified that the RCEM-EMI and IDEM are effective robust design methods for two simple examples discussed in Sections 3.10 and 4.9 and the comprehensive examples, multiscale simulation-based MESMs design problems, discussed in Chapter 5 and 6. In the next section, it is argued that the proposed RCEM-EMI and IDEM in this dissertation are useful for general multiscale simulation-based systems design problems.

7.3. THEORETICAL PERFORMANCE VALIDATION OF THE HYPOTHESES

As discussed in Section 1.5, theoretical performance validation represents the ability to produce useful results beyond the chosen example problems. This requires a "leap of faith" which is eased by the process of building confidence. This involves determining the characteristics of the example problems that make them representative of general

classes of problems. Based on the utility of the method for these example problems, its usefulness for general classes of problems is inferred.

For empirical structural validation, it is argued in Sections 5.2 and 6.2 that the example problems are collectively representative of a general class of problems, defined by the following characteristics:

- Input variables may have variability caused by natural randomness, which becomes variability in control and noise factors.
- Simulation, analysis, or experiment includes unparameterizable variability in results that may be caused by uncertain sources that cannot be configured as numeric parameters, such as random micro-structure changes, human errors, random topology defects, etc.
- Unparameterizable variability causes large system performance deviation, which must be considered in exploration of a design space.
- Quantification of the non-deterministic system behavior requires a large amount of sampling.
- Nonlinear dynamic materials analysis, such as the Reactive Powder Metal Mixture (RPMM) shock simulation, requires intensive computing resources that make it difficult for designers to collect a large amount of data.
- In a material system analysis and simulation, simplification processes for efficient modeling and calculation are usually incorporated, which causes model structure uncertainty.
- Due to the limited system knowledge, simulation and analysis models may not be consistent with reality.

- A multiscale simulation-based design problem is usually associated with a complex design process due to coupled, shared, and interdependent variables.
- Uncertainty in a simulation or analysis model may be propagated along the multiscale simulation chain.

This is intended to be a list of the signature properties of the examples for which the effectiveness of the RCEM-EMI and the IDEM has been demonstrated. Some of these properties and associated opportunities for future work are discussed in Section 7.4. In Chapters 5, and 6, it has been demonstrated that the RCEM-EMI and the IDEM are effective for the example problems with these characteristics. Therefore, there is reason to believe that the RCEM-EMI and IDEM are effective for *general* classes of problems with these characteristics.

In addition, the RCEM-EMI and IDEM may be applicable to even broader classes of problems, as discussed in Section 7.4. The capabilities, advantages, and limitations of the RCEM-EMI and IDEM for the general classes of problems represented by the example problems are summarized in Sections 7.2.1 through 0 and are not repeated here. The next step is to highlight the achievements and contributions to the fields of design methodology and materials design that have been established by answering the research questions and demonstrating and validating the research hypotheses.

7.4. ACHIEVEMENTS AND CONTRIBUTIONS

The achievements and contributions of this dissertation are divided into three categories. First, there are contributions to the field of design methodology. These contributions are directly related to Hypotheses 1, 2, and 4 proposed in Chapter 1 and the

establishment of the Robust Concept Exploration Method with Error Margin Indices (RCEM-EMI) and the Inductive Design Exploration Method (IDEM). Second, in the course of applying these design methodologies, a framework for multiscale simulation-based robust materials design under uncertainty is established based on the Multifunctional Energetic Structural Materials design problem in Chapters 5 and 6. Finally, there are contributions to the field of engineering information technology, which are directly related Hypotheses 3 and the establishment of Graphical Robust Design Process Model (GRDPM). In this section, these two categories of achievements and contributions are highlighted.

7.4.1. Systems Design Methodology

The main contribution of this dissertation is establishment of two **new types of robust design**, namely Type III and IV robust design, which have been overlooked in the previous studies of system-based engineering design.

- Type III robust design is proposed as an extension of existing robust design methodology. Type III robust design focuses on obtaining design solutions that are insensitive to variability or uncertainty embedded within the model or function used. As discussed in Sections 1.3.3 and 1.3.4, Type I and II robust design is designing an insensitive system to uncertainty or variability in input parameters (control and noise factors), such as operating condition, geometry, etc. On the other hand, Type III robust design is proposed in order to consider **the uncertainty or variability in the function relationship between input parameters and responses of a system.** The uncertainty in the function relationship is originated from unparameterizable variability in a system, lack of

sampling data, and limited knowledge of a system. These uncertainty and variability have been overlooked in the studies of systems design since these are often insignificant at product scale level. However, **we claim that Type III robust design must be employed for designing extremely small and/or complex systems, incorporating uncertain models, expensive simulations and experiments, and non-deterministic system behavior.**

- Robust Concept Exploration Method with Error Margin Index (RCEM-EMI) is established for identifying Type I~III robust solutions. Based on the RCEM-EMI, designers may search for a ranged set of design specifications that is robust to not only the uncertainty in input parameters (i.e., deviations in noise or control factors) but also the uncertainty embedded in a system function as unparameterizable variability. The RCEM-EMI is especially useful for designing a system based on non-deterministic simulation with heavy calculations or expensive real experiments since it incorporates with an efficient metamodeling technique for computationally expensive non-deterministic simulation models.
- The Error Margin Index (EMI) is established as a metric for the degree of robustness to Type I~III system uncertainties. The EMI alleviates designers from the difficulties in trade-off between mean performance achievement and performance disperses due to uncertainty.

The identification of Type III robust design and the establishment of the RCEM-EMI for Type I~III robust design is one of the main contributions to the field of systems design methodology.

- Another important contribution to the field of systems design methodology is the proposition of Type IV robust design. Type IV robust design focuses on obtaining a design solution that is insensitive to the propagated uncertainties in a chain of multiple models. Compared to Type I~III robust design, the propagated uncertainty in design and analysis chains is not originated from the variability in systems or the errors in the observation of systems. Instead, the uncertainty comes from a process based on a series of multiple design tasks and/or inter-related analysis and simulation models. If a designer considers multiple inter-related models as a single large model (all-in-one approach; see Section 4.1), then Type IV robust design might not be necessary. However, multidisciplinary analyses and simulations of a complex system limit the seamless integration. For example, it is virtually impossible to integrate all simulations and analyses employed in designing a car. Moreover, multiscale, multiphysics models employed for predicting material behaviors cannot be integrated as a single analysis model; this requires too much computational resource. For example, it is impossible to incorporate ab initio (atomic level) model for analyzing a cantilever beam. Therefore, it is required to divide those complex systems as multiple sub-systems or multiscale models. In this case, we claim that Type IV robust design plays an important role in the complex systems (materials) design, since designers must consider the propagated uncertainty in those simulation and analysis chains.
- The Inductive Design Exploration Method (IDEM) is established for achieving Type I~IV robust design solutions. The IDEM is particularly useful for designing a complex system that incorporates with multiple (multiscale, multidisciplinary,

and multi-physics) analysis, simulation, and experiments. In the IDEM, an inductive (top-down) feasible range search algorithm, called Inductive Discrete Constraint Evaluation, is a unique technique that has not been tried in the field of systems design methods. Based on the IDEM, designers may find not only a single robust solution but also ranged sets of feasible design specifications, which other design exploration algorithms cannot provide. The IDEM is a computationally efficient method since it incorporates with the metamodeling technique used in the RCEM-EMI for capturing non-deterministic system behavior. Since, in the IDEM, the uncertainty analyses (function evaluation) and design exploration processes are completely decoupled, parallel computation is easily and effectively applicable.

The identification of Type IV robust design and the establishment of the IDEM for Type I~IV robust design is another main contribution to the field of systems design methodology.

7.4.2. Multiscale Simulation-based Materials Design

In this section, the contribution of this dissertation to the field of materials design is providing a systematic design method for multiscale simulation-based materials design. The details are discussed as follows.

- One of the contributions to the field of materials design is establishing a framework for incorporating the structure-property relationship with a design of materials. A systematic approach for quantifying the amount of variability in predicting a material property due to random microstructure variation is established. A large number of samples are required in order to consider the

random variability of a material property in a design of materials using previous methods. However, most computational models for predicting structure-property relationship of materials incorporate with computationally intensive simulations or analyses. In this dissertation, an integrated metamodeling and prediction interval estimation is proposed and used for design exploration; this approach saves a large amount of computational expenses. Since this approach requires even fewer samples than traditional approaches, it is also appropriate for designing with experimental data.

- In this dissertation, uncertainty types in multiscale simulation-based materials design are classified. This is an important study since a design method should be carefully selected based on the types of uncertainty in computational material models. Various classifications provided by researchers are reviewed. The most appropriate classification for the categorization of the uncertainties in the models is suggested. Examples of the uncertainties classification for the microscale Al+Fe_2O_3 shock simulation model are presented.
- Another contribution of this dissertation to the field of materials design is the development of a robust materials design framework based on non-deterministic simulation models. As stated earlier, a computationally efficient uncertainty quantification method is employed for characterizing non-deterministic material model (i.e., material system) behavior. Based on the quantifying method, an efficient design exploration method including the Error Margin Indices and compromise Decision Support Problem is developed. These two mathematical constructs provide efficient means (i.e., RCEM-EMI) for exploring a design space

and finding a design specification of materials that are multi-functional and robust to non-deterministic behavior in computationally efficient manner. In this dissertation, material behaviors are characterized as engineering equations using metamodeling techniques since the engineering equation of the materials in this study is unknown in literature. However, the RCEM-EMI is also useful when engineering equations of materials are known but some parameters of the equations are uncertain with some confidence level. This is discussed again in the following section as future work.

- A multiscale robust materials design framework is established in this dissertation. The IDEM is employed to design a material system based on multiscale phenomena. In contrast to the traditional (i.e., bottom-up, deductive) materials design approach, the inductive (i.e., top-down) approach is applied to specify the microstructure of a material given by the required performance. Using the IDEM, material designers may search for ranged sets of materials structure specifications not only a single solution. As shown in the multiscale materials design example in Chapter 6, the uncertainty in the microscale materials simulation model is propagated and expanded through the continuum level simulation. The final performance estimation includes a large amount of uncertainty. The uniqueness of this framework is that the propagated uncertainty through the multiscale simulation chain is considered in the robust design exploration in order to mitigate the effect on the final performance of the designed materials.
- Another contribution to the field of materials design is the development of two interfacing techniques of multiscale models and DOE modules. One is interfacing

between distributed multiscale simulation models, and the other between simulation models and a DOE module. For the interface between distributed multiscale simulation and analysis models, metamodeling techniques are employed instead of a direct simulation-to-simulation plug-in. In this way, materials designers save the expense of integrating heterogeneous computing codes into one platform; this integration is sometimes virtually impossible. To facilitate an efficient computing interface between simulation models and DOE. We developed an automated distributed computing infrastructure for the process of dispatching inputs, pre-processing, calculation, post-processing, and collecting outputs. This automated infrastructure is particularly useful for simulating a large number of samples each of which requires intensive computation.

7.4.3. Engineering Information Technology

The contribution of this dissertation to the field of engineering information technology is the development of a graphical, semantic model for describing complex design processes incorporating various types of uncertainties. Unlike other process models, such as IDEF0, P-diagram, etc., this graphical process model, called Graphical Robust Design Process Model (GRDPM), is specially implemented for describing 'design processes' which are a series of tasks specifying design variables with given requirements. Uncertainties in design tasks, such as variability in control factors (design parameters), noise factors, associated simulations or experiments, and identified design specifications, are explicitly and graphically represented in the model. Therefore, designers may capture the degree of uncertainties associated to each task in a design process. Decision-makings in a series of design tasks are described as required reliabilities against the uncertainties

(i.e., required Hyper-Dimensional Error Margin Indices) and corresponding designed parameters (i.e., feasible spaces in design spaces). we believe that the GRDPM is useful for describing any complex design processes as well as the multiscale materials design processes in which uncertainties are associated.

In this section, the contributions of this dissertation to the fields of design methodology, materials design, and engineering information technology are discussed. However, there are a number of limitations and opportunities for future improvement, which are discussed in the following section.

7.5. LIMITATIONS AND FUTURE WORK

In this section, the limitations in the implemented methods and case studies are discussed in detail. The opportunities for future works are proposed from the limitations.

The limitations in the RCEM-EMI and the opportunities for improvements are as follows.

- The worst case scenario in Eq. (3.16) for quantifying the variability in response due to variability in control factors could be too conservative, which means the response deviation could be over-estimated. In this dissertation, the worst case scenario is used for its computational efficiency. For better accuracy, we recommend directly using the metamodel for uncertainty quantification. Since the metamodels (a mean regression model and its prediction interval) for the random errors in RCEM-EMI are obtained and those models can simulate the non-deterministic behavior of the system model, we may easily perform Monte

Carlo method or Latin Hypercube sampling based on the metamodels without increasing computational expenses.

- An argument regarding the mathematical construct of the EMI has been raised. This argument is that the EMI cannot explicitly convey the designer's preferences since an EMI is calculated based on a set of combination of mean location and performance deviation as shown in Figure 3.9. For this reason, an EMI with a smaller distribution and a mean closer to a requirement limit could be identical to an EMI with a large distribution and a mean farther from the limit. In some cases, however, a designer may prefer the larger distribution whose mean is located farther from the limit. In order to improve this limitation, we may have a few options.

  One of them is to separate the mathematical combination of performance mean and variance in order to control them individually. Two individual goals for mean and variance are created in the cDSP formulation. Formulating an objective function composed of deviation variables, we may either select the Archimedean or Preemptive formulation. In the Archimedean formulation, it is necessary to study trade-off between the achievement of mean and variance, as mentioned in Section 5.8. In order to extend design freedom in downstream activities, designers may find sets of design specifications at which system performances (i.e., means and variances) lie on a Pareto frontier. In the Preemptive formulation, designers prioritize multiple goals (i.e., performance means and variances) and find system variables by sequentially minimizing deviation functions. Another alternative of the EMI is to use preference

functions. Utility function (Myerson, 1991; Otto and Antonsson, 1993) or Taguchi's Loss function discussed in Section 2.3.1 are useful for customizing the designer's preference. Using the preference functions, designers should consider about the uncertainty in a formulated preference function itself.

The EMI goal formulation, however, is still valid and **useful to identify robust solution if a designer is not concerned about system performance once the performance satisfies a requirement limit**. For example, if a single activated cell in a SVE is good enough to react the whole SVE of the MESM, then designers will not care about the number of reacted cells. Instead, they will focus on weather the SVE will include at least one activated cell or not. In this example, we believe that the EMI goal formulation is more reasonable. In addition, **the simplicity of the EMI construct eliminates backward performance check regarding performance requirement limits, which is necessary in the separate mean and variance goal formulation approach.** Finally, as mentioned in Section 5.8, **the EMI construct facilitates extending the EMI from a single performance index into a hyper-dimensional index that is obtained based arbitrary shaped constraint boundaries in a hyper-dimensional space** (c.f., Figure 4.13)**.** Therefore, as a future work, it is recommended to evolve the EMI to be flexible enough to incorporate designer's preferences as well as the advantages that the current EMI construct has.

The limitations and future research opportunities in the IDEM are as follows.

- The GRDPM could be extended further to a computer interpretable model using XML (eXtensible Modeling Language) (W3C, 2005) or other information modeling protocols. The computer interpretable information model may be connected to the coded IDEM so that designers automatically execute a top-down robust design process by configuring the network of a design process by the GRDPM. A generalized computer code for the IDEM needs to be implemented so that it could be easily customized for various types of design tasks.
- One of the main limitations of the IDEM is the errors due to the discretization of a design space. For improving the performance of exploring a design space, the exact border boundary generation algorithm is introduced; however, the discretization errors are not avoidable while checking the feasibility of a mean performance based on discretized feasible and infeasible points. This limitation is discussed in detail in Section 4.7.1 and Figure 4.11. The finer resolution of the discretization of a design space may reduce the errors; however, it should also require more computing power for evaluating feasible spaces. Therefore, it is necessary to develop an efficient algorithm for further improvement of the accuracy without sacrificing the feasibility evaluation performance.
- Another limitation for the IDEM is that the number of design variables explored for the feasibility evaluation (i.e., Discrete Constraints Evaluation) is limited. If the number of design variables increases, then the number of discrete evaluation points increases in the order of power; therefore, it is virtually impossible to include many (above nine) design variables for the

evaluation. In Chapter 4, it is recommended to reduce the design variables by screening process; however, another algorithm to evaluate a discrete design space is necessary. A technique for uneven spacing between discrete points, smaller spacing around constraints border, could be recommended for this improvement.

In addition to the limitations and future work for improving the robust design methodology, future work for enhancing the framework of multiscale materials design is recommended as follows.

- As shown in the examples of Chapters 5 and 6, the obtained responses of the material performances (i.e., the number of reaction initiation site and the average hot spot temperature at first reaction initiation) include a large amount of variability due to the random microstructure changes. This variability is reduced by increasing the size of the statistical volume element. Reduced response variability requires a smaller number of samples for obtaining an accurate metamodel. However, increasing the size of the statistical volume element is limited to the required computing resources, since much more intensive computing power is required for analyzing the larger volume element. In this dissertation work, the largest size of a statistical volume element that can be analyzed by our computing power is selected; however, it is shown that the response variability is still large. The recommended future work is to reduce this response variability and also systematically to select the most appropriate statistical volume element size. In order to reduce the response variability, we may define a new definition of a system performance response

that is robust to the random microstructure changes. Otherwise, we should strategically trade off the element size with the number of samples for the most accurate decision with the minimum resources.

- The design space of the Al+Fe_2O_3 material system needs to be extended to cover a larger range of particle sizes. In the examples of Chapters 5 and 6, the design space is determined by the scope of the simulation capability. Since the design decision is on the border of the design space, extended study incorporating the larger design space as the simulation capability is enhanced. The number of the design variables in the case study needs to be extended including volume fraction of constituents, standard deviations of particle size, and particle velocity. We have previously studied the effect of the volume fractions of the constituents (Seepersad, et al., 2004) and those parameters are not included in this dissertation. However, the interaction effects between the volume fraction and the particle sizes of each constituent need to be characterized and incorporated to searching the MESMs design specification.
- In this dissertation, the MESM case studies include microscale and continuum level simulation. However, as discussed in Section 1.1.2, there are smaller time and length scale simulations (i.e., Ab Initio calculation and Molecular Dynamics simulation) and a larger scale simulation (i.e., projectile level simulation) that are under development in the entire multiscale simulation chain for the MESMs design. Those simulations need to be incorporated with design process logically and computationally interfaced each other. In addition, the experimental results being processed need to be compared with the

developed computational models for the purpose of validation. From the experiment group, the material processing needs to be characterized in order to establish process-structure relationship of the MESMs, which enables for designers to tailor not only material structures but also material processing parameters for achieving proper material performances.

- As a long term future research, we have a challenge for developing a systematic framework for integrated design of materials-product-process. The relationship in materials design (i.e., process-structure-property-performance relationship) may be extended to product design (i.e., part-subassembly-assembly-product) with the support of appropriately designed design processes for a specific product. A conceptual framework with a simple example of a material-product integrated design is published by Choi and coauthors (Choi, et al., 2005). System design and designing design process integration is under development. Initial works are published by Panchal and coauthors (Panchal, et al., 2005)

APPENDIX A

ADDITIONAL SIMULATION AND DESIGN RESULTS IN CHAPTER 6

In this appendix, the data obtained for the validation purposes in Chapter 6 are listed.

A.1 SIMULATION RESULTS FOR THE DEMONSTRATION OF PROPAGATED UNCERTAINTY

In Section 6.2.2, 18 repeated simulations along the multiscale MESMs simulation chain illustrated in Figure 6.7 are performed in order to validate the appropriateness of the example (i.e., empirical structure validation). The histograms of simulation results at each scale level are illustrated in Figure 6.9, demonstrating propagated uncertainty in the simulation chain. In Table A.1, the obtained data used for this demonstration are listed.

Table A.1 Data for uncertainty propagation test

Ra Al (x1 mm)	Ra Fe203 (x2 mm)	Vf void (x3 mm)	Ra Void (x4 mm)	T_ignit (1000 K)	acFe
0.00075	0.0004	0.04	0.0004	1.1285	18.844
0.00075	0.0004	0.04	0.0004	1.613	0
0.00075	0.0004	0.04	0.0004	1.417	9.3702
0.00075	0.0004	0.04	0.0004	1.526	0
0.00075	0.0004	0.04	0.0004	1.483	4.9369
0.00075	0.0004	0.04	0.0004	1.192	17.14
0.00075	0.0004	0.04	0.0004	1.137	18.633
0.00075	0.0004	0.04	0.0004	1.26878	14.972
0.00075	0.0004	0.04	0.0004	1.07795	20.076
0.00075	0.0004	0.04	0.0004	1.427	8.7781
0.00075	0.0004	0.04	0.0004	1.697	0
0.00075	0.0004	0.04	0.0004	1.312	13.392
0.00075	0.0004	0.04	0.0004	1.10607	19.36
0.00075	0.0004	0.04	0.0004	1.189	17.357
0.00075	0.0004	0.04	0.0004	1.456	7.3685
0.00075	0.0004	0.04	0.0004	1.237	15.821
0.00075	0.0004	0.04	0.0004	1.456	7.3685
0.00075	0.0004	0.04	0.0004	1.55431	0

A.2 DISCRETE FEASIBLE POINTS OBTAINED USING THE IDEM

In Figure 6.20, the discrete feasible solution points obtained using the IDEM with HD-$EMI_{acFe} \geq 1$ and HD-$EMI_{Tignit} \geq 0.9$ and the exact boundary points at HD-$EMI_{Tignit} = 0.9$ are illustrated. The illustrated points are the feasible points at $x2$=0.0002. All the obtained feasible points are listed in Table A.2.

Table A.2 Discrete feasible points with satisfying HD-$EMI_{acFe} \geq 1$, HD-$EMI_{Tignit} \geq 0.9$

Mean Ra Al (x1 mm)	Mean Ra Fe2 (x2 mm)	Vf Voids (x3 mm)	Mean Ra Voids (x4 mm)	HD-EMI_{Tignit}
0.0009	0.0004	0.02	0.0002	0.90189
0.0005	0.0002	0.04	0.0002	0.99677
0.0007	0.0002	0.04	0.0002	0.97468
0.0009	0.0002	0.04	0.0002	0.96665
0.0005	0.0002	0.09	0.0002	1.0254
0.0007	0.0002	0.09	0.0002	0.94172
0.0005	0.0002	0.1	0.0002	1.2468
0.0007	0.0002	0.1	0.0002	1.1406
0.0009	0.0002	0.1	0.0002	1.0529
0.0011	0.0002	0.1	0.0002	0.98226
0.0013	0.0002	0.1	0.0002	0.92773
0.0005	0.0003	0.02	0.0003	0.95959
0.0007	0.0003	0.02	0.0003	0.96493
0.0009	0.0003	0.02	0.0003	0.98468
0.0005	0.0002	0.03	0.0003	1.0305
0.0007	0.0002	0.03	0.0003	1.0208
0.0005	0.0002	0.09	0.0003	0.97645
0.0005	0.0002	0.1	0.0003	1.2116
0.0007	0.0002	0.1	0.0003	1.1071
0.0009	0.0002	0.1	0.0003	1.0207
0.0011	0.0002	0.1	0.0003	0.95123
0.0013	0.0003	0.02	0.0004	0.92353
0.0011	0.0002	0.03	0.0004	0.91203
0.0013	0.0002	0.03	0.0004	0.94522
0.0005	0.0002	0.09	0.0004	0.95139
0.0005	0.0002	0.1	0.0004	1.2023
0.0007	0.0002	0.1	0.0004	1.0987
0.0009	0.0002	0.1	0.0004	1.013
0.0011	0.0002	0.1	0.0004	0.94411
0.0005	0.0002	0.02	0.0005	0.97819
0.0007	0.0002	0.02	0.0005	0.98334
0.0009	0.0002	0.02	0.0005	1.0037

0.0011	0.0002	0.02	0.0005	1.0391
0.0005	0.0002	0.09	0.0005	0.94945
0.0005	0.0002	0.1	0.0005	1.2184
0.0007	0.0002	0.1	0.0005	1.1149
0.0009	0.0002	0.1	0.0005	1.0293
0.0011	0.0002	0.1	0.0005	0.96042
0.0013	0.0002	0.1	0.0005	0.90721
0.0011	0.0002	0.02	0.0006	0.92977
0.0013	0.0002	0.02	0.0006	0.97983
0.0005	0.0002	0.09	0.0006	0.97024
0.0005	0.0002	0.1	0.0006	1.2598
0.0007	0.0002	0.1	0.0006	1.1557
0.0009	0.0002	0.1	0.0006	1.0695
0.0011	0.0002	0.1	0.0006	1.0001
0.0013	0.0002	0.1	0.0006	0.94637
0.0015	0.0002	0.1	0.0006	0.90753
0.0005	0.0003	0.1	0.0006	0.92335
0.0015	0.0002	0.02	0.0007	0.96205
0.0005	0.0002	0.09	0.0007	1.0138
0.0007	0.0002	0.09	0.0007	0.93259
0.0007	0.0002	0.1	0.0007	1.2213
0.0009	0.0002	0.1	0.0007	1.134
0.0011	0.0002	0.1	0.0007	1.0635
0.0013	0.0002	0.1	0.0007	1.0088
0.0015	0.0002	0.1	0.0007	0.96918
0.0005	0.0003	0.1	0.0007	0.99195
0.0007	0.0003	0.1	0.0007	0.90097
0.0015	0.0002	0.02	0.0008	0.90602
0.0005	0.0002	0.09	0.0008	1.0805
0.0007	0.0002	0.09	0.0008	0.99795
0.0009	0.0002	0.09	0.0008	0.93119
0.0009	0.0002	0.1	0.0008	1.2233
0.0011	0.0002	0.1	0.0008	1.1513
0.0013	0.0002	0.1	0.0008	1.0953
0.0015	0.0002	0.1	0.0008	1.0545
0.0005	0.0003	0.1	0.0008	1.0841
0.0007	0.0003	0.1	0.0008	0.9908
0.0009	0.0003	0.1	0.0008	0.91387
0.0005	0.0002	0.08	0.0009	0.91577
0.0007	0.0002	0.09	0.0009	1.0867
0.0009	0.0002	0.09	0.0009	1.0182
0.0011	0.0002	0.09	0.0009	0.96478
0.0013	0.0002	0.09	0.0009	0.9256
0.0015	0.0002	0.09	0.0009	0.9
0.0013	0.0002	0.1	0.0009	1.2068
0.0015	0.0002	0.1	0.0009	1.1647
0.0007	0.0003	0.1	0.0009	1.1047

0.0009	0.0003	0.1	0.0009	1.0252
0.0011	0.0003	0.1	0.0009	0.96119
0.0013	0.0003	0.1	0.0009	0.9118
0.0005	0.0004	0.1	0.0009	0.95789
0.0005	0.0002	0.08	0.001	1.0062
0.0007	0.0002	0.08	0.001	0.93937
0.0011	0.0002	0.09	0.001	1.074
0.0013	0.0002	0.09	0.001	1.0333
0.0015	0.0002	0.09	0.001	1.0065
0.0005	0.0003	0.09	0.001	0.997
0.0007	0.0003	0.09	0.001	0.92141
0.0011	0.0003	0.1	0.001	1.0949
0.0013	0.0003	0.1	0.001	1.0432
0.0015	0.0003	0.1	0.001	1.0057
0.0007	0.0004	0.1	0.001	1.0068
0.0009	0.0004	0.1	0.001	0.93395
0.0005	0.0005	0.1	0.001	0.92396

REFERENCES

Aitkin, M., 1987, "Modelling Variance Heterogeneity in Normal Regression Using GLIM," *Applied Statistics,* Vol. 36, No. 3, pp. 332-339.

Allen, J. K., R. S. Krishmachari, J. Masetta, D. Pearce, D. Rigby and F. Mistree, 1990, "Fuzzy Compromise: An Effective Way to Solve Hierarchical Design Problems," *Proceedings Third Air Force/NASA Symposium on Recent Advances in Multidisciplinary Analysis and Optimization*, San Francisco, California, pp. 141-147.

Amemiya, T., 1977, "A Note on a Heteroscedastic Model," *Journal of Econometrics,* Vol. 6, pp. 365-370.

Asay, J. R. and M. Shahinpoor, Eds., 1993, *High-Pressure Shock Compression of Solids*, Springer-Verlag, New York.

Ashby, M. F., 1999, *Materials Selection in Mechanical Design,* Butterworth-Heinemann, Oxford, UK.

Askeland, D. R., 1994, *The science and engineering of materials,* PWS Publishing Company, Boston.

Austin, R., 2005, "Numerical Simulation of the Shock Compression of Microscale Reactive Particle Systems," *M.S. Thesis,* Woodruff School of Mechanical Engineering, Georgia Institute of Technology, Atlanta.

Austin, R., D. L. McDowell and D. J. Benson, 2005, "Numerical simulation of shock wave propagation in spatially-resolved reactive particle systems," *Modeling and Simulation in Materials Science and Engineering,* Submitted.

Ayyub, B. M. and R.-J. Chao, 1997, "Uncertainty Modeling in Civil Engineering with Structural and Reliability Applications," *Uncertainty Modeling and Analysis in civil engineering* (B. M. Ayyub, Ed.), CRC Press, New York**,** pp. 3-32.

Bascaran, E., F. Mistree and R. B. Bannerot, 1987, "Compromise: An Effective Approach for Solving Multi-objective Thermal Design Problems," *Engineering Optimization,* Vol. 12, No. 3, pp. 175-189.

Belytschko, T., J. Fish, T. R. J. Hughes and T. Oden,2004, *Simulation Based Engineering Science: A Report on a Workshop*.

Benson, D. J., 1994, "An analysis by direct numerical simulation of the effects of particle morphology on the shock compaction of copper powder," *Modelling Simul. Mater. Sci. Eng.,* Vol. 2, pp. 535-550.

Benson, D. J., 1995, "The calculation of the shock velocity - particle velocity relationship for a copper powder by direct numerical simulation," *Wave Motion,* Vol. 21, pp. 85-99.

Benson, D. J., 1995, "A multi-material Eulerian formulation for the efficient solution of impact and penetration problems," *Computational Mechanics,* Vol. 15, pp. 558-571.

Benson, D. J. and P. Conley, 1999, "Eulerian finite-element simulations of experimentally acquired HMX microstructures," *Modelling Simul. Mater. Sci. Eng.,* Vol. 7, pp. 333-354.

Booth, R. S., 1967, "Random search for zeroes," *Journal of Mathematical Analysis and Applications,* Vol. 20, No. 2, pp. 239-257.

Box, G. E. P., 1988, "Signal-to-Noise Ratios, Performance Criteria and Transformation (with discussion)," *Technometrics,* Vol. 30, No. 1, pp. 1-17.

Box, G. E. P. and R. D. Meyer, 1986, "DISPERSION EFFECTS FROM FRACTIONAL DESIGNS," *Technometrics,* Vol. 28, No. 1, pp. 19-27.

Bras, B. and F. Mistree, 1993, "Compromise Decision Support Problem for Axiomatic and Robust design," *Advances in Design Automation,* Vol. 65, pp. 359-369.

Brooks, R. J. and A. M. Tobias, 1996, "Choosing the Best Model: Level of Detail, Complexity, and Model Performance," *Mathl. Comput. Modeling,* Vol. 24, No. 4, pp. 1-14.

Byrne, D. M. and S. Taguchi, 1986, “The Taguchi Approach to Parameter Design,” *40th Annual Quality Congress Transactions*, pp. 370-376.

Cagan, J. and B. C. Williams, 1993, "First-Order Necessary Conditions for Robust Optimality," *ASME Advances in Design Automation*, Albuqueque, NM, pp. 539-549.

Chan, L. K. and T. K. Mak, 1995, “A Regression Approach for Discovering Small Variation Around a Target,” *Applied Statistics. Journal of the Royal Statistical Society Series C,* Vol. 44, No. 369-377.

Chen, W., 1995, "A Robust Concept Exploration Method for Configuring Complex Systems," *Ph.D. dissertation,* School of Mechanical Engineering, Georgia Institute of Technology, Atlanta, Georgia.

Chen, W., J. K. Allen, D. Mavris and F. Mistree, 1996, “A Concept Exploration Method for Determining Robust Top-Level Specifications,” *Engineering Optimization,* Vol. 26, pp. 137-158.

Chen, W., J. K. Allen, F. Mistree and K.-L. Tsui, 1995, "Integration of Response Surface Methods with Compromise Decision Support Problem in Developing a General Robust Design Procedure," *ASME Design Automation Conference*, Boston, Massachusetts, pp. 485-492.

Chen, W., J. K. Allen, K.-L. Tsui and F. Mistree, 1996, “A Procedure for Robust Design: Minimizing Variations Caused by Noise Factors and Control Factors,” *Transactions of the ASME,* Vol. 118, pp. 478-485.

Chen, W., R. Garimella and N. Michelena, 2001, “Robust Design for Improved Vehicle Handling Under a Range of Maneuver Conditions,” *Engineering Optimization,* Vol. 33, No. 3, pp. 2-22.

Chen, W. and K. Lewis, 1999, “A Robust Design Approach for Achieving Flexibility in Multidisciplinary Design,” *AIAA Journal,* Vol. 37, No. 8, pp. 982-989.

Chen, W., T. W. Simpson, J. K. Allen and F. Mistree, 1996, "Using Design Capability Indices to Satisfy a Ranged Set of Design Requirements," *Advances in Design Automation*, Irvine, CA. 96-DETC/DAC-1090.

Chen, W., T. W. Simpson, J. K. Allen and F. Mistree, 1999, "Satisfying Ranged Sets of Design Requirements Using Design Capability Indices as Metrics," *Engineering Optimization,* Vol. 31, pp. 615-639.

Chen, Y., 2001, "Computer-Aided Design for Rapid Tooling: Methods for Mold Design and Design-for-Manufacture," *Ph.D. Dissertation,* Woodruff School of Mechanical Engineering, Georgia Institute of Technology, Atlanta, Georgia.

Choi, H.-J., 2001, "A Framework for Distributed Product Realization," *M.S. Thesis,* Woodruff School of Mechanical Engineering, Georgia Institute of Technology, Atlanta, Georgia.

Choi, H.-J., R. Austin, J. K. Allen, D. L. McDowell, F. Mistree and D. J. Benson, 2005, "An Approach for Robust Design of Reactive Powder Metal Mixtures Based on Non-deterministic Micro-Scale Shock Simulation," *Journal of Computer-Aided Materials Design,* Vol. 12, No. 1, pp. 57-85.

Choi, H.-J., R. Austin, J. Shepherd, J. K. Allen, D. L. McDowell, F. Mistree and D. J. Benson, 2004, "An Approach for Robust Micro-Scale Materials Design under Unparameterizable Variability," *10th AIAA/ISSMO Multidisciplinary Analysis and Optimization Conference*, Albany, NY. AIAA-2004-4331.

Choi, H.-J., J. H. Panchal, K. J. Allen, D. Rosen and F. Mistree, 2003, "Towards a Standardized Engineering Framework for Distributed, Collaborative Product Realization," *ASME Computers and Information in Engineering Conference*, Chicago, IL. DETC2003/CIE-48279.

Das, D., 2005, "A noniterative load flow algorithm for radial distribution networks using fuzzy set approach and interval arithmetic," *Electric Power Components and Systems,* Vol. 33, No. 1, pp. 59-72.

Davidian, M. and R. J. Carroll, 1987, "Variance Function Estimation," *Journal of the American Statistical Association,* Vol. 82, No. 400, pp. 1079-1091.

Der Kiureghian, A., 1989, "Measures of Structural Safety under Imperfect State of Knowledge," *J. Structural Eng.,* Vol. 115, No. 5, pp. 1119-1139.

Dolbow, J., M. A. Khaleel and J. Mitchell,2004, *Multiscale Mathematics Initiative: A Roadmap*, U.S. Department of Energy.

Du, X. and W. Chen, 2000, "A Methodology for Uncertainty Propagation and Management in Simulation-Based Systems Design," *AIAA Journal,* Vol. 38, No. 8, pp. 1471-1478.

Du, X. and W. Chen, 2000, "Towards a Better Understanding of Modeling Feasibility Robustness in Engineering Design," *ASME Journal of Mechanical Design,* Vol. 122, No. 4, pp. 385-394.

Du, X. and W. Chen, 2002, "Efficient Uncertainty Analysis Methods for Multidisciplinary Robust Design," *AIAA Journal,* Vol. 40, No. 3, pp. 545-552.

Dubois, D. and H. Prade, 1978, "Operations on Fuzzy Numbers," *International Journal of Systems Science,* Vol. 9, pp. 613-626.

Dubois, D. and H. Prade, 1979, "Fuzzy Real Algebra: Some Results," *Fuzzy Sets and Systems,* Vol. 2, No. 4, pp. 327-348.

Engel, J. and A. F. Huele, 1996, "Generalized linear modeling approach to robust design," *Technometrics,* Vol. 38, No. 4, pp. 365-373.

Engineous Inc., 2001, *Product Overview: iSIGHT,* http://www.engineous.com/overview.html

Giunta, A. A., V. Balabanov, D. Haim, B. Grossman, W. H. Mason, L. T. Watson and R. T. Haftka, 1997, "Aircraft Multidisciplinary Design Optimization Using Design of Experiments Theory and Response Surface Modelling," *Aeronautical Journal,* Vol. 101, No. 1008, pp. 347-356.

Glejser, H., 1969, "A New Test for Heteroscedasticity," *Journal of the American Statistical Association,* Vol. 64, pp. 316-323.

Gong, G. and F. J. Samaniego, 1981, "Pseudo-maximum Likelihood Estimation: Theory and Application," *The Annals of Statistics,* Vol. 9, pp. 861-869.

Grego, J. M., 1993, "Generalized linear models and process variation," *Journal of Quality Technology,* Vol. 25, No. 4, pp. 288-95.

Gu, X. and J. E. Renaud, 2001, "Implicit Uncertainty Propagation for Robust Collaborative Optimization," *ASME Advances in Design Automation Conference*, Pittsburgh, PA. DETC2001/DAC-21118.

Gu, X., Renaud, J.E., Batill, S.M., Brach, R.M., Budhiraja, A.S., 2000, "Worst Case Propagated Uncertainty of Multidisciplinary Systems in Robust Design Optimization," *Structural and Multidisciplinary Optimization,* Vol. 20, No. 3, pp. 190-213.

Haftka, R. T., 1985, "Simulation Analysis and Design," *AIAA Journal,* Vol. 23, No. 7, pp. 1099-1103.

Hao, F. and J.-P. Merlet, 2005, "Multi-criteria optimal design of parallel manipulators based on interval analysis," *Mechanism and Machine Theory,* Vol. 40, No. 2, pp. 157-171.

Harvey, A. C., 1976, "Estimation Regression Models With Multiplicative Heteroscedasticity," *Econometrica,* Vol. 44, pp. 461-465.

Hasan, O. A. and M. C. Boyce, 1995, "A Constitutive Model for the Nonlinear Viscoelastic Viscoplastic Behavior of Glassy Polymers," *Polymer Engineering and Science,* Vol. 35, No. 4, pp. 331-344.

Haukass, T.,2003, *Types of Uncertainties, Elementary Data Analysis, Set Theory, Reliability and Structural Safety*. Lecture Notes, University of British Columbia.

Ignizio, J. P., 1983, "Generalized Goal Programming: An Overview," Vol. 5, No. 3, pp. 179-197.

Iman, R. L., J. C. Helton and J. E. Campbel, 1981, "An Approach to Sensitivity Analysis of Computer Models, Part1. Introduction, Input Variable Selection and Preliminary Variable Assessment," *Journal of Quality Technology,* Vol. 13, No. 3, pp. 174-183.

Iman, R. L., J. C. Helton and J. E. Campbel, 1981, "An Approach to Sensitivity Analysis of Computer Models, Part2. Ranking of Input Variables, Response Surface Validation, Distribution Effect and Technique Synopsis," *Journal of Quality Technology,* Vol. 13, No. 4, pp. 232-140.

Isukapalli, S. S., A. Roy and P. G. Georgopoulos, 1998, "Stochastic Response Surface Methods (SRSMs) for Uncertainty Propagation: Application to Environmental and Biological Systems," *Risk Analysis,* Vol. 18, No. 3, pp. 351-363.

Jin, R., X. Du and W. Chen, 2003, "The Use of Metamodeling Techniques for Optimization under Uncertainty," *Journal of Structural & Multidisciplinary Optimization,* Vol. 25, No. 2, pp. 99-116.

Jobson, J. D. and W. A. Fuller, 1980, "Least Squares Estimation When the Covariance Matrix and Parameter Vector Are Functionally Related," *Journal of the American Statistical Association,* Vol. 75, pp. 176-181.

Kennedy, M. C. and A. O'Hagan, 2000, "Predicting the output from a complex computer code when fast approximations are available," *Biometrika,* Vol. 87, No. 1, pp. 1-13.

Kim, N. H., H. Wang and N. V. Queipo, 2004, "Efficient Shape Optimization under Uncertainty Using Polynomial Chaos Expansions and Local Sensitivities," *ASCE Joint Specialty Conference on Probabilistic Mechanics and Structural Reliability*, Albuquerque, New Mexico. Paper Number 12-202.

Kirkpatrick, S., 1984, "Optimization by simulated annealing: quantitative studies," *Journal of Statistical Physics,* Vol. 34, No. 5-6, pp. 975-986.

Klepaczko, J. R., T. Sasaki and T. Kurokawa, 1993, "On Rate Sensitivity of Polycrystalline Aluminum at High Strain Rates," *Trans. Japan Soc. Aero. Space Sci.,* Vol. 36, No. 113, pp. 170-187.

Klir, G. J. and B. Yuan, 1995, *Fuzzy Sets and Fuzzy Logic,* Prentice Hall, Upper Saddle River, NJ.

Koch, P. N., T. W. Simpson, J. K. Allen and F. Mistree, 1999, "Statistical Approximations for Multidisciplinary Design Optimization: The Problem of Size," *Journal of Aircraft,* Vol. 36, No. 1, pp. 275-286.

Krishnamachari, R., 1991, "Designing with Fuzzy Compromise Decision Support Problems," *M.S. Thesis,* Department of Mechanical Engineering, University of Houston, Houston, Texas.

Kroo, I., S. Altus, R. Braun, P. Gage and I. Sobieski, 1994, "Multidisciplinary Optimization Methods for Aircraft Preliminary Design," *5th AIAA/USAF/NASA/ISSMO Symposium on Multidisciplinary Analysis and Optimization*, Panama City, FL, pp. 697-707.

Lewis, K. and F. Mistree, 1998, "The Other Side of Multidisciplinary Design Optimization: Accommodating a Multiobjective, Uncertain, and Non-Deterministic World," *Engineering Optimization,* Vol. 31, No. 2, pp. 161-189.

Lin, Y., K. Krishnapur, J. K. Allen and F. Mistree, 1999, "Robust Design: Goal Formulations and a Comparison of Metamodeling Methods," *1999 ASME Design Engineering Technical Conferences*, Las Vegas, Nevada. DETC99/DAC-8608.

Lu, X., V. Narayanan and S. Hanagud, 2003, "Shock Induced Chemical Reactions in Energetic Structural Materials," *13th American Physical Society Topical Conference on shock compression of condensed matter*, Portland, Oregon.

Marston, M., J. K. Allen and F. Mistree, 2000, "The Decision Support Problem Technique: Integrating Descriptive and Normative Approaches in Decision Based Design," *Journal of Engineering Valuation and Cost Analysis,* Vol. 3, No. 2, pp. 107-129.

Mavris, D. N., O. Bandte and D. A. DeLaurentis, 1999, "Robust Design Simulation: A Probabilistic Approach to Multidisciplinary Design," *Journal of Aircraft,* Vol. 36, No. 1, pp. 298-307.

McDowell, D. L.,1998, *New Directions in Materials Design Science and Engineering (MDS&E)* Georgia Institute of Technology and Morehouse College, Atlanta, GA, Sponsored by the U.S. National Science Foundation.

McDowell, D. L.,2004, *Design of Multifunctional Energetic Structural Materials (MESMs)* Georgia Institute of Technology Atlanta, GA, Sponsored by AFOSR MURI.

McKay, M. D., W. J. Conover and R. J. Beckman, 1979, "A Comparison of Three Methods for Selecting Values of Input Variables in the Analysis of Output from a Computer Code," *Technometrics,* Vol. 221, pp. 239-245.

Merzhanov, A. G., 1966, "On Critical Conditions for Thermal Explosion of a Hot Spot," *Combustion and Flame,* Vol. 10, pp. 341-348.

Messine, F., 2004, "Deterministic global optimization using interval constraint propagation techniques," *RAIRO - Operations Research,* Vol. 38, No. 4, pp. 277-293.

Mistree, F., O. F. Hughes and B. A. Bras, 1992, "The Compromise Decision Support Problem and the Adaptive Linear Programming Algorithm," *Structural Optimization: Status and Promise* (M. P. Kamat, Ed.), AIAA, Washington, D.C., Vol. 150**,** pp. 251-290.

Murnaghan, F. D., 1937, "Finite deformations of an elastic solid," *American Journal of Mathematics,* Vol. 49, pp. 235-260.

Myers, R. H. and D. C. Montgomery, 1995, *Response Surface Methodology: Product and Process Optimization Using Designed Experiments,* Wiley, New York.

Myers, R. H. and D. C. Montgomery, 1995, *Response Surface Methodology,* A Wiley Interscience Publication, New York.

Myerson, R. B., 1991, *Game Theory: Analysis of Conflict,* Harvard University Press, Cambridge, MA.

Nair, V. N., 1992, "Taguchi's Parameter Design: A Panel Discussion," *Technometrics,* Vol. 34, pp. 127-161.

Nair, V. N. and D. Pregibon, 1988, "Analyzing Dispersion Effects From Replicated Factorial Experiments," *Technometrics,* Vol. 30, pp. 247-256.

Neter, J., M. H. Kutner, C. J. Nachtsheim and W. Wasserman, 1996, *Applied Linear Statistical Models,* IRWIN, Chicago.

Nikolaidis, E., 2005, "Types of Uncertainty in Design Decision Making," *Engineering Design Reliability Handbook* (E. Nikolaidis, D. M.nGhiocel and S. Singhal, Eds.), CRC Press, New York**,** pp. 8.1-8.20.

NIST, 1993, *Integrated Definition for Functional Modeling (IDEF 0),* http://www.idef.com/Downloads/pdf/idef0.pdf

Oberkampf, W. L., S. M. DeLand, B. M. Rutherford, K. V. Diegert and K. F. Alvin, 1999, "A New Methodology for the Estimation of Total Uncertainty in Computational Simulation," *AIAA Non-Deterministic Approaches Forum*, St. Louis, MO. Paper No. 99-1612.

Olson, G. B., 1997, "Computational Design of Hierarchically Structured Materials," *Science,* Vol. 277, pp. 1237-1242.

Otto, K. N. and E. K. Antonnson, 1993, "Extensions to the Taguchi Method for of Product Design," *ASME Journal of Mechanical Design,* Vol. 115, No. 1, pp. 5-13.

Otto, K. N. and E. K. Antonsson, 1991, "Extensions to the Taguchi Method of Product Design," *Third International Conference on Design Theory and Methodology*, Miami, Florida, pp. 21-30.

Otto, K. N. and E. K. Antonsson, 1993, "The Method of Imprecision Compared to Utility Theory for Design Selection Problems," *Design Theory and Methodology - DTM '93* (T. K. Hight and L. A. Stauffer, Eds.), ASME, New York, Vol. DE-Vol. 53**,** pp. 167-173.

Otto, K. N. and E. K. Antonsson, 1993, "Tuning Parameters for Engineering Design," *ASME Journal of Mechanical Design,* Vol. 115, No. 1, pp. 14-19.

Panchal, J. H., H.-J. Choi, J. Shepherd, J. K. Allen, D. L. McDowell and F. Mistree, 2005, "A Strategy for Simulation-Based Design of Multiscale, Multi-functional Products and Associated Design Processes," *ASME DETC05*, Long Beach, CA. DETC2005-85316.

Parkinson, A., C. Sorenson and N. Pourhassen, 1993, "A General Approach for Robust Optimal Design," *ASME Journal of Mechanical Design,* Vol. 115, No. 1, pp. 74-80.

Pedersen, K. and J. Emblemsvag, 2000, "Validating Design Methods & Research: The Validation Square," *2000 ASME Design Engineering Technical Conference*, Baltimore, Maryland. DETC00/DTM-14579.

Phadke, M. S., 1989, *Quality Engineering using Robust Design,* Prentice Hall, Englewood Cliffs, New Jersey.

Phoenix Integration Inc., 2001, *Phoenix Integration: Products,* http://www.phoenix-int.com/products/index.html

Qian, Z., C. C. Seepersad, V. R. Joseph, C. F. J. Wu and J. K. Allen, 2004, "Building Surrogate Models based on Detailed and Approximate Simulations," ASME DETC04, Salt Lake City, UT. DETC2004/DAC57486.

Ross, P. J., 1988, *Taguchi Techniques for Quality Engineering,* McGraw-Hill, New York, NY.

Sargent, R. G., 2003, "Verification and Validation of Simulation Models," *2003 Winter Simulation Conferences*, New Orleans, LA, pp. 37 - 48.

Seepersad, C. C. and J. K. Allen, 2003, "Robust Topological Design of Cellular Materials," *ASME Advances in Design Automation*, Chicago, IL. DETC2003/DAC-48772.

Seepersad, C. C., M. G. Fernandez, J. H. Panchal, H.-J. Choi, J. K. Allen, D. L. McDowell and F. Mistree, 2004, "Foundations for a Systems-Based Approach for Materials Design," *10th AIAA/ISSMO Multidisciplinary Analysis and Optimization Conference*, Albany, NY. AIAA-2004-4300.

Seepersad, C. C., R. S. Kumar, J. K. Allen, F. Mistree and D. L. McDowell, 2004, "Multifunctional Design of Prismatic Cellular Materials," *Journal of Computer-Aided Materials Design,* Vol. 11, No. 2-3, pp. 163-181.

Shoemaker, A. C., K. L. Tsui and J. Wu, 1991, "Economical Experimentation Methods for Robust Design," *Technometrics,* Vol. 33, No. 4, pp. 415-427.

Simpson, T. W., W. Chen, J. K. Allen and F. Mistree, 1996, "Conceptual Design of a Family of Products Trough the Use of the Robust Concept Exploration Method," *AIAA/USAF/NASA/ISSMO Symposium on Multidisciplinary Analysis and Optimization*, Bellevue, WA. AIAA 96-4161.

Simpson, T. W., J. R. A. Maier and F. Mistree, 2001, "Product Platform Design: Method and Application," *Research in Engineering Design,* Vol. 13, No. 1, pp. 2-22.

Simpson, T. W., T. T. Mauery, J. J. Korte and F. Mistree, 1998, "Comparison of Response Surface and Kriging Models for Multidisciplinary Design

Optimization," *7th AIAA/USAF/NASA/ISSMO Symposium on Multidisciplinary Analysis & Optimization*, St. Louis, MI. AIAA-98-4755.

Simpson, T. W., J. D. Peplinski, P. N. Koch and J. K. Allen, 2001, "Metamodels for Computer-based Engineering Design: Survey and Recommendations," *Engineering with Computers,* Vol. 17, pp. 129-150.

Sobieszczanski-Sobieski, J.,1988, *Optimization by Decomposition: A Step from Hierarchic to Non-Hierarchic Systems,* NASA Technical Memorandum, NASA Langley Research Center.

Sobieszczanski-Sobieski, J. and R. T. Haftka, 1997, "Multidisciplinary Aerospace Design Optimization: Survey of Recent Developments," *Structural Optimization,* Vol. 14, No. 1, pp. 1-23.

Su, J. and J. E. Renaud, 1997, "Automatic Differentiation in Robust Optimization," *AIAA Journal,* Vol. 35, No. 6, pp. 1072-1079.

Suh, N. P., 1990, *The Principles of Design,* Oxford University Press, New York.

Sundaresan, S., K. Ishii and D. R. Houser, 1995, "Robust optimization procedure with variations on design variables and constraints," *Engineering Optimization,* Vol. 24, No. 2, pp. 101-109.

Swadi, S. and A. Bui,1991, *Application of Fuzzy Sets and Bayesian Statistics in the Design of Aircraft Tires*, Department of Mechanical Engineering, University of Houston.

Taguchi, G., 1987, *System of Experimental Design: Engineering Methods to Optimize Quality and Minimize Costs,* UNIPUB/Kraus International Publications.

Taguchi, G., 1993, *Taguchi on Robust Technology Development: Bringing Quality Engineering Upstream,* ASME Press, New York.

Theil, H., 1971, *Principles of Econometrics,* John Wiley, New York.

Torquato, S., 1991, "Random heterogeneous media: microstructure and improved bounds on effective properties," *Applied Mechanics Review,* Vol. 44, pp. 37-76.

Tsui, K.-L., 1992, “An Overview of Taguchi Methods and Newly Developed Statistical Methods for Robust Design,” *IIE Transactions,* Vol. 24, No. 5, pp. 44-57.

Tsui, K.-L., 1996, “A Critical Look at Taguchi's Modeling Approach for Robust Design,” *Journal of Applied Statistics,* Vol. 23, No. 1, pp. 81-95.

Vining, G. G. and R. H. Myers, 1990, “Combining Taguchi and Response Surface Philosophies: A Dual Response Approach,” *Journal of Quality Technology,* Vol. 22, pp. 38-45.

W3C, 2005, *Extensible Markup Language (XML),* http://www.w3.org/XML/

Wang, H. V., 2001, "Computer-Aided Design Methods For The Additive Fabrication Of Truss Structure," *M.S. Thesis,* Woodruff School of Mechanical Engineering, Georgia Institute of Technology, Atlanta.

Welch, W. J., T.-K. Yu, S. M. Kang and J. Sacks, 1990, “Computer experiments for quality control by parameter design,” *Journal of Quality Technology,* Vol. 22, No. 1, pp. 15-22.

Workshop Report,2004, *Simulation Based Engineering Science*. Arlington, VA, National Science Foundation**:** 1-18.

Wujek, B., J. E. Renaud, S. M. Batill and J. B. Brockman, 1996, “Concurrent Subspace Optimization Using Design Variable Sharing in a Distributed Computing Environment,” *Concurrent Engineering: Research and Applications,* Vol. 4, No. 4, pp. 361-377.

Xiao, A., H.-J. Choi, R. Kulkani, K. J. Allen, D. Rosen and F. Mistree, 2001, "A Web-based Distributed Product Realization Environment," *Computers and Information in Engineering Conference*, Pittsburgh, PA. DETC01/CIE-21766.

Xiao, A., S. Zeng, J. K. Allen, D. W. Rosen and F. Mistree, 2002, "Collaborating Multidisciplinary Decision Making Using Game Theory and Design Capability Indices," *9th AIAA/ISSMO Symposium on Multidisciplinary Analysis and Optimization*, Atlanta, GA. AIAA 2002-5617.

Xiu, D. and G. E. Karniadakis, 2003, "A new stochastic approach to transient heat conduction modeling with uncertainty," *International Journal of Heat & Mass Transfer,* Vol. 46, No. 24, pp. 4681-4693.

Xu, D. and S. L. Albin, 2003, "Robust optimization of experimentally derived objective functions," *IIE Transactions (Institute of Industrial Engineers),* Vol. 35, No. 9, pp. 793-802.

Yu, J. and K. Ishii, 1994, "Robust Design by Matching the Design with Manufacturing Variation Patterns," *ASME Design Automation Conference*, Minneapolis, MN, pp. 7-14.

Zimmermann, H. J., 1978, "Fuzzy Programming and Linear Programming with Several Objective Functions," *Fuzzy Sets and Systems,* Vol. 1, pp. 45-55.

VITA

Hae-Jin Choi was born in Gunsan, Jeonbook, Korea on October 5, 1970. He grew up in Jeonju city and attended Jeonju High School. He earned a Bachelor of Science degree in Mechanical Engineering from Yonsei University (Seoul, Korea) in 1995. He earned a Master of Science degree in Mechanical Engineering from the same university. His work was funded by Hyundai Heavy Industry Co. In 1998, he joined in WEBS System Co. as a system consultant where he awarded Orion Inc. and Century Co. funded projects. He earned another Master of Science degree in Mechanical Engineering from the Georgia Institute of Technology in 2001. His graduate work is funded by Air Force Office of Scientific Research MURI 1606U81.